# WINDING MOVEMENT AND CONDITION MONITORING OF POWER TRANSFORMERS IN SERVICE

by

MENGGUANG WANG

B.Sc., Xian Jiaotong University, P.R. China, 1982
M.Sc., The University of British Columbia, 1991

A THESIS SUBMITTED IN PARTIAL FULFILMENT OF
THE REQUIREMENTS FOR THE DEGREE OF

DOCTOR OF PHILOSOPHY
in
THE FACULTY OF GRADUATE STUDIES

(Department of Electrical and Computer Engineering)

We accept this thesis as conforming
to the required standard

The University of British Columbia

July 2, 2003

Department of Electrical and Computer Engineering

The University of British Columbia
Vancouver, Canada

Date July 28, 2003

## *ABSTRACT*

*Power transformers are the most expensive pieces of equipment in a power substation. It is very important to prevent failures and detect problems in a transformer as early as possible. This thesis reviews the diagnostic and monitoring tests and equipment available to assess the condition of transformers and to provide an early warning of potential failure.*

*One problem that is particularly difficult to detect is winding looseness, which can cause movement of the windings and may cause transformer failure. If the looseness or movement can be detected over time, action can be taken to prevent such failures.*

*Frequency Response Analysis (FRA) techniques have the potential to detect winding problems, but the method also contains some uncertainty. In this thesis, Experiments on off-line and on-line FRA techniques were performed both in the laboratory and on transformers in the field throughout North America. New data assessment methods were developed that will help interpret future on-site transformer condition assessment tests.*

*The key test circuit parameters and their effects on frequency response measurements were studied, covering issues such as the effects that external measurement leads and high voltage bushings on the test results, measuring shunt impedance, requirements for recording equipment, the measurement frequency ranges to identify winding problems, the measurement frequency range related to the amount of winding movement, criteria to be used for winding movement ranking, etc.*

*A computer simulation was conducted on a simplified network transformer model. The principal findings from the simulation are similar to the experimental work.*

*Based on the experimental investigation of the FRA method and the transformer model simulation, a new FRA technique was developed that is feasible for on-line applications or for monitoring on-site. To overcome the shortcomings of the existing FRA method, such as frequency limitations and on-line application, the High-Frequency Internal Frequency Response Analysis method (HIFRA) was developed. It uses an injected wide-band frequency signal through the transformer bushing, in combination with an internal FRA measurement. This new technique is very promising for future application for on-line FRA measurements.*

## TABLE OF CONTENTS

## LIST OF TABLES

## LIST OF FIGURES

## GLOSSARY OF ABBREVIATIONS

AI – artificial intelligence
C tap – high voltage bushing capacitance tap
DBPC – dibutyl paracresl
DGA – dissolved gas analysis
DF – dissipation factor
DP – degree of polymerization
EMTP – Electromagnetic Transients Program
FFT – fast Fourier transform
FRA – frequency response analysis
FRA (I) - FRA impulse method
FRA (S) - FRA swept frequency method
FRSL – frequency response of stray losses
FT – Fourier transform
GST – grounded specimen test
HIFRA – high frequency internal frequency response analysis
HV – high voltage
I (f) – current as a function of frequency
IFT – interfacial tension
KV – kilovolts
kVA – kilo volt-amps
LV – low voltage
LVI – low voltage impulse
MVA – mega volt-amps
NIF – node-to-node impedance function
OFAF – oil forced air forced
OLTC – on-load tap changers
PD – partial discharge
PEMI – high voltage pulse generator
RSG – recurrent surge generator
RVM – recovery voltage measurment
STFT – short-time Fourier transform
TDCG – total dissolved combustible gas
TF – transfer function
UST – ungrounded specimen test
V (f) – voltage as a function of frequency
WT – wavelet transform

## ACKNOWLEDGEMENT

I wish to express my profound gratitude to my advisor, Dr. KD Srivastava, for taking me on as his student and for his valuable guidance, suggestions and patience though the years.

I would like to thank Dr. Prabha Kundur, CEO of Powertech Labs Inc. for his kindly encouragement and support.

I would like to thank Mr. Jan Zawadzki, Director of the Power Engineering Lab at Powertech, for his support.

Mr. John Vandermaar, Manager of the Power Engineering Lab, provided inspiration, complete support, and valuable discussion and suggestions. His encouragement and help made the completion of this thesis possible.

Thanks to Dr. J. Marti for his assistance and useful discussion on modelling of transformers.

I would also like to thank the professors in the Department of Electrical and Computer Engineering whose courses I took, and my Powertech Labs colleagues who, in one way or another, helped me during my thesis work.

Last but not least, I would like to thank my mother, my husband and my son for giving me their full support, understanding and patience over the years. Without their support, I would not have been able to finish my study program.

# CHAPTER I OVERVIEW

## 1.1 Introduction

The use of transformers is widespread throughout modern interconnected power systems. In a large public power utility, there can be from a few hundred to over one thousand 69 kV to 500 kV transformers in the sub-transmission and transmission network (excluding the lower voltage distribution network). The size of these transformers ranges from as low as a few kVA to several hundred MVA, with replacement costs ranging from a few hundred dollars to millions of dollars.

Power transformers are usually very reliable within their 20-35 year design life. With proper maintenance, a transformer can remain in service as long as 60 years. However, the catastrophic in-service failure of a transformer is potentially dangerous to utility personnel and the public through explosion and fire, while slow oil leakages from transformers may damage the environment. Failed transformers are costly to repair or replace, and may result in significant loss of revenue through outages.

As transformers age, their internal condition degrades which increases the risk of failure. Failures are usually triggered by severe conditions such as lightning strikes, switching transients, short-circuits or other incidents. When the transformer is new, it has sufficient electrical and mechanical strength to withstand unusual system conditions. As it ages, its insulation strength can degrade to the point that it cannot withstand system events such as short circuit faults or transient overvoltages.

Utilities must prevent these failures and maintain their valuable inventory of transformers in good operating condition. Traditionally, routine preventive maintenance programs have been used, combined with regular testing. As the utility industry is gradually deregulated, increasing efforts are being made to reduce maintenance costs and equipment inventories. This has led to reductions in routine maintenance, reductions in spare transformer capacity, and increases in average loading. These changes are occurring at a time when the average age of transformers in service is increasing and approaching the end of nominal design life.

There is also a trend in the industry to move from traditional time-based maintenance programs to condition-based maintenance. Instead of doing maintenance at regular, pre-determined intervals, it is only carried out if the equipment is suspected to be deteriorating. Hence, there is an increasing need for better non-intrusive diagnostic and monitoring tools to assess the internal condition of transformers. If a problem is found, the transformer can then be repaired or replaced before it fails.

Utilities use a variety of testing and monitoring techniques. The literature review in Chapter II reviews existing monitoring and diagnostic methods and looks at future trends. One important problem in transformer diagnostics is the detection of winding movement. As transformers age, the insulation structure compresses. This leads to a reduction in clamping pressure on the winding, which allows the winding to move. A transformer winding can also become distorted (localized movement) due to short circuit forces on the winding. Loose or distorted windings can cause mechanical or electrical failure. The focus of this thesis is to research the most effective methods to detect this problem with winding looseness.

## 1.2 Proposed Work

The accumulated knowledge from field testing of transformers suggests that the most effective monitoring technique is the frequency response analysis (FRA) method. The main objective of this research is to gain a much better understanding of the FRA test method, and to make the test more practical in service and the data simpler to interpret. To accomplish this goal a four-part work program is proposed.

### Task 1: Test System

The test system used to carry out the FRA test will be modelled using the Electromagnetic Transients Program (EMTP) to study the effect of test set-up parameters such as lead lengths, size, shunt impedance etc. The results will be used to optimise the test arrangement and to determine the critical parameters for obtaining good test data. It is important that these effects are understood to ensure that the test results are repeatable when the time period between tests is long (possibly years) and the personnel doing the tests change and/or are inexperienced. A simplified transformer model similar to the model shown in Figure 1.1 will be used to study the test leads/set-up. The internal electromagnetic and circuit structure of a practical transformer is very

complex, with an array of distributed circuit parameters. The model used for the transformer will only be detailed enough to give a reasonable simulation of a typical transfer function for the purpose of studying the effect of the test circuit.

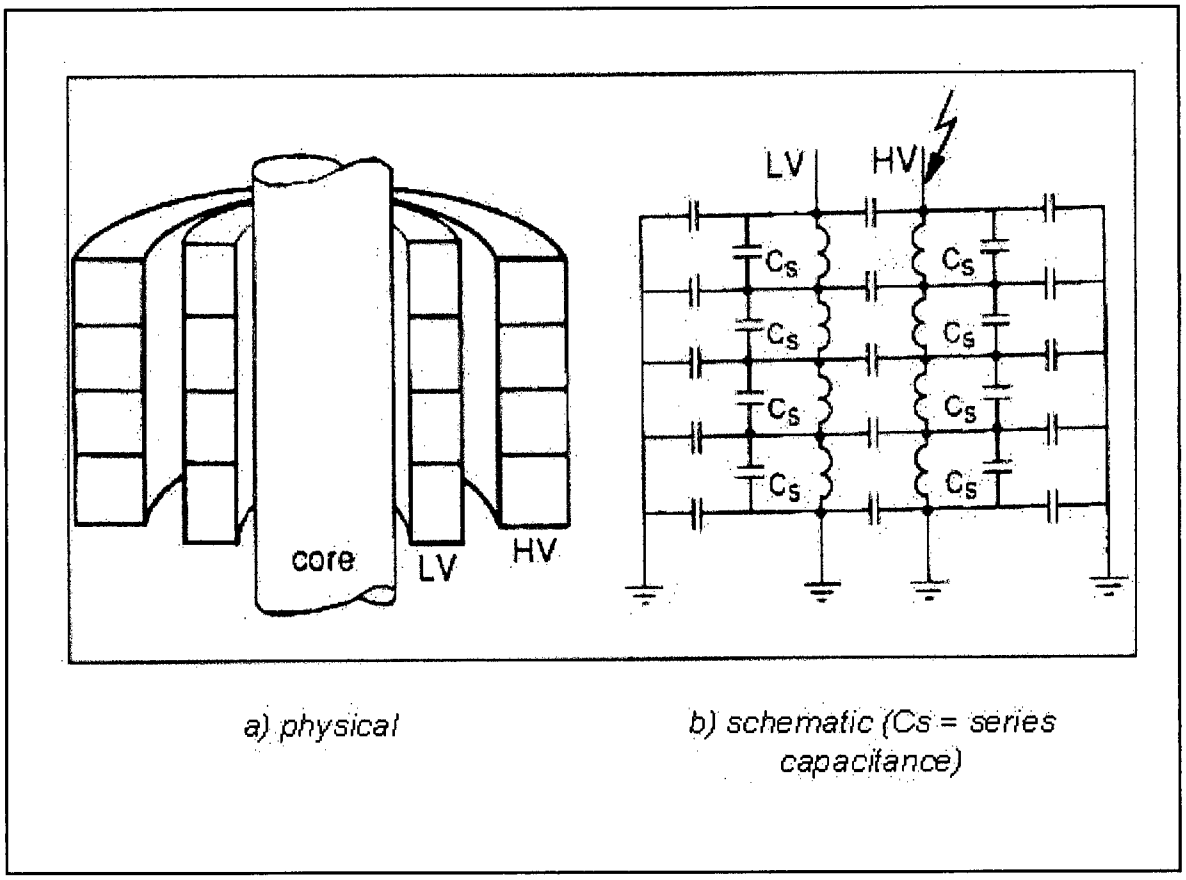


Figure 1.1 - Simplified transformer model

Task 2: Measurement Parameters

The parameters of the test circuits and even the test method used vary a great deal between researchers. The frequency range used, the shunt impedance, the location of the test (top or bottom of the transformer) and the length and type of leads used for the test set-up all differ. It is not clear how these factors influence the test results. In order to get a better understanding of the effect of the parameters on the FRA test, and to improve it, the results of field tests, laboratory tests and the modelling work of Task 1 will be compared in Task 2.

Task 3: On-line Testing

The cost of performing an FRA test can be greatly reduced if the test is carried out on-line (transformer connected to the power system and energized). The savings due to reduced testing and set-up costs are estimated to be up to $5k, while the savings from not requiring an outage for an off-line test (transformer de-energized and isolated from the power system) could be as high as $25k. Tests will be carried out on-line on a transformer in-service in a utility substation, using transients generated by switching operations as the input signal. The results will be analysed to determine the feasibility, sensitivity and repeatability of on-line testing. The bushing taps on the high voltage (HV) and low voltage (LV) bushings will be used in these trials to obtain the input and output signals. To reduce the voltage at the tap to safe levels, additional capacitance will be added at the capacitance tap. Overvoltage protection and 60 Hz filtering will be required at the capacitance tap. A suitable prototype circuit has been designed and manufactured, and it will be tested and modified as required.

Tests will be carried out on-line on a transformer in-service in a utility substation, using transients generated by switching operations as the input signal. The results will be analysed to determine the feasibility, sensitivity and repeatability of on-line testing. The bushing taps on the high voltage (HV) and low voltage (LV) bushings will be used in these trials to obtain the input and output signals. To reduce the voltage at the tap to safe levels, additional capacitance will be added at the capacitance tap. Overvoltage protection and 60 Hz filtering will be required at the capacitance tap. A suitable prototype circuit has been designed and manufactured, and it will be tested and modified as required.

Task 4: Data Processing and Interpretation for Maintenance Decision Making

The data obtained through an off-line FRA test can be noisy, due to interference from noise sources in the substation. The signals obtained on-line may also be subject to interference. An experienced engineer does a visual interpretation of the signal signatures obtained to determine if there has been any significant winding deformation. Techniques to reduce the noise in the signals and to simplify the data analysis techniques will be studied to obtain algorithms that can be used for data analysis. These techniques will include measuring the difference in total area under the curves and measuring the sum of the differences in signal magnitude, as a function of frequency.

The aim of this task is to develop an interpretation technique that can be carried out fairly simply by less experienced personnel. The technique must determine if the transformer under test is in good condition, is deteriorating but needs no immediate action, or has deteriorated to the point that it needs to be taken out of service and opened.

In proceeding with this investigation, it is recognized that a large power transformer is a very complex electromagnetic structure. Simple four-terminal measurements, without de-tanking the transformer, are dependent upon the complex parameters that define the internal windings and upon the external measuring system parameters that may vary from one on-site test to another. Hence, an extensive and comprehensive program of field testing will be necessary.

# CHAPTER II LITERATURE REVIEW

## 2.1 Power Transformer Failures and Problems

Generally, transformer failures can be defined as follows [1, 2]:

- Any forced outage due to transformer damage in service (e.g. winding damage, tap-changer failure)
- Any problem that requires removal of the transformer to a repair facility, or which requires extensive field repair (e.g. excessive gas production, high moisture levels)

Transformer failures can be broadly categorized as electrical, mechanical or thermal. The cause of a failure can be internal or external. Table 2.1 lists typical causes of failures. In addition to failures in the main tank, failures can also occur in the bushings, in the tap changers or in the transformer accessories.

Table 2.1 - Typical failure causes

| Internal | External |
|---|---|
| Insulation deterioration | Lightning strikes |
| Loss of winding clamping | System switching operations |
| Overheating | System overload |
| Oxygen | System faults (short circuit) |
| Moisture | |
| Solid contamination in the insulating oil | |
| Partial discharge | |
| Design & manufacture defects | |
| Internal winding resonance | |

The failure pattern of transformers follows a "bathtub" curve as shown in Figure 2.1. The first part of the curve is failures due to infant mortality, the second part of the curve is the constant failure rate, and the last part of the curve is failures due to old age.

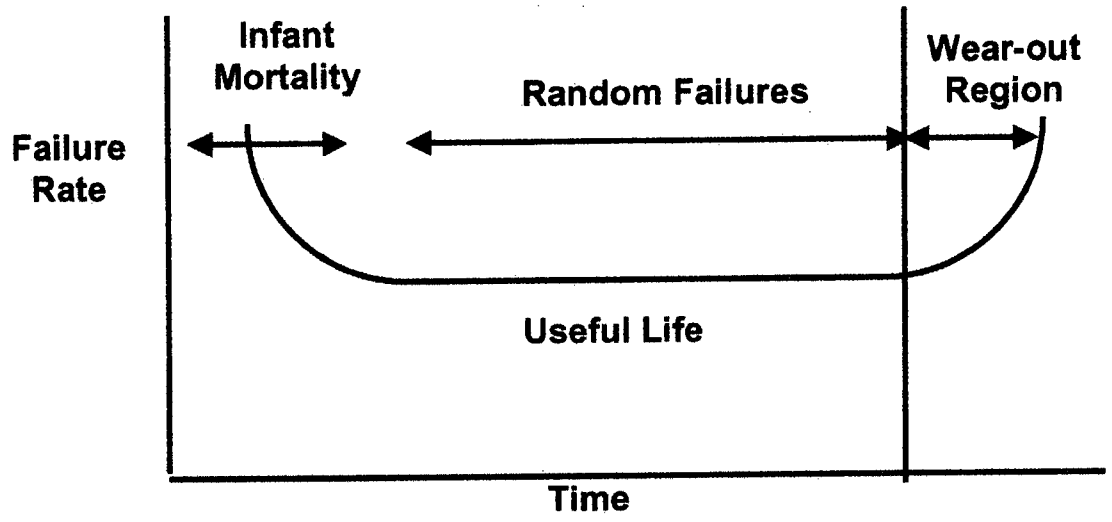


Figure 2.1 - Bathtub failure curve

In addition to normal aging, a transformer may develop a fault that results in faster than normal aging, resulting in a higher probability of failure.

Power transformers have proven to be reliable in normal operation, with a global failure rate of 1% to 2% per year. A large investment was made in generating capacity beginning shortly after the Second World War and continuing into the early 1970s, resulting in a transformer inventory that, in theory, is fast approaching end of life [3]. The end of life of a transformer is typically defined as the loss of mechanical strength of the solid insulation in the windings. These power transformers are at the last stage of the "bathtub" curve. They are expected to have an increasing failure rate in the next few years.

A survey [4] reports that the main causes of transformer failure (51% of transformer failures over a five-year period) were due to the following problems:

- Moisture, contamination and aging which caused the transformer internal dielectric strength to decrease
- Damage to the winding or decompression of the winding under short circuit forces
- Damage to the transformer bushings caused by loss of dielectric strength of the internal insulation.

An American utility has reported four single-phase EHV autotransformer failures due to transformer winding resonance [5]. All of the failures involved the breakdown of the no-load tap changers immediately after the transmission system was energized. The utility also experienced three 25/765 kV, 500 MVA generator step-up transformer failures and two 765 kV, 80 MVA reserve auxiliary transformer failures. All of the failures were dielectric in nature [6].

A survey done by a CIGRE working group on failures in large power transformers [1] found that about 41% of failures were due to on-load tap changers (OLTCs) and about 19% were due to the windings. The failure origins were 53% mechanical and 31% dielectric. On transformers without on-load tap changers, 26.6% of failures were due to the windings, 6.4% were due to the magnetic circuit, 33.3% were due to terminals, 17.4% were due to the tank and dielectric fluid, 11% were due to other accessories and 4.6% were due to the tap changer. Figure 2.2 shows the percentage failure distribution for power transformers with on-load tap changers. Figure 2.2 also shows that a significant fraction of the failures may be attributed to changes in the transformer windings, such as loss of clamping pressure.

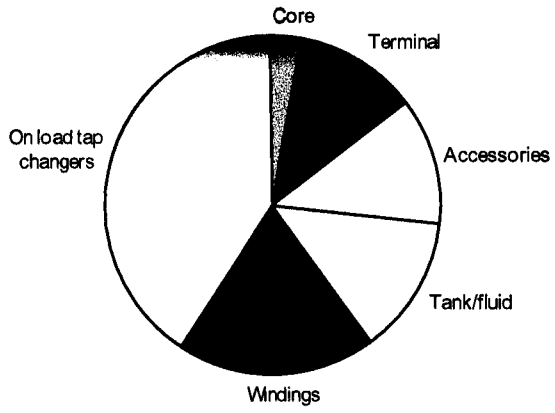


Figure 2.2 – Percentage failure of power transformer with on-load tap changers [1]

Another report presents transformer failure data in South Africa [7]. This failure analysis was based on 131 power transformers in the voltage range of 88 kV to 765 kV, with ratings from 20 MVA to 800 MVA. The failure modes are shown in Figure 2.3. Both ageing of transformers and internal damage to the winding structure from short circuits would contribute to winding looseness and undesirable movement under normal load current cycling. Failure statistics for

large transformers that had been in service between 15 and 25 years are shown in Figure 2.4 [4].

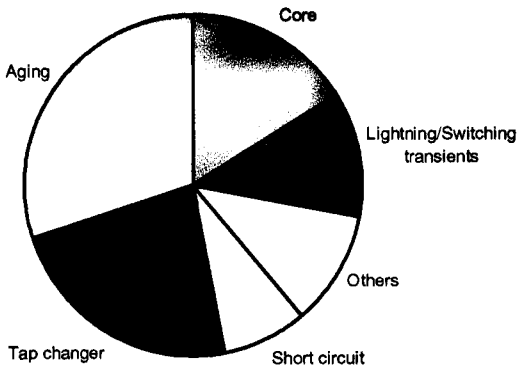


Figure 2.3 – Percentage of failures of power transformers with and without on-load tap changers [7]

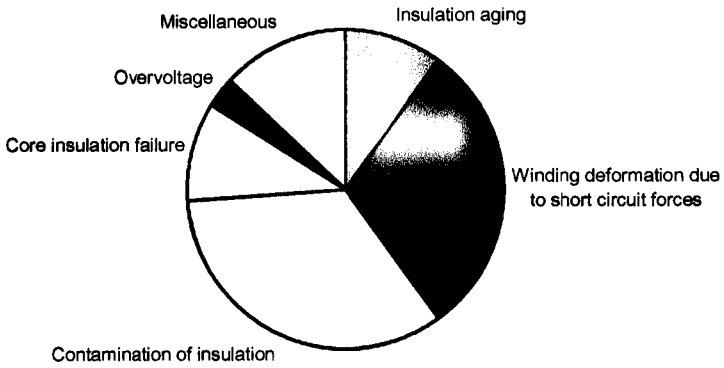


Figure 2.4 – Failure of transformers 15 to 25 year old [4]

These surveys and research results indicate that the key sources of transformer failure are load tap changers, windings, insulation ageing and contamination. Winding deformation and insulation aging are very significant contributors to field failures of transformers.

Another paper [8] reports that the average number of transformer failures over a four-year period (1975 to 1979) was 2.6 failures per year per 100 transformers.

The cost and time to repair and replace a power transformer is very substantial. The repair and replacement of a 345/138 kV transformer normally takes about 12 to 15 months. When a spare transformer is readily available, the time needed for replacement of a failed unit can be in the range of 2 to 3 months.

## 2.2 Transformer Life Management

The fundamental objective of transformer life management is to promote the longest possible service life and to minimize lifetime operating costs. The importance of this issue over the past 10 to 15 years has led to a lot of research [9-15]. In general, transformer life is equal to the life of the insulation, which depends on its mechanical strength and electrical integrity. Insulation degradation can be hydrolytic, oxidative and thermal. Life evaluation of a transformer takes into consideration aging that may lead to major failures, and the aging and life of a transformer has been defined as the life of the paper insulation [10]. Aging mechanisms for insulation have been identified as follows:

- Applied mechanical forces
- Thermal aging (chemical reactions)
- Voltage stresses
- Contamination.

The transformer is subjected to mechanical forces during transportation and to electromagnetic forces caused by system short circuits and inrush current. Vibration and thermal forces, generated by different thermal expansion rates in different materials, can cause long-term degradation of the paper. Dielectric failure may eventually occur when the mechanical forces rupture the insulation. The compressive mechanical forces on the cellulose paper can cause material flow and cause the clamping pressure to lessen. Thus the ageing of the paper insulation determines the ultimate life of the transformer, although other factors may contribute to an earlier failure.

Thermal aging of transformer insulating materials is associated with the chemical reactions that occur within the materials. These chemical reactions are caused by pyrolysis oxidation and hydrolysis, and are accelerated by increased levels of temperature, oxygen and moisture content. As the cellulose paper breaks down chemically, its mechanical properties also begin to fail. The paper insulation becomes brittle to the point of almost falling apart, but it still retains an acceptable level of dielectric strength.

The temperature of a transformer has a major impact on the life of the insulation. Current industry standards limit maximum allowable hot spot temperatures in transformers with conventional oil-paper insulation to 140°C. Continuous on-line monitoring of the transformer oil temperature, along with a thermal model of the transformer, can give an estimate of the loss of life of the transformer due to over-heating.

End of life for a transformer may be dictated by a single factor or by any combination of factors. Considerable attention has been given to paper aging as a cause of transformer failure. While it is undoubtedly a factor in reducing the life of a transformer, it does not automatically lead to failure. Some other influence is normally required, such as mechanical shock. In industry loading guides (e.g. IEC, ANSI and IEEE standards) the principal factor for end of life relates only to the transformer's thermal factor. A classical method of calculating the remaining life of a transformer has been the Arhennius-Dakin formula:

$$\text{Remaining life} = Ae^{B/T}$$

where A = initial life; B = constant, depending on the properties of the material studied; and T = absolute temperature in °Kelvin

The other factors affecting the probability of failure are not as easily quantified as thermal aging. A more comprehensive approach is clearly needed to evaluate the remaining life of a transformer as a whole. To assess the overall condition a transformer reliably, several monitoring techniques are in use or under investigation. The most common monitoring/testing methods used for transformer condition assessment are given in [11, 16, 17-79].

Traditional routine tests include transformer ratio measurement, winding resistance, short circuit impedance and loss, excitation impedance and loss dissipation factor, capacitance, and applied and induced potential. These tests usually provide information on faults in windings, winding conductor and joint problems, winding deformation, oil moisture and contamination and insulation dielectric problems. Specialized tests for transformer condition assessment include partial discharge measurement, frequency response analysis, vibration analysis, infrared examination, voltage recovery and degree of polymerization. These tests detect problems such as local partial discharge, winding looseness and displacement, slack winding and mechanical faults, hot spots on connections, moisture in paper and aging of paper, and insulation degradation.

Oil tests are used extensively. They consist of dissolved gas analysis (DGA) with ratio analysis, furan analysis, water content, resistivity, acidity, interfacial tension (IFT) and dissipation factor (DF). These detect oil incipient faults, overheating, aging of paper, dryness of oil-paper and aging of oil.

Life assessment of large transformers may be performed to [12]:

- monitor the condition of transformers and provide an early warning of faults
- diagnose problems when transformers exhibit signs of distress or following the operation of protective equipment
- determine whether a transformer is in a suitable condition to cope with unusual operating conditions
- obtain reference results to assist in the interpretation of subsequent tests
- assist in planning a replacement strategy for transformers
- satisfy the requirements for insurance coverage

Various testing and monitoring methods are reviewed in detail in the next section.

## 2.3 Monitoring and Diagnostic Methods

In general, the term *monitoring* describes basic parameter measurement with threshold alarms. The term *diagnostics* indicates the addition of sophisticated analysis, such as an expert system capable of providing an assessment of equipment condition and suggested actions.

There are a variety of tools available to evaluate the condition of transformers [25, 58, 67, 68, 80-84]. Some are traditional diagnostic methods that have been in widespread use for many years. Others are non-traditional methods that are either in use or still in the research stage.

### 2.3.1 Traditional Methods of Diagnosis

#### 1) Oil Testing

Testing of the winding insulating oil is one of the most common methods to evaluate the condition of transformers in service. Thermal and electrical faults in the oil can lead to oil degradation.

Dissolved Gas Analysis

Under abnormal electrical or thermal stresses, insulating oils break down to liberate small quantities of gases. The composition of these gases is dependent upon the type of fault. By means of dissolved gas analysis (DGA), it is possible to distinguish faults such as partial discharge (corona), overheating, and arcing in a variety of oil-filled equipment. A number of samples must be taken over a period of time to discern trends and to determine the severity and progression of incipient faults. The gases-in-oil tests commonly evaluate the concentration of hydrogen, methane, acetylene, ethylene, ethane, carbon monoxide, carbon dioxide, nitrogen and oxygen. The relative ratios and the amount of gas detected in each sample are used to detect problems with the insulation structure [62, 85-93].

*Cellulosic decomposition* - the thermal decomposition of oil-impregnated cellulose insulation produces carbon oxides (CO, $CO_2$) and some hydrogen and methane ($H_2$, $CH_4$) due to the oil.

*Oil decomposition* – mineral transformer oils are mixtures of many different hydrocarbon molecules, and the decomposition processes for these hydrocarbons in thermal or electrical faults are complex. Heating in the oil produces ethylene as the principal gas.

Information from the analysis of gases dissolved in insulating oil is one of the most valuable tools in evaluating the health of a transformer, and has become an integral part of preventive maintenance programs. Data from DGA can:

- provide advanced warning of developing faults
- monitor the rate of fault development
- confirm the presence of faults

- provide a means for conveniently scheduling repairs
- monitor condition during overload.

DGA data by itself does not always provide sufficient information with which to evaluate the integrity of a transformer system. Manufacturing data and the history of the transformer in terms of maintenance, loading practices, previous faults, etc. are all an integral part of the information required to make an evaluation.

In general, there are three steps involved in DGA. The first is to establish whether or not a fault exists. In-service transformers always have some fault gases dissolved in their oil. Only when these levels exceed a threshold value is a fault suspected. Several recommended safe values have been published, some of which are listed Table 2.2.

Table 2.2 – Selected fault gas limits

| Gas | Dornenburg/Stritt | IEEE | Bureau of Reclamation | Age Compensated |
|---|---|---|---|---|
| Hydrogen | 200 | 100 | 500 | 20n+50 |
| Methane | 50 | 120 | 125 | 20n+50 |
| Ethane | 35 | 65 | 75 | 20n+50 |
| Ethylene | 80 | 50 | 175 | 20n+50 |
| Acetylene | 5 | 35 | 7 | 5n+10 |
| Carbon Monoxide | 500 | 350 | 750 | 25+500 |
| TDCG* (total of above) | | 720 | | 110n+710 |
| Carbon Dioxide | 6000 | 2500 | 10000 | 100n+1500 n=yrs in service |

* Total Dissolved Combustible Gas

The second step is to determine the type of fault. The two methods in common use are the key gases method and gas ratios method [17,18,21-23,29,31-32,39,42,48,59,61,63,79]. Key gases involve plotting all the total dissolved combustible gases (TDCG) as a percentage of their total in a histogram. Each fault type will give a distinctive pattern characterized by a key gas, generally the most abundant. For example, high levels of hydrogen with low levels of

other gases are characteristic of partial discharge. The ratio method requires the calculation of ratios of gases to each other, such as methane to hydrogen. Three or four such ratios are used for diagnosis. The most widely used are Roger's ratios, where the severity of the fault is established by comparison of the levels of gases with threshold levels and their rate of generation. At least two consecutive samples are needed to calculate the rates of fault generation.

A list of key gases and their related faults is shown in Table 2.3.

Table 2.3 – Key gases and related faults

| **Key Gas** | **Characteristic Fault** |
|---|---|
| $H_2$ | Partial Discharge |
| $C_2H_6$ | Thermal Fault <300°C |
| $C_2H_4$ | Thermal fault 300°C-<700°C |
| $C_2H_2$, $C_2H_4$ | Thermal Fault > 700°C |
| $C_2H_2$, $H_2$ | Discharge of Energy |

For a detailed discussion consult IEEE Std. C57.104-1991, *IEEE Guide for the Interpretation of Gases Generated in Oil-Immersed Transformers.*

Insulating oil quality

The condition of the oil greatly affects the performance and the service life of transformers. A combination of electrical, physical and chemical tests can be performed to measure any changes in the oil's electrical properties, as well as the extent of contamination and degree of deterioration of the insulating oil. The results are used to establish preventive maintenance procedures that avoid costly shutdowns and premature equipment failure and extend the service life of the equipment.

There are many insulating oil tests available. Table 2.4 shows the most commonly used and their significance.

Table 2.4 - Common oil tests

| Type of Test | ASTM Method | Significance/Effects |
|---|---|---|
| Dielectric Breakdown | D877, D1816 | Moisture, particles, cellulose fibres/lower dielectric strength |
| Neutralization Number | D644, D974 | Acidic products from oil oxidation/ sludge, corrosion |
| Interfacial Tension (IFT) | D971 | Presence of polar contaminants, acids, solvents, varnish |
| Colour | D1500 | Darkening indicates contamination or deterioration |
| Water Content | D1533 | Excessive paper decomposition/lower dielectric strength |
| Power Factor | D924 (100, 25 C) | Dissolved metals, peroxides, acids, salts/overheating |
| Oxidation Inhibitor (DBPC*) | D2668, D1473 | Low levels result in accelerated oil aging |
| Metals in Oil | | Indicative of pump wear, arcing or sparking with metal |

* Dibutyl Paracresol

Threshold levels for these oil tests are specified in ASTM D3487 (for new oils) and IEEE guide 637-1985 (for service oils).

As paper degrades, a number of specific furanic compounds are produced and dissolved in the oil. The presence of these compounds is related to the strength of the paper, as measured by its degree of polymerization (DP). Measurement of furans and phenols in oil is a convenient, non-invasive method to assess the condition of the paper insulation. Transformer oil samples should be analyzed for furans and phenols when one or more of the following conditions exist:

- Overheating or overloading of the transformer
- High level of carbon monoxide or carbon dioxide
- Rapid decrease of interfacial tension without a corresponding increase in acid number
- Sudden darkening of the oil and a sudden increase of the moisture content of the oil
- The transformer is over 25 years old

Furan measurement is still a relatively new technique and its interpretation is dependent on many operational and historical factors. However, the guidelines in Table 2.5 provide some assistance.

Table 2.5 - Furan guidelines

| 2-Furaldehyde (ppm) | Degree of Polymerization | Extent of Degradation |
|---|---|---|
| 0 – 0.1 | 800 – 1200 | Insignificant |
| 0.1 – 0.5 | 700 – 550 | Significant |
| 1.0 – 2.0 | 500 – 450 | Cause for concern |
| >10 | <300 | End of life |

The degree of polymerization (DP) estimated from furan analysis provides an average value. However, paper in transformers usually does not age uniformly so there will be areas where degradation is more severe.

3) Power Factor Testing

Insulation power factor is the ratio of the resistive current component to the total leakage current under an applied voltage. Power factor measurement is an important source of data in monitoring transformer and bushing condition. In general, equipment for measuring power factor has three basic modes of operation: 1) grounded specimen test (GST); 2) GST guard; and 3) ungrounded specimen test (UST). The three measurement modes allow for measurement of the current leaking back to the test set on each lead individually and together. A power factor of less than 1% is generally considered to be good, 1%-2% is questionable, and a power factor that exceeds 2% requires action to be taken. In practice, the evaluation is not only based on a single power factor data point, but is also based on the history of change in the power factor.

Measurement of a transformer's capacitance and power factor at voltages up to 10 kV (at 50 Hz or 60 Hz) has long been used for both routine testing and diagnosis. The acceptance value should be less than 0.5%. Reference [63] categorizes the inter-winding power factor as: dry

<0.5%; medium <1.5%; wet >1.5%. This evaluation also takes into account the transformer's power factor history. The test requires an outage and isolation of the transformer, and can be done on high voltage winding to ground, high to low voltage winding, low voltage winding to ground, high to tertiary voltage winding, low to tertiary voltage winding, and the tertiary voltage winding to ground insulation. The test is used to detect problems with the transformer bushings and to evaluate the condition of the oil-paper insulation structure [17,18,42,48,60,63,94].

3) Winding Resistance

Winding resistance is used to indicate the condition of the winding conductor and tap change contact. The test requires an ohmmeter capable of accurately measuring resistance in the range of 20 Ω down to fractions of an Ω. Winding resistance varies with oil temperature. During the test, the temperature should be recorded. For future comparison, the resistance should be converted to a reference temperature. Measurement of transformer winding resistance requires an outage and isolation of the transformer. Variations of more than 5% may indicate a damaged conductor in a winding [22].

4) Winding Ratio

The ratio of the transformer windings is the number of primary winding turns divided by the number of secondary winding turns. The ratio test is useful in determining if there are any shorted turns or open winding circuits. The measured ratio should be within 0.5% of the ratio of the rated voltages between the windings, as noted on the transformer nameplate. All tap positions and all phases should be measured. The test can be performed at a very low voltage.

5) Excitation Current

An excitation current test provides the no-load losses of the transformer. Changes in these losses can indicate changes in the core. This test is difficult to carry out on site since it requires a substantial power supply, and is of limited usefulness. It is done routinely only in a factory setting [22,29,42,48,63]. Excitation current is measured by applying a rated voltage to the primary winding with the secondary winding open-circuited. The current must be accurately measured and recoded at the same voltage level for future comparison. The excitation current should have no more than a 5% variation between tests.

6) 60 Hz Impedance Testing

A transformer's 60 Hz impedance is measured by short-circuiting the low voltage winding of the transformer and measuring the input current, voltage and power, normally with the rated current in the shorted winding. It is usually only performed in the factory, before and after short circuit testing of a transformer to detect movement. It is only sensitive to relatively large changes in the winding, which is difficult to do on site due to the size of the power source required for the test (typically rated ≥1 MVA [23,42,49]). The ratio of voltage to current should be within 2% for each phase, and should not vary more than 2% between tests. A variation of more than 2% for transformers over 10 MVA indicates the possibility of winding distortion. For transformers less than 10 MVA, the allowable variation is 2% for circular coils and 7.5% for non-circular concentric coils. A greater variation indicates the possibility of mechanical distortion of the winding [95].

7) Thermography

Infrared emission testing is used to check the surface temperature of the transformer on-line. It is useful for detecting thermal problems with a transformer, such as cooling system blockages, and for locating electrical connection problems and indicating the hot spots [34,42,45].

Infrared imagers "see" the heat radiation from objects just like a photographic camera "sees" visible light. This heat is radiated from, reflected by, or transmitted through the object being imaged. Black and white thermograms (heat pictures) show hot areas in white and cold areas in black, unless stated otherwise. In colour thermograms, white and red areas are usually hotter, while black and blue areas are colder.

Infrared thermography provides the heating patterns for the load that was on the equipment at the time that the scan was performed. Any abnormal conditions can be located from the scan. The severity of overheating from the scan can be categorized as follows:

| Classification | Temperature Rise* |
|---|---|
| Attention: | 0° to 9 °C |
| Intermediate: | 10° to 20° C |
| Serious: | 21° to 49° C |
| Critical: | >50° C |

* - Temperature rise is defined as the difference in temperature between a reference point on the transformer at normal temperature and the point of concern.

### 2.3.2 Non-traditional Transformer Monitoring Techniques

New developments in testing and monitoring techniques for power transformers have flourished in recent years.

1) In-service Partial Discharge Testing

Partial discharge (PD) in a transformer degrades the properties of the insulating material and can lead to eventual failure [23]. There are two commonly used PD detection methods: detection of the acoustic signals, and measurement of the electrical signals produced by the PD [29]. PD can also be detected indirectly using chemical techniques, such as measuring the degradation products produced by the PD. The acceptable PD limit for new transformers is dependent on the voltage and size of the transformer, but ranges from <100 pC to <500 pC.

PD pulses generate mechanical stress waves that propagate through the surrounding oil (in the range of 100 kHz to 300 kHz) [37]. Acoustic emission sensors for detecting these waves are mounted either on the transformer tank wall or inside the transformer tank in the oil. If multiple sensors are used, the PD can be located based on the arrival time of the pulses at the sensors. The sensitivity of the test is dependent on the location of the PD. The signal is attenuated by the oil and winding structure, so that the deeper the PD is located inside the winding, the greater the attenuation. Piezoelectric sensors and fibre optic sensors can be used to measure PD. Recent research shows that optical sensors have a potential sensitivity that is much higher

than normal external tank-mounted piezoelectric sensors for PD detection [96]. Fibre optic sensors also could potentially be placed inside the winding.

PD causes high frequency low amplitude disturbances on the applied voltage and current waveforms that can be detected electrically. Electrical PD signals can be measured at a number of different locations, including bushing tap current or voltage and neutral current [17,18,23,24,28-29,39,42,48,53-54,58,65,71,76,79]. Techniques using detection of ultra high frequency signals (typically 1 GHz to 2 GHz) have been developed to detect PD in gas-insulated substations, and this method is also being applied to transformers. The work shows some promise for PD detection in transformers [47,64].

Acoustic methods of PD detection are limited by signal attenuation, while electrical PD measurements are limited by electromagnetic interference problems. Equipment is commercially available that will continuously monitor and evaluate internal PD on-line, using both acoustic and electrical methods.

Investigations are underway to improve acoustic detection of PD and to study electrical detection for in-service monitoring [97]. The goal is to be able to detect and, ideally, locate PD levels with a minimum sensitivity of at least 100 pC.

2) Recovery Voltage Measurement

The recovery voltage measurement (RVM) [98-102] method is used to detect the condition of oil-paper insulation and the water content of the insulation. The RVM method relies on the principle of interfacial polarization of composite dielectric materials; that is, the build up of space charges at the interfaces of oil-paper insulation due to impurities and moisture. A dc voltage is applied to the insulation for a period of time. The electrodes are then short-circuited briefly, after which the short circuit is removed to examine the rate of voltage build-up or the polarisation profile. The time constant associated with this peak recovery voltage gives an indication of the state of the insulation. The main parameters derived from the polarization spectrum are the maximum value of the recovery voltage, the time to peak value and the initial rate of rise of the of recovery voltage.

The test results give an indication of the state of the oil-paper insulation structure of the transformer. It requires a transformer outage to carry out the test [18,23,43,48,54,63,69-70]. This method is very controversial as to its suitability for direct measurement of the moisture content in oil, due to the strong dependence of the results on the geometry and construction of the insulation system of a transformer. Figure 2.5 shows a typical RVM curve for an old transformer that is in good condition. Figure 2.6 shows an example of a transformer in poor condition.

The main drawbacks to this test are the long outage that can be required and the reliability of the interpretation of the results.

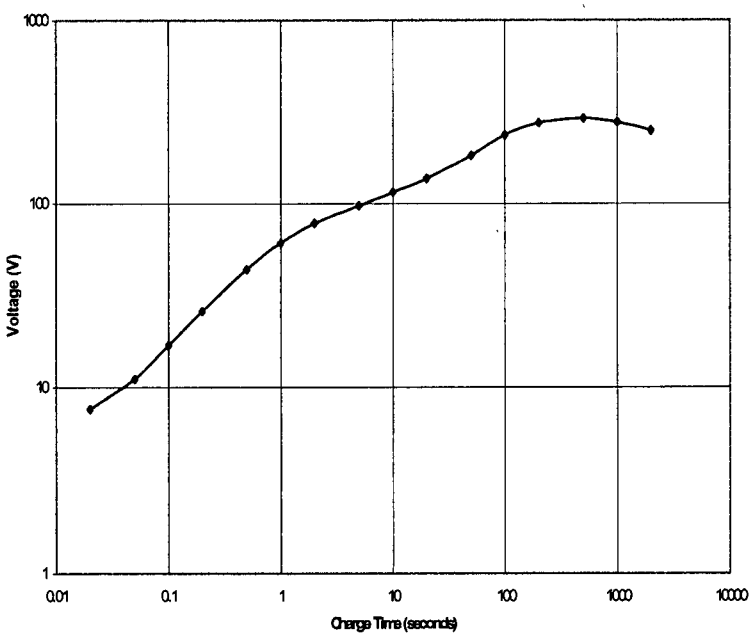


Figure 2.5 – Typical RVM curve for a transformer in good condition

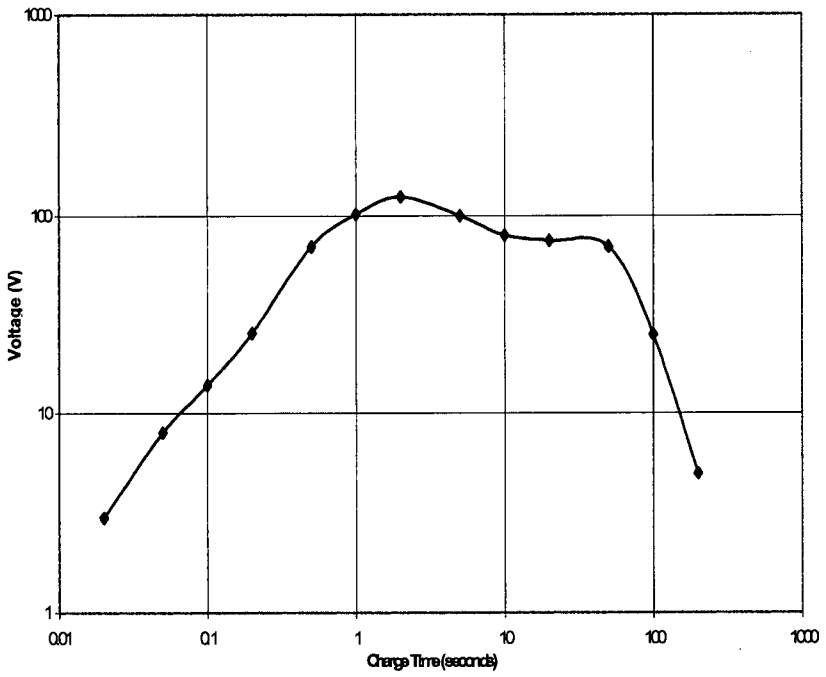


Figure 2.6 – Typical RVM curve for a transformer in poor condition

3) Winding Insulating Oil Testing/Monitoring

In addition to the insulating oil tests that are routinely carried out on transformer windings (see Section 2.3.1 1), there are other oil tests that can provide information on the condition of the transformer. These include particle count, metals in the oil, furan analysis, aniline point, corrosive sulphur, and oxidation stability.

Today, many transformers have equipment installed that continuously monitors oil condition in service. The most widely used systems measure hydrogen content. Systems that measure moisture and other gases are also available. The hydrogen and composition sensors use semiconductor or fuel cell technology. More complex sensors that use infrared technology and gas chromatography can detect several or all of these gases.

4) Tap Changer/Motor Monitoring

Oil testing is also used for tap changer oil. Gas in oil analysis can help to determine deterioration of the contacts [19,29,42,45,53-54,58,62,65,66,67].

Monitoring of tap changer temperature can detect problems such as contact overheating, while acoustic analysis of the switching operation can detect faults in the selector switch and diverter switch [54]. Tap changer motor currents can be monitored to obtain a signature every time the tap changer moves, and changes in this signature will identify problems in the tap changer. Bearing monitors are used to detect bearing wear on transformer oil pumps [28].

5) Internal Temperature Measurement

The traditional method to measure the temperature of a transformer winding is to measure the top and bottom oil temperature of the transformer and estimate the hot spot temperature. Fibre optic equipment has now been developed that is able to monitor the temperature two different ways: distributed temperature measurement and point temperature measurement.

With distributed temperature measurement, the temperature of the winding is monitored along its entire length using a fibre optic cable. The technology used in fibre optic sensors is capable of measuring the full range of temperature encountered in transformers. This system could be used in service if a fibre optic cable could be laid along the transformer winding during construction of the transformer [23,53]. However, optical fibre is very expensive and needs to be handled with extreme care. When installed in a transformer, it would be subjected to high mechanical stresses (squeezing and buckling). . For these reasons, the application of fibre optic temperature sensors to transformer windings so far has been mainly limited to laboratory research and design studies.

With point temperature measurement, insulated sensors and associated cables are installed directly at the transformer hot spots. The best time to install these sensors is during transformer construction, at the locations indicated by thermal modeling of the transformer. It is also possible to retrofit a fibre optic sensor to an existing transformer, but this is difficult to do.

Temperature monitoring systems are also being installed in on-load tap changers, since monitoring of temperature trends has been found to be a useful indicator of degradation of tap changer contacts [23,29,52,53-54,56].

6) On-line Power Factor Measurement

Two commercial systems are now available to measure bushing condition on-line, based on detecting changes in their capacitance and power factor. Both systems place sensors on the bushing capacitance taps to measure the bushing leakage currents. One system uses an electric field sensor to measure the bus voltage phase angle and calculates the capacitance and dissipation factor from the measured data. The other system measures the bushing currents from the three phases and plots the sums on a polar plot. Any shift in the resultant currents indicates a change in capacitance or dissipation factor of one of the bushings. These measurements can give sufficient warning of an impending bushing failure so that the bushing can be replaced before a catastrophic failure occurs.

7) Power Factor vs. Frequency Measurement (Dielectric Spectroscopy)

The measurement of power factor over a broad range of frequencies from a low of 1 mHz to 1 kHz or higher has been used to evaluate insulation condition [17,43,51,60]. Interference can be easily detected as an irregularity, since transformer insulation usually has a smooth power factor-frequency characteristic. The power factor-frequency characteristic allows for a more complete diagnosis of the examined insulation. At the lower frequency range, pressboard dielectric loss is the main factor. At the medium frequency range, oil conductivity is the dominant contributor. At the higher frequency range, pressboard and oil volume determined the dielectric loss. Different aging mechanisms can be detected and identified at their respective frequency ranges.

8) Detection of Winding Movement

One of the most serious problems, and a problem that is particularly difficult to detect, is movement or distortion of the transformer winding. Forces on the winding during short circuits on the transformer can cause winding distortion. Reduction or loss of winding clamping can cause winding movement. This can result in a transformer fault that will cause damage to the

transformer, and may result in an explosive failure. Traditionally, the only way to evaluate the winding condition of a large power transformer has been to drain the oil from the transformer and carry out an internal inspection. Various techniques have been investigated to detect and/or monitor this problem [17-19,21,23,25,29,36,41,48,52,55,57,59,61,75,79].

Some research work has focused on using transformer vibration signals to detect winding looseness and developing the analysis techniques for interpreting the vibration data [103-106]. The method is based on looking for changes in the transformer's vibration signature to detect movement in the winding. Vibration analysis has the advantage that it does not require an extended outage, and the transformer does not have to be disconnected from the system. However, it has not been found to be as reliable as the frequency response analysis test, and is not as widely used.

In the frequency response test (FRA), the transformer is isolated from the system and the magnitude of the impedance or admittance of the transformer is measured as a function of frequency (typically to at least 2 MHz) [12,19,23,36,38-39,41,52-53,55,57,63,72,75,77-78,80-81,83,107-115]. This gives a fingerprint of the transformer. The test is repeated over time and the fingerprints from two or more tests are compared.

Two test methods commonly used to carry out the FRA test are the swept frequency test method and the pulse test method. The swept frequency method applies a variable frequency voltage or a white noise voltage to the high voltage winding and records the response in another winding or terminal. This technique is more widely used in Europe than in North America. The pulse test method, also known as the Low Voltage Impulse (LVI) test method, is a similar technique more commonly used in North America. With this technique, a pulse signal is applied to the high voltage winding and the response is recorded in another winding or terminal. Research indicates that the pulse method is most sensitive for the detection of small winding movements and winding clamping looseness [107]. Figure 2.7 compares FRA test results for a transformer with some movement to the results for a transformer in good condition. The transformer admittances (I(f)/V(f)) were derived from the Fourier transform of the measured transformer neutral current from the high voltage winding (I(f)), divided by the Fourier transform of the measured input voltage applied to the transformer high voltage winding (V(f)). In general, the greater the difference between the two signatures, the greater the movement in

the transformer. The test requires experienced personnel to compare the two signatures and evaluate the severity of the movement.

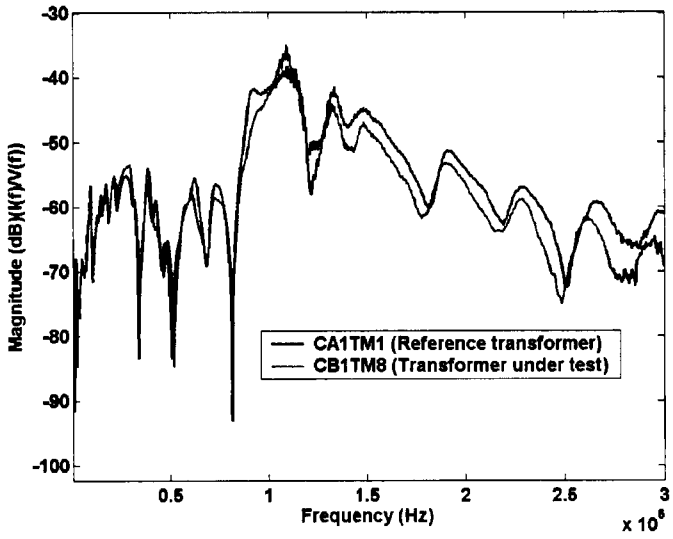


Figure 2.7 – Comparison of FRA test results
(I(f)/V(f) – Fourier transform of measured high voltage winding neutral current/Fourier transform of measured input voltage across high voltage winding)

The conventional off-line FRA test requires a transformer outage. Work has been carried out in Europe and North America to use the transient voltages generated during switching operations as the driving signal to measure the transformer admittance [78,116]. If such an on-line FRA test could be developed, where the transformer remains connected to the power system, it could reduce or eliminate the need for outages to carry out an FRA test.

The FRA test is being used extensively. The drawbacks of the test are that it requires an outage, an initial reference test with the transformer in good condition, great consistency in the test set-up from one test to the next, and experienced personnel to interpret the data. Despite these drawbacks, FRA has been found to be the most effective test in detecting winding movement.

Another technique used to detect winding displacement is the frequency response of stray losses (FRSL). This test is done over a range of frequencies from 20 Hz to over 600 Hz [25-27]. It is thought not to be as sensitive to winding movement as the FRA test, due to its lower measurement frequency range.

The principal focus of this investigation is the evaluation of existing techniques most commonly used to detect winding movement and looseness. Therefore, the variations of FRA test techniques will be critically examined and novel improvements to this well-established technique will be explored.

### 2.3.3 Diagnostic Software and Expert Systems

Diagnostic software, which gives a more definite indication of transformer problems than conventional analysis, is under investigation by many researchers and utilities [66,74,79].
A great deal of research work has been done on software to interpret transformer oil test data such as gas, moisture content and dielectric strength, and to correlate the data with transformer insulation condition. Expert systems have been developed that give an alarm signal to system operators.

Some systems have been developed to detect transformer partial discharge signals and give early warnings of partial discharge in faulty transformers [97]. Equipment using acoustic emission sensors and specialized software has been successful in detecting partial discharge and locating the origin of the discharge. The sensors are mounted externally on the transformer tank wall and three-dimensional source location techniques are applied to locate the source of the detected signals.

Artificial intelligence (AI) modeling techniques have been developed to diagnose transformer faults, but they are not widely used and do not yet appear to be effective [66,74,79]. There is no indication in the published literature that AI systems are being considered for analysis of the FRA test. The use of an expert system would reduce the manpower and financial overhead required to perform transformer condition monitoring, and should provide utilities with more accurate results.

### 2.3.4 Comments on Transformer Diagnostic Techniques

Many monitoring techniques have been developed to allow for the early detection of different types of transformer defects. The problem of loss of clamping/winding deformation is

particularly important, as it will result in catastrophic failure of the transformer if it is left undetected. With the increasing use of condition-based maintenance, and with a transformer inventory that is aging, it is particularly important to focus on this problem.

The FRA test method has proven effective in detecting this problem. Other methods that are in use, such as vibration analysis, have not been as successful. However, the FRA/LVI method still needs improvement, particularly in its sensitivity and the overall understanding of the factors affecting the measurement results. For these reasons, this thesis will focus on the FRA diagnostic technique.

## 2.4 Trends in Monitoring and Diagnostic Techniques

The most widely used tests for diagnosing the condition of transformers are oil tests and off-line power factor testing at reduced voltages. The use of other tests (both off-line and on-line) is increasing, but is limited by a number of factors:

Cost: The high cost of testing and monitoring can make it difficult to justify. The purchase price of the equipment is only one of the cost factors. For off-line tests, the cost of isolating the transformer and performing the test can be substantial, and the long outage time required by tests such as the recovery voltage meter method can make them difficult to carry out. For on-line tests, the installation costs for the monitoring equipment can be a major factor.

Data interpretation: The interpretation of tests often requires experienced personnel (experts). Incorrect interpretation of the data can lead to false conclusions about transformer condition.

Reliability: The degradation of a transformer occurs over a period of years. Sensors and electronic equipment installed on transformers must be able to perform over many years with minimal maintenance.

Compatibility: Typically, systems from one supplier are completely incompatible with those of other suppliers.

Since the number of aging transformers is increasing, the use of non-traditional diagnostic and monitoring techniques is expected to increase. As the techniques become more widely used, the cost of the equipment will decrease and the reliability of the methods will increase. The

interpretation and understanding of the data obtained from tests such as FRA, RVM, and vibration testing will improve. In particular, standard analysis techniques that are currently being developed will enable field personnel to more easily use the test results, and will reduce the need for interpretation by experts. Software that combines the results of different tests and gives an overall assessment of condition is expected to become more widely available, and continuous on-line monitoring of transformers will increase.

As the cost of equipment decreases and the performance of the sensors improves, it will be easier to justify the installation of sophisticated monitoring systems on transformers. Standardization will make it possible to integrate systems and data from different suppliers. The use of wireless technologies within the substation to communicate between the transformer and control room will make monitoring equipment more effective.

The ultimate goal of developing advanced transformer monitoring and diagnostic techniques is to have a set of devices/systems to monitor and anticipate transformer failure, so that appropriate action can be taken before a forced outage occurs.

## 2.5 Power Transformer Modelling and Equivalent Circuits

Transformer modeling plays a very important role in determining the dynamic characteristics of a transformer for simulating internal resonance, transient response, transfer function and steady state analysis.

The published literature on transformer modeling is extensive. In the early years, many researchers tried to establish analytical models to present the transient behaviour of transformer windings. Studies were done on surge response of iron core windings by non-linear integro-differential equations and traveling wave theory for the calculation of impulse voltage distribution on transformer windings. More recently, work has been done on calculating the model parameters through the internal and external models based on electromagnetic theory network analysis and geometry [117-122].

There are different ways to model a transformer. They can be categorized as follows:

1. Internal models: These models are based on the internal physical geometry and properties of the transformer. All parts of the transformer (including the winding, core, lead, tank, etc) are modeled based on their electrical characteristics.

   Internal models can be further subdivided into two types:
   *Detailed models*: the major physical elements of the transformer are included.

   *Reduced models*: the number of elements is reduced to simplify the model and make it easier to analyse.

2. External models: External models, also known as black box models, are based on using a mathematical model to describe the input/output characteristics of the transformer. These models do not require any knowledge of transformer internal construction. The characteristics of the transformer are measured at the terminals over the frequency range of interest and a model is developed from these characteristics.

Both types of model can be further classified as low frequency (60 Hz to a few kHz range), medium frequency (kHz range) or high frequency (MHz range). At higher frequencies, magnetic circuits (steel core) can be ignored since the magnetic excitation inductance can be considered to be open.

It is important that the transformer model meets the need for a particular analytical usage. The external models are not suitable for the modeling of winding displacements, as they just present the behavior of the transformer at its terminals and do not account for minor internal physical changes. With terminal models, it is not possible to simulate internal changes to the transformer and examine the effect of the changes.

To simulate winding movement, it is necessary to use detailed physical models such as those that comprise a network of resistors, capacitors, inductors and magnetic circuits. The physical models are based on the winding lumped equivalent circuit and its geometry. All parts of the transformer must be considered in the model. To be useful at higher frequencies, individual transformer parts such as the winding must be separated into small sections and each section

modeled separately. For example, the capacitance of each section of the winding modeled to the core, to the tank and to other winding sections must be included in the model. If the model contains sufficient detail, changes can be made in the appropriate parts to simulate changes such as movement in the transformer winding. The response of the network to the changes can then be calculated. The higher the frequency, the more detail the model must simulate.

In theory, the transformer can be modeled in sufficient detail to accurately duplicate the measured phenomena. In practice, however, this can be very difficult. The programs used to analyze the models are limited by the number of components they can handle. This forces a reduction in the model details and limits the ability to completely model the transformer response, particularly at higher frequencies. The size of the matrix that needs to be analyzed by the software increases at the rate of the square of the number of elements in the model, which means that the size of the model can quickly exceed the computing capacity of all but the most powerful computers. It can also be very difficult to obtain enough details about the transformer design to establish the parameters for the model. Transformer manufacturers normally will not provide such details due to commercial considerations.

Singh [123] has reported a transformer model that works on determining the transfer function of a power transformer. Experimental measurements were carried out to determine the neutral current and the frequency spectrum of the current. The calculated values for both neutral current and frequency response analysis were found to be in good agreement with the measured results. The electrical network represents the high voltage winding in 15 sections and the tapping winding in 10 sections. Each section consists of self-inductance and mutual inductances, with respect to all other sections in the HV and tapping windings. The series and shunt capacitances of the section are calculated on the basis of disc separation and distances, with reference to core, tank and other windings. The equivalent electrical network is solved for obtaining the neutral current in the winding for the same investigation. The theoretical calculations for three different tapping positions (maximum, normal and minimum) were carried out for both neutral current and frequency.

One reference presents a power transformer model that uses the equivalent circuit [124] shown in Figure 2.8. A single winding model transformer has been considered. Five equal numbers of sections are taken to form a model of an entire winding. The equivalent circuit is a ladder

network, which consists of self-inductance and mutual inductance as well as series, and shunt capacitances. This model is used for calculating the transfer function of the winding.

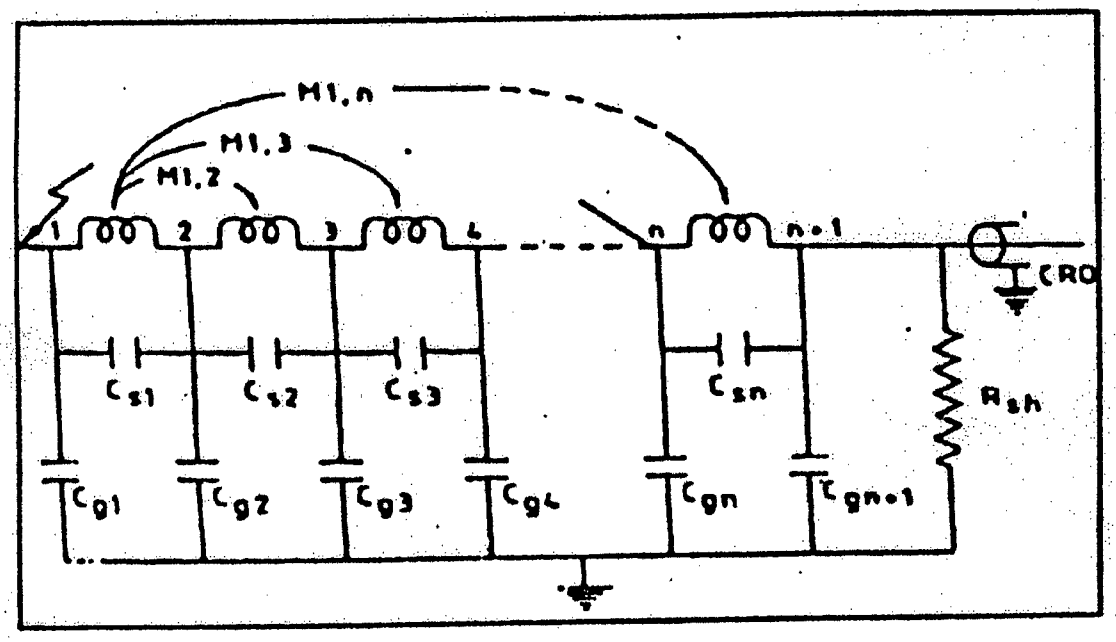


Figure 2.8 – Simple transformer equivalent circuit

The turn failure in the winding will cause a change in the values of the network parameters. The calculation results show that the shift of resonance frequency of the network varies as the percentage of the turn failure. However, the highest change in the frequency observed is only 4% with a failure of 10% of the winding. The results show that the frequency sensitivity of the windings is low and hence it may be difficult to locate the position of a fault in the winding (calculating frequency range from 0 MHz to 1.5 MHz).

A hybrid model was developed by G. B. Gharehpetian et al. [122] to get around the problem of the model size exceeding the capability for analysis. The paper states that *"a model of a transformer valid for the MHz frequency range requires that every turn be represented and that all mutual couplings, inductive and capacitive, with every other turn be included. Manipulating such a model would need the capability of the largest computers."* Their model combines a detailed coil-by-coil model and inter-coil black box models. When the researchers made measurements on a 220 /35 kV 50 MVA transformer, they found unexpected inter-coil winding resonances in the frequency range of several MHz.

## 2.6 System Identification and Parameter Estimation of Power Transformers

When diagnosing transformers, it is advantageous to have a detailed knowledge of their transient response for electrical signals in a wide frequency range.

There are many different approaches to calculating the transfer functions. The most common of these methods is the approximation of the transmission behaviour of the coils by modeling their interior impedances.

These methods are often effective only for limited frequency ranges, up to a maximum frequency of 1 MHz, which may not be sufficient. Additionally, the calculated transfer functions depend on the models used, making them valid only for specific transformers. Thus, for each different apparatus new models must be constructed and their suitability verified in an extensive series of experiments.

However, for some applications it is sufficient to calculate the transmission behaviour of the device. For this, an analytical method can be used with which measured frequency responses are approximated in the frequency domain.

Reference [125] presents an analytical method for computing the transfer function of transformers. A transfer function of the form in Equation 2.1 below is used to describe the measured frequency response:

$$F_c(j\omega) = \frac{b_0 + b_1(j\omega) + b_2(j\omega)^2 + ... + b_Z(j\omega)^Z}{a_0 + a_1(j\omega) + a_2(j\omega)^2 + ... + a_p(j\omega)^p} \quad (2.1)$$

The relative frequency response measured vs. calculated error is determined by the equation below:

$$\delta(j\omega) = \frac{F_c(j\omega) - F_m(j\omega)}{F_m(j\omega)} \quad (2.2)$$

Equation 2.2 is a measure for the judgment of the difference between the calculated frequency response $F_c$ and the measured frequency response $F_m$.. This error should be minimized in the frequency range of interest and should also be independent of the frequency. The maximum likelihood method is also used in the calculation.

At the start of an approximation, the structure of the transformer's transfer function is usually unknown. Thus, it must be calculated with the help of the measured frequency response. According to the reference [125], the mean approximation error is as follow:

$$\bar{\delta} = \sqrt{\frac{\sum_{i=1}^{N} |\delta(j\omega)|^2}{N}} \qquad (2.3)$$

Equation 2.3 is a suitable criterion for a quantitative judgment. Starting from a minimum structure, the number of poles and zeros of the transfer function is increased successively until the mean approximation error decreases to its least value.

This analytical method was verified by calculating the transfer functions of a distribution transformer and a power transformer up to 5 MHz.

Reference [126] presents research work on parametric identification in potential transformer modeling. A wideband lumped parameter equivalent circuit of a potential transformer can be determined through parametric system identification by the Least Squares method. The results show that the equivalent circuit model of this method is able to describe a potential transformer from 50 Hz to 300 kHz.

An integrated approach for high accuracy and low order model identification is presented in reference [127]. The specific identification algorithm given in the paper is the integrated frequency domain operability range space extraction and least square parameter estimation algorithm (IFORSELS).

Several papers discuss system identification by different methods [128-131]. A frequency-domain, subspace-based algorithm is used in the identification of two power transformers. Studies indicate that transformer frequency response is divided into low, medium, and high frequency ranges and second order works [108,126,132]. The non-linear least squares method is applied to obtain an appropriate transfer function to model the frequency response of a particular transformer from 50 Hz to 1 MHz. The models obtained by this approach provide a poor fit to the data and, in particular, are not capable of modeling high frequency dynamics of a transformer.

Another study [133] focuses on mathematical models of transformers rather than their equivalent circuits. This study shows that once an accurate analytic model of a transformer under consideration is available, it is possible to derive a transformer equivalent circuit by a suitable transformation if necessary. This study also indicates that transformer dynamics vary from one transformer to another, which makes it difficult to derive a transformer equivalent circuit valid for all ranges of power transformers. Nevertheless, a mathematical model adequately describes a transformer for the purposes of studying its time domain response and monitoring its condition in service.

Transformer failures are usually accompanied by the generation of new modes and the disappearance of old modes. Existing mode shapes and natural frequencies are also subject to dramatic changes. This variation of model structure makes it difficult to correlate winding deformations to the elements of a transformer equivalent circuit.

Mathematical models are sufficient for a study of the transient response of a transformer and for monitoring its condition in service. The development of an analytical model could be the first step towards deriving a transformer equivalent circuit to match the frequency response of the model. The traditional second or third order transformer equivalent circuits do not capture the dynamics of realistic power transformers. The combination of finite element methods with the subspace-based identification algorithms may produce accurate transformer equivalent circuits from frequency response data.

Reference [134] presents work on using frequency domain data to identify the transformer equivalent circuit. Transformers were defined as high, medium and low frequency models. The Matlab program was used for the calculation. However, the data set was small and more

investigation needs to be done in this field. The proposed method could have the benefits of being quick, relatively simple, and easily implemented for effective, non-intrusive transformer condition monitoring.

High frequency models based on the node-to-node impedance function (NIF) model were used in [135,136] to study radio frequency electromagnetic interference in converter stations and to predict transformer transient response.

The system identification method uses the external characteristics of the transformer to simulate the transformer equivalent circuit, similar to a black box model approach. It is not suitable for this study. This type of transformer model aims to fit the external characteristics of a transformer but not the internal physical arrangement. To be able to relate external characteristics of the transformer to the internal physical changes in the transformer, the model used must be based on the transformer's physical characteristics.

## 2.7 Signal Processing Methods Used in Transformer Testing and Diagnostics

The following methods of signal analysis have been used in transformer high voltage testing and condition monitoring:

- Fourier transform or fast Fourier transform analysis (FT/FFT)
- Short-time Fourier transform analysis (STFT)
- Wavelet transform analysis (WT)

These mathematical techniques play an important role in detection of transformer winding problems such as partial discharge and winding movement.

### 2.7.1 Fourier Transform (FT)

The Fourier transform is a frequency domain analysis that mainly deals with stationary signals. The basic equation is as follows:

$$X(f) = \int_{-\infty}^{+\infty} x(t) e^{-2j\pi ft} dt \qquad (2.4)$$

The analysis coefficients X (f) define the notion of global frequency in a signal. As shown in Equation 2.4, they are computed as inner products of the signal with sine wave basis functions of infinite duration. As a result, Fourier analysis works well if x(t) is composed of a few stationary components. Any abrupt change in time in a non-stationary signal x(t) is spread out over the whole frequency axis in X(f). Therefore, an analysis adapted to non-stationary signals requires more than the Fourier transform.

Fourier transform analysis has been widely used in signal analysis, including high voltage impulse testing, to detect winding failure. It is independent of the input waveform and characterizes the winding condition. Fourier transforms have also been used in recent years in "before and after" analysis of transformer short circuit tests to detect winding movement. It has gradually been used more in transformer condition monitoring in the field to detect transformer winding looseness and winding faults.

### 2.7.2 Short-time Fourier Transform (STFT)

If a signal is not narrow-band, the instantaneous frequency averages different spectral components in time. To become accurate in time, therefore, a two-dimensional time-frequency representation S(t, f) of the signal x(t) is needed to compose spectral characteristics depending on time, the local frequency f being defined through an appropriate definition of S(t, f).

Consider a signal x(t), and assume it is stationary when seen through a window g(t) of limited extent, centred at time location $\tau$. The Fourier transform equation of the windowed signals $x(t)g^*(t-\tau)$ yields the Short-time Fourier transform (STFT)

$$STFT(\tau, f) = \int x(t) g^*(t-\tau) e^{-2j\pi ft} dt \qquad (2.5)$$

which maps the signal into a two-dimensional function in a time-frequency plane ($\tau$, f).

The parameter f in Equation 2.5 is similar to the Fourier frequency. Many properties of the Fourier transform carry over to the STFT. The analysis depends critically on the choice of the window g(t).

The STFT windows with a finite length of the signal result in poor frequency resolution. Only a band of the frequencies are used, but not the exact frequency components existing in the signal. When a wider window is used, it can improve frequency resolution. However, according to the uncertainty principle (Heisenberg inequality), given by the relation,

$$\text{Time-Bandwidth product} = \Delta t \, \Delta f \geq 1/4\pi$$

the signal results in poor time resolution. The time-frequency plane cannot give both accurate time and frequency resolution. This indicates that a narrow window results in a spectrum with good time resolution and poor frequency resolution, while a wider window results in a spectrum with poor time resolution and good frequency resolution.

### 2.7.3 Wavelet Transform Analysis (WT)

A Wavelet is described as a "little" wave, in the sense of being of short duration with finite energy which integrates to zero; hence its suitability for transients.

A Fourier series requires periodicity of all the time functions involved, which effectively means that the basis functions used in Fourier analysis are precisely located in frequency but exist for all time. The frequency information of a signal calculated by the classical Fourier transform is an average over the entire time duration of the signal. If there is a local transient signal over some small interval of time in the lifetime of the signal, the transient will contribute to the FT but its location on the time axis will be lost. Traditional Fourier analysis does not consider frequencies that evolve with time (i.e., non-stationary signals).

One technique that overcomes these problems to a certain extent is the windowed FT (STFT). However, the drawback is STFT's fixed window width, which does not provide the requisite good resolution in both time and frequency that is an important characteristic for analyzing transient signals comprising both high and low frequency components. A wide window gives

good frequency resolution but poor time resolution, whereas a narrow window gives good time resolution but poor frequency resolution. A windowed-FT approach could be applied with a sequence of windows of different widths to get more detail on transient location, but this option is unwieldy and time consuming.

Wavelet analysis overcomes the limitations of the Fourier methods by employing analyzing functions that are local both in time and frequency. Wavelet transform (WT) is well suited to wideband signals that are not periodic and may contain both sinusoidal and impulse components, as is typical of fast power system transients. In particular, the ability of wavelets to focus on short-time intervals for high-frequency components improves the analysis of signals with localized impulses and oscillations, which particularly adapts to give the appropriate resolution.

WT is a transform with variable window length. It is used for non-stationary signals. The basic idea of wavelets is that of analyzing a signal according to scale. WT decomposes a signal from the time domain to a time-scale domain. These different levels of resolution use a set of basis functions that are obtained from a single prototype function $\psi(t)$, known as the "mother wavelet". From the decomposed signals, it is possible to recover the original time domain signal without losing any information. A wavelet has to be thought of as a function located at a position *b* and having a scale *a*. By performing scaling and translation operations on the mother wavelet $\psi(t)$, a family of continuous wavelet functions is created and can be denoted, where *a*, $b \in \Re$ ($a \neq 0$) are the scaling and translation parameters, respectively.

$$\Psi_{a,b}(t) = \frac{1}{\sqrt{|a|}} \Psi\left(\frac{t-b}{a}\right) \qquad (2.6)$$

As the value of *b* changes, the location of the wavelet moves along the horizontal axis, allowing any events to be represented in time or space. When *a* changes, the shape of the wavelet changes in scale, making the steps in time smaller. These narrower and smaller steps allow representation of greater detail of higher resolution [137].

The continuous-time wavelet transform is defined in Equation 2.7. As can be seen, the wavelet transform is a function of two variables.

$$CWT(a,b) = \frac{1}{\sqrt{a}} \int_{-x}^{\infty} x(t)\, g\left(\frac{t-b}{a}\right) \quad dt \qquad (2.7)$$

The discrete wavelet transform (DWT) is defined in Equation 2.8.

$$DWT(m,k) = \frac{1}{\sqrt{a_0^m}} \sum x(n)\, g\left(\frac{k - nb_0 a_0^m}{a_0^m}\right) \qquad (2.8)$$

Wavelet transforms can be used as a de-noising technique for many applications. WT is also used in non-stationary signal analysis such as transient analysis. Examples of wavelet transform applications for transformer monitoring include analysis of partial discharge data and transformer impulse test data [138-140].

## CHAPTER III WINDING MOVEMENT DETECTION AND EXISTING PROBLEMS

### 3.1 Power Transformer Winding Movement Detection and Diagnostic Methods

This chapter discusses the methods commonly used to detect winding movement and their effectiveness in field testing of transformers. As mentioned in earlier chapters, transformer windings are subjected to dynamic mechanical forces induced by load and short-circuit currents in service. These forces can reach levels as high as 100 $N/mm^2$ [141-142] when the transformer is subjected to a short circuit. The short circuit forces can be up to 1600 times as great as the normal load forces. To prevent the winding from moving, the transformer is designed with a system of mechanical clamps. The transformer windings are normally pre-stressed in the factory by this clamping system. Two basic types of winding are used in power transformers, core form windings and shell form windings. They are shown in Figures 3.1 and 3.2.

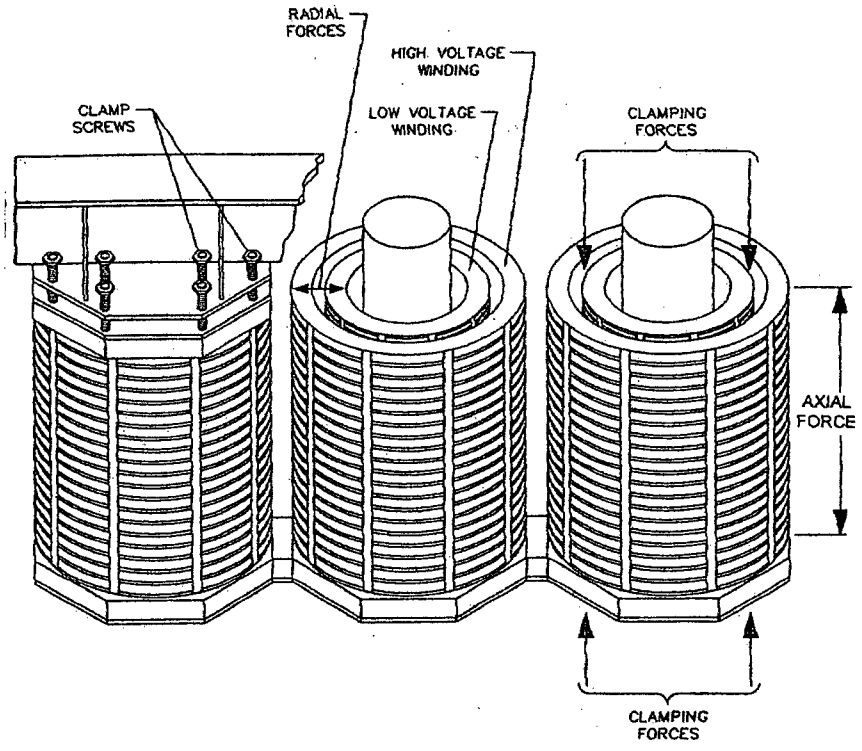


Figure 3.1 – Core form transformer winding

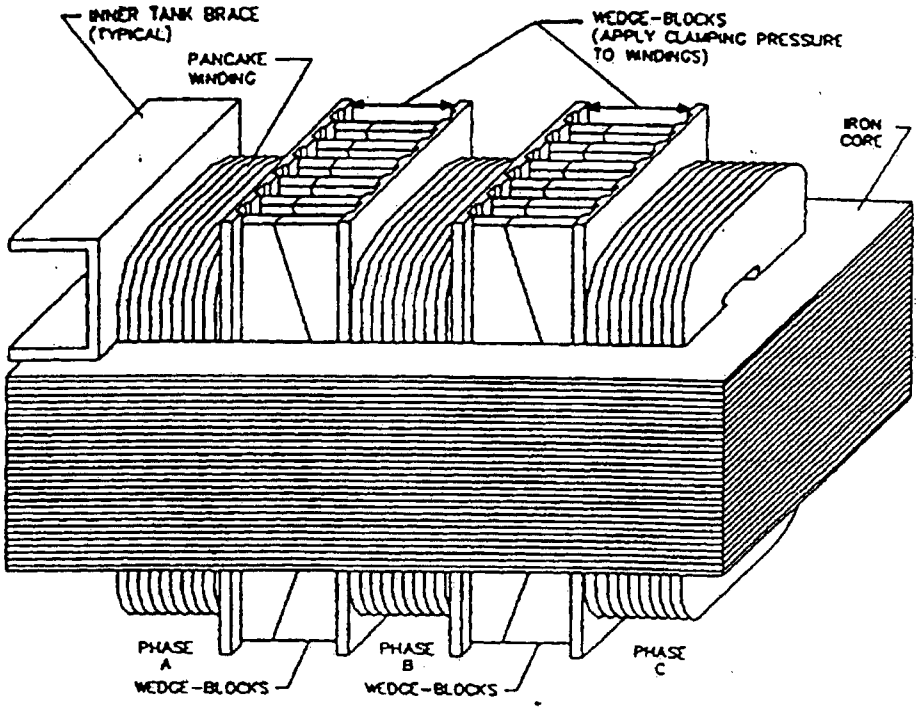


Figure 3.2 – Shell form transformer winding

The core form design has the winding essentially outside the core, while the shell form design has the winding essentially inside the core. The core form transformer winding is mechanically weaker, under short circuit conditions, than the shell form winding. Since the core is outside the winding in the shell form design, it helps contain the short circuit forces. This is not the case with the core form design. Despite the mechanical advantages of the shell form winding, the core form design is used in most power transformers. This is mainly due to the fact that the core form design is much easier and therefore cheaper to manufacture. It is also easier to locate problems with the core form transformer since more of the winding is accessible, and it is easier to re-clamp a core form winding by inserting additional wedges over a larger circumference of the winding.

The winding column is stressed by the clamping system and can resist the dynamic force induced by short circuit currents in service. However, the continuous action of the clamping force may cause permanent deformation of the paper insulation. This leads to a reduction of the clamping force or, in extreme cases, to a complete loss of clamping pressure. If clamping pressure is lost, the winding becomes prone to bulging or displacement, caused by the

unavoidable short circuit currents. Winding displacement can also occur under normal operating conditions. When moved, the brittle, aged paper insulation can be crushed and its dielectric strength reduced. This is considered to be an incipient fault, since the next overvoltage can initiate a breakdown and lead to the destruction of the transformer.

Transformer windings may also loosen when the transformer is dried after oil processing, or over years of service and mechanical vibration. Many large power transformers in North American utility systems have been in service longer than their design life. These transformers are still functioning, but their cellulose insulation has aged and lost its elasticity. As the transformer inventory ages the risk of failure, due to loss of clamping pressure, increases.

The winding leads are also clamped to prevent their movement under short circuit forces. This clamping is subject to loosening over time, which increases the risk of them moving under short circuit forces.

Some utilities try to control winding displacement by periodical internal inspections of the transformer and tightening of the clamps. However, if the aged paper has lost some of its spring-back ability, the clamping force will decrease in a few months rather than a few years. Even a moderate short circuit current can then deform the winding. Early detection of these displacements is essential to ensure reliable operation of aged, large and expensive transformers.

When transformer windings, the winding clamping structure, or the clamping structure for the leads has problems, the possible degradation can be summarized as follows:

- Radial distortion of conductors
- Axial deformation of conductors
- Twisting of conductors
- Breaking of clamping supports

The possible faults and defects that these failures can lead to are:

- Shorted turns
- Combustible gas production
- Change in impedance
- Change in excitation current
- Change in capacitance

Various test methods have been used to detect these problems, with varying degrees of success:

Radial distortion, axial deformation, twisting of conductor

- Visual inspection – This is the most effective method of detecting winding movement and loss of clamping pressure. The oil is drained from the transformer and personnel enter the transformer to perform an inspection. The drawback is the high cost of the long outage (as much as five weeks) and the cost of doing the inspection.
- Leakage reactance percentage impedance – This test measures the transformer impedance at 60 Hz. It will detect winding problems only if they are severe, and is therefore not very effective.
- Oil screen, dissolved gas analysis – Analysis of the transformer oil cannot directly detect the problem. It sometimes will detect the effects of winding problems such as partial discharges.
- Capacitance – The capacitance of the winding is measured at low frequency. If there is winding movement, the capacitance will change. The problem with this test is that it is not sensitive enough. It requires a large change for it to be detectable.
- Frequency response analysis (FRA) - The FRA measures the transadmittance of the transformer. It is the most effective technique presently available that does not require opening the transformer.

Damage to conductor clamping support

- Visual inspection
- Winding resistance
- Dissolved gas analysis
- Acoustic partial discharge detection
- Frequency response analysis (FRA)

## 3.2 Low Voltage Impulse Test and Frequency Response Analysis Test Principles

In the past, direct detection of winding movement could only be done by carrying out a visual inspection or by the analog low voltage impulse (LVI) test. Before digital recording techniques were used in the measuring system, the LVI method was only successfully used in laboratory tests for detection of winding movement before and after short circuit tests. Attempts were made to do the LVI test in the field but the results were not reproducible, as the input waveform could not be reproduced identically over extended periods of time.

With the advent of digital techniques, it is possible to obtain the transfer function of the transformer based on measurement of the input and output signals. This produces a unique signature that does not depend on the input waveform.

### 3.2.1 Low Voltage Impulse Test Method

The low voltage impulse test method (LVI) of winding movement detection is based on applying a low voltage pulse into one winding of a transformer and measuring the response current or voltage from another winding. Lech and Tyminski [109] proposed this winding displacement detection method in the 1960s. A low voltage square pulse was applied to the examined winding terminal and the response was recorded with an analog scope. A change in the winding geometry causes changes in the oscillation pattern, and a deformation or displacement of a coil can be detected by comparison of the response oscillograms recorded before and after the short circuit.

Initially, this method was used during short circuit tests of power transformers in a high power laboratory. As the method was recognized as an effective diagnostic tool, its use was extended

to the diagnosis of large power transformers in service. The transformers were inspected at regular time intervals, and at each inspection the response records were taken and examined for any changes since the previous oscillograms.

Analog oscillograms were used to collect the data when the test was first used. As digital recorders became available, they were used instead. However, the limited resolution of the early designs of digital recorders did not permit more advanced signal processing [81].

Figure 3.3 shows a typical LVI measurement circuit (high voltage winding neutral current measurement) and Figure 3.4 shows typical measured test results.

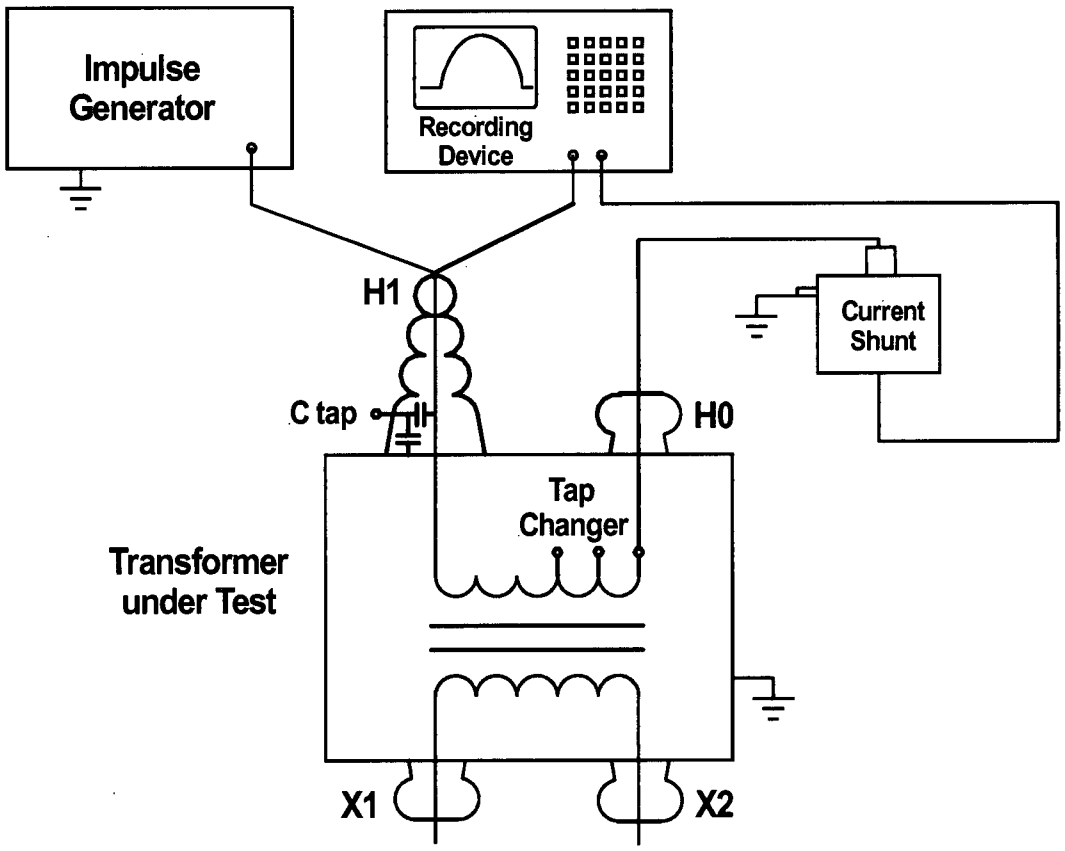


Figure 3.3 – LVI measurement circuit

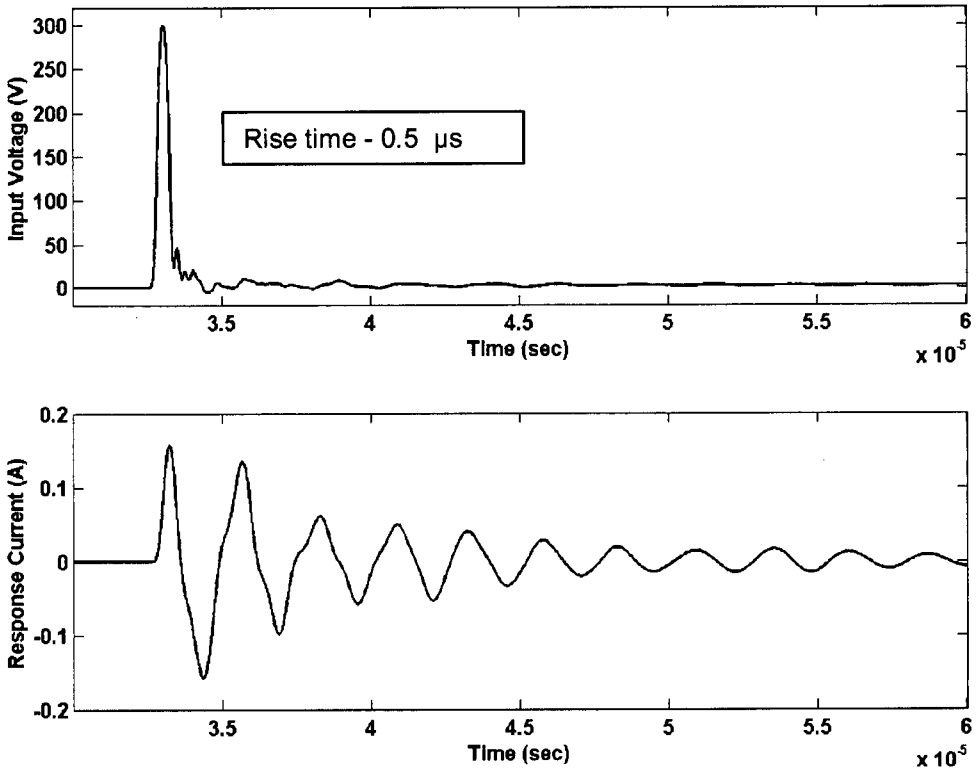


Figure 3.4 – LVI measurement results

By overlaying the oscillograms of the response (output) waveforms and comparing the two waveforms taken at different times on the same transformer, the internal condition of the transformer as related to winding movement or deformation can be determined.

The problem with this test method is that small changes in the input waveform can cause a large change in the response signal. The input waveform that the signal generator applies to the transformer can change in the generator (aging of components, changes in temperature of the instrument, etc) or because of a change in the loading of the transformer caused by movement in the winding. The change in the output signal caused by this change in the input signal is comparable to the change caused by winding movement. This made it difficult or impossible to reliably determine if the changes in the response signal were due to changes in the transformer or due to the input signal changes caused by the signal generator. This is not a problem during short circuit testing of transformers, since the initial reference test (before the short circuit test) and the comparison test (after the short circuit test) are both done within a few hours, or at most a few days. Changes in the source waveform are not expected in such a short

time period. Tests on in-service transformers, however, are typically done, at most, once a year. Small changes in the signal generator's output are very likely over these longer time periods.

Figure 3.5 shows the effect of a small change in the input voltage signal. The change in the response current is significant. Figure 3.6 shows the calculated percent difference.

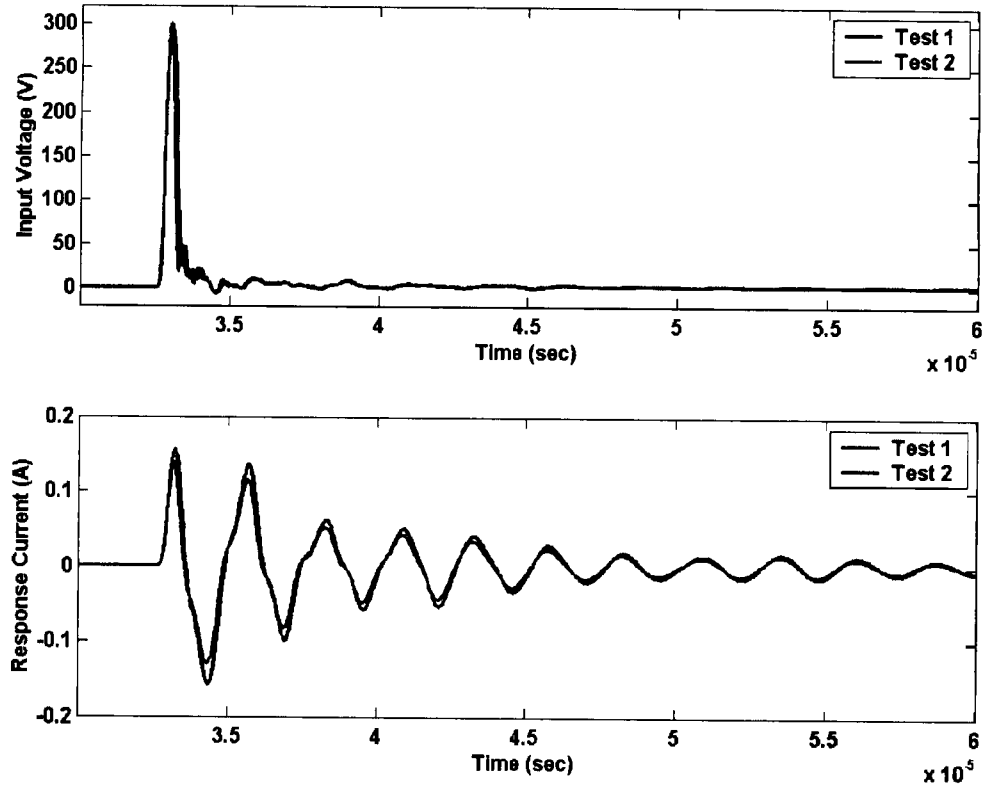


Figure 3.5 – Effect of input voltage change on response

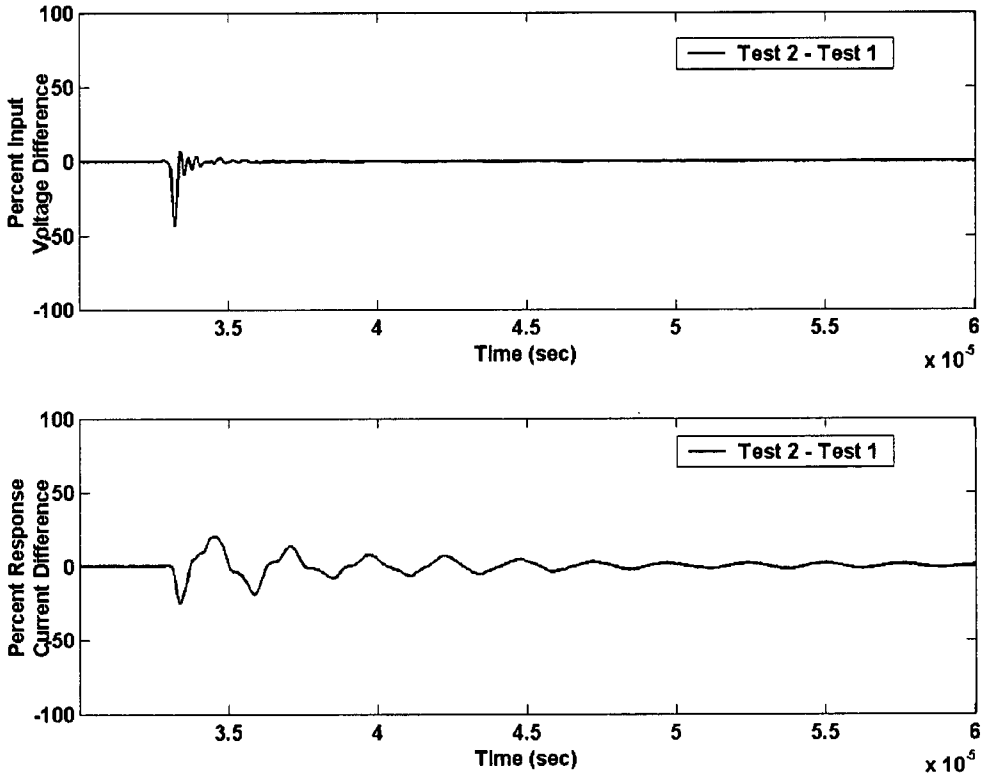


Figure 3.6 – Input voltage change differences

### 3.2.2 FRA Test Method

In the late 1980s and early 1990s, digital signal processing techniques made it possible to eliminate the problems with the LVI technique caused by changes in the input waveform. Instead of comparing the output waveforms, a Fourier transform is done on the input and output signals. The transformer is considered as a linear network. The magnitude of the transfer function is used as the transformer signature. This is described in Equation 3.1.

$$|TF(f)| = \left| \frac{Output(f)}{Input(f)} \right| \qquad (3.1)$$

This quotient (transfer function) represents the winding transadmittance signature of the transformer. The transadmittance eliminates the effect of changes in the input signal. The test is repeated over time, or on identical transformers, and the transfer functions are compared to

detect winding movement [75]. The phase angle of the transadmittance is also measured, but is not commonly used in the analysis since industry experience shows that the phase angle data do not provide useful additional information for interpreting the amount of winding movement. The assumption that the transformer is a linear network is very important; otherwise the transfer function (signature) would be dependent on the shape and magnitude of the input signal. Experimental results show that this is valid assumption.

This refined LVI method is commonly called the frequency response analysis test (FRA). Any method that puts sufficient energy to obtain usable signals at the required frequencies can be used to do this test. For example, white noise could be used as the signal source. In practice, however, two FRA methods are commonly used by the power industry. One uses a voltage impulse as the input signal (FRA (I)) and the other uses a swept frequency source (FRA (S)). The test is typically done with a maximum frequency range of 1 MHz to 3 MHz. The equipment used for the FRA (S) method will record data up to 10 MHz, but in practice the higher frequencies cause complications and cannot be used. For example, the higher the frequency of measurement, the more impact that the changes in the placement of the test lead have on the test result. The FRA (I) method has an advantage in that it has the potential to be done on-line, which is not possible with the swept frequency method. Due to the potential ability of the FRA (I) method to be used on-line and thus reduce the test costs, this research work focused mainly on the FRA (I) method.

Figure 3.7 shows a typical FRA (I) test result. The FRA (I) test results are typically plotted with a linear scale on the Y-axis, while the FRA (S) test results are typically plotted with a log scale on the Y-axis. The log scale is generally used on the FRA (S) test method because it is the normal display mode of the test equipment used for the test. The FRA (I) plots can easily be converted to a log scale; the choice of the type of scale used is based on individual preferences.

Figure 3.8 shows the effect of a small change in the input voltage on the signals. It is apparent that even though the response current changes, the transadmittance does not. Figure 3.9 shows the calculated percent difference. The change in the response current is significant, but there is no measurable difference in the transadmittance.

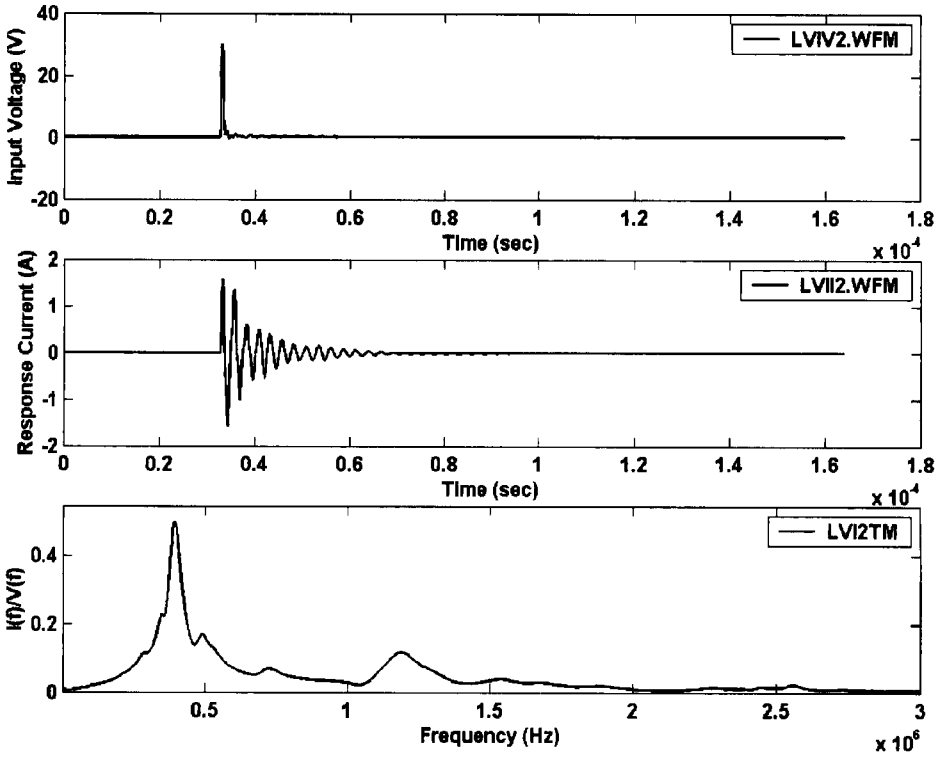


Figure 3.7 – FRA (I) measurement results

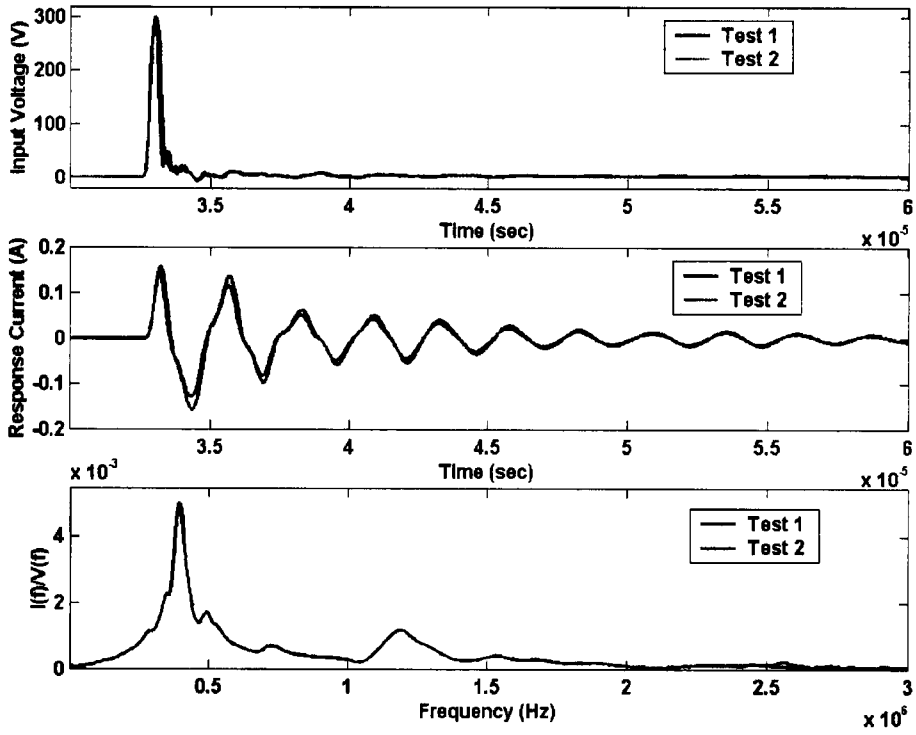


Figure 3.8 – Effect of input voltage change on transadmittance

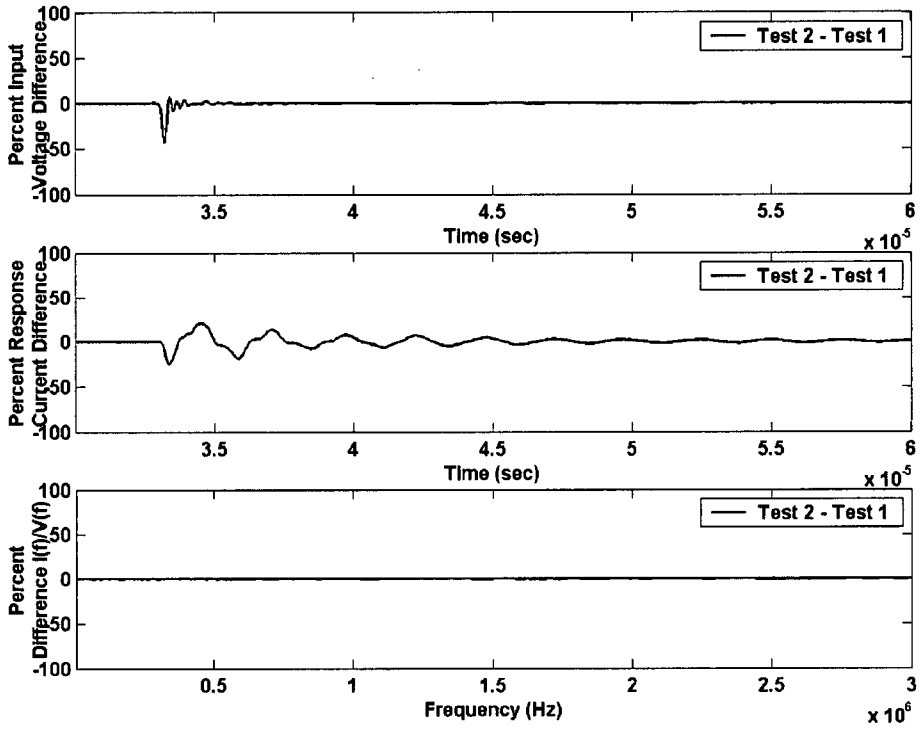


Figure 3.9 – Input voltage change differences

Much attention has been given to the FRA test in recent literature. Sensitivity, repeatability, digital data storage and freedom from the configuration of the external wiring are all being studied. The winding transadmittance or transfer function when plotted against frequency is a series of resonant frequency poles that constitute the unique winding signature. There are some publications that present methods to give criteria for analysis of the FRA test results [143]. However, few references present fault location techniques, which would give information on the location of the damage to the transformer. At present, interpretation of the results is generally done by experienced personnel using a visual comparison of the results to determine the condition of the transformer. These experts evaluate the degree of change in the magnitude and frequency shifts of the transfer function to determine if the changes are severe enough to warrant an internal inspection of the transformer. The complex nature of transformer windings has prevented direct correlation of changes in FRA test results to specific changes in the transformer.

Short circuit forces that result in the axial displacement of concentric windings will reduce the distributed inter-winding capacitance [110], because the effective overlapping surface area of

the windings is reduced. The distributed capacitance between the inner winding and core, and the outer winding and tank, may of course also change. The net effect of this displacement will influence winding response.

Winding looseness (i.e., loss of clamping) gives rise to an overall change in the axial dimensions of a winding. These changes can be directly "viewed" by the FRA test. By definition, winding looseness implies that the winding is either free to move axially or has axially moved. The changes to the axial dimensions alter the inter-turn separations and equate directly to changes in the inter-turn capacitance. This alters the centre frequency of resonant modes on the winding.

When a transformer is manufactured, the windings are compressed using a hydraulic press and a fairly even distribution of axial movement is achieved on each winding. Test results show two significant features:

1. The centre frequency of resonant modes reduces with reducing axial length. This is consistent with an increase in series capacitance due to a reduction in inter-turn separation, and is consistent with field experience with the FRA test.
2. The frequency shift is experienced over a wide frequency range, with the amount of shift being approximately the same at all frequencies. This is consistent with the well-distributed nature of the displacement.

It is desirable to be able to model the transformer tested, in order to relate changes in the FRA test results to the internal condition of the transformer. If a sufficiently detailed model could be developed for the transformer being tested, it would not be necessary to have an initial reference signature. The problem is that the transformer is very difficult to model with sufficient accuracy over a large frequency range. There are many models that have been developed for transformers, but they are mainly designed for power system studies and they do not model the inside details of the transformer. There are low frequency models available for the windings, but they are not valid for the frequency ranges used for the FRA test. As well, a different model would be required for each transformer and each FRA measurement, since each transformer and test set-up is unique. The length of test leads, the circuit layouts, and other factors affect the test measurement results. The best way to detect winding movement is to have a reference signature for comparison when doing the FRA test analysis.

## 3.3 Other Methods to Detect Winding Movement

The FRA test is not the only diagnostic test that is designed solely to detect winding movement indirectly. Some research work has been done on using acoustic vibration methods to detect winding movement [144]. However, the acoustic vibration technique has not been as effective as the FRA test in the diagnosis of transformer internal condition. It can only be used to provide reference information [111].

The principle of the detection of winding displacement by vibration is to monitor the vibrations picked up by acoustic sensors, usually, accelerometers mounted on the tank wall. Changes in the vibration pattern should be indicative of changes to the winding. In the work done in [111] it was found that the vibration signals measured did not contain any significant energy above about 2500 Hz. The results showed that as the winding became loose there tended to be an increase in the energy content at higher frequencies (500 Hz to 2500 Hz). However, changes in the vibration signatures did not correlate to winding changes as well as in the FRA test. The vibration data were found to be a useful tool to rank transformers for further testing by other methods such as the FRA test, but it was not a good test for determining if a transformer should be opened.

Japanese researchers [145] undertook a study to measure the coupling vibration of power transformers under short circuit conditions. The results indicated that the vibration of the windings increases when the variation of electromagnetic force caused by the movement of the windings is taken into account. The non-linearity of winding stiffness and internal damping reduce the increase in winding vibration. The researchers also plotted the power frequency impedance change vs. winding displacement (a 10 cm axial displacement caused approximately a 0.3% change in impedance). This curve indicates that the transformer power frequency impedance is insensitive to the transformer winding displacement.

Another method for detecting winding movement was studied by South African researchers [144]. In this method, a hydraulically coupled system is installed between the transformer winding and the core clamp structure, and hydraulic fluid is transmitted to a remote receiver transducer. The core is displaced by the hydraulic forces acting upon it, giving an output signal that is a function of the forces on the piston. The forces themselves are a function of the

position of the actuator in the transmit cylinder; hence, the dc output signal is a function of piston displacement. When this method was experimented with in a reactor winding, the equivalent of 1.7 mm winding shrinkage was detected in the clamping system. The drawback to this method is that it requires the installation of additional equipment on the transformer. It also may not be able to detect winding movement caused by short circuit forces.

Hydro Quebec has taken an interesting approach [25-27], involving the measurement of stray load loss across a range of frequencies. The technique, referred to as *frequency response of stray losses* (FRSL), is based on the observation that axial winding displacement causes an increase in stray losses. For the FRSL test, the transformer is short circuited on the secondary and the primary winding is supplied with low voltage at frequencies in the range of 20Hz to 400 Hz. The technique is considered to be sensitive down to an axial displacement of the order equivalent to winding separation, although it is considered to be insensitive to radial displacement. This method is far less sensitive than the FRA test since it uses a much lower frequency.

A group of Russian researchers has assessed the effect of compression strength and deformation of transformer windings on transformer electromagnetic and mechanical frequency characteristics. In particular, this group has developed a procedure for the disassembly-free assessment of winding compression residual strength [146]. When the de-energized transformer, with disconnected buses, is loaded by a mechanical pulse, changes that occur in the electrical voltage that characterizes free damped mechanical vibrations of the core elements are registered on the transformer lead-ins. The winding compression strength is assessed on the basis of certain regularities in the voltage spectral composition changes. This procedure allows detection, in some cases, of unfixed elements of the design inside a transformer (e.g., magnetic shunts on tank walls). The procedure was tested on more than 50 transformers. Satisfactory coincidence was observed between diagnosed compression strengths and actual compression strengths.

Unlike the FRA test, where it is now possible to purchase purpose-built commercial equipment, none of these alternative methods is in widespread use.

## 3.4 Restatement of the Research Objectives

The FRA test method is the only tool that has been proven effective for the detection of a serious and potentially costly problem in transformers. The test circuit parameters and their effects on the measurements have been studied in this research work by doing laboratory tests, field tests and model studies, using a simplified model. The issues studied include:

- A comparison of the two commonly used methods, FRA (I) and FRA (S),
- The effect of the external measurement leads and the high voltage bushing
- The effect of the measuring shunt impedance
- The best measurement frequency range
- The relationship of the measurement frequency range to the amount of winding movement
- The criteria for ranking winding movement
- Whether the test can be done on-line to eliminate the need for an outage
- The best way to process the data
- The feasibility of relating FRA measurements on a transformer to any specific physical changes in the internal winding structure

In this research work, the goal is to gain a better understanding of the FRA test and to improve the test method. The issues are discussed in the following chapters.

# CHAPTER IV EXPERIMENTAL WORK ON FRA METHODS

The FRA (I) method is based on applying a low voltage pulse to a transformer winding and measuring the output to obtain the transfer function. The FRA (I) test method is effective, but in practice many factors affect the measurement results. By investigating and clarifying these factors, the interpretation of test data and evaluation of transformer condition will be improved. This chapter describes the experimental work carried out and the results.

## 4.1 FRA (I) Test Procedure

The FRA test and the test circuit have been described in general in Section 3.2. For the FRA tests done in this work, a recurrent surge generator (RSG) was used to generate the voltage impulse. This generator generates pulses at the rate of 30 pulses/second. The typical pulse has a pulse width of 2 μs at a peak voltage of 300 V. The rise time of the impulse can vary from about 0.2 μs to 1 μs, depending on the transformer being tested. In most cases, the rise time was about 0.5 μs. A 12.5 Ω shunt was used (except as noted), terminated by 50 Ω at the oscilloscope. Figure 4.1 shows the typical test circuit, with a detailed circuit of the impulse voltage source and the transformer winding connections. The components of the RSG are adjustable. They are set to obtain a voltage pulse with the fastest possible rise time to maximize the high frequency content. The voltage input into the transformer is measured with a high frequency oscilloscope probe and the current is measured with a high frequency coaxial current shunt equipped with non-inductive resistors. The signals are recorded with a digital oscilloscope at a sampling rate of 50 MHz (unless otherwise noted).

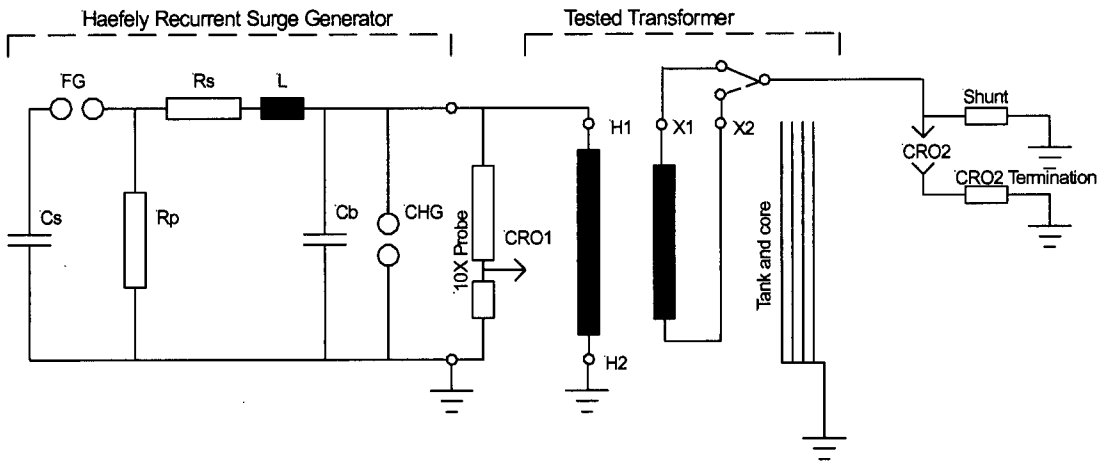


FG –generator firing gap

CHG - chopping gap ("ON" position)

CR01 – oscilloscope channel 1 - applied voltage measurement

CR02 – oscilloscope channel 2 - transferred current measurement

CRO2 – oscilloscope channel 2 termination – 50 Ω

Shunt – 12.5 Ω

Cs – 47 nF, Rp – 15 kΩ, Rs –3.3 Ω, L – 10 μH, Cb – 3.3 nF

Figure 4.1 – FRA test circuit

In order to repeat the measurements under the same conditions, data on the test leads and the exact circuit used for each test must be recorded. This is necessary as the impedance of the leads is significant compared to the transformer impedance. If different leads or a different circuit arrangement is used, the resultant signature will be different. Tests were done with all the equipment on top of the transformer to minimize the length of the leads required (minimum impedance). All the instrumentation used was calibrated at regular intervals to ensure the accuracy of the measurements. The typical circuit details are given in Figure 4.2.

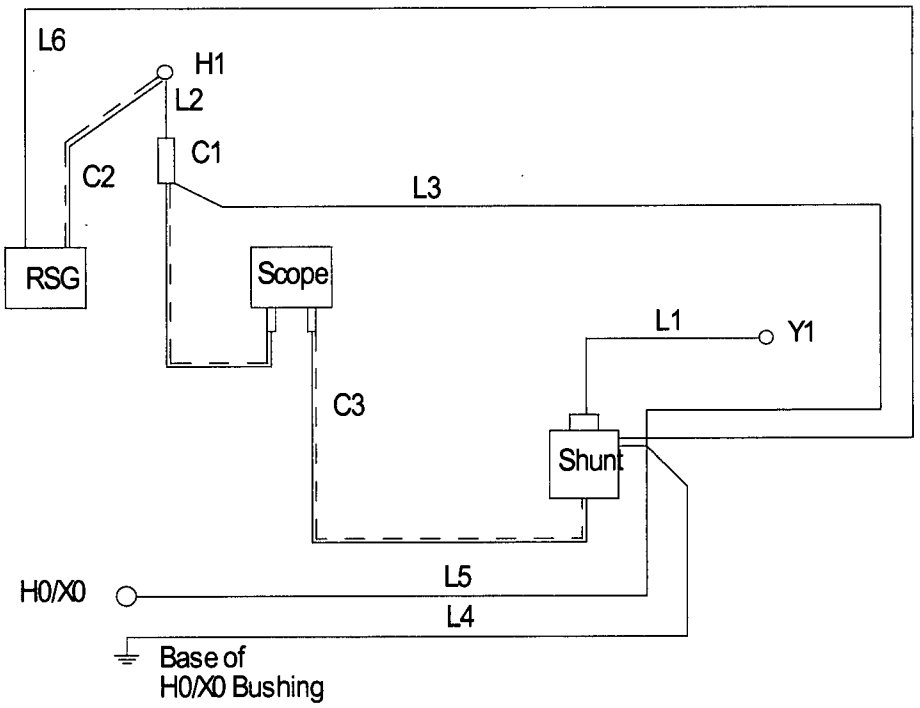


L1 - speaker wire size #10, twin, 6 meter

L2 - speaker wire size #10, twin, 2.5 meter

L3 - speaker wire size #10, twin, 5.5 meter

L4 - size #2, single, 2.5 meter

L5 - size #2, single, 2.5 meter

L6 - speaker wire size #10, twin, 3.21 meter

C1 - 10X probe, Tektronix Type P6150; 13 pF, 10 MS, 3.0 meter

C2 - RG58 C/U, 6 meter

C3 - RG58 C/U, 2.11 meter - terminated by 50 Ω

Current shunt - R=12.5 Ω

Figure 4.2 – Typical circuit and test leads description

The oscilloscope used for the testing had an eight-bit vertical resolution. To make valid measurements with the FRA test, the vertical resolution should be at least 12 bits [38]. To improve the vertical resolution, multiple pulses were averaged. The increase in vertical resolution is determined by the following equation:

$$\text{Pulses Averaged} = 2^{X} \text{ where } X = \text{additional bits resolution} \quad (4.1)$$

By averaging 256 pulses, the resolution increases from 8 bits to 16 bits. In this work, a minimum of 250 pulses were averaged. The additional bits resolution is:

$$\text{Additional Bits Resolution} = \text{Log(pulses averaged)/Log(2)} \qquad (4.2)$$

Averaging the signal has the additional benefit of filtering out random noise that may be present in the substation.

## 4.2 FRA (I) Measurements in the Field

Off-line FRA measurements were performed on a wide variety of in-service power transformers throughout Canada and the United States. After making arrangements for outages on large transformers and traveling to the sites, data were collected on different transformer types and conditions. Often planned outages were delayed or cancelled at the last minute due to changes in system conditions. Figures 4.3 and 4.4 show typical examples of transformers that were tested. Figures 4.5 and 4.6 show the construction of transformer windings.

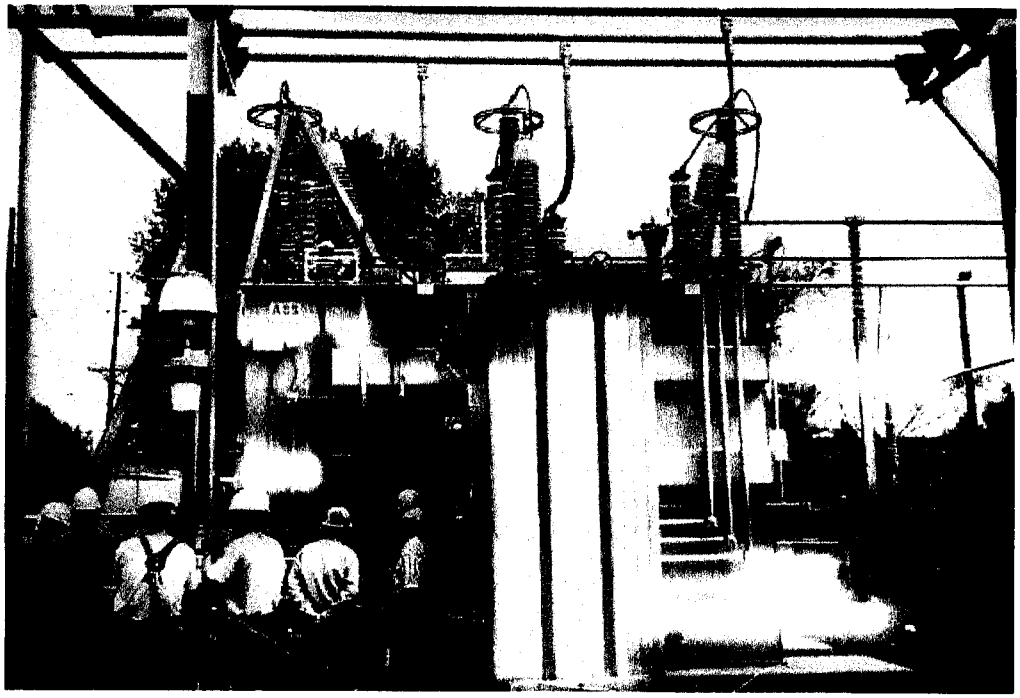

Figure 4.3 – Three-phase, 138 KV transformer

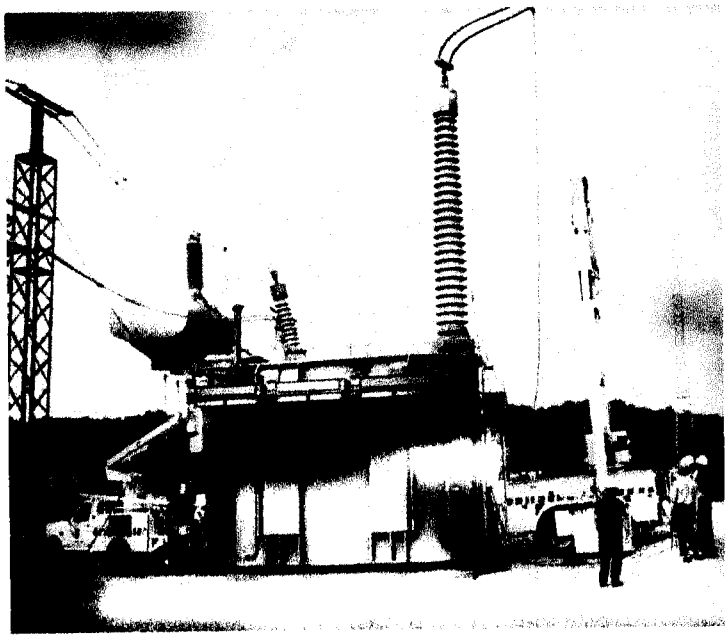

a) Single phase, 765 kV Transformer

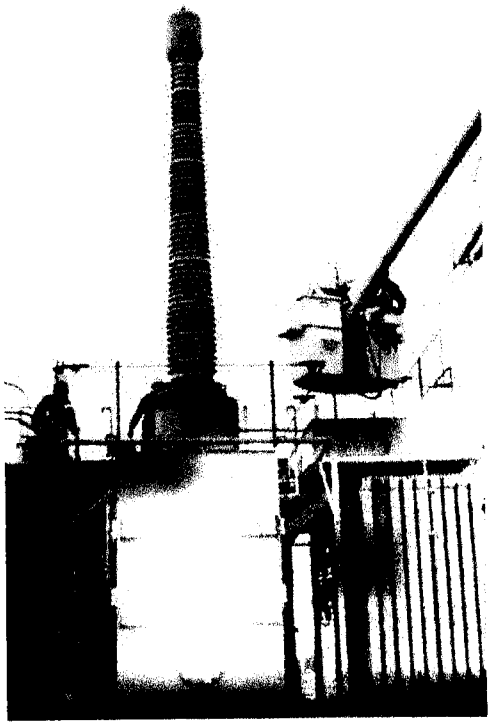

b) Single Phase, 500 kV Transformer

Figure 4.4 – Single phase Transformers

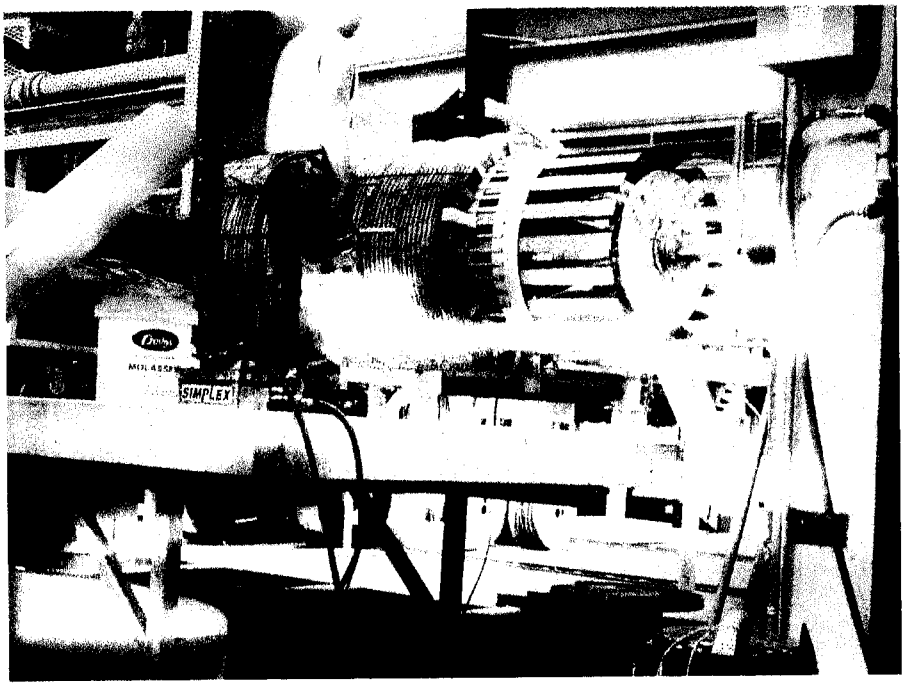


Figure 4.5 – 500 kV transformer winding under construction

a) Winding coil being compressed before assembly

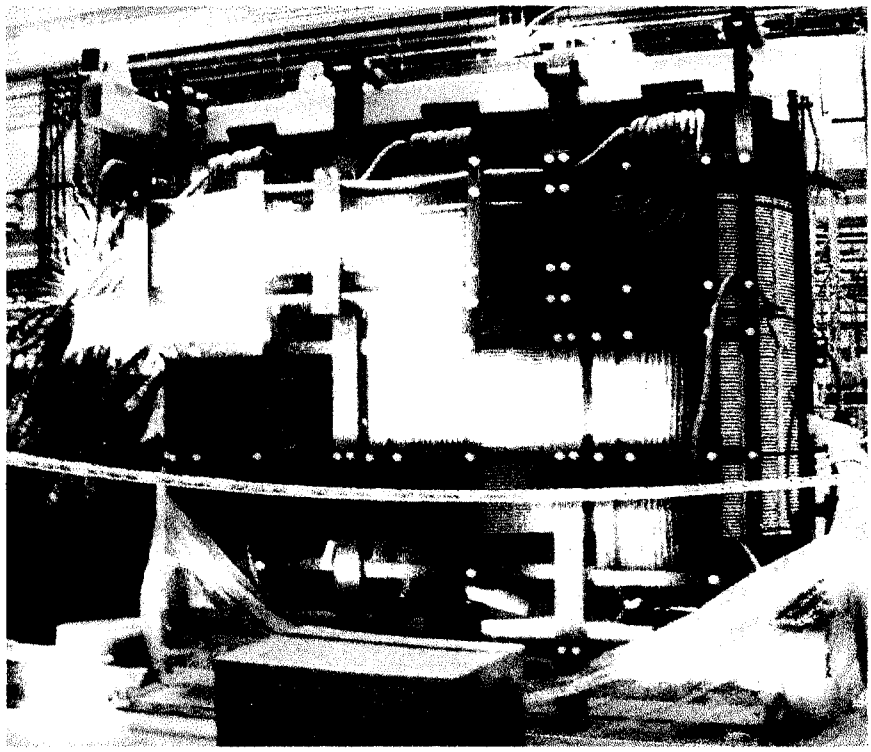

b) Complete 3-phase winding

Figure 4.6 – 500 kV, 3-phase transformer windings before tanking

In order for engineers to interpret such data and to predict the condition of the transformer windings, the effect of measurements under different test configurations and conditions must be understood. In this section measurement results using the FRA (I) method under different conditions are presented. Eight different cases are described, looking at the effects of the following parameters:

| | |
|---|---|
| Case 1: | Transformer tap changer position |
| Case 2: | Phase tested on a three-phase transformer |
| Case 3: | Transformers of identical design |
| Cases 4, 5: | Repeatability of the test over time |
| Case 6: | Transformers of different designs |
| Case 7: | Loose winding clamping vs. tight winding clamping |
| Case 8: | Effect of removing oil from the transformer |

In all eight cases, the FRA (I) measurement (I(f)/V(f)) was derived from the Fourier transform of the measured current (I(f)), divided by the Fourier transform of the measured input voltage applied to the transformer high voltage winding (V(f)). The current measured was either the high voltage winding current or the coupled current in a second winding. Figure 4.7 shows the circuit for Case 1 and Cases 3-6, Figure 4.8 shows the circuit for Case 2, and Figure 4.9 shows the circuit for Cases 7 and 8.

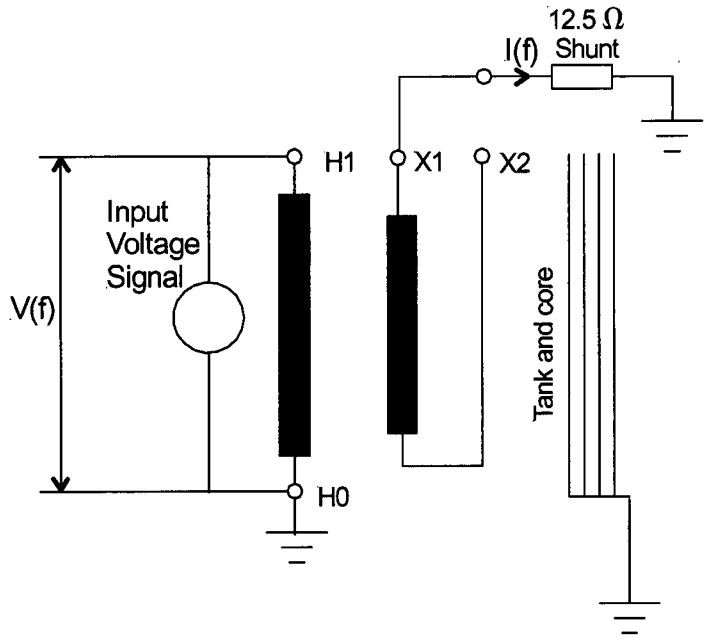


Figure 4.7 – Single phase test circuit – current measured on secondary winding

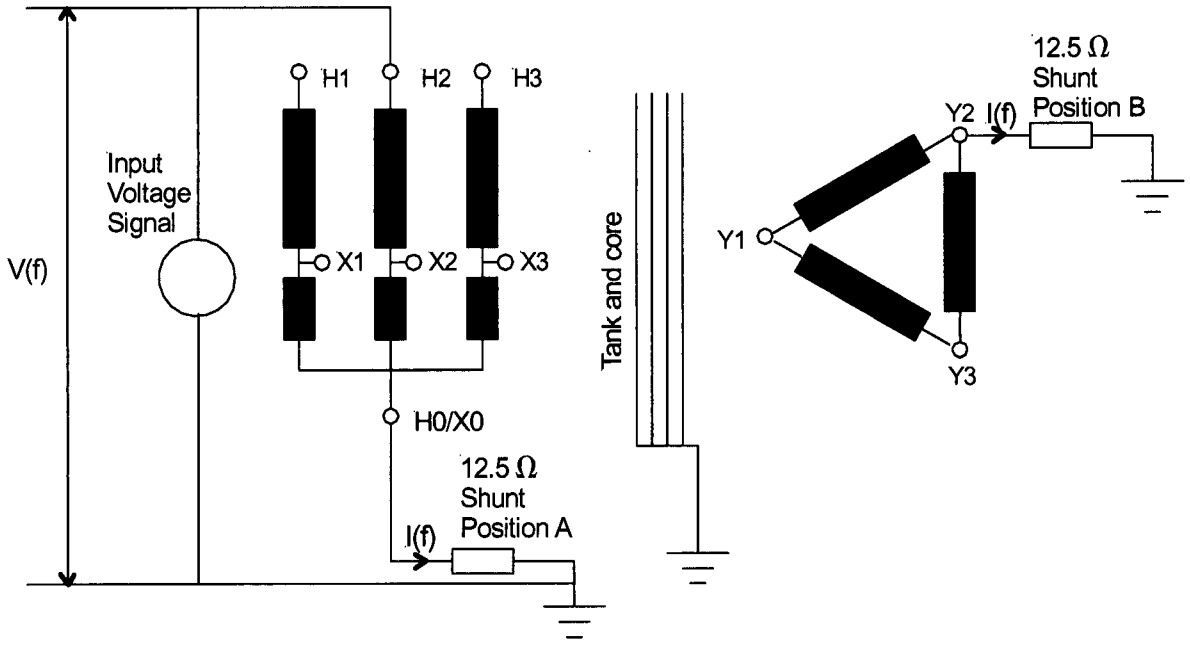


Figure 4.8 – Three phase test circuit – current measured on neutral (postion A) or tertiary (position B)

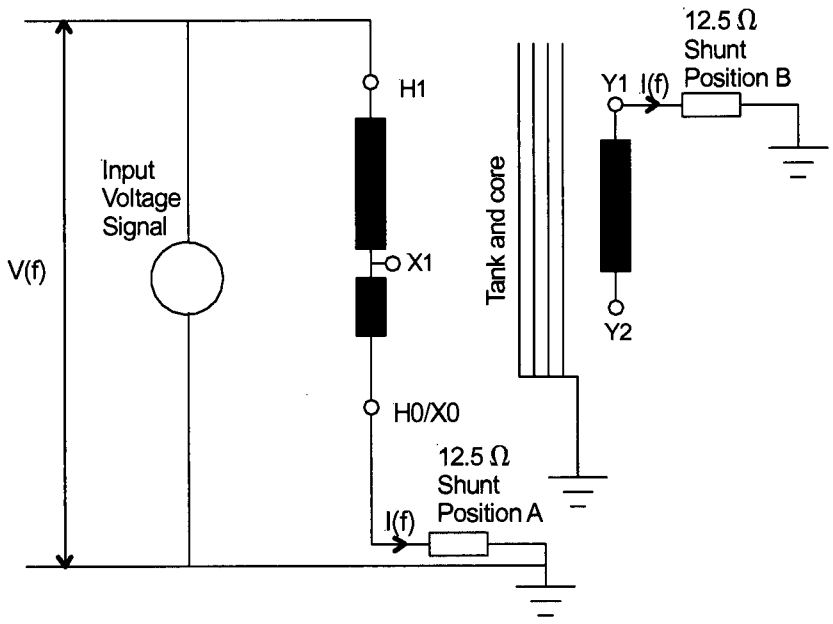


Figure 4.9 – Single phase test circuit – current measured on neutral (postion A) or tertiary (position B)

**Case 1: Effect of Tap Changer Position**

The transformer ratings were as follows:

| | |
|---|---|
| Phase: | Single phase |
| Voltage: | 236 kV (HV winding) – 111 kV (LV winding) |
| Power rating: | 50 MVA |
| Type: | Core form, two windings |

FRA (I) measurements were done at tap position 1 (260 kV) and tap position 23 (210 kV), between the high voltage to low voltage windings. Figure 4.10 compares the measurements, showing that the FRA results are affected by the tap position. The amount of change depends on the transformer winding design and type, and the location of the tap changers.

When a different transformer tap changer position is used in the FRA test, the total effective turns of winding involved in the test circuit are different and the winding parameters (such as inductance and capacitance) change. This causes a change in the FRA signature. The change is significant and may be falsely interpreted as winding movement. Therefore, in order to compare two FRA results, the transformer tap must be in the same position for both tests.

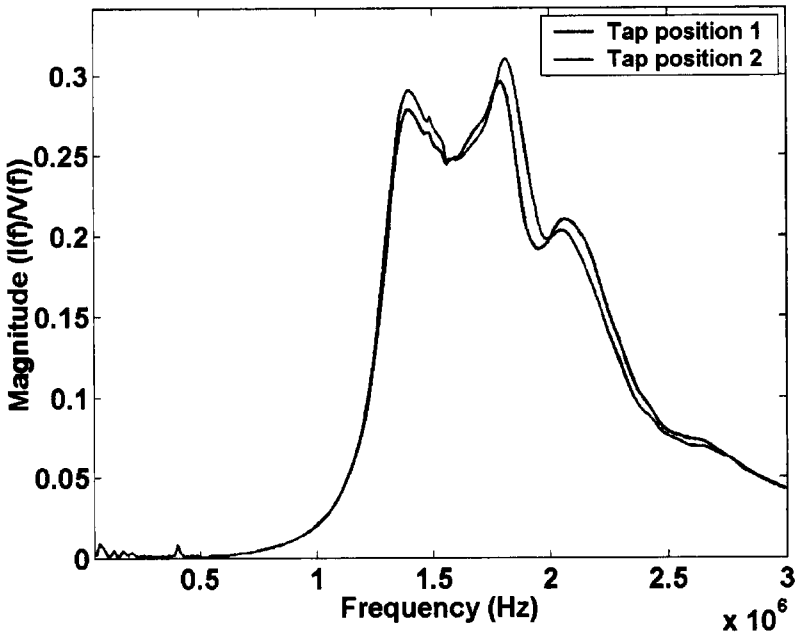


Figure 4.10 – Single phase two winding transformer measurement at different tap positions

**Case 2: Effect of FRA Measurements on Different Phases**

The transformer ratings were as follow:

| | |
|---|---|
| Phase: | Three-phase |
| Voltage: | 330 kV (HV winding) – 138 kV (LV winding) |
| Power rating: | 300 MVA |
| Type: | Core form auto transformer with tertiary |

Instead of comparing FRA test results over time, it has been suggested that they could be compared on different phases of a transformer. Comparison was therefore done for all three phases. The FRA measurements were made both on the high voltage winding-to-neutral and from one winding to another. Figure 4.11 shows the measurement between the high voltage input and the neutral terminal. Figure 4.12 shows the measurement between the high voltage and the tertiary windings. The measurement results show that a three-phase power transformer can have different FRA results from phase to phase. The differences can be very large, indicating that it is not valid to compare phases to detect movement.

The windings of different phases of a transformer are located in different physical positions in the transformer, and the leads to the bushings and the tap changer can be of different lengths. These differences result in different phase-to-ground and phase-to-phase impedances and lead impedances in series with the windings.

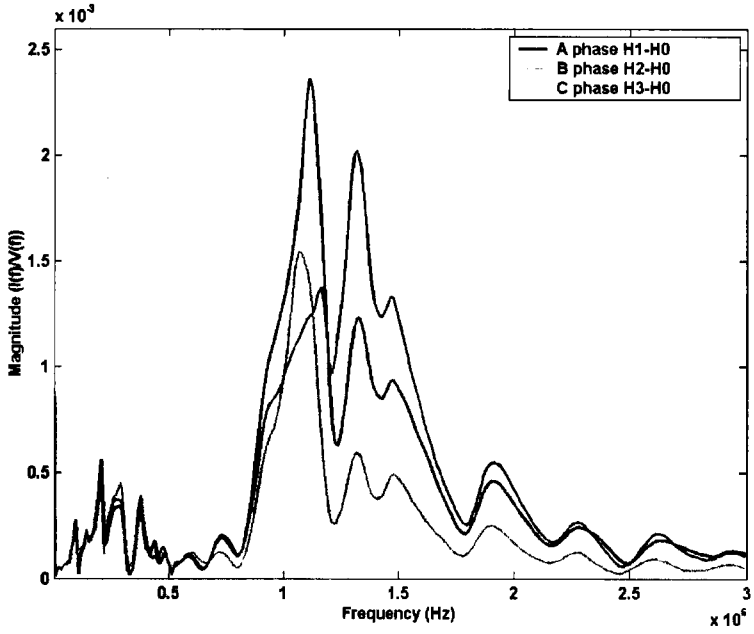


Figure 4.11 – Three-phase transformer FRA (I) measurement on each phase (high voltage terminal to neutral terminal)

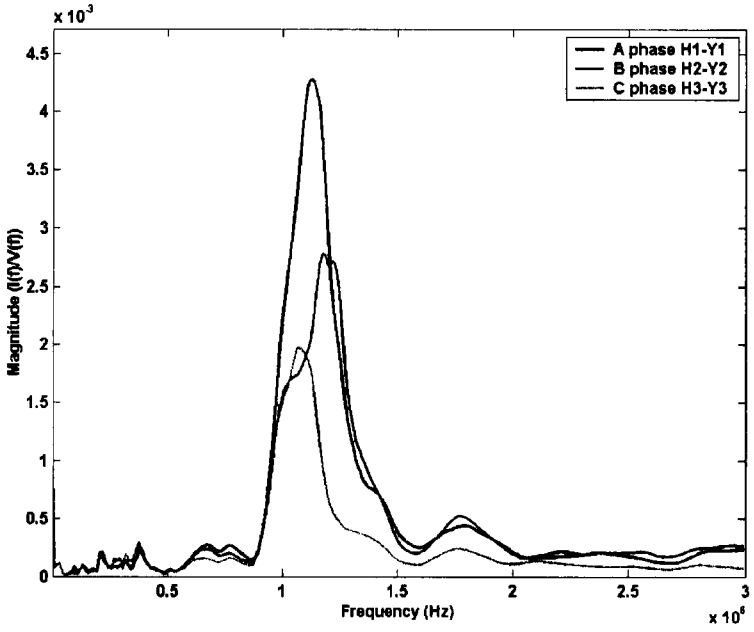


Figure 4.12 - Three-phase transformer FRA (I) overlay (high voltage to tertiary winding)

**Case 3: Effect of FRA Measurements on Two Transformers of Identical Design**

Transformer ratings were as follows:

| | |
|---|---|
| Phase: | Single phase |
| Voltage: | 137.4 kV (HV winding) – 16 kV (LV winding) |
| Power rating: | 15 MVA |
| Type: | Core form, two windings |

Figures 4.13 and 4.14 show the FRA (I) measurements done on two transformers of the same design. Transformer B was manufactured nine years after Transformer A. The results show a remarkable similarity between the two transformers in spite of the difference in their age, indicating that it is valid to compare transformers of the same design. The manufacturing tolerances, even over a period of nine years, were such that there was no significant difference in the FRA (I) results.

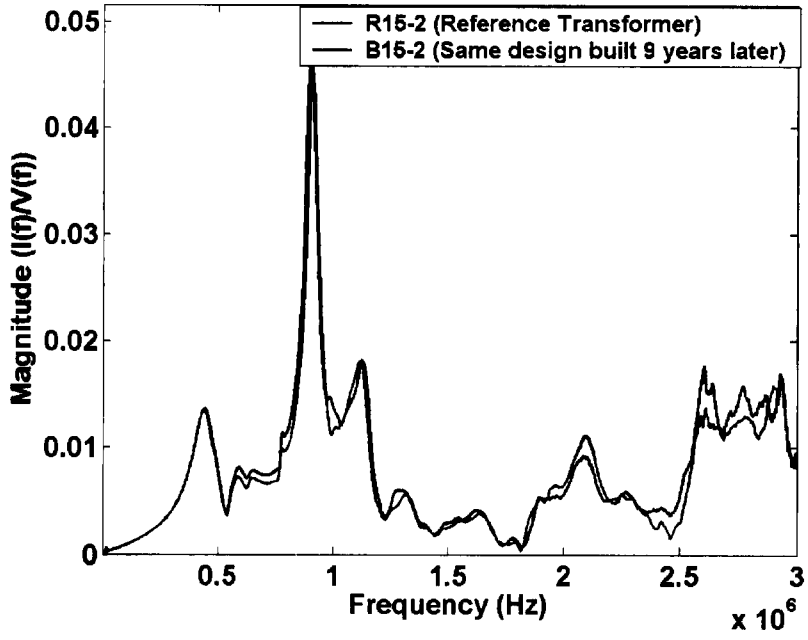


Figure 4.13 - Comparison of two transformers with the same design (overlaid)

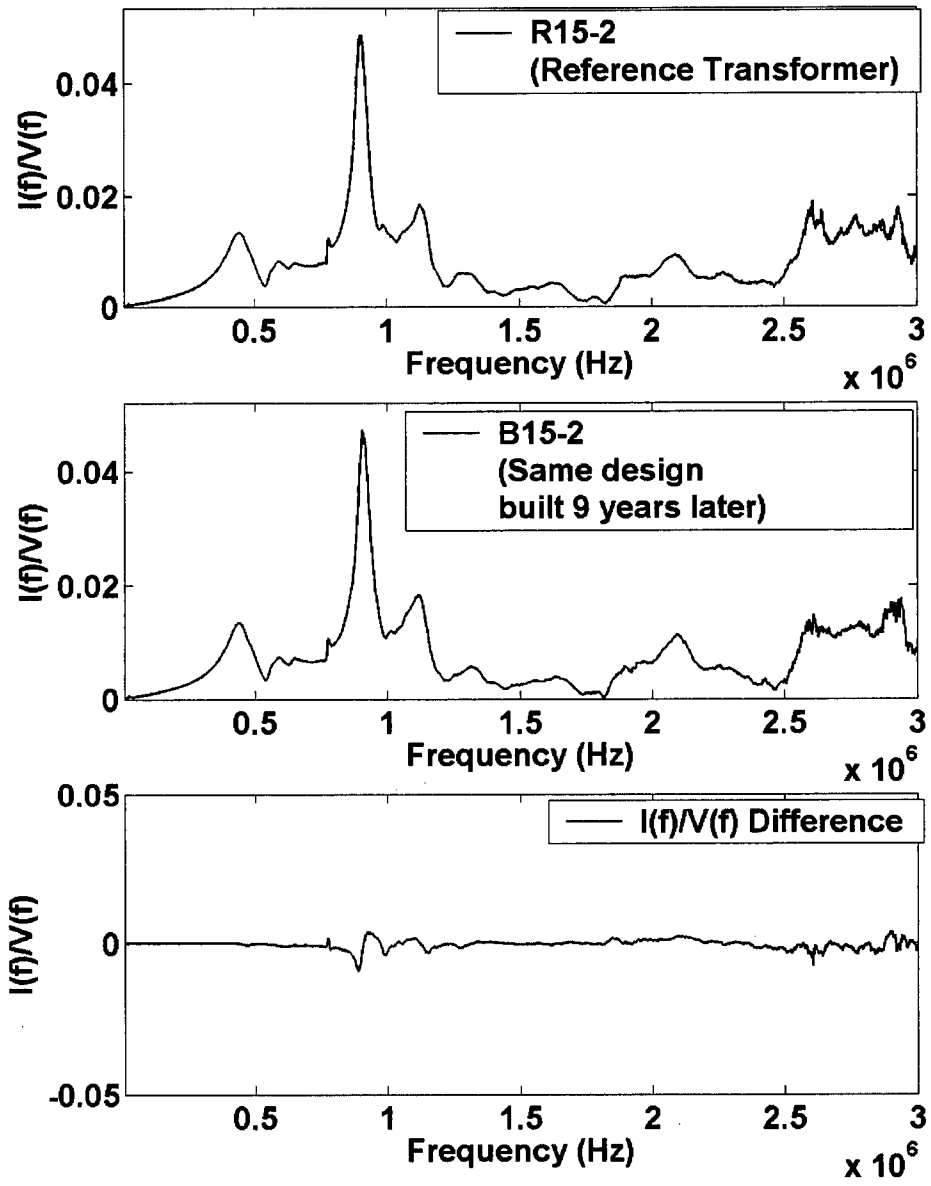


Figure 4.14 - Comparison of two transformers with the same design (difference)

**Case 4: Effect of FRA Measurements on a Transformer Over Time (no change in the transformer)**

The transformer ratings were as follows:

Phase: Single phase
Voltage: 137.4 kV (HV winding) – 16 kV (LV winding)
Power rating: 15 MVA
Type: Core form, two windings

Figures 4.15 and 4.16 show two FRA (I) measurements done on the same transformer one year apart. All other measurement factors remained the same. This transformer was not subjected to any severe duty during this year, and was considered to have remained in good condition over its service life. If the FRA is to be used to detect movement in a transformer over the life of a transformer, which can be 30 years or more, it must be possible to repeat the FRA at extended intervals with the confidence that changes in the results are due to transformer changes and not due to test equipment variation/changes. Figures 4.12 and 4.13 show that over the one year in service between tests on this transformer there was no significant change in the FRA (I) results. The test is repeatable over time, and if there is no change in the transformer the test result will be the same.

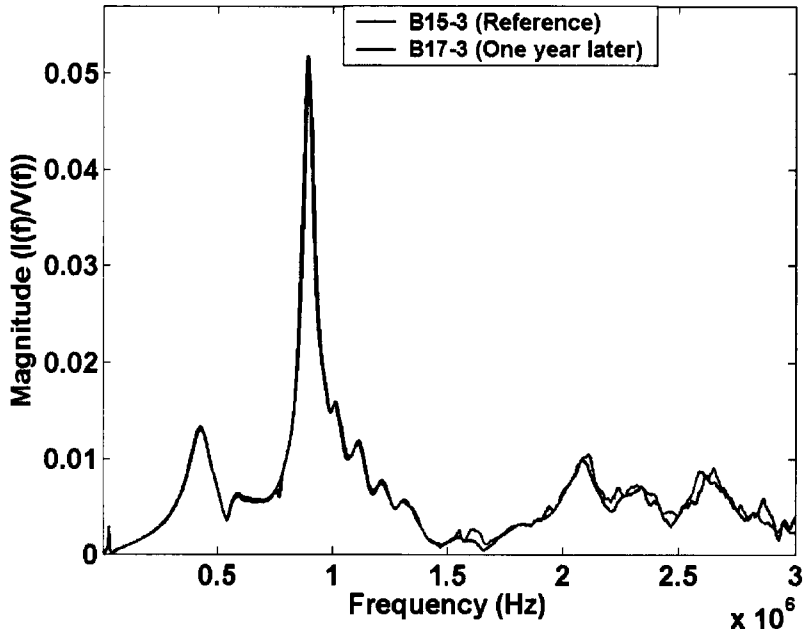


Figure 4.15 - FRA (I) measurements one year apart (transfer function overlaid)

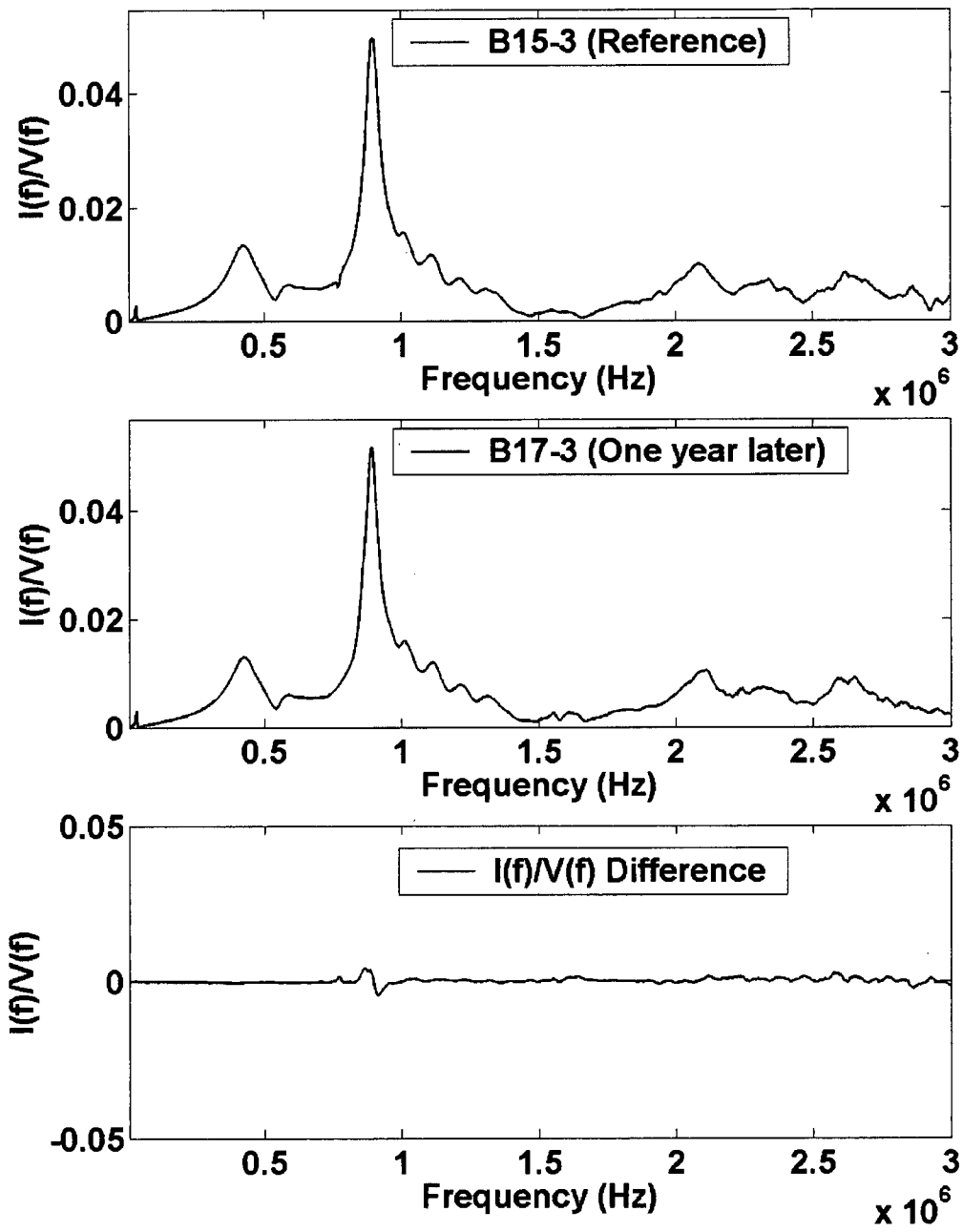


Figure 4.16 – Comparison between the reference test and a test one year later

**Case 5: Effect of FRA Measurements on a Transformer Over Time (some change in the transformer)**

The transformer ratings were as follows:

| | |
|---|---|
| Phase: | Single phase |
| Voltage: | 137.4 kV (HV winding) – 16 kV (LV winding) |
| Power rating: | 15 MVA |
| Type: | Core form, two windings |

Figures 4.17 and 4.18 show two FRA (I) measurements done on a transformer one year apart. The results show some changes. This was consistent with the duty on the transformer, which had been subjected to severe operating conditions over the one-year period that could have caused some winding movement.

Cases 4 and 5 demonstrate the ability of the FRA test to be used over time and retain the ability to detect winding movement.

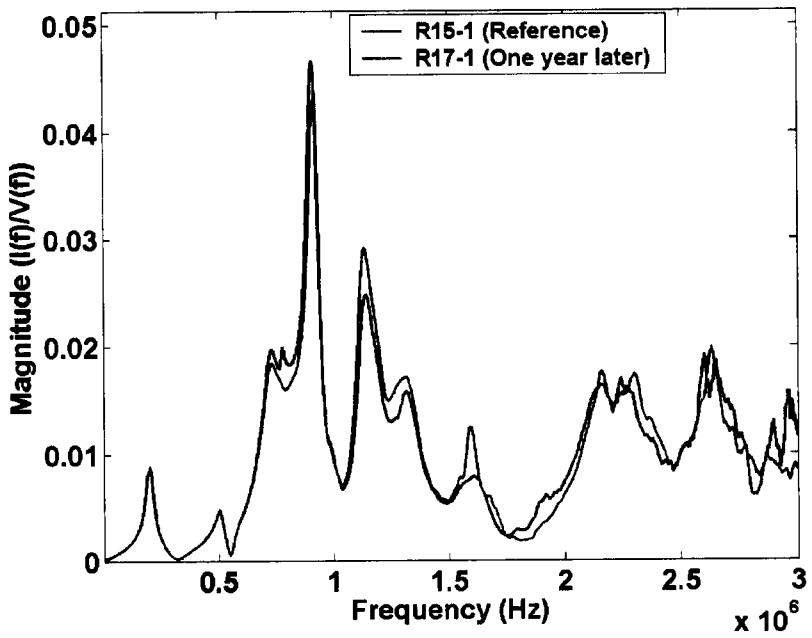


Figure 4.17 - FRA (I) Measurements one year apart (transfer function overlaid)

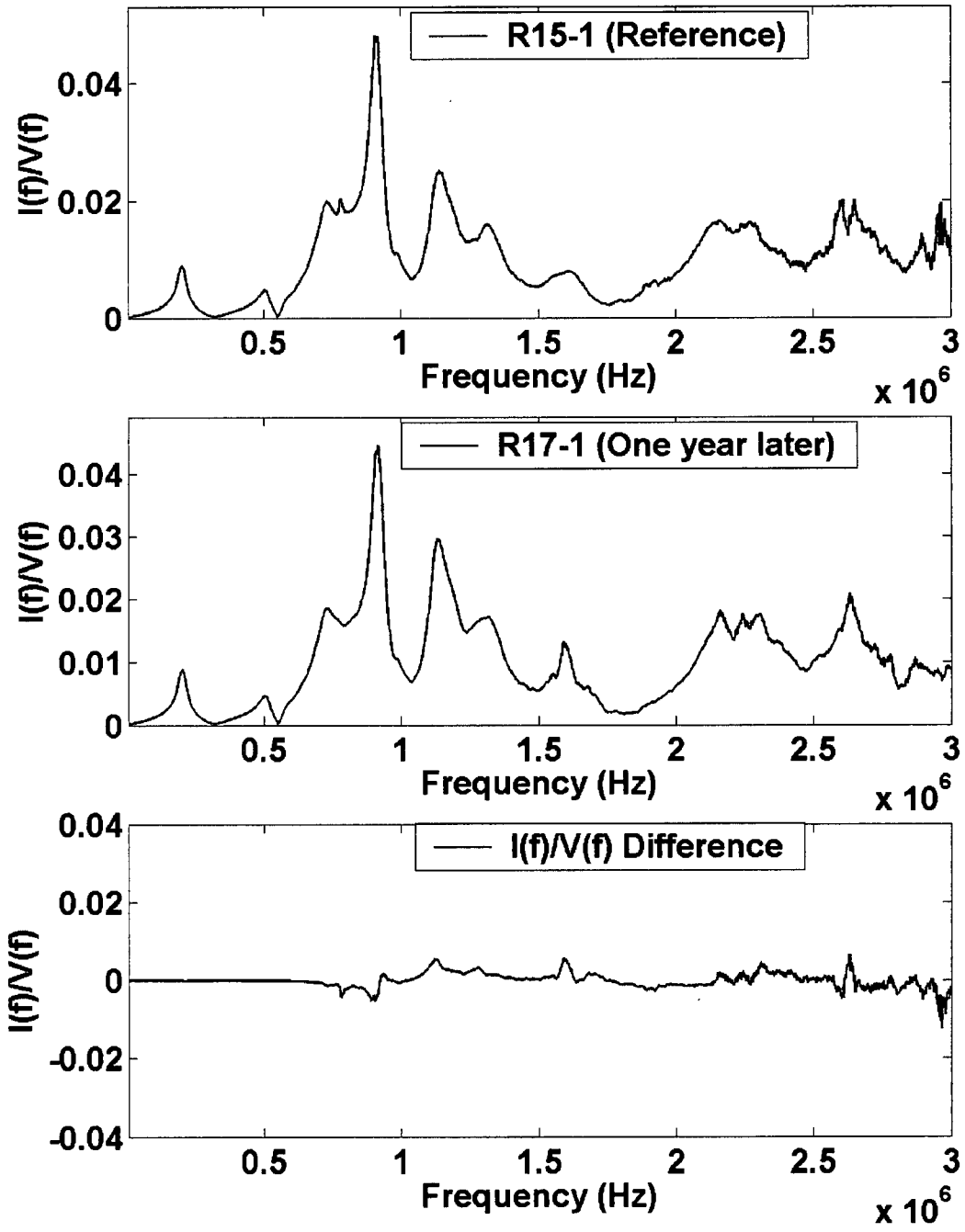


Figure 4.18 – Comparison between the reference test and a test one year later

**Case 6: Effect of FRA Measurements on Transformers of Different Designs**

The transformer ratings were as follows:

| | |
|---|---|
| Phase: | Single phase |
| Voltage: | 137.4 kV (HV winding) – 16 kV (LV winding) |
| Power rating: | 15 MVA |
| Type: | Core form, two windings |

Figures 4.19 and 4.20 show the results of FRA (I) tests on two transformers with identical ratings (MVA, kV, number of taps, etc.), but with a different internal design. The measurements were done between the high voltage and low voltage windings. One transformer is used as A - phase and the other as B - phase in a three-phase bank. The figures show that the transformers have very different FRA results when the design is different, even if they have the same rating. The internal winding geometry of transformer designs vary, even if they have the same rating. This means that the winding capacitance and inductance are not identical and will give different transfer functions (signatures). This case study demonstrates that it is not possible to do a comparison between transformers of the same rating if they are not of the same design.

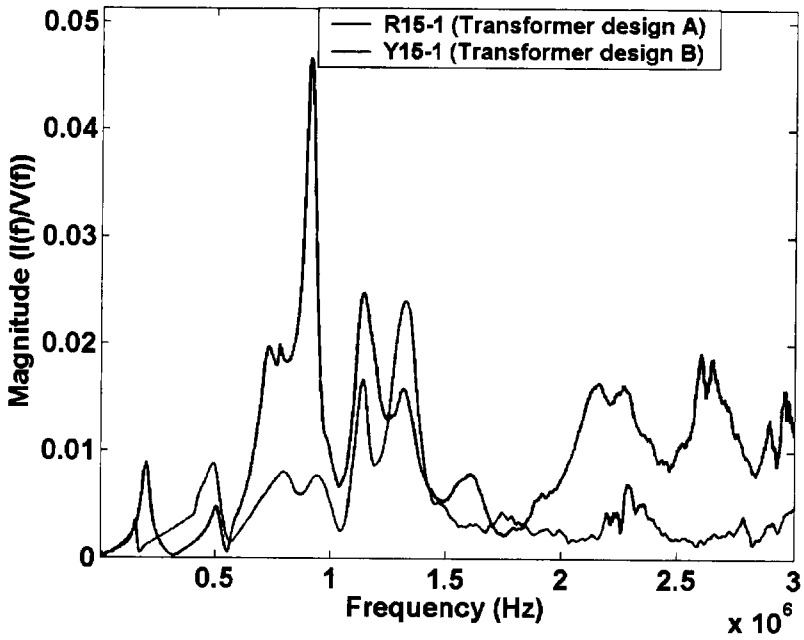


Figure 4.19 – Comparison of two transformers with different internal design (overlaid)

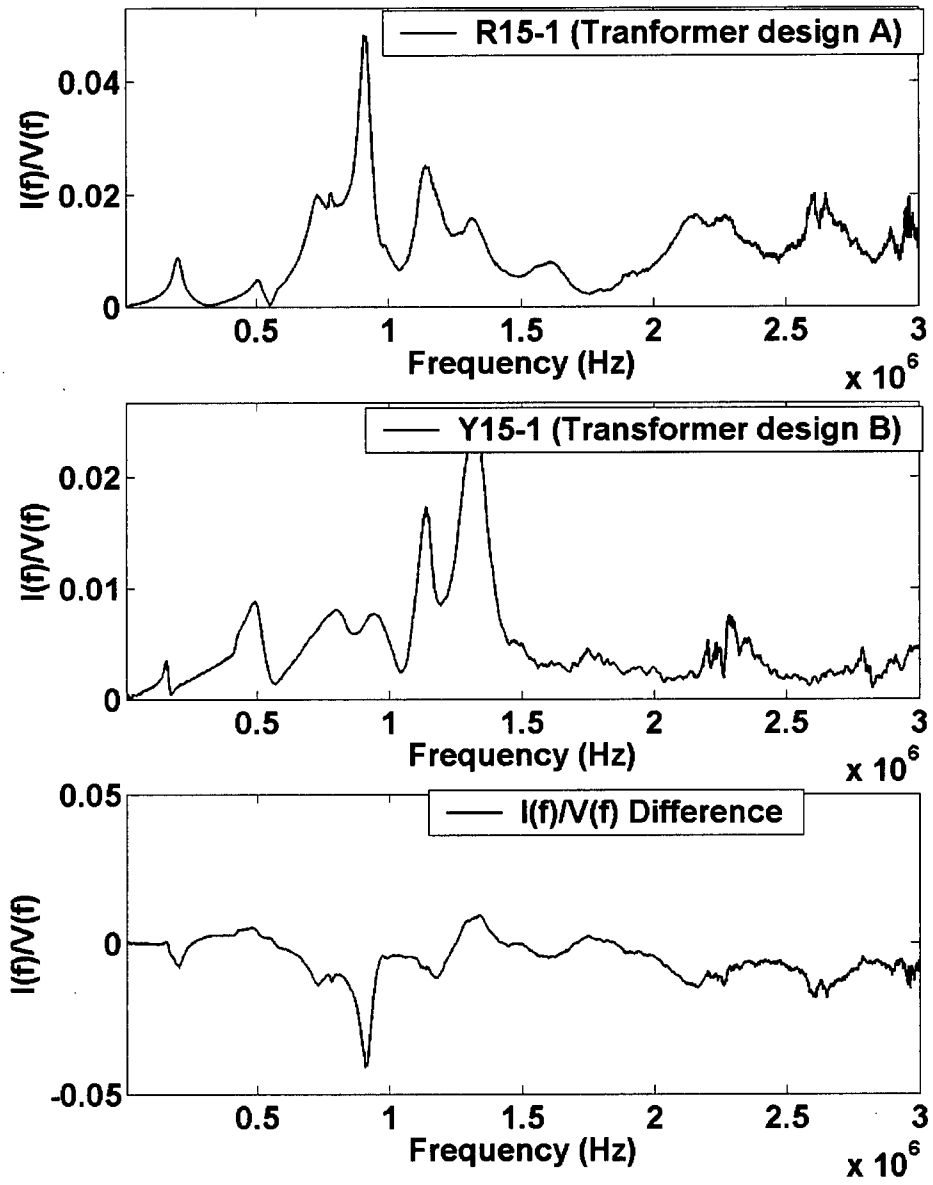


Figure 4.20 – Comparison of two transformers with different internal design

**Case 7: Effect of Loose Winding Clamping vs. Tight Winding Clamping (before and after re-clamping)**

The transformer ratings were as follows:

Phase: Single phase
Voltage: 295.9 kV (HV winding) – 139.715 kV (LV winding)
Power rating: 400 MVA
Type: Core form, auto transformer with a tertiary winding

Figures 4.21 to 4.24 show the results of FRA (I) tests on a transformer with loose winding clamping and on the same transformer with tight winding clamping. When the transformer was first tested, it had moderately loose winding clamping. Although the winding did require re-clamping, it had not reached the stage where there was a serious risk of transformer failure. The transformer was re-clamped and the test was repeated. Figures 4.21 and 4.22 show the test results with the voltage pulse input to the same high voltage bushing and measurement of the neutral current. Figures 4.23 and 4.24 show the measurement of the current coupled into the tertiary winding (Y1).

These figures clearly show the ability of the FRA (I) test to detect loss of winding clamping pressure before the loss has reached the stage that the transformer is at serious risk. Changes in the winding clamping cause variations in the winding geometry, resulting in different winding parameters (such as capacitance and turn-to-turn magnetic coupling). These changes alter the FRA signature.

The figures also demonstrate that measurement to the second winding (tertiary) is more sensitive than measurement of the neutral current.

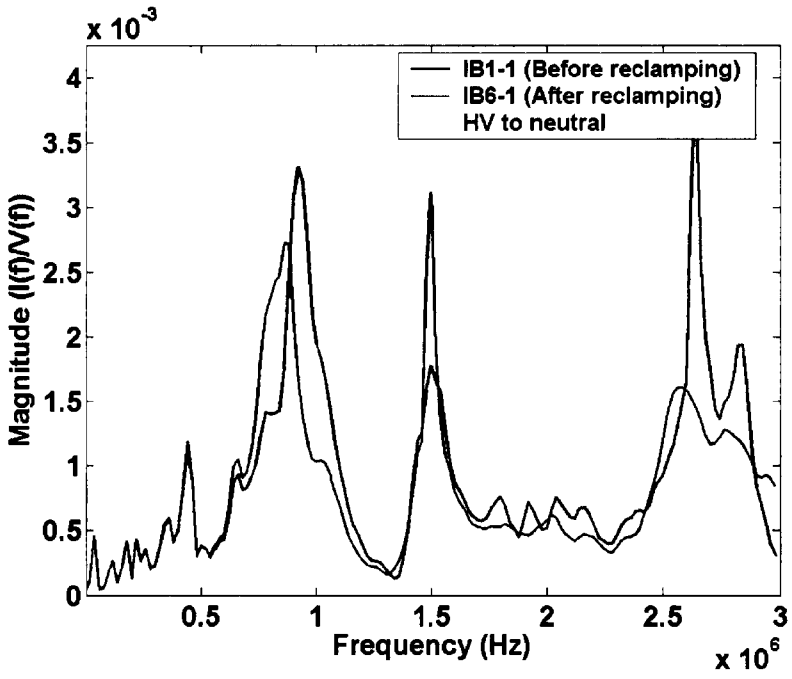


Figure 4.21 – Comparison before and after re-clamping (high voltage to neutral)

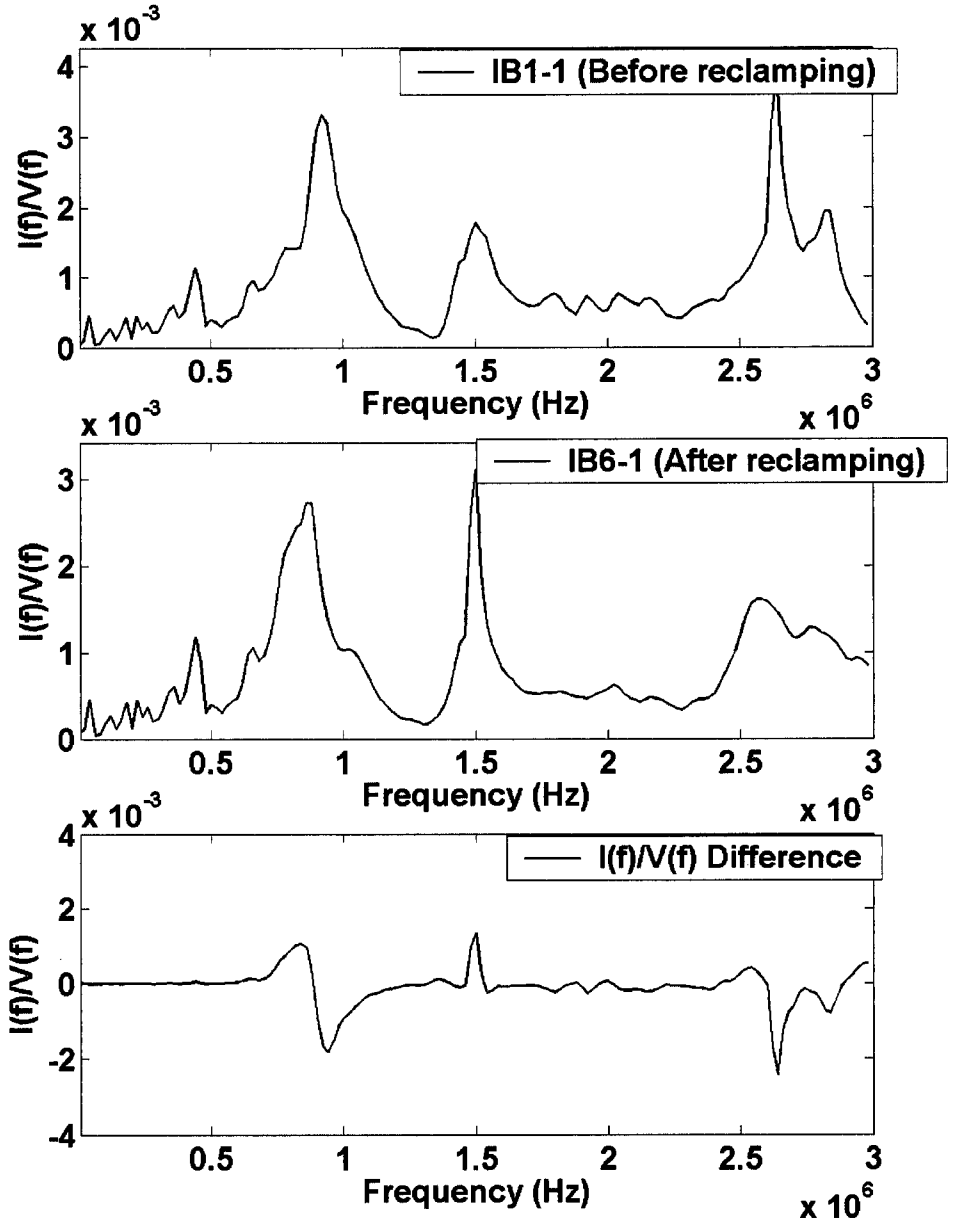


Figure 4.22 – Comparison before and after re-clamping (high voltage to neutral difference)

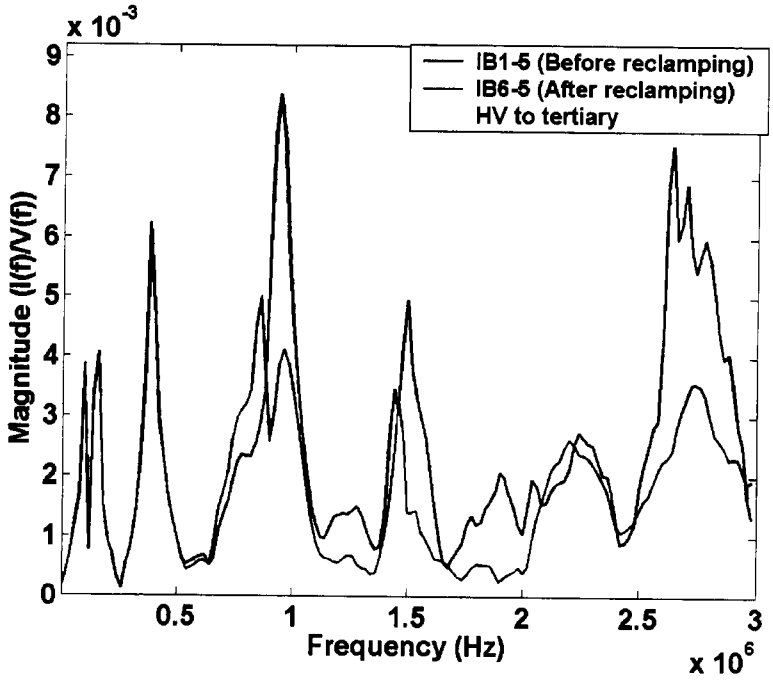


Figure 4.23 – Comparison before and after re-clamping
(high voltage to tertiary winding overlaid)

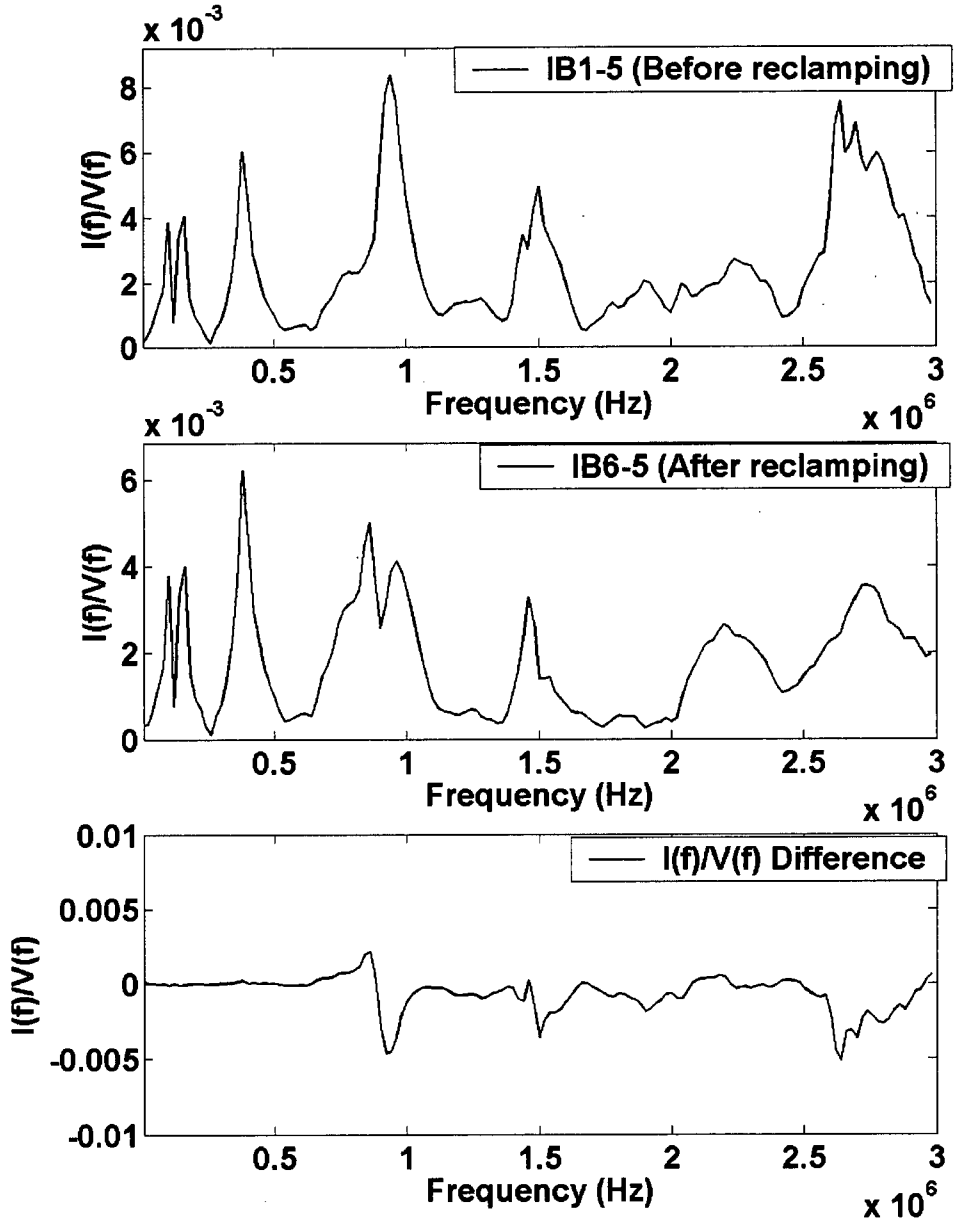


Figure 4.24 – Comparison before and after re-clamping
(high voltage to tertiary winding difference)

**Case 8: Effect of Removing Oil**

The transformer ratings were as follows:

| | |
|---|---|
| Phase: | Single phase |
| Voltage: | 295.9 kV (HV winding) – 139.715 kV (LV winding) |
| Power rating: | 400 MVA |
| Type: | Core form, auto transformer with a tertiary winding |

Figures 4.25 to 4.31 show the results of FRA (I) tests on a transformer before and after clamping, with oil and then without oil. The FRA (I) measurements were done in two test configurations: input to the high voltage winding, H1 and output current measured on H0; and input to the high voltage winding and coupled current on the tertiary winding terminal Y1. The transformer was first tested with oil in the transformer, then the oil was drained and the winding was re-clamped. FRA (I) tests were done without oil before and after the re-clamping. Finally, the FRA (I) test was done again after the transformer had been re-filled with oil.

The FRA measurement results show that in the frequency range below 0.5 MHz there is no significant admittance changes before and after re-clamping, either with or without oil; however, the existence of oil had a significant impact above 0.5 MHz. The resonant frequencies (peaks in the signatures) shifted in frequency and magnitude (Figure 4.25 with oil, Figure 4.26 without oil and Figures 4.29 and 4.30). The capacitances between windings and from the windings to ground are reduced with the oil out of the transformer, as the dielectric constant of the oil is higher than air. With the lower capacitance, the resonant frequencies are increased, since resonance is inversely proportional to the capacitance.

At the frequency range above 0.5 MHz, the FRA results start to show the re-clamping effect, both with and without oil. The FRA measurement with oil is more sensitive than without oil. The magnitude changes were much larger with the oil than without the oil. The results (Figure 4.31) also show that the two measurement configurations (H1-Y1 and H1-H0) had a similar sensitivity to the detection of the re-clamping changes.

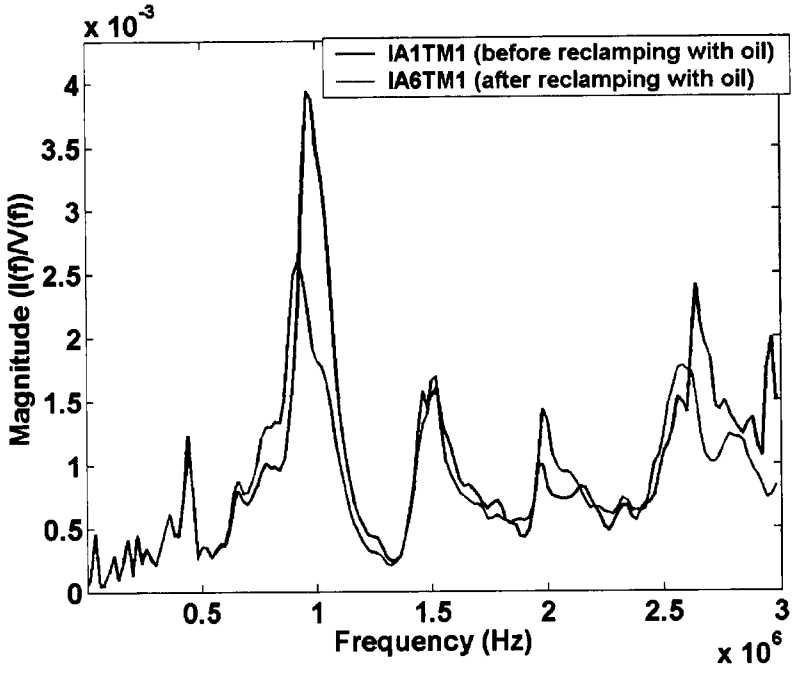


Figure 4.25 - FRA (I) Comparison before and after re-clamping with transformer oil (HV winding H1-Y1)

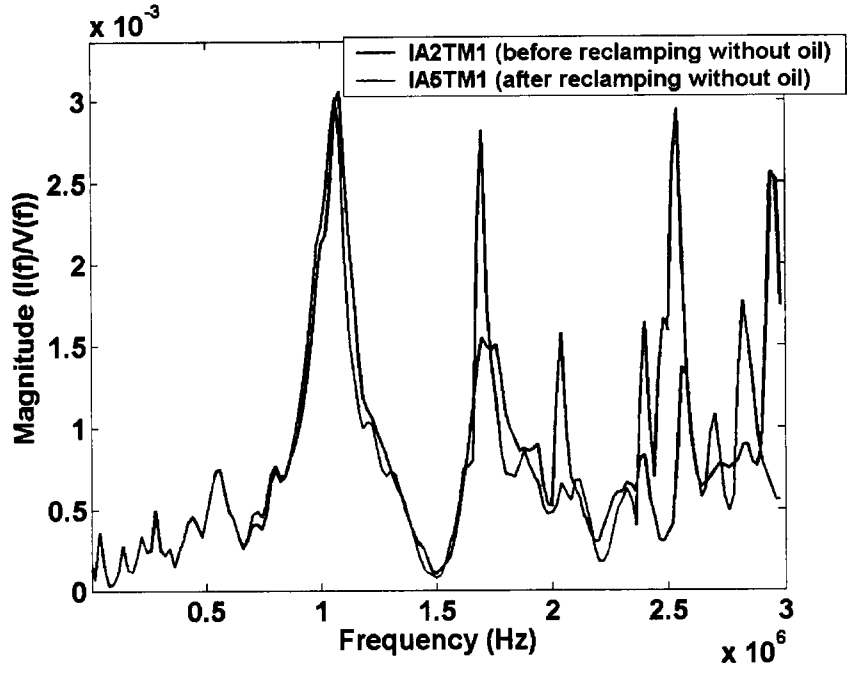


Figure 4.26 - FRA (I) Comparison before and after re-clamping without transformer oil (HV winding H1-H0)

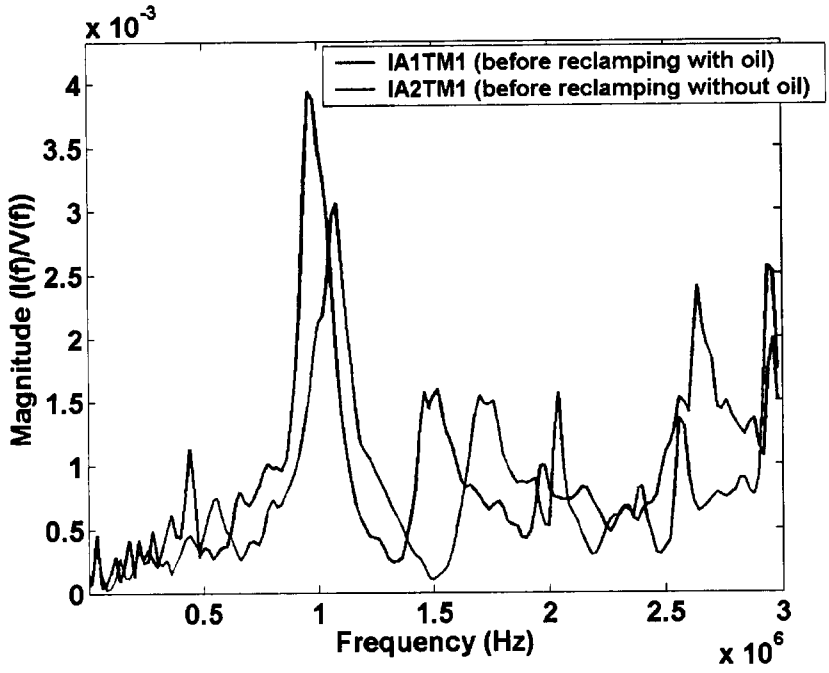


Figure 4.27 - Comparison before re-clamping with and without transformer oil (HV winding H1-H0)

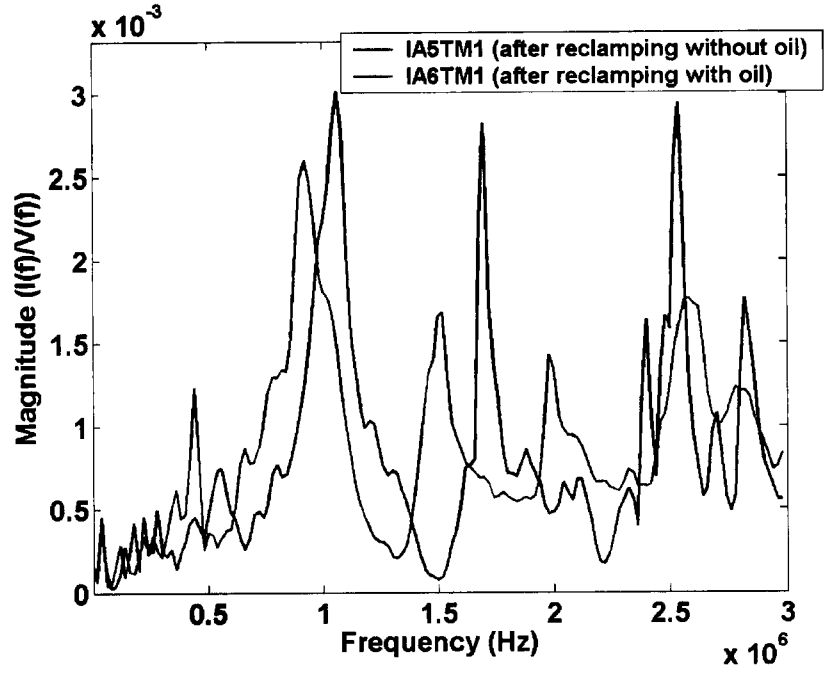


Figure 4.28 - Comparison after re-clamping with and without transformer oil (HV winding H1-H0)

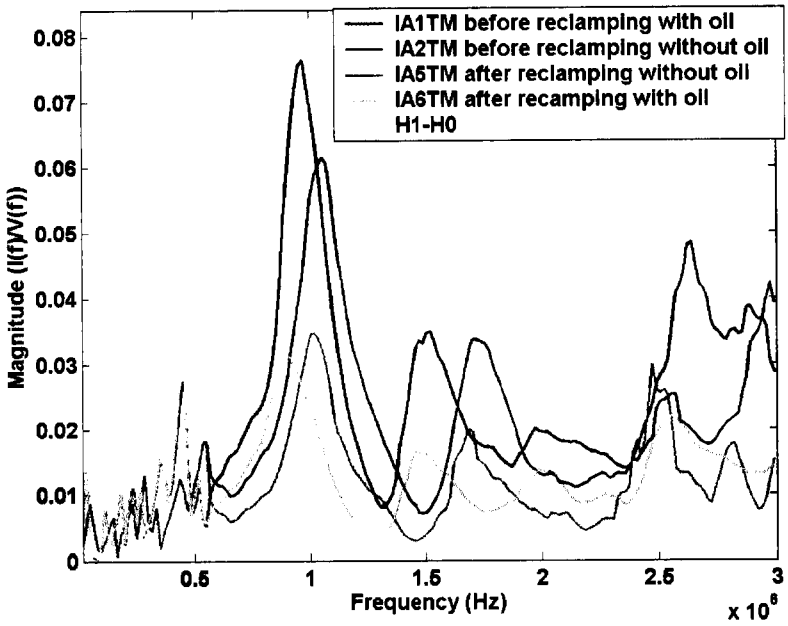


Figure 4.29 - Comparison before and after re-clamping with and without transformer oil (HV winding H1-H0)

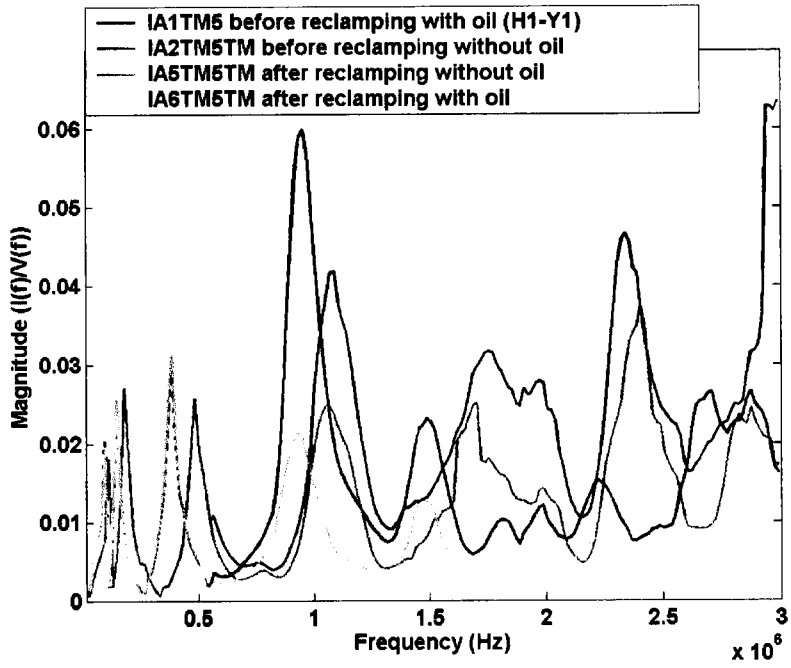


Figure 4.30 - Before and after re-clamping with and without transformer oil (HV winding H1-Y1)

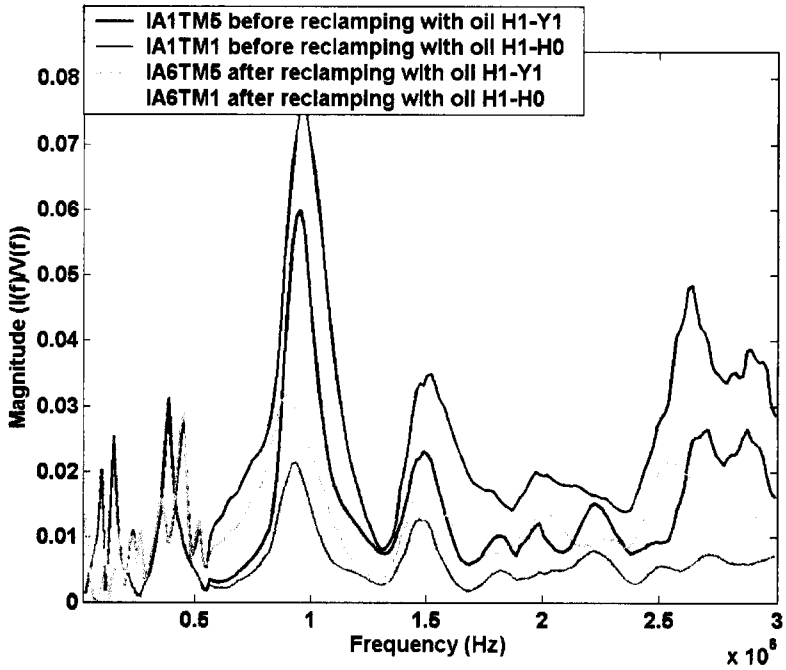


Figure 4.31 - Before and after re-clamping with transformer oil (comparison of two configurations - H1-Y1 and H1-H0)

These test cases demonstrate a number of important characteristics of the FRA test:

- FRA measurement with different tap positions produces different signatures. The differences are sufficient to require that tests must be repeated on the same tap position.
- The signature of different phases on a three-phase transformer can be significantly different. This is caused by construction differences such as lead placement, lead length, bushing placement, etc.
- Transformers of the same design have the same FRA signature if they are in identical condition. Therefore, a comparison between transformers of the same design can be used to detect winding movement if a signature over time is not available.
- Transformers with different internal designs will have different FRA signatures, even if they have the same ratings.
- The FRA test is repeatable over time if the test arrangement used has not been changed. If there is no internal change in the transformer, the FRA results will be the same. If the internal winding condition has changed, the FRA results will show changes

- A loss of clamping of a transformer will change the FRA signature. Based on the experimental data, the transfer admittance of the transformer will in general show a reduction in the magnitude of the dominant resonant frequencies after re-clamping. This phenomenon is due to changes in the parallel insulation resistance between winding discs, as explained in Appendix A (Simulation Results).
- A transformer with and without oil will show changes in the FRA results if there are changes in the transformer. The FRA results without oil will show a shift to a higher frequency. The FRA measurement with oil is more sensitive than tests without oil.

## 4.3 Experimental Laboratory Work on the Off-Line Test Method

### 4.3.1 Comparison of the Two FRA Off-line Test Methods

The two standard off-line methods used to perform the Frequency Response Analysis (FRA) test were compared to determine their suitability for the detection of winding damage and movement in a power transformer. The impulse FRA (I) test was compared to the swept frequency FRA (S) test on the same 345-kV autotransformer to determine if both methods are effective, interchangeable, and have the sensitivity to detect winding movement and other problems.

The two test methods are based upon the same mathematical and electrical principles relating to excitation and response of a complex network. The two methods rely on different sources of excitation, lead arrangement, instrument positions, and separate methods of resolving the response to the frequency domain. The FRA (I) method uses a series of identical impulses, which by definition contain all frequency components necessary to create a relationship between response magnitude and frequency when the Fourier transform is applied. The FRA (S) method uses a sine wave that is swept through the frequencies of interest. The instruments used directly produce the relationship required between the input signal and the response as a function of frequency.

The goals in comparing these two methods were to:

1. Determine if both methods are suitable for the purpose of detecting winding movement
2. Determine the effect of signal source arrangement, lead configuration, and grounding arrangement, and the inter-changeability of source and leads

3. Investigate the limits of detectable changes and the sensitivities for various types of internal deformations, etc.

The transformer used for these investigations was a single-phase 345/230-kV shell-form autotransformer rated 200 MVA, without tertiary. The windings were distributed around a horizontally supported core. Figure 4.32 shows an external view of the transformer. Figure 4.33 shows a general view of the internal arrangement of the coils. The winding diagram is shown in Figure 4.34. The winding is inter-distributed along the axial length of the core to minimize leakage flux. Winding distortions and shorting were confined to a location close to the low voltage X terminal in the common winding, due to limitations in access to the winding.

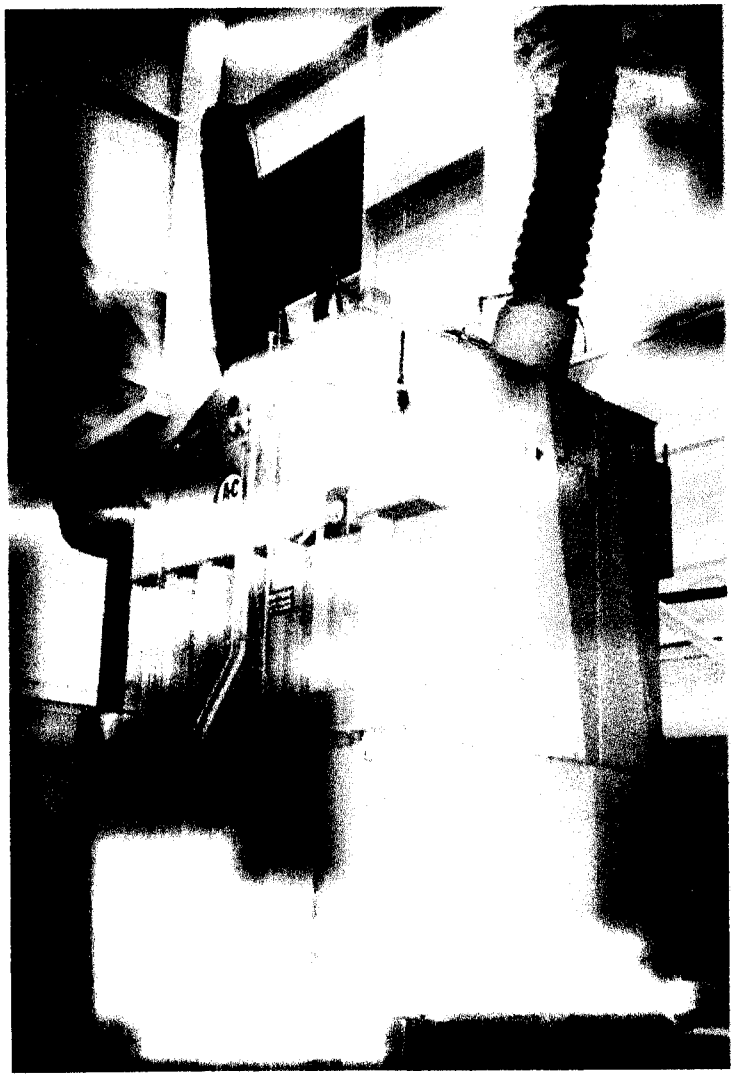

Figure 4.32 – Tested transformer (external view)

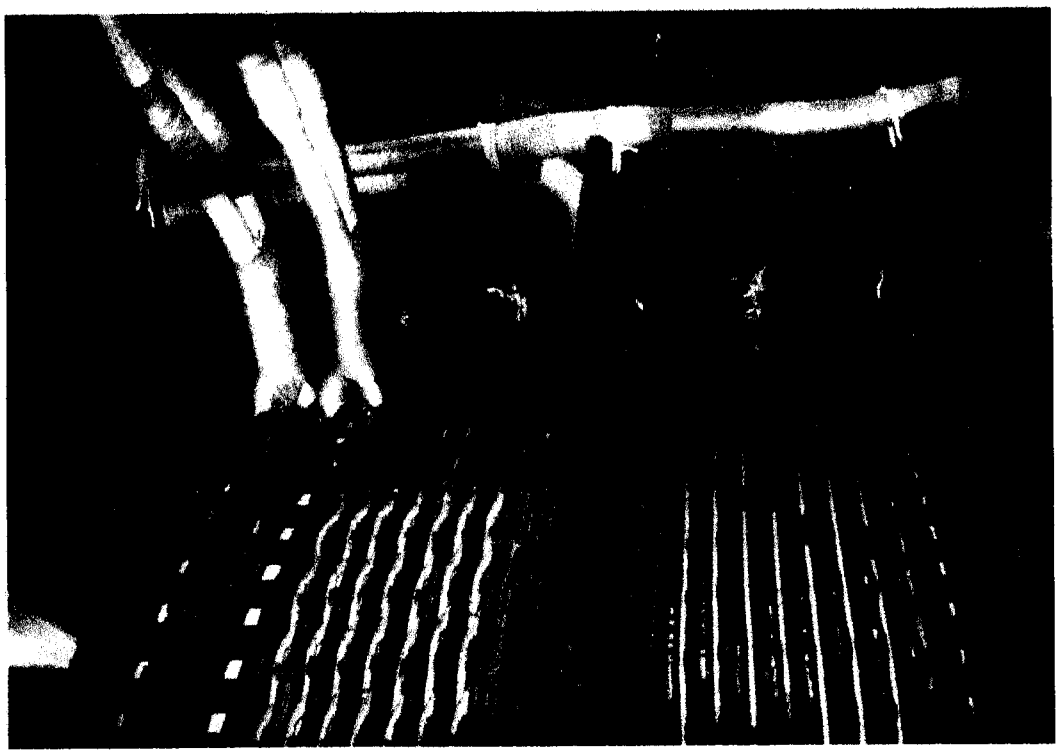

Figure 4.33 – Tested transformer (internal view)

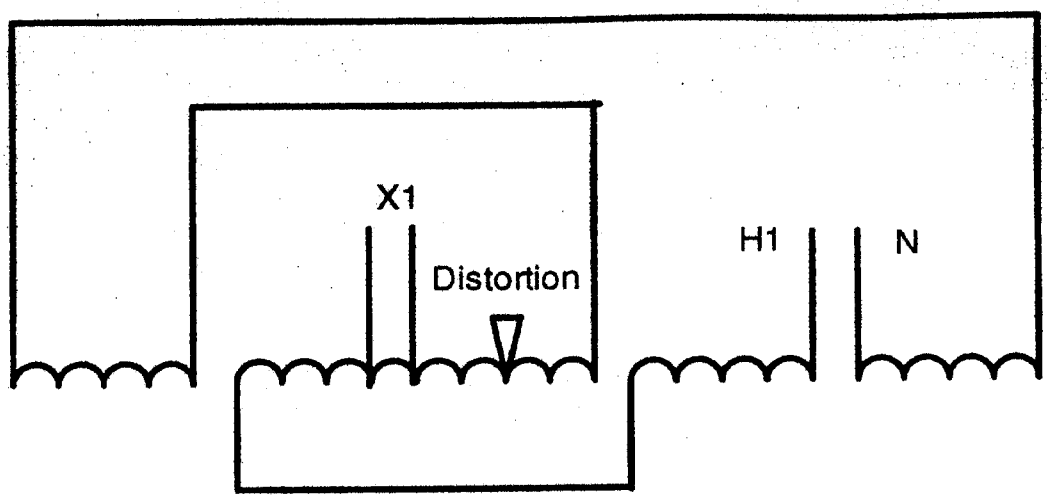


Figure 4.34 – Test transformer winding diagram

### 4.3.2 Comparison Tests Performed

The comparison tests were performed without oil in the transformer. In general, the FRA measurement has a higher sensitivity with the transformer in the oil-filled condition. This is because the higher dielectric constant of the oil compared to air increases the capacitive coupling, particularly at higher frequencies where capacitance is more dominant[1].

The FRA (S) is normally performed by energizing the winding and measuring the response of the winding at the other end, leaving other terminals ungrounded. The measurement system consisted of a HP 8751A network analyzer. The network analyzer was located at the floor level. Three triaxial cables were run from the analyzer to the bushing terminals, one as a signal source and two for measuring the input and output voltages. A diagram of the system is shown in Figure 4.35. The measured transfer function of the winding is the ratio of $V_{out}$ to $V_{in}$ in the frequency domain. Both $V_{out}$ and $V_{in}$ are measured with respect to the grounded transformer tank.

The comparisons were made primarily in the frequency range of 5 kHz to 3 MHz. The swept frequency tests, however, were run from 5 Hz to 10 MHz. Accordingly, some results from these very low or very high swept frequency ranges will also be discussed.

The FRA (I) measurement system consists of a recurrent surge generator (RSG) to generate the impulse signal and a current shunt to convert the response current signal to a voltage. The system is normally located on top of the transformer to minimize lead lengths. The impulse signal from the RSG is applied to the transformer by coaxial cable. The applied impulse signal and the output signal from the current shunt are measured and recorded on a digital oscilloscope. Figure 4.36 shows a diagram of the system. The recorded signals are analyzed to obtain the transfer function of the winding in the frequency domain.

Tests to determine comparative detection capabilities for various deformations were then conducted with each system in the normally used configuration (i.e., FRA (S) with instruments at ground level and FRA (I) with instruments on top of the transformer). The normal leads and grounding connections for the respective systems were also used.

The transformer was modified to simulate a number of typical lead, winding and grounding problems. Modifications to the transformer were performed in the following sequence:

1. One of the two neutral leads was disconnected to simulate a fault induced burn-off.
2. The disc winding was wedged open axially to simulate localized axial distortion.
3. Two turns of the winding were shorted near the X1 terminal in the common section.
4. The flux control shield around the winding was first ungrounded and then provided with two ground points.
5. Partial and complete winding turns within a disc were distorted radially.

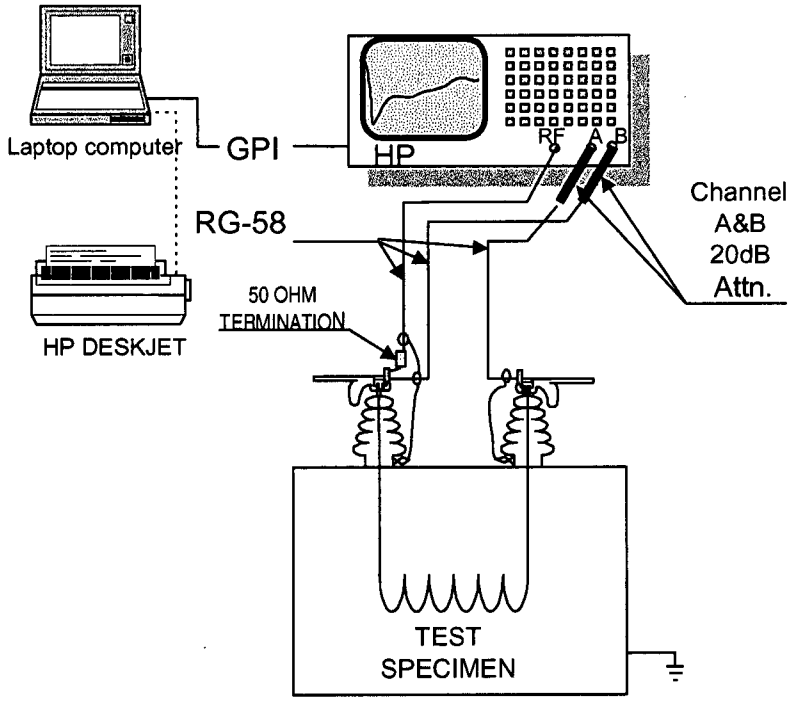


Figure 4.35 – FRA (S) test configuration

[1] Data on the effect of oil in the transformer on the FRA test was presented in Section 4.2.

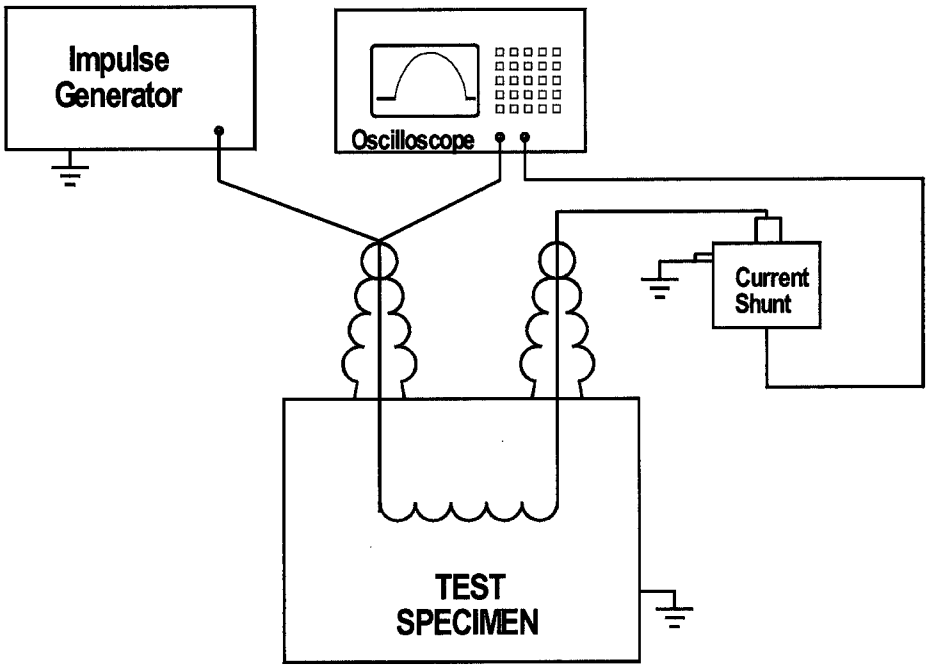


Figure 4.36 – FRA (I) test configuration

### 4.3.3 Results

#### 4.3.3.1 Inter-changeability of Methods

The upper curves of Figure 4.37 show a comparison of results when using the FRA (S) lead arrangement (long leads) at the bottom of the transformer with both input signal sources. The waveforms have a similar shape over the entire frequency range. Using the FRA (I) lead arrangement (short leads) on top of the transformer with both sources results in waveforms not quite as similar, as can be seen in the lower curves of Figure 4.37[2].

An interesting inter-comparison of the same data can be made by looking at the extreme cases of interchanging the sources into the other position and leads. Comparing Configurations (1) and (16) or Configurations (12) and (5) shows that large differences exist as a result of a change in source position and leads. Nevertheless, there is some similarity in response when using the longer swept frequency leads with the two different sources. This is attributed to the difference of shunt value (FRA (I) - 10 Ω) and termination impedance (FRA (S) - 50 Ω)

[2]The FRA (I) curves are at a lower dB level than FRA (S) curves. They were shifted down in all the graphs in this

compared to the impedance of the whole circuit, which includes winding impedance, leads impedance and shunt or termination impedance. When using the long leads, the percentage of shunt/termination impedance impact to the circuit is smaller. When using the shorter leads, the percentage of shunt/termination impedance impact to the circuit is larger[3].

The conclusions from the inter-changeability studies are:

- The two methods (FRA (S) and FRA (I)) are not directly interchangeable with each other due to differences in equipment. However, the test results are comparable enough to conclude that differences in the results are due to differences in the set-up and instrumentation (i.e., leads, position, grounding, and circuit and measurement impedances), not the test method. Accordingly, the methods can be considered interchangeable if the two methods are done under identical set-up conditions.

- With the FRA (S) method and the lead lengths used in this study, signal lead movement can result in some small differences in response. With both methods, a consistent lead arrangement is required for repeatability.

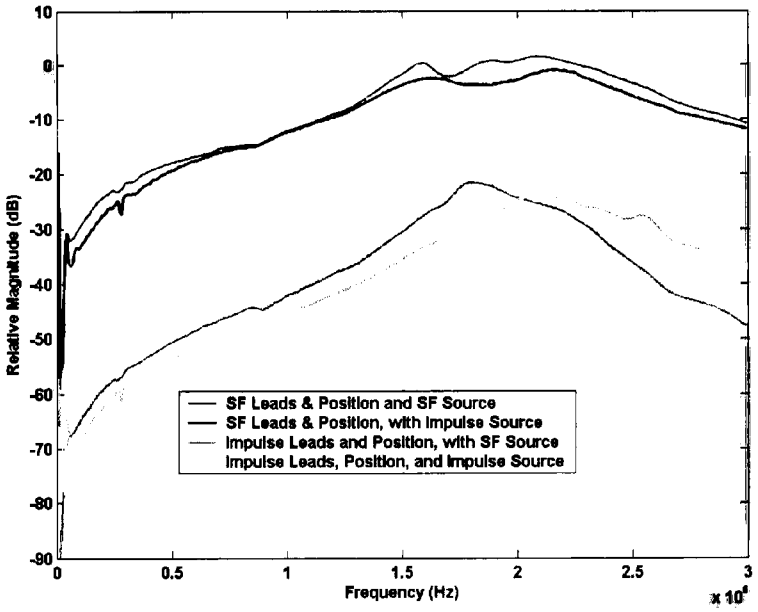


Figure 4.37 – Inter-changeability of the FRA (S) and FRA (I) methods
(FRA (I) results shifted down to simplify comparison)

section to make it easier to compare the two test procedures.

[3] This is discussed in more detail in Section 6.2.

4.3.3.2 Detection and Sensitivity

The detection and sensitivity results are discussed in the order of transformer modifications described in Section 4.3.2.

Neutral Disconnection: One of the two neutral leads was disconnected to simulate burn-off damage, as shown in Figure 4.38. The response of the two methods to this type of deformation is shown in Figure 4.39. Both methods are sensitive to this type of problem in the frequency range of about 1-3 MHz.

Axial Distortion: To achieve axial distortion of the pancake coils, a plastic wedge was driven between them, causing a localized separation of about 3 cm, as shown in Figure 4.40. Some of the adjacent insulating structure was removed, as shown, to make it easier to insert the wedge. Figures 4.41 and 4.42 show the response of the measurement methods to this type of distortion from both the H1-N and X1-N winding connections. It is interesting to see that the FRA (I) method shows more displacement when exciting the full winding (H1-N), while the swept frequency method shows more change when exciting the common winding where the distortion was localized.

Shorted Turns: Two adjacent spiral turns of a pancake coil assembly were shorted in the same location as indicated above. Figure 4.43 shows the method of shorting. This type of problem was easily detected by both methods in the response of H1-N, as shown in Figure 4.44.

Radial Distortion: The winding was radically distorted by pulling up one or more spiral windings from the pancake coil. Part of one turn (8 of 13 layers of conductor) was pulled up for "moderate" distortion. All of the first turn and two layers of the second turn were pulled up for "severe" radial distortion.

These modifications are shown in Figure 4.45. The comparative responses to measurements on the H1-N winding are shown in Figure 4.46. The FRA (S) method was found to be insensitive to this type of distortion. Through enlargement of the applicable portion of the curve some changes can be seen, but they are not significant relative to the signal level. The comparison for the X1-N winding is shown in Figure 4.47. Again, the FRA (I) method is more

sensitive. For this connection, the FRA (S) method does, however, exhibit some observable differences.

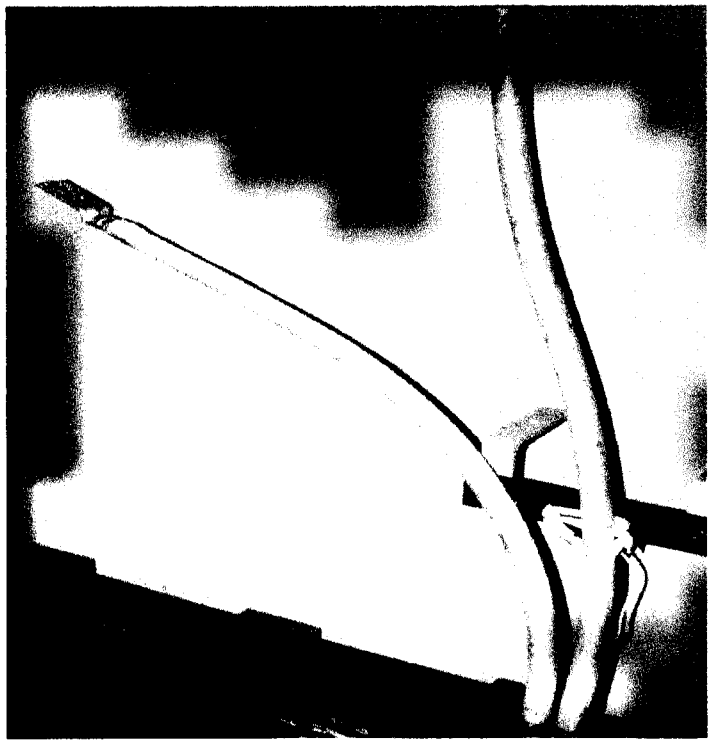

Figure 4.38 – Transformer neutral disconnected

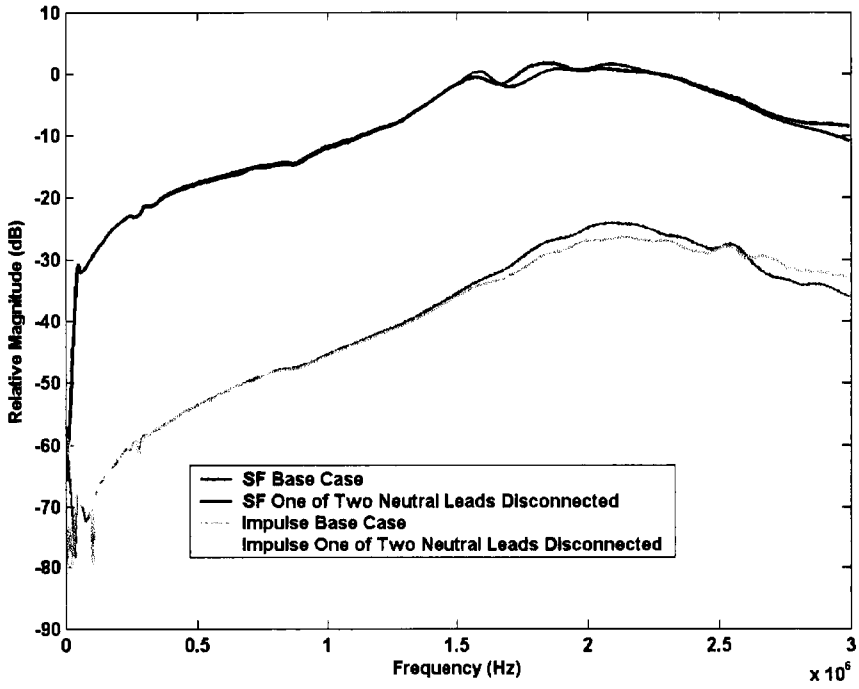


Figure 4.39 – Neutral disconnected test results

(FRA (I) results shifted down to simplify comparison)

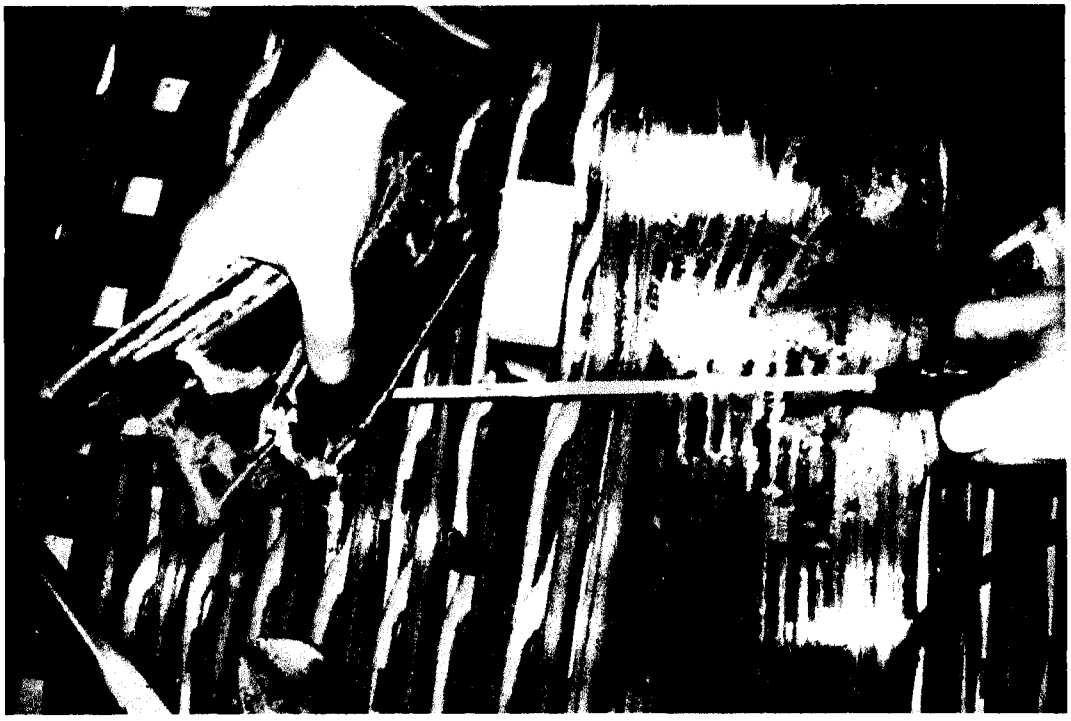

Figure 4.40 – Axial distortion on transformer

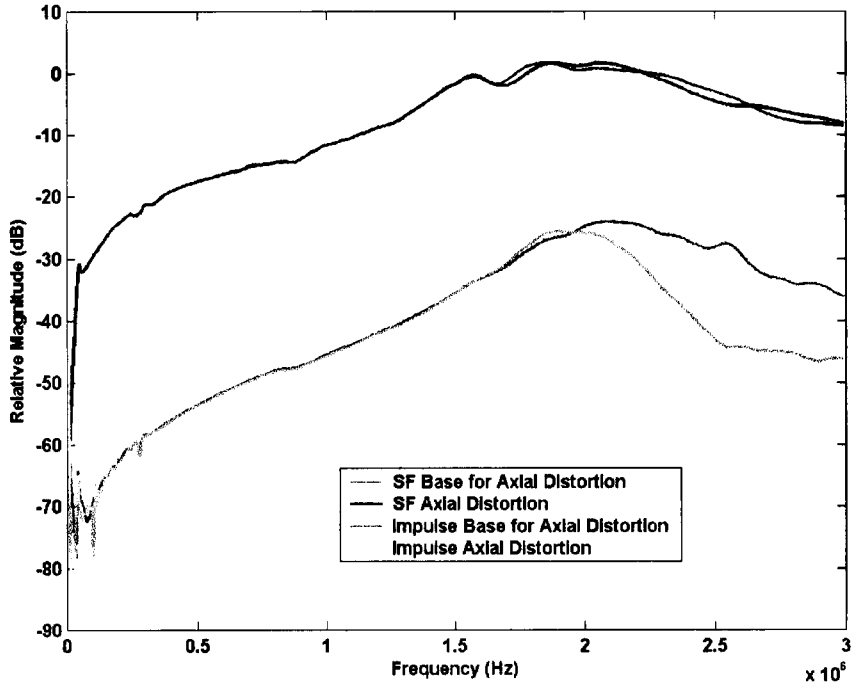


Figure 4.41 – Axial distortion test results – H1 to N
(FRA (I) results shifted down to simplify comparison)

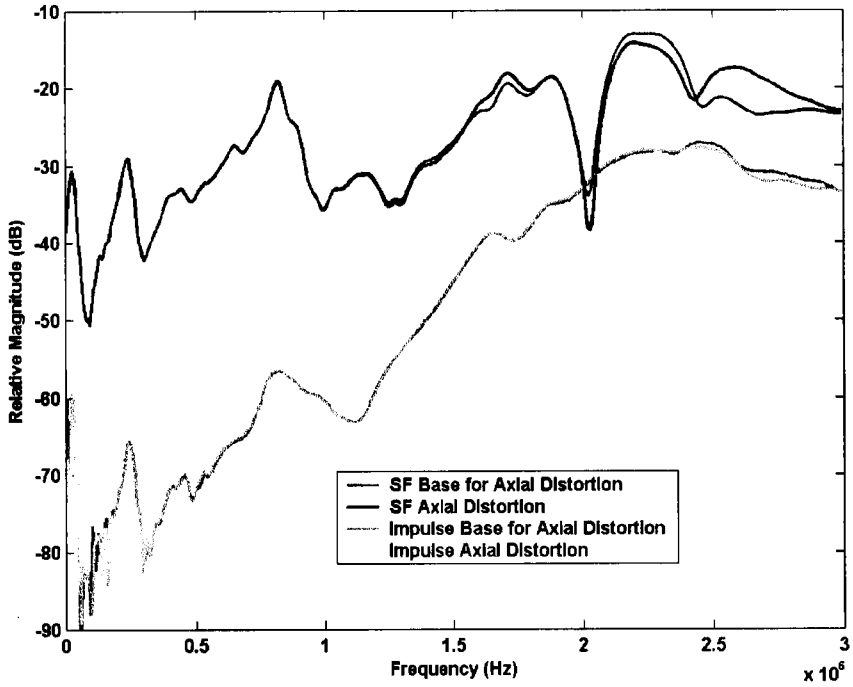


Figure 4.42 – Axial distortion test results – X1 to N

(FRA (I) results shifted down to simplify comparison)

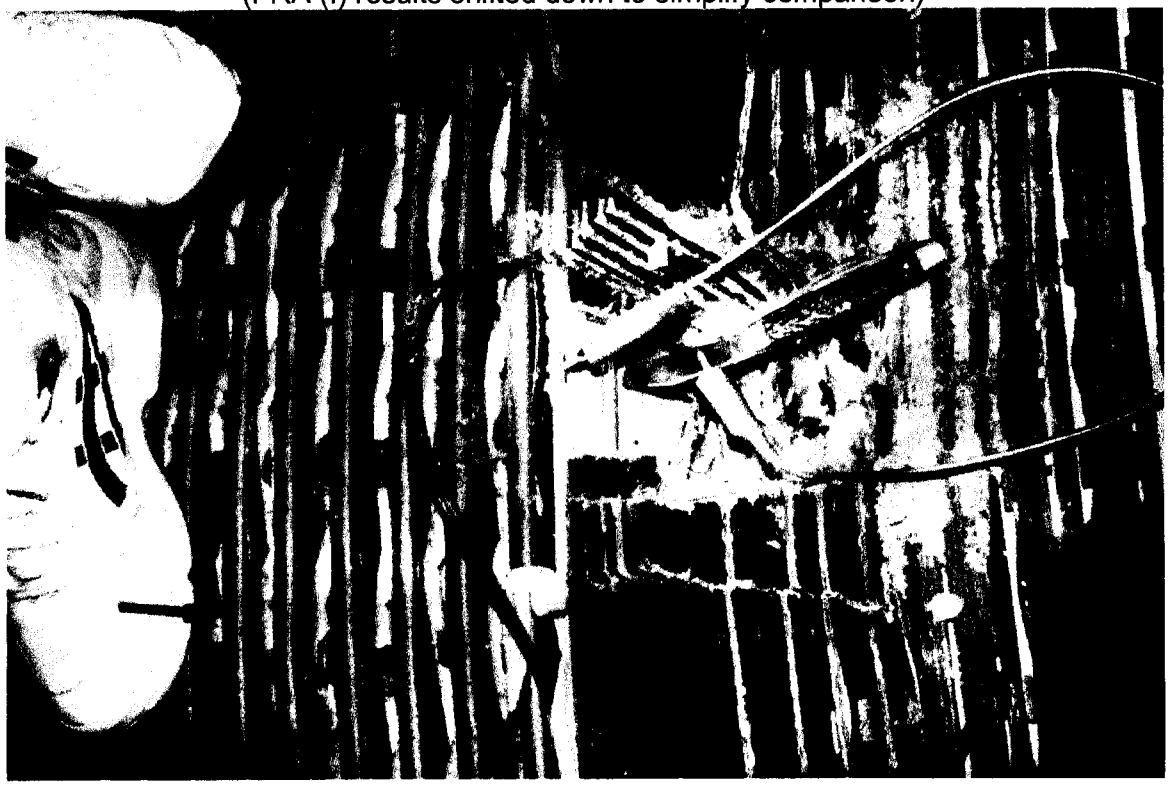

Figure 4.43 – Shorted turns on transformer

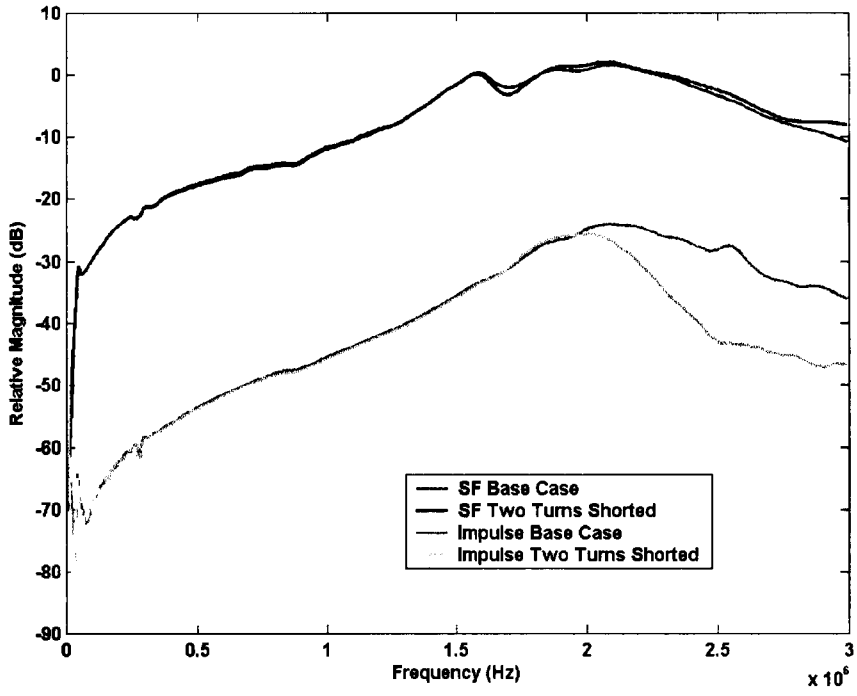


Figure 4.44 – Shorted turns test results
(FRA (I) results shifted down to simplify comparison)

Figure 4.45 – Radial distortion on the transformer winding

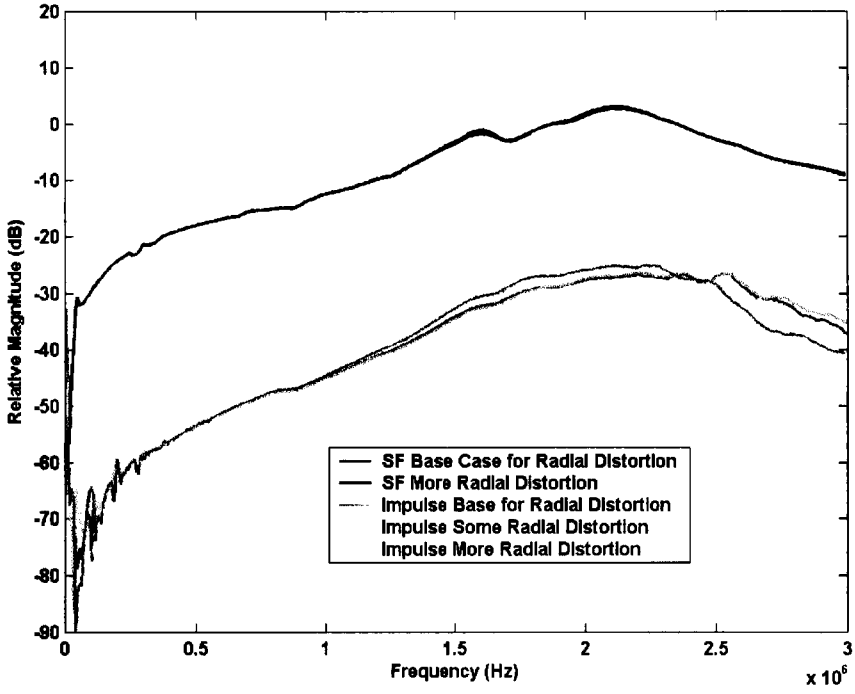


Figure 4.46 – Radial distortion test results – H1 to N
(FRA (I) results shifted down to simplify comparison)

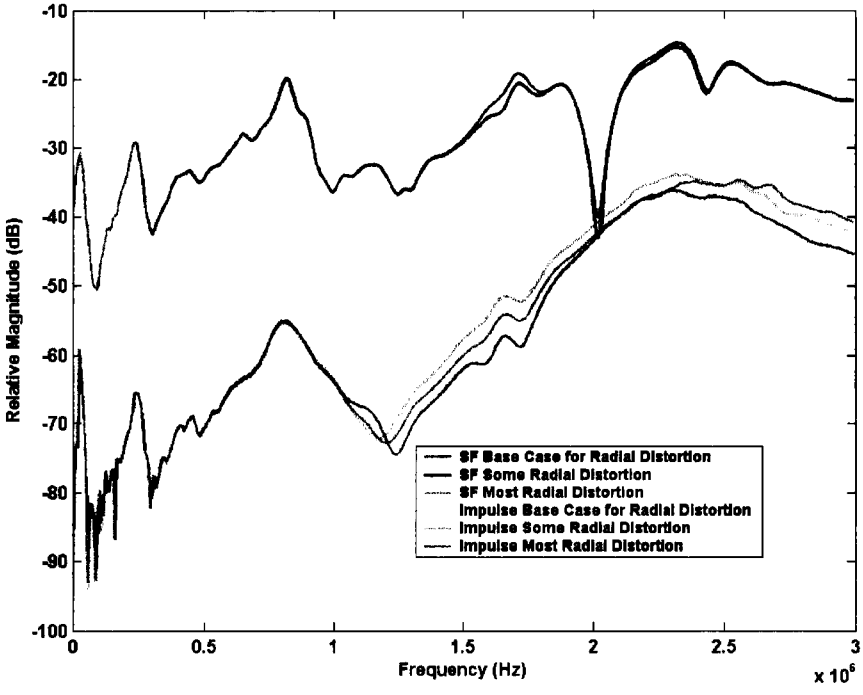


Figure 4.47 – Radial distortion test results – X1 to N
(FRA (I) results shifted down to simplify comparison)

### 4.3.4 Discussion of Results

It is clear from these tests that both the impulse FRA (I) test method and the swept frequency FRA (S) method are capable of detecting winding deformation in laboratory experiments. The extent of the winding deformations that were simulated in these experiments was less than what would be expected from actual transformer faults. Both methods are sensitive to changes in instrument location, lead and grounding arrangements, and circuit impedances. Repeatability is dependent upon consistent arrangement of these parameters. Both methods were sensitive to axial winding deformation. Both methods are viable in the field, but the measurement parameters are important for greater sensitivity and repeatability. The transformer impedance at the higher frequencies is quite low (e.g., 1 Ω). The ground level instrument location and higher series measurement impedance (50 Ω vs. the 10 Ω of the impulse shunt) cause the observed lower sensitivity of the FRA (S) method for some tests.

## 4.4 Experimental Laboratory and Field Work on the On-Line Test Method

### 4.4.1 On-line FRA Method

Performing the FRA test using the normal impulse or swept frequency methods requires a transformer outage and isolation of the transformer from the system to obtain the signature. If the test could be done on-line, with the transformer connected to the power system and energized, it would be easier to perform at lower cost, and it could be done more frequently. This would make it possible to detect trends in the transformer condition and detect problems earlier.

It has been proposed to use the signals generated by switching operations on the high voltage side of the transformer to obtain the driving source voltage for an on-line FRA test and to measure the signals using the transformer bushing taps [55,78].

Experimental work was done by Hydro Quebec to develop a system for the simultaneous recording of the input transient over-voltage and the winding output transient current, without disconnecting the transformer [147].

Other researchers have reported on power transformer condition monitoring by using a chirp signal to obtain the transformer transfer function off-line/on-line [112]. These researchers found that the configuration of the measurement set-up, frequency range and terminations play an important role in getting reproducible fault-indicating results.

To implement the FRA test on-line, several questions need to be answered including:

- Can the HV input transients be measured using the bushing taps?
- What is the impact on the admittance results using input waveforms different than the normal short rise time chopped pulses?
- What is the impact of the sampling rate on the results?
- What is the impact of a single shot signal vs. averaging multiple pulses?

A series of tests were carried out in the laboratory to answer these questions and to evaluate the feasibility of doing on-line FRA tests. On-line FRA field measurements were made on a 230/138 kV, 1-phase and a 330/138, 3-phase transformer to test the method. These are noted in the following section.

A potential alternative to the on-line test technique is to inject a signal into the high voltage bushing capacitance tap on one winding and to measure the response in another winding. Some laboratory tests were done in the high voltage laboratory of Powertech Labs to evaluate the feasibility of this technique[4].

### 4.4.2 Laboratory Tests

The laboratory test program began with a series of FRA (I) tests on a 100 kVA, 90 kV - 600 V, single-phase transformer. The high voltage bushing on this transformer had a capacitance tap and a tapped high voltage winding. Tests were done in the 90 kV and 16.6 kV tap positions, without the transformer being energized.

Table 4.1 lists the first series of tests, where the input was measured directly using the bushing tap. The waveform and the digitizer parameters were varied. There was no load on the transformer

secondary and both the X1 and X2 terminals were ungrounded. This series of tests was aimed at demonstrating the influence of different input signals (conventional FRA pulse vs. a standard lightning impulse), the effectiveness of averaging of multiple pulses and the limitations of the sampling rate. Figure 4.48 shows the transformer winding configuration.

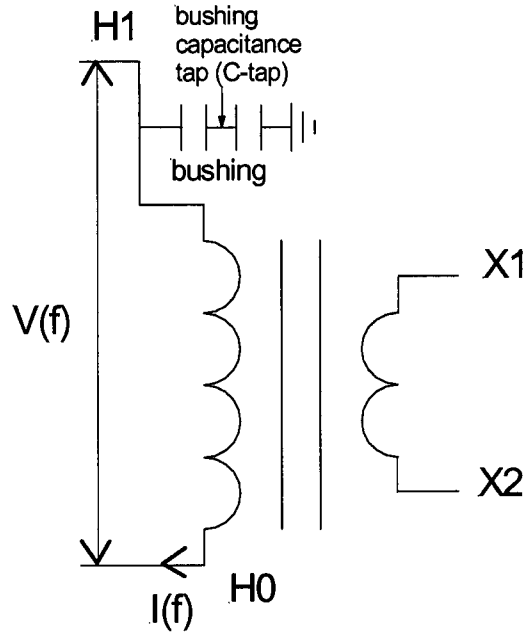


Figure 4.48 – 90 kV transformer winding configuration

Table 4.1 - 90 kV transformer tests

| Figure No. | Input Signal Terminal | Input Signal Type | Number of Pulses Averaged | Sampling Rate (Ms/s) | Input Measurement Terminal | Output Measurement Terminal | Tap Position (kV) |
|---|---|---|---|---|---|---|---|
| 4.50 | H1 | FRA* | 250 | 50 | H1 | H0 current | 90 |
| 4.51 | H1 | FRA* | 250 | 50 | C-Tap | H0 current | 90 |
| 4.52 | H1 | LI** | 250 | 50 | H1 | H0 current | 90 |
| 4.53 | H1 | LI** | 250 | 50 | C-Tap | H0 current | 90 |
| 4.54 | H1 | LI** | 1 | 50 | H1 | H0 current | 90 |
| 4.55 | H1 | LI** | 1 | 10 | H1 | H0 current | 90 |
| 4.56 | H1 | LI** | 1 | 5 | H1 | H0 current | 90 |

*Conventional FRA test pulse - <1/<1 μs,
**Standard lightning impulse waveform – 1.2/50 μs

[4] They had to be scheduled for periods when the laboratory was not being used for other tests.

The results from this test series show that the sampling rate of 5 Ms/s is too low for FRA measurement, and that even 10 Ms/s is too low. The measurement results from the input signal measured at the top of the high voltage bushing and at the bushing capacitance show significant differences. The admittances from lightning impulse and FRA pulse had the same results up to 3 MHz. In the frequency range above 3 MHz, the admittance from the lightning impulse input had a very "noisy" result.

For on-line data to be recorded effectively from transformers in the field, the data must be retrieved under a variety of transformer load conditions. To study the effect of load on the transformer transfer function, the test series listed in Table 4.2 was carried out on a 25 kVA, 14.4 kV-240 V distribution class transformer. Figure 4.48 shows the transformer winding configuration. The sampling rate was 50 Ms/s on all these tests and 250 impulse waveforms were averaged. This series of tests focused on studying the influence of the transformer secondary load conditions. The input voltage V(f) was measured across the high voltage winding and the current was measured on the H2 terminal of the high voltage winding. Four types of load condition were applied to the transformer secondary (low voltage winding), as follows:

a. open circuit
b. short circuit
c. resistive load of 3.9 ohm
d. inductive load of 100 mH

A lightning impulse was used as the input signal for all tests except for the condition with a short on the secondary winding. For this condition, a test was done with an FRA pulse for comparison with the lightning impulse.

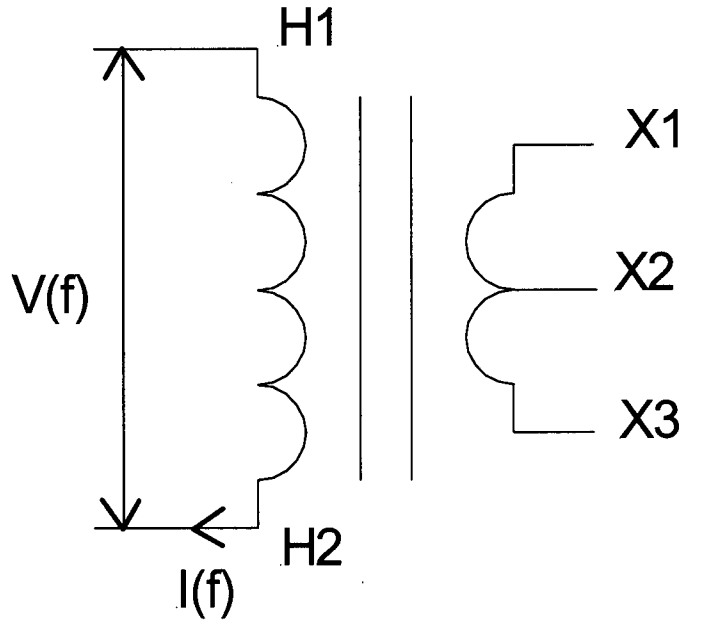


Figure 4.49 – 14.4 kV transformer winding configuration

Table 4.2 - 14.4 kV transformer tests

| Figure No. | Input Signal Terminal | Input Signal Type | Secondary Load (X1-X3) | Input Measured | Output Measured | Tap Position (kV) | Secondary Ground Terminal |
|---|---|---|---|---|---|---|---|
| 4.57 | H1 | LI* | Open | H1 | H2 current | 14.4 | None |
| 4.58 | H1 | LI* | 3.9 Ω | H1 | H2 current | 14.4 | None |
| 4.59 | H1 | LI* | Short | H1 | H2 current | 14.4 | None |
| 4.60 | H1 | LI* | 100 mH | H1 | H2 current | 14.4 | None |
| 4.61 | H1 | LI* | Open | H1 | H2 current | 14.4 | X1 |
| 4.62 | H1 | LI* | Short | H1 | H2 current | 14.4 | X1 |
| 4.63 | H1 | FRA** | Short | H1 | H2 current | 14.4 | X1 |

*Standard lightning impulse waveform – 1.2/50 μs
**Conventional FRA test pulse - <1/<1 μs

The data show that load on the secondary winding had very little effect on the test results in the measured frequency range. However, floating or grounding the secondary (terminal X1) had a significant effect on the test results.

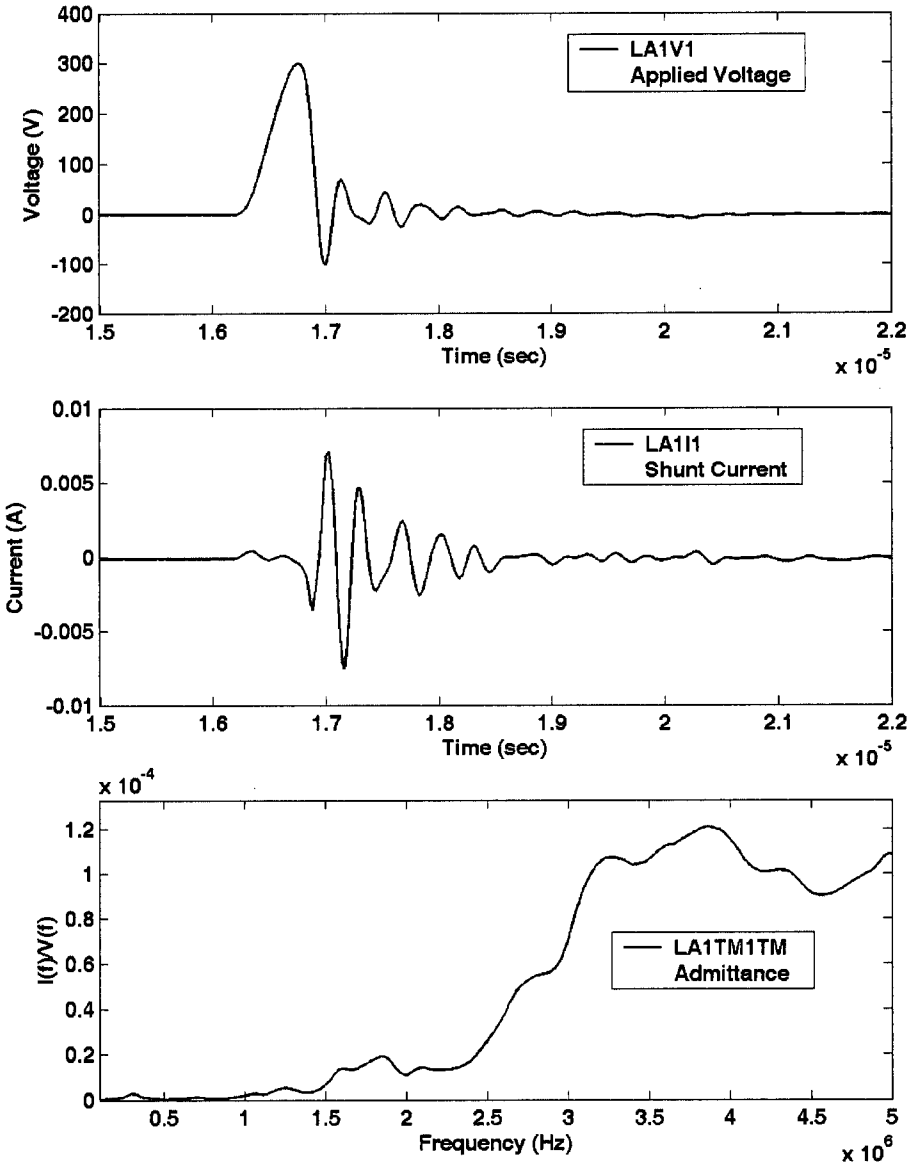


Figure 4.50 - Input waveform – FRA pulse, avg. 250 pulses, 50 Ms/s rate
Input measured – voltage on H1
Output measured – H0 current

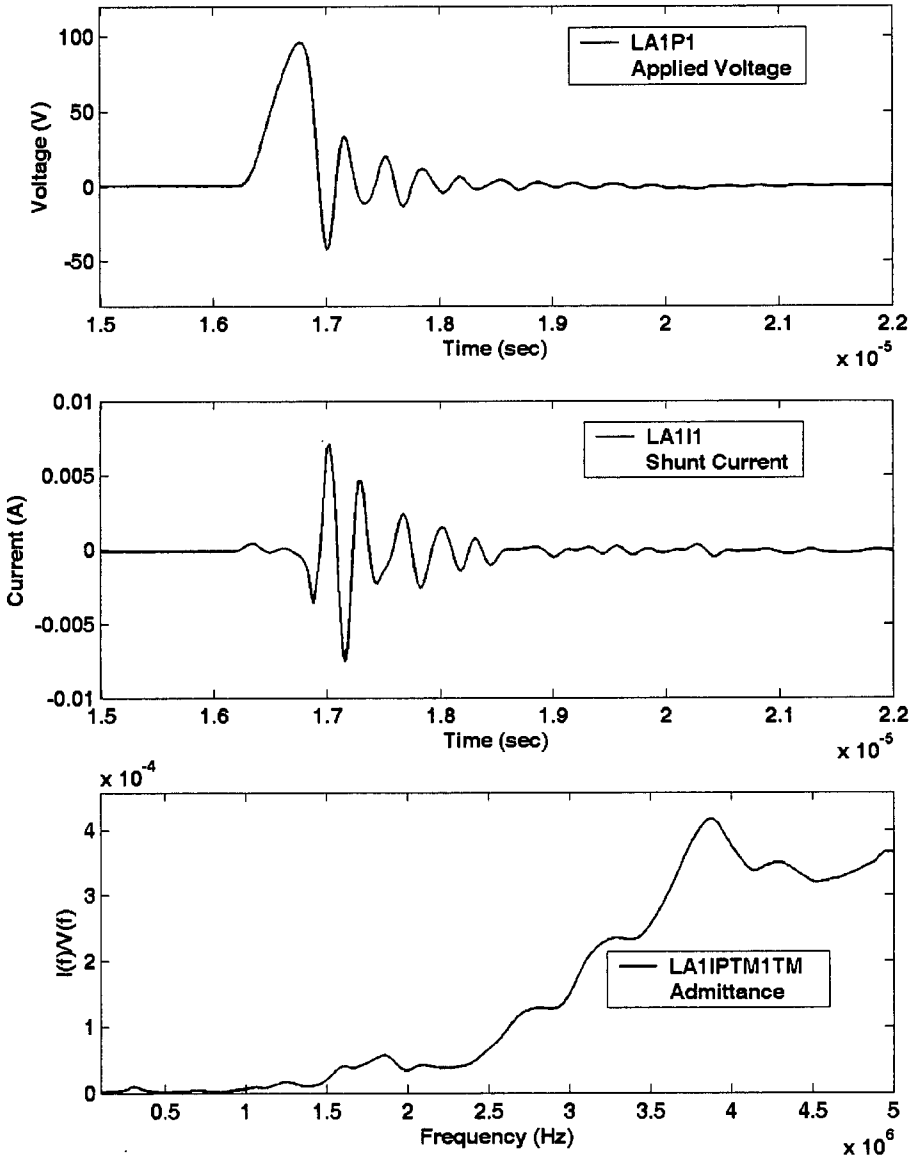


Figure 4.51 - Input waveform – FRA pulse, avg. 250 pulses, 50 Ms/s rate
Input measured – voltage on bushing tap
Output measured – H0 current

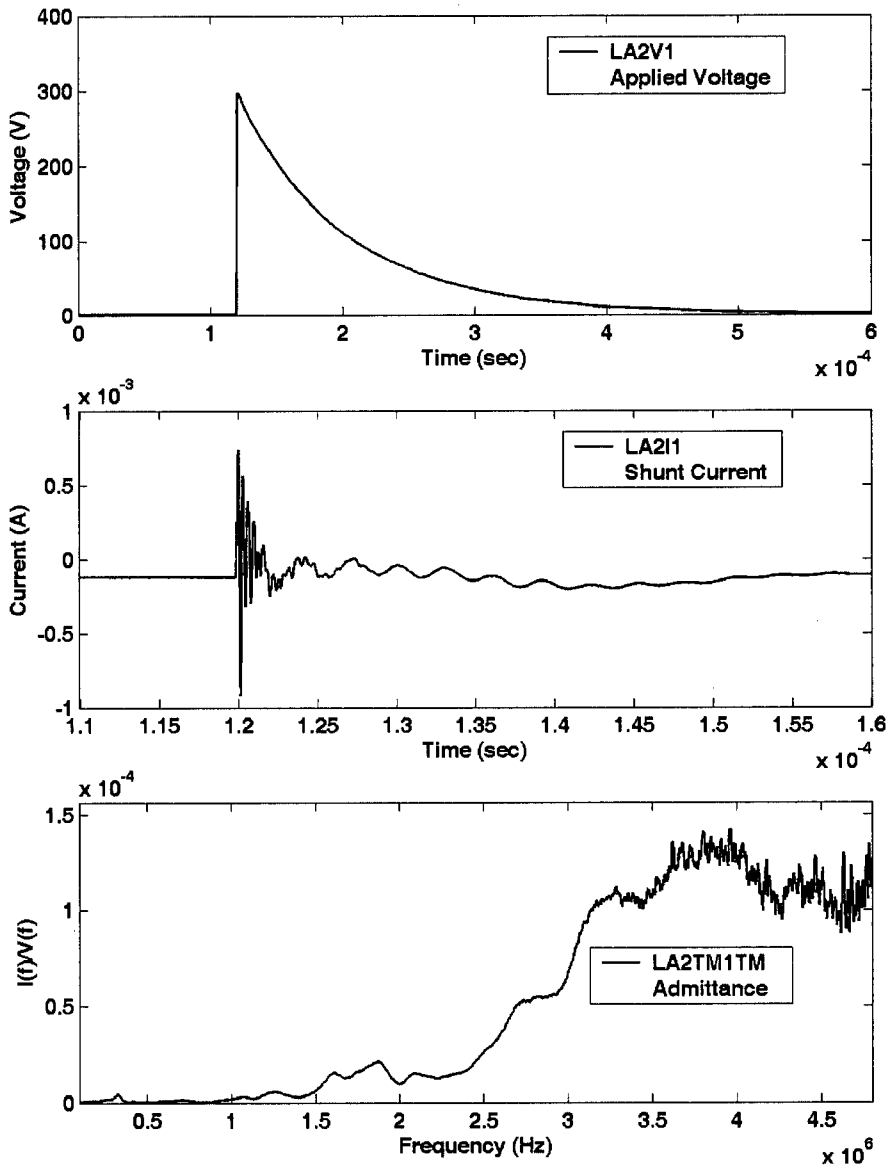


Figure 4.52 - Input waveform – LI, avg. 250 pulses, 50 Ms/s rate
Input measured – voltage on H1
Output measured – H0 current

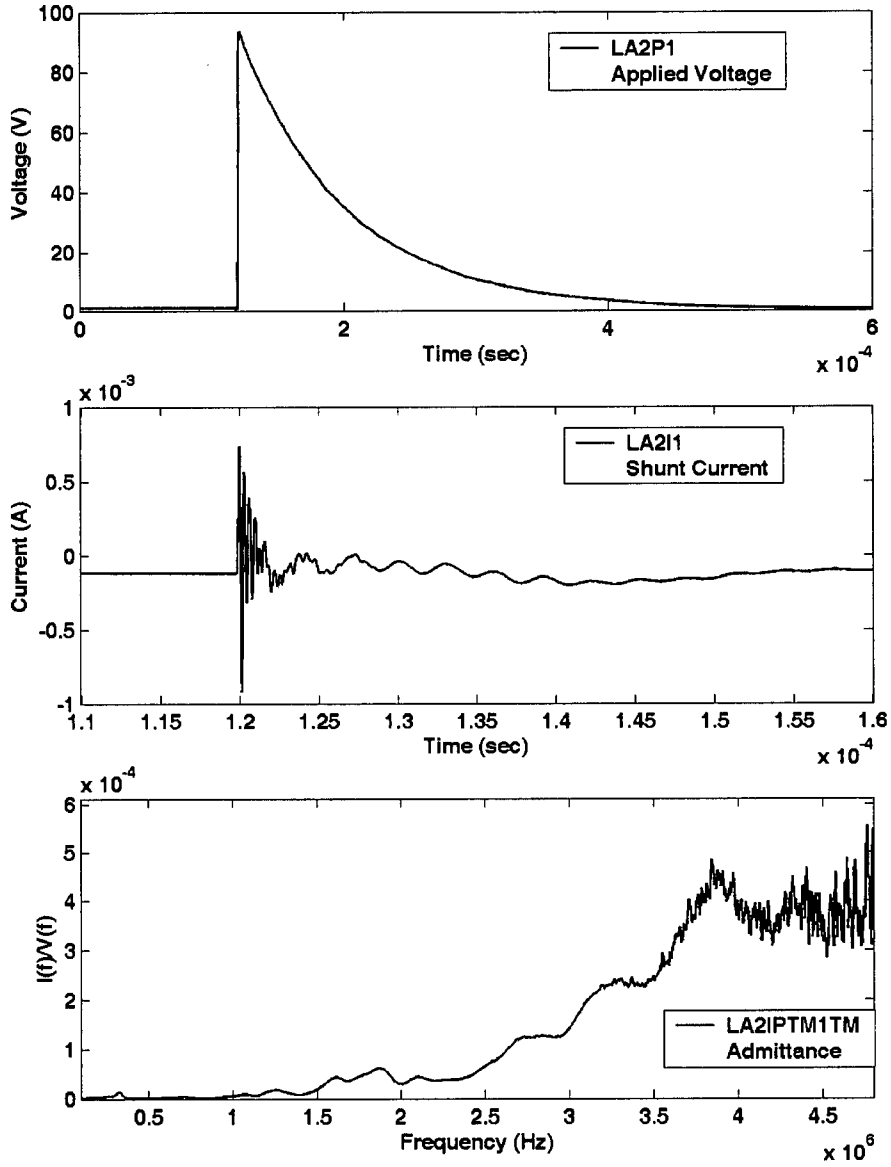


Figure 4.53 - Input waveform – LI pulse, avg. 250 pulses, 50 Ms/s rate
Input measured – voltage on bushing tap
Output measured – H0 current

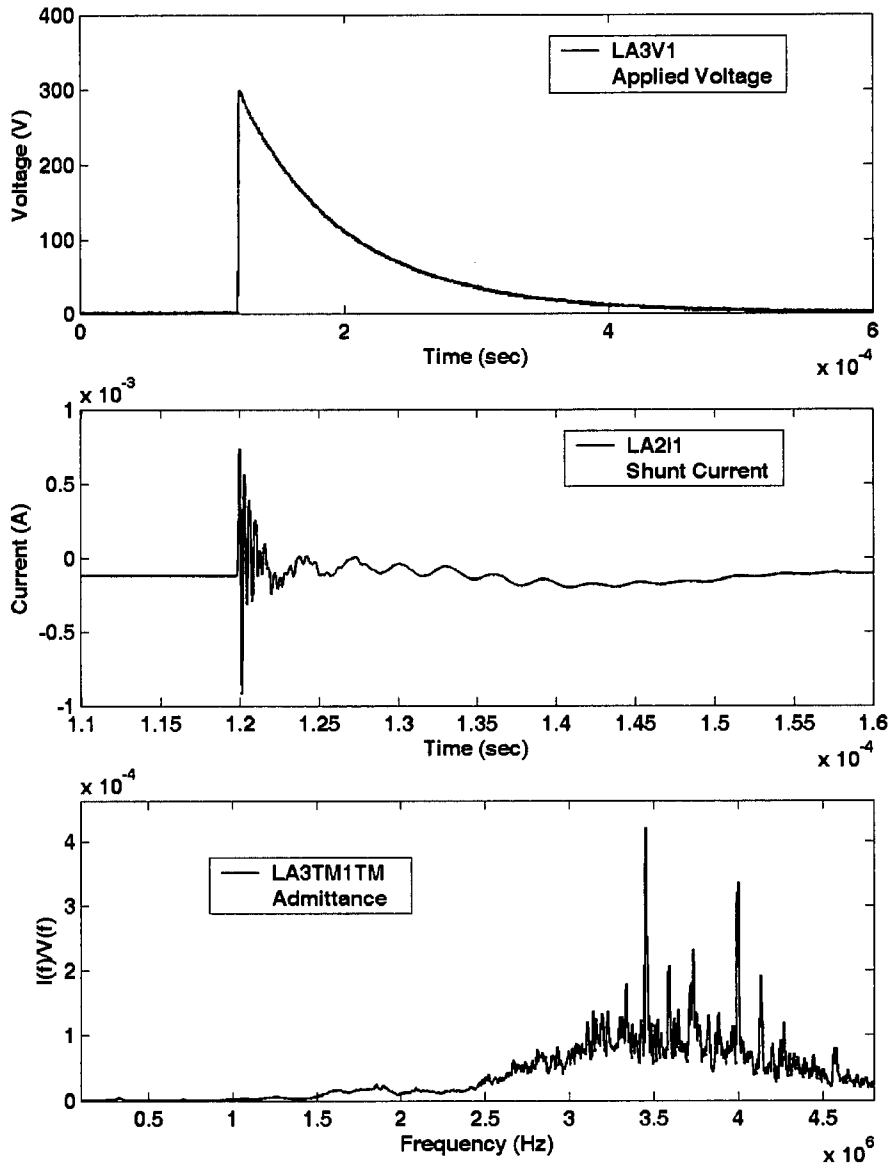


Figure 4.54 - Input waveform – LI, single shot, 50 Ms/s rate
Input measured – voltage on H1
Output measured – H0 current

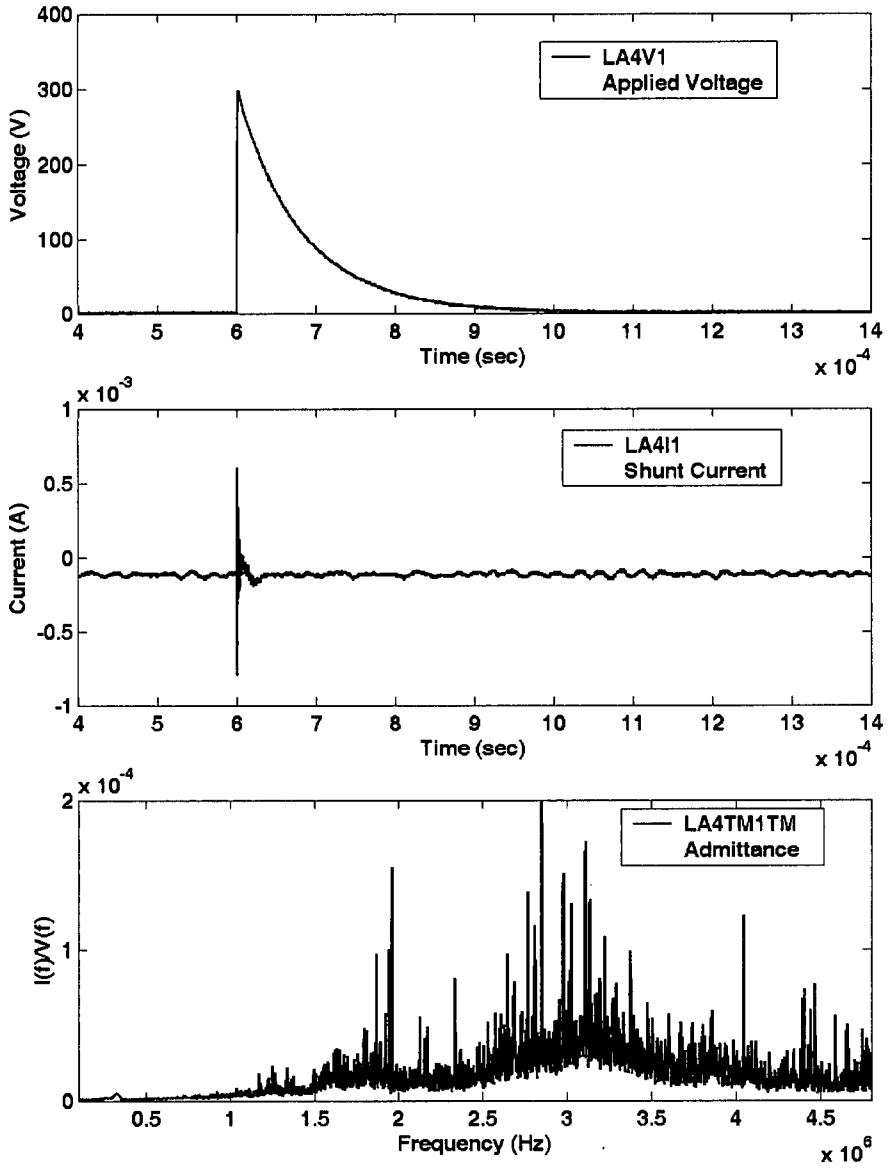


Figure 4.55 - Input waveform – LI, single pulse, 10 Ms/s rate
Input measured – voltage on H1
Output measured – H0 current

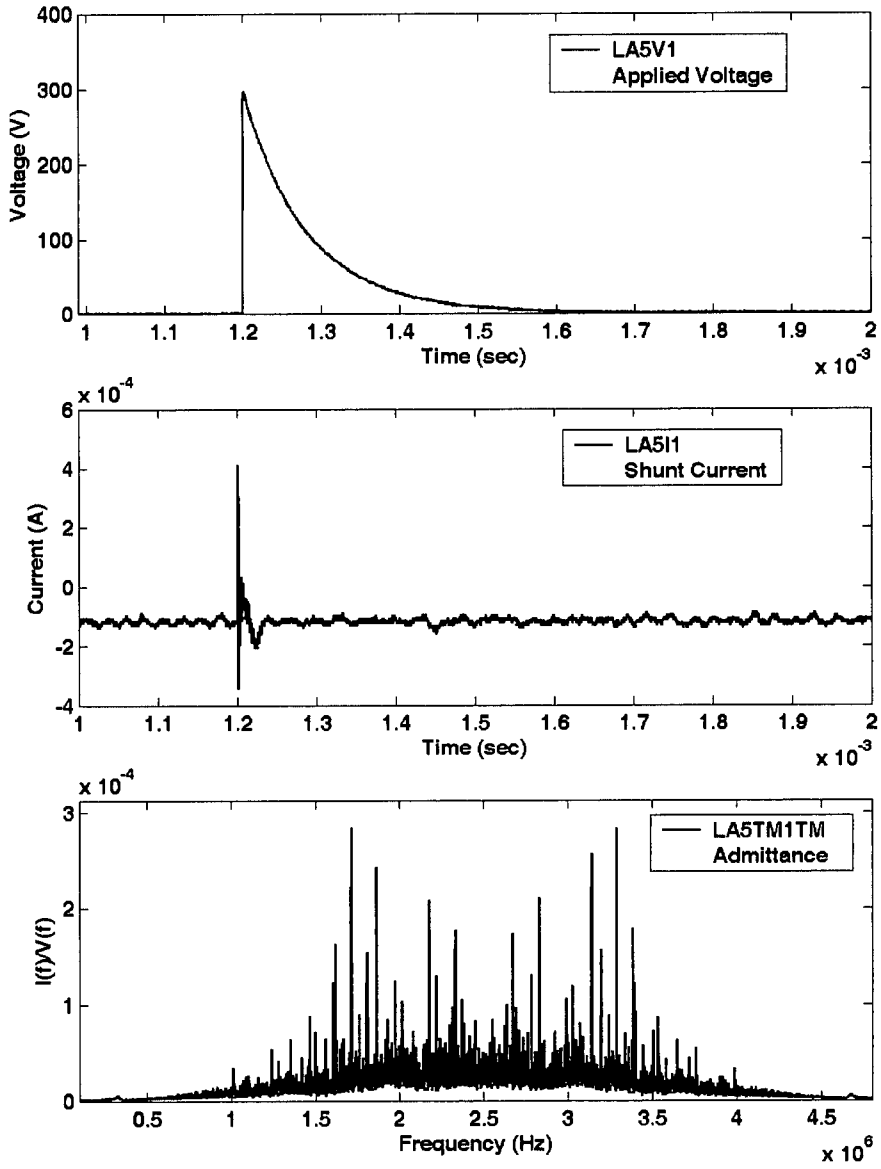


Figure 4.56 - Input waveform – LI, single impulse, 5 Ms/s rate
Input measured – voltage on H1
Output measured – H0 current

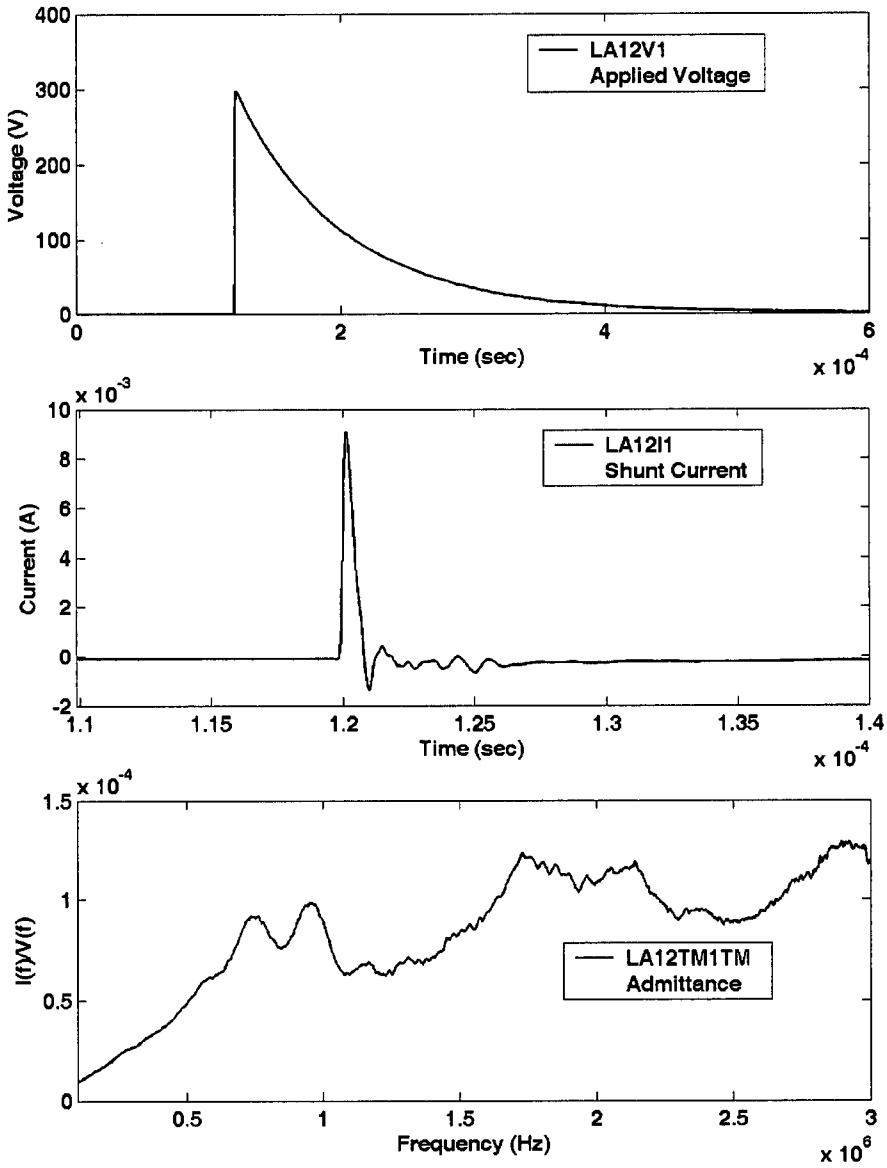


Figure 4.57 - 14.4 kV Transformer: X1, X3 floating
Input waveform – Lightning impulse, 250 shots avg., 50 Ms/s rate
Input measurement – H1
Load condition – secondary open (no load)
Output – HV winding current (H2)

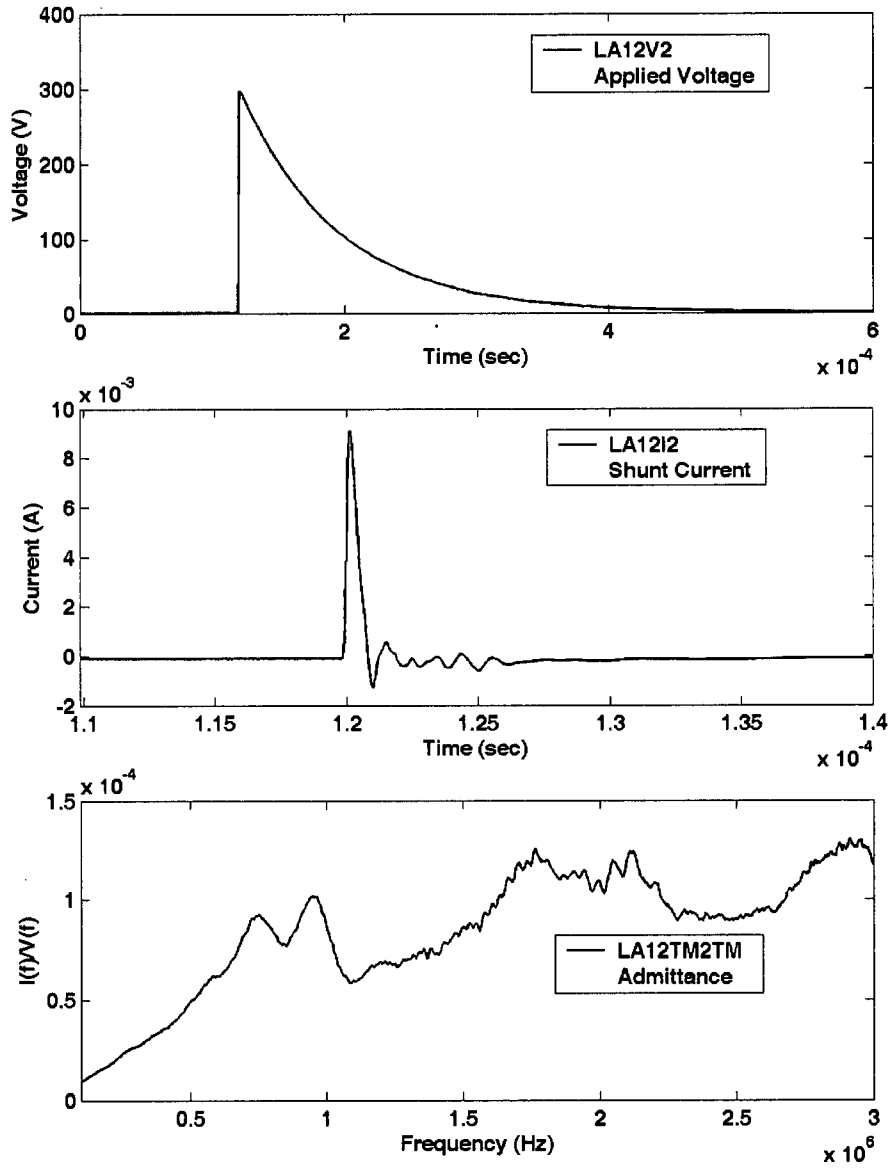


Figure 4.58 - 14.4 kV Transformer, X1, X3 floating
Input waveform – Lightning impulse, 250 shots avg.,50 Ms/s rate,
Input measurement – H1
Load condition – secondary with 3.9 Ω
Output – HV winding current (H2)

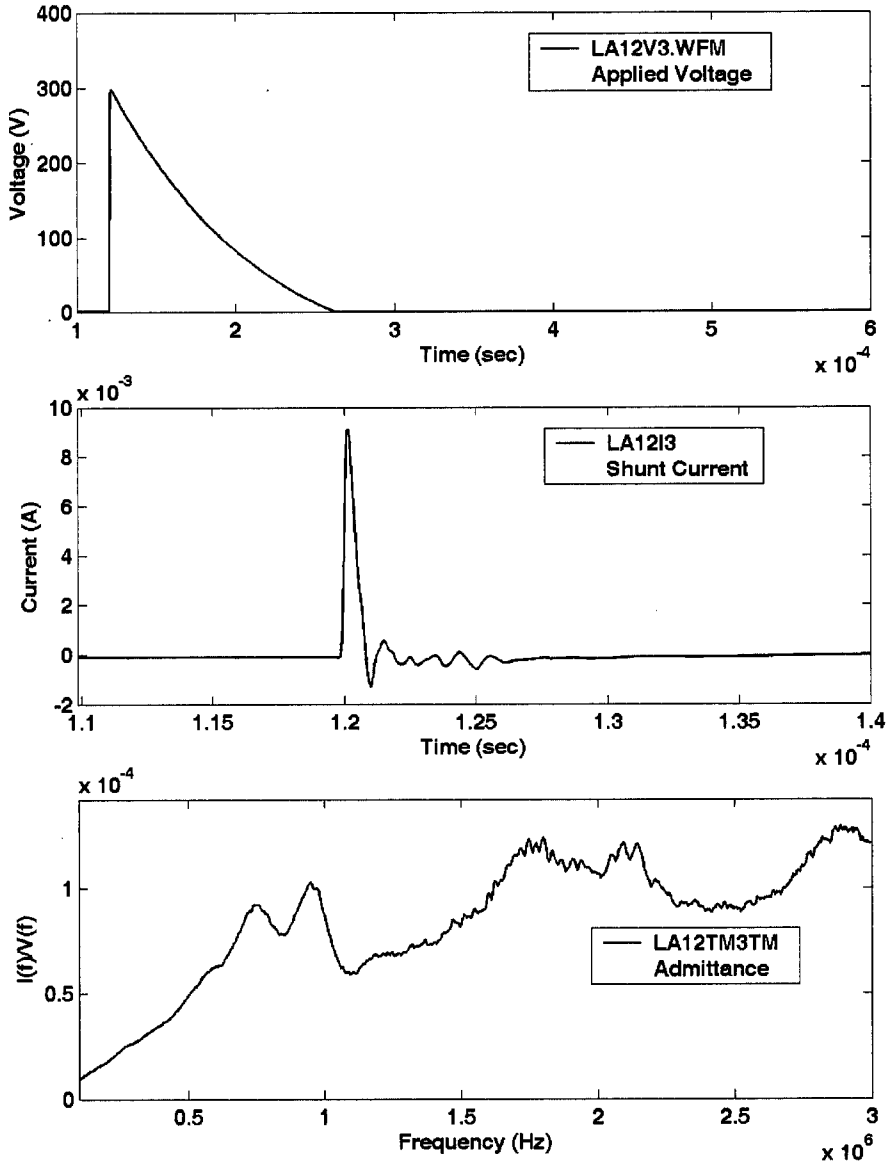


Figure 4.59 - 14.4 kV Transformer, X1, X3 floating
Input waveform – Lightning impulse, 250 shots avg., 50 Ms/s rate
Input measurement – H1
Load condition – secondary shorted
Output – HV winding current (H2)

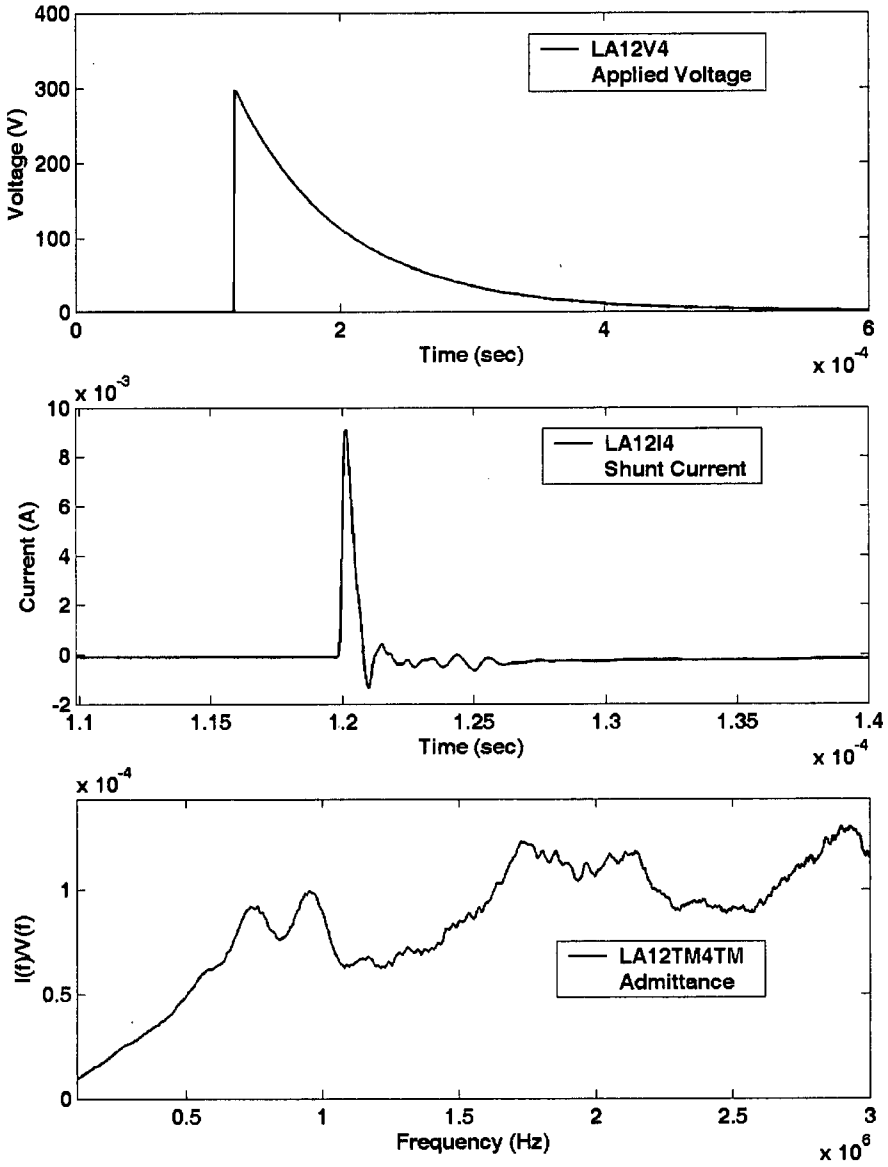


Figure 4.60 - 14.4 kV Transformer, X1, X3 floating
Input waveform – Lightning impulse, 250 shots avg., 50 Ms/s rate,
Input measurement – H
Load condition – secondary with 100 mH
Output – HV winding current (H2)

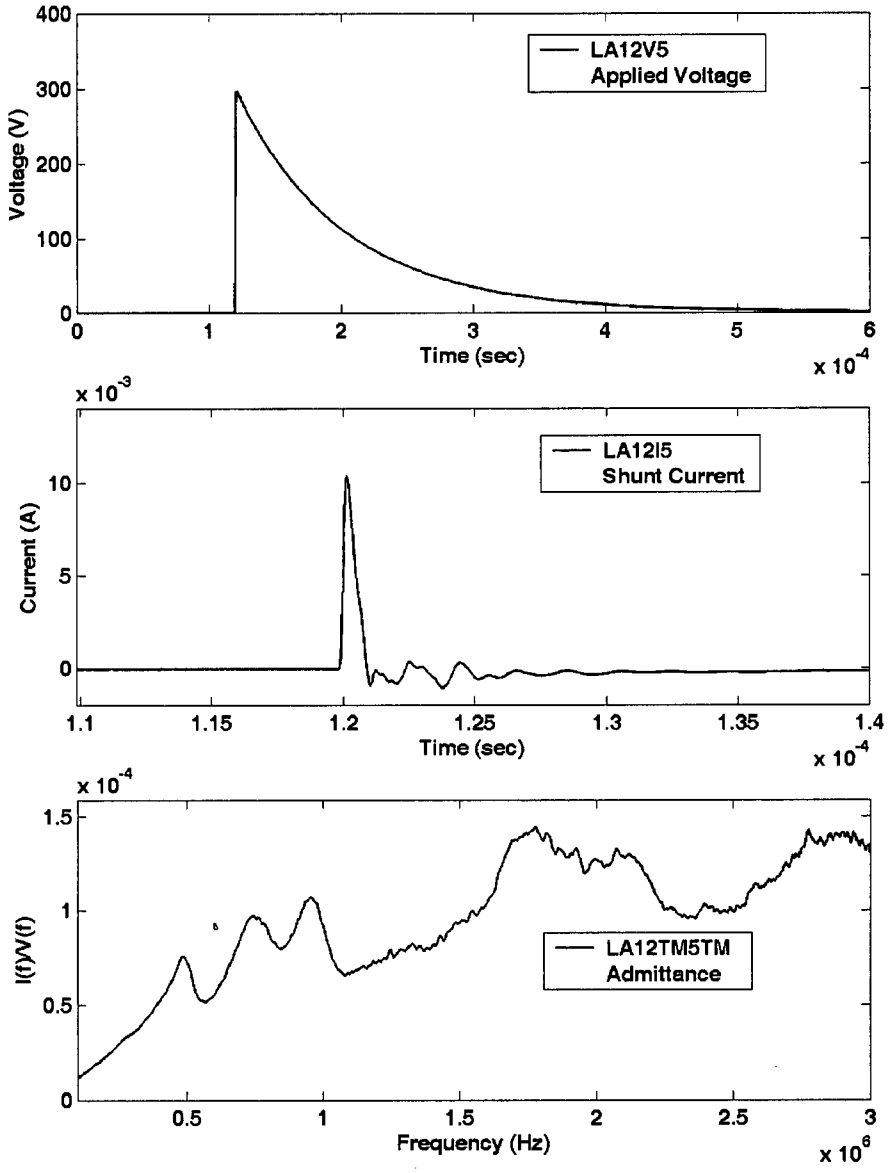


Figure 4.61 - 14.4 kV Transformer, X1, X3 floating
Input waveform – Lightning impulse, 250 shots avg., 50 Ms/s rate,
Input measurement – H1
Load condition – secondary open (no load)
Output – HV winding current (H2)

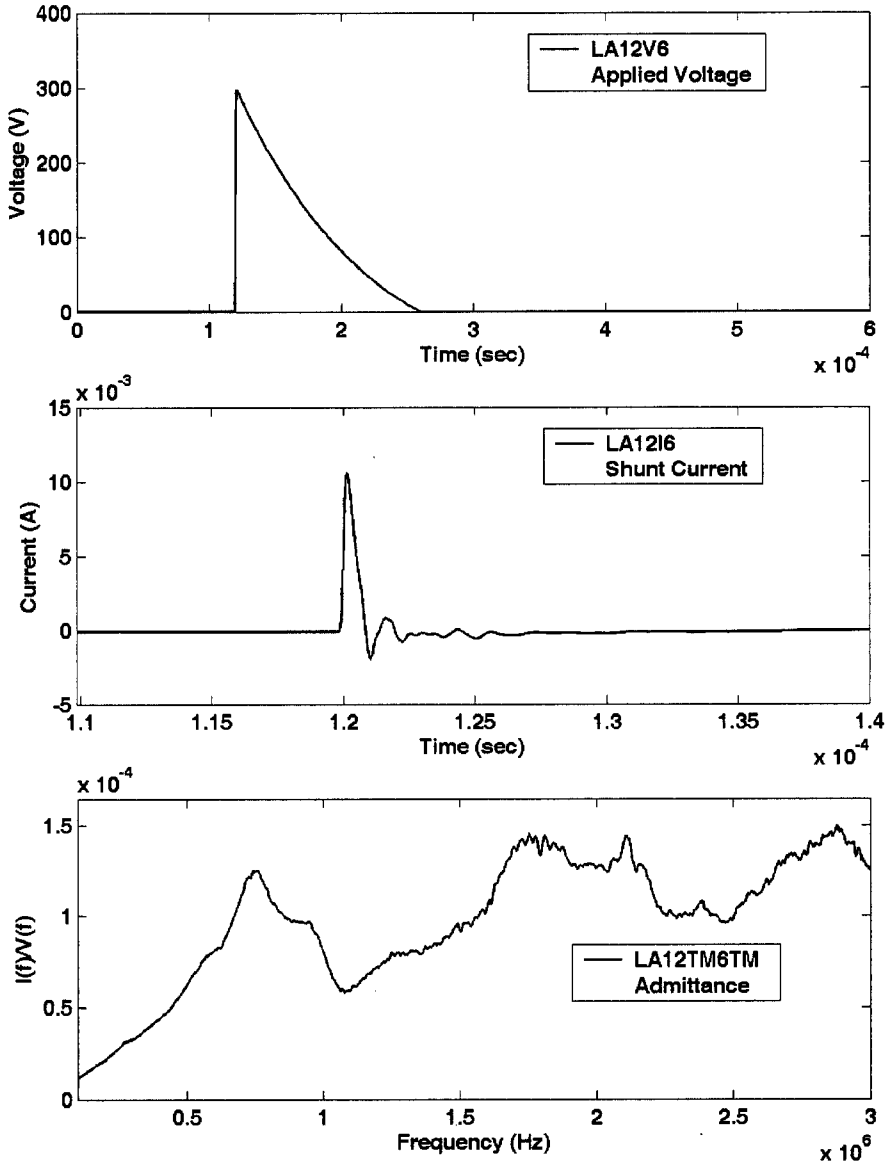


Figure 4.62 - 14.4 kV Transformer, X1, X3 floating
Input waveform – Lightning impulse, 250 shots avg.,50 Ms/s rate,
Input measurement – H1; Load condition – secondary shorted (X1-X3)
Output – HV winding current (H2)

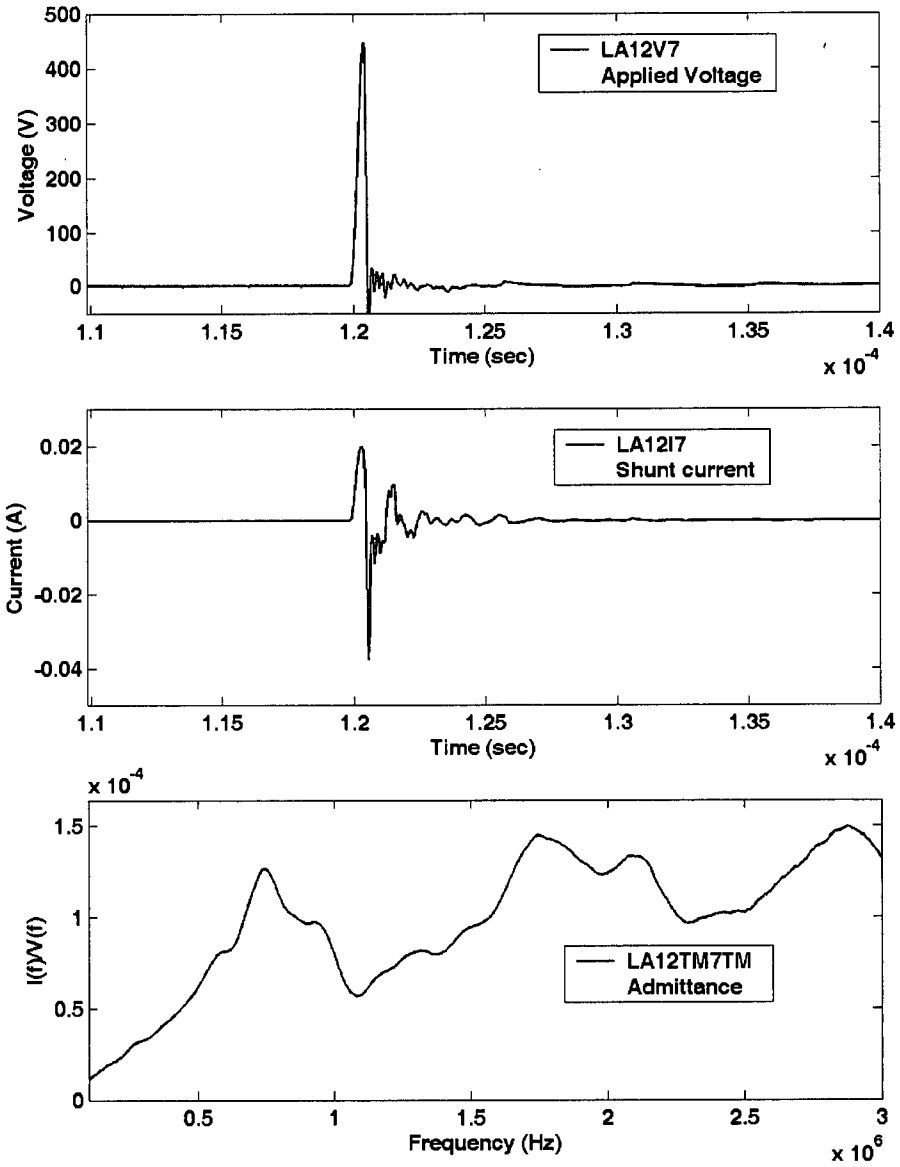


Figure 4.63 - 14.4 kV Transformer, X1, X3 floating
Input waveform – traditional LVI impulse, 250 shots avg., 50 Ms/s rate,
Input measurement – H1
Load condition – secondary shorted (X1-X3)
Output – HV winding current (H2)

The laboratory investigations in this section were aimed at evaluating the potential of doing on-line FRA testing using power system switching transients as the input signal source. The parameters explored were input source requirements, recording requirements (sampling rate, single shot vs. average multiple impulses), effect of measuring the input voltage by using the high voltage bushings capacitance taps and the impact of the transformer load.

The findings from the tests can be summarized as follows:

- With a lightning impulse input signal, the maximum usable frequency is 3.5 MHz, even when signal averaging is used to improve the vertical resolution of the eight-bit digitizer. With a single shot, the usable frequency drops to 2.5 MHz.
- If the bushing capacitance tap is used to measure the input signal, it will provide the same FRA test results as a direct measurement, up to a maximum frequency of 2 MHz.
- The sampling rate used for the single shot measurements has a major impact on the usable bandwidth. The maximum usable frequency was about 2.5 MHz with a 50 MHz sampling rate, 1 MHz with a 10 MHz sampling rate and 0.5 MHz with a 5 MHz sampling rate.
- The load applied to the secondary winding of the transformer had only a slight effect on the FRA test results.

It is concluded that the frequency content of even a lightning impulse will not be adequate for doing on-line FRA tests. A pulse source with a higher frequency content is required if measurements are to be done up to at least 3 MHz. The high voltage bushing capacitance tap has the potential to measure the input voltage for frequencies up to 2 MHz. A minimum sampling rate of 50 MHz should be used for on-line and single shot measurements. Surprisingly, the transformer secondary load had very little impact on the FRA measurement results up to 3 MHz. This finding would need to be investigated further to determine under what conditions it applies.

### 4.4.3 Transformer Test Results

The transformer tests show that it is feasible to use the bushing capacitance tap to measure the FRA signal. Figure 4.64 shows an overlay of the admittance measured directly and the admittance measured using the capacitance tap. For this test, the output of the capacitance tap was measured directly with no additional components connected to the tap.

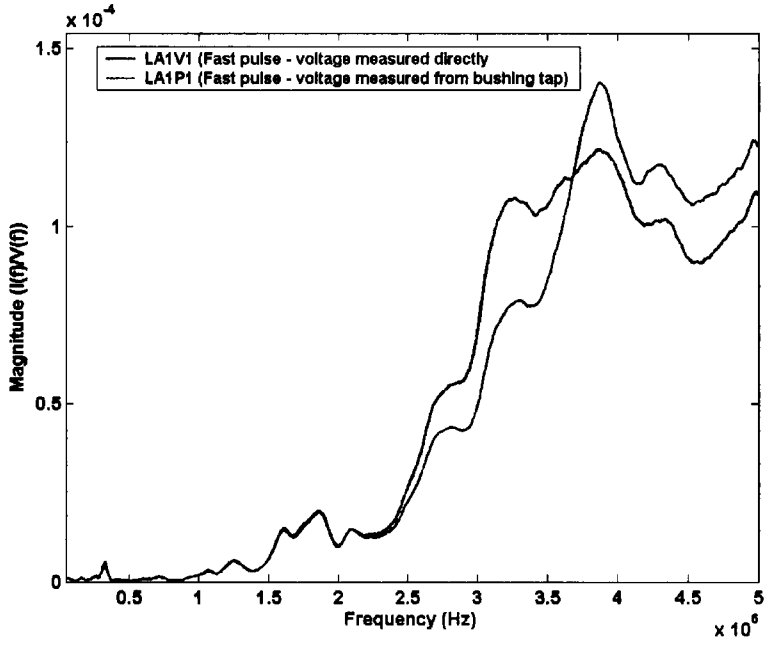


Figure 4.64 - Comparison of admittance with voltage measured directly and at bushing capacitance tap (C-tap)

Up to 2.5 MHz, the admittance is very similar, but above 3 MHz there is a large difference. Overall, the results are very good below 2 MHz. The differences at the higher frequencies are caused by the frequency response characteristics of the bushing tap. Internal resonances in the bushing cause the output signal to increase in the range from approximately 2.5 MHz to 3.5 MHz. Above 3.5 MHz, the bushing inductance begins to dominate and the voltage signal decreases.

Figure 4.65 shows an overlay of the admittance recorded using the conventional FRA pulse and a lightning impulse. It can be seen that there is no significant difference, except that at the higher frequencies the admittance measured with the lightning impulse is very "noisy". The measured transadmittance appears "noisy" because the lightning impulse waveform does not contain sufficient energy at the higher frequencies.

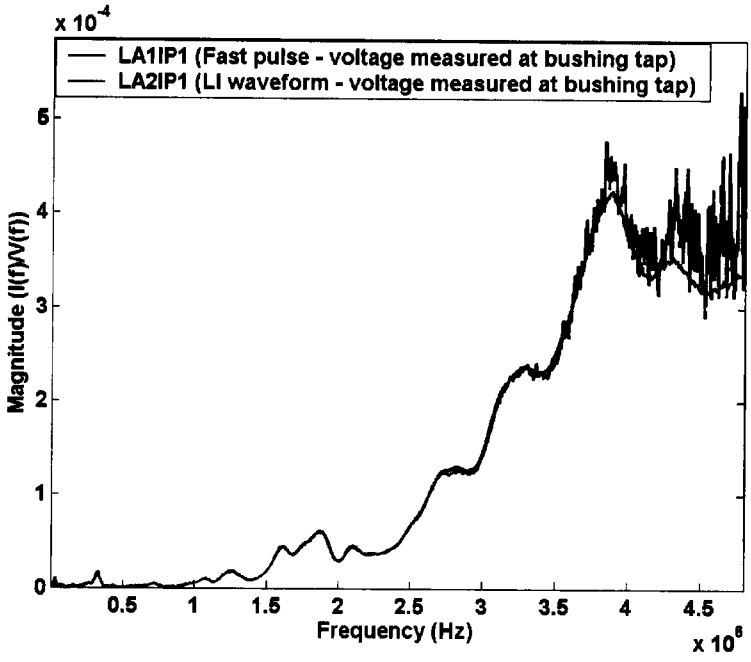


Figure 4.65 - Comparison of the admittance with FRA impulse and lightning impulse

When the single shot measurements were compared with averaging of 250 pulses, the noise level was found to be significantly higher with the single shot. The noise level in the measured signal was also very high with sampling rates of 10 Ms/s and 5 Ms/s. Further work needs to be done if the sampling rate is to be reduced (to reduce equipment cost). For example, adding an analogue anti-aliasing filter to the system or applying digital processing techniques may reduce the noise level in the signals.

The tests done to evaluate the effect of load on the secondary terminals of the transformer show very little difference in frequency response signatures when the load was changed from an open circuit to a short circuit. The effect was far less than expected. Field tests with various loads would be required to confirm these results on large power transformers.

### 4.4.4 Bushing Tap Coupling Box

The typical high voltage bushing consists of a high voltage capacitance in series with a capacitance brought out to a bushing tap. This capacitance tap is normally grounded in service. The tests on the 90 kV transformer showed that it should be possible to use the normally grounded high voltage bushing tap to measure the system transient voltages when doing the FRA test on-line. However, to use the bushing as a voltage divider an additional capacitance needs to be added in parallel with the capacitance tap to increase the voltage divider ratio. This is required to reduce the output voltage generated by the system transients to below the maximum voltage rating of the capacitance tap. Otherwise, the bushing insulation will puncture and the bushing will need to be replaced. In addition, the bushing tap coupling box must also filter out the 60 Hz voltages from the output to prevent excessive 60 Hz voltages at the tap in service, reduce the output voltage to a level suitable for the measuring equipment, and have an output impedance of 50 Ω to match to the measuring cable and measuring equipment.

In initial attempts to design a suitable coupling box, it was found that reducing the internal inductance of the coupling circuit was absolutely critical to a useful output signal. If the inductance were too high, the output signal would have excessive high frequency oscillation and would not be useable. The total capacitance used had to be kept as low as possible, since the internal inductance of the capacitors was a significant portion of the total circuit inductance. The requirement to reduce the capacitance to decrease the inductance conflicts with the requirement to increase the capacitance to reduce the output voltage level. The capacitors had to be mounted in a coaxial arrangement to make the system work.

A bushing tap coupling box that met the requirements was designed and tested. Figure 4.66 shows the schematic of the coupling box and Figures 4.67 and 4.68 show photographs of the box. A 360 kV bushing was used to develop and test the coupling box. It had a primary capacitance of 420 pF and a secondary capacitance of 6350 pF. These are typical values for high voltage bushings.

Figure 4.69 shows the transfer function of the bushing, using a standard lightning impulse waveform as the input signal to the bushing high voltage terminal. The results show a good response up to approximately 1 MHz. Above 1 MHz, the ratio starts to increase due to bushing and coupling box resonances.

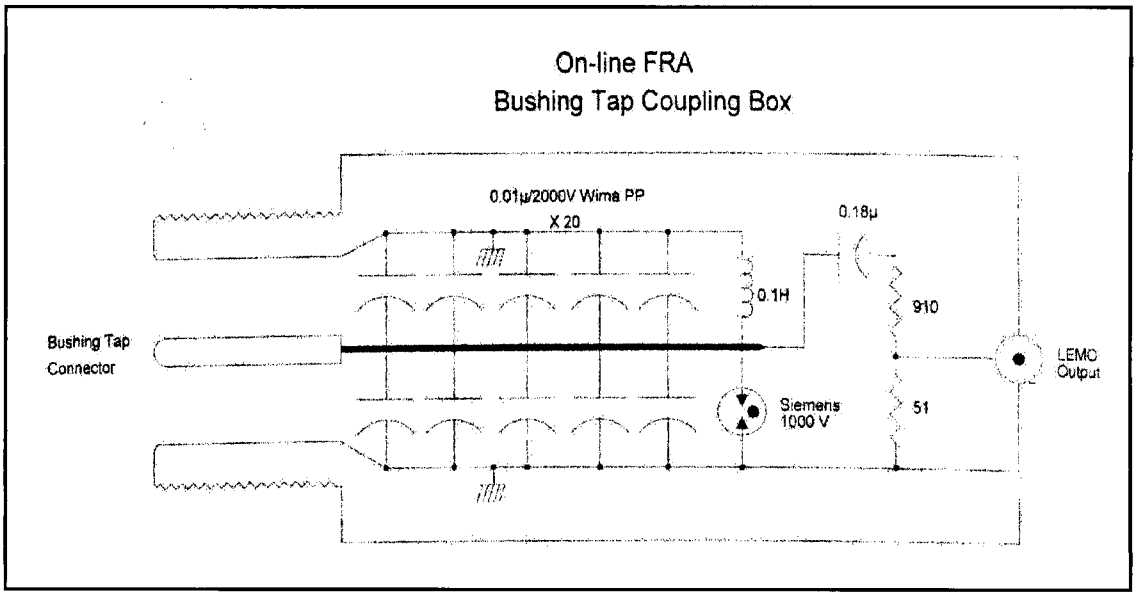


Figure 4.66 – Bushing tap coupling box

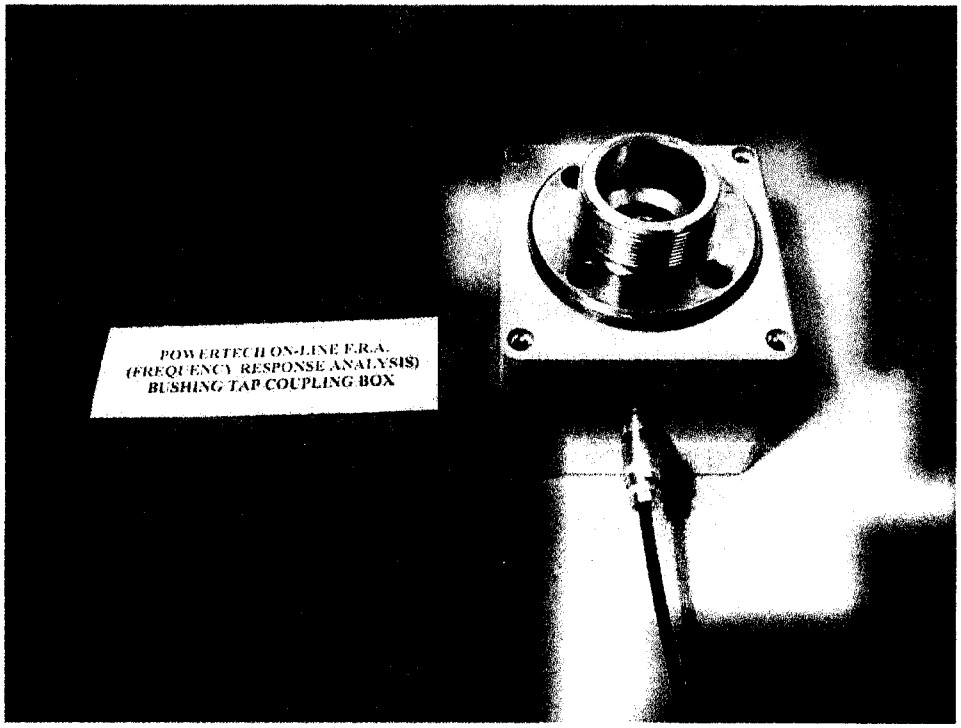


Figure 4.67 – Bushing coupling box (external view)

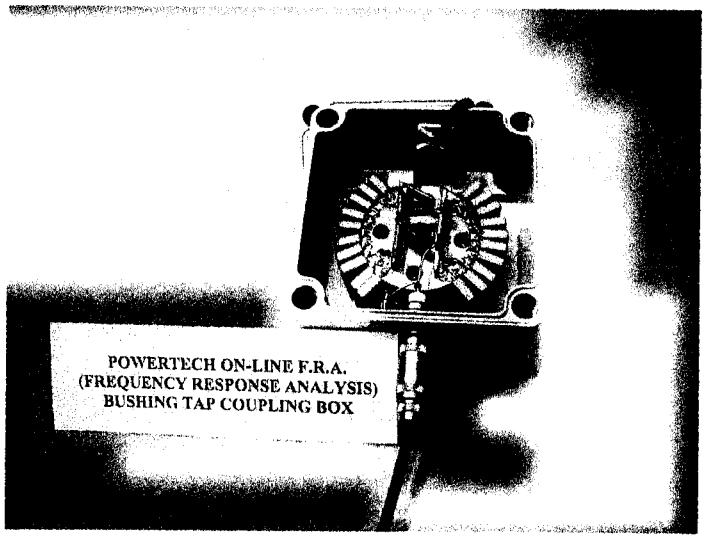


Figure 4.68 – Bushing coupling box (internal view)

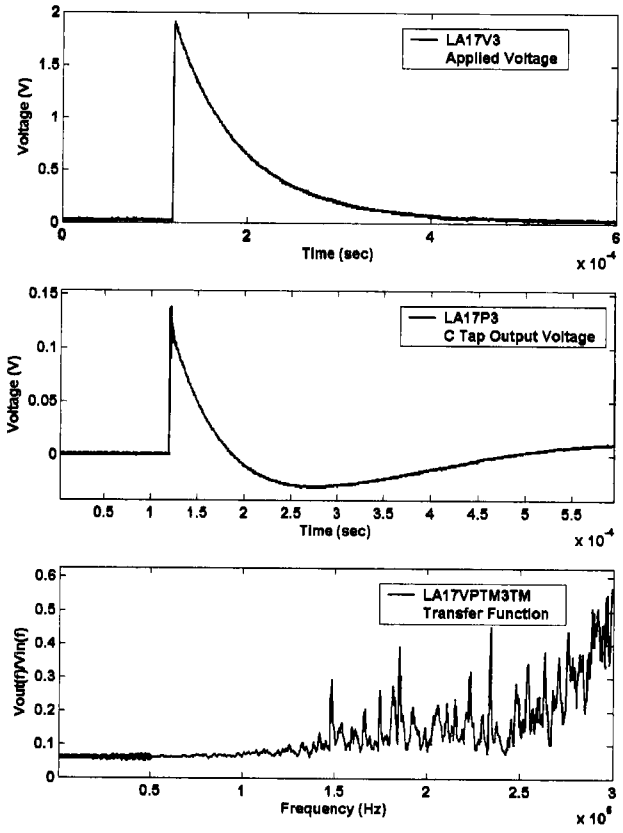


Figure 4.69 - Bushing tap termination test on bushing
Input waveform – standard LI, 250 shots avg., 50 Ms/s rate,
Input applied and measured at bushing H1 terminal,
Output measured at bushing tap termination output
(with 50 Ω termination)

### 4.4.5 Signal Injection Tests

A potential alternative method for performing an on-line test is to inject a signal into the high voltage bushing capacitance tap on the winding and to measure the response in another winding. Some tests were done to evaluate the feasibility of this technique. Conventional FRA signals were injected into the capacitance tap on the high voltage winding of the 90 kV transformer and the output signal was measured on the secondary winding X1 terminal. Table 4.3 lists the tests done to evaluate this technique.

The results showed that it is possible to inject and measure a signal into the transformer through the bushing tap. However, the frequency response signature changes with changes to the external impedance connected to the HV bushing. This would make it difficult to obtain consistent signatures.

Table 4.3 - Signal injection tests

| Figure No. | Test Condition |
|---|---|
| 4.70 | No bus on HV terminal (H1) |
| 4.71 | 9.4 m long bus on HV terminal (H1) |
| 4.72 | Signal injected into bushing capacitance tap (C-tap) through a 60 Hz filter |
| 4.73 | 718 VAC on HV terminal (H1) |

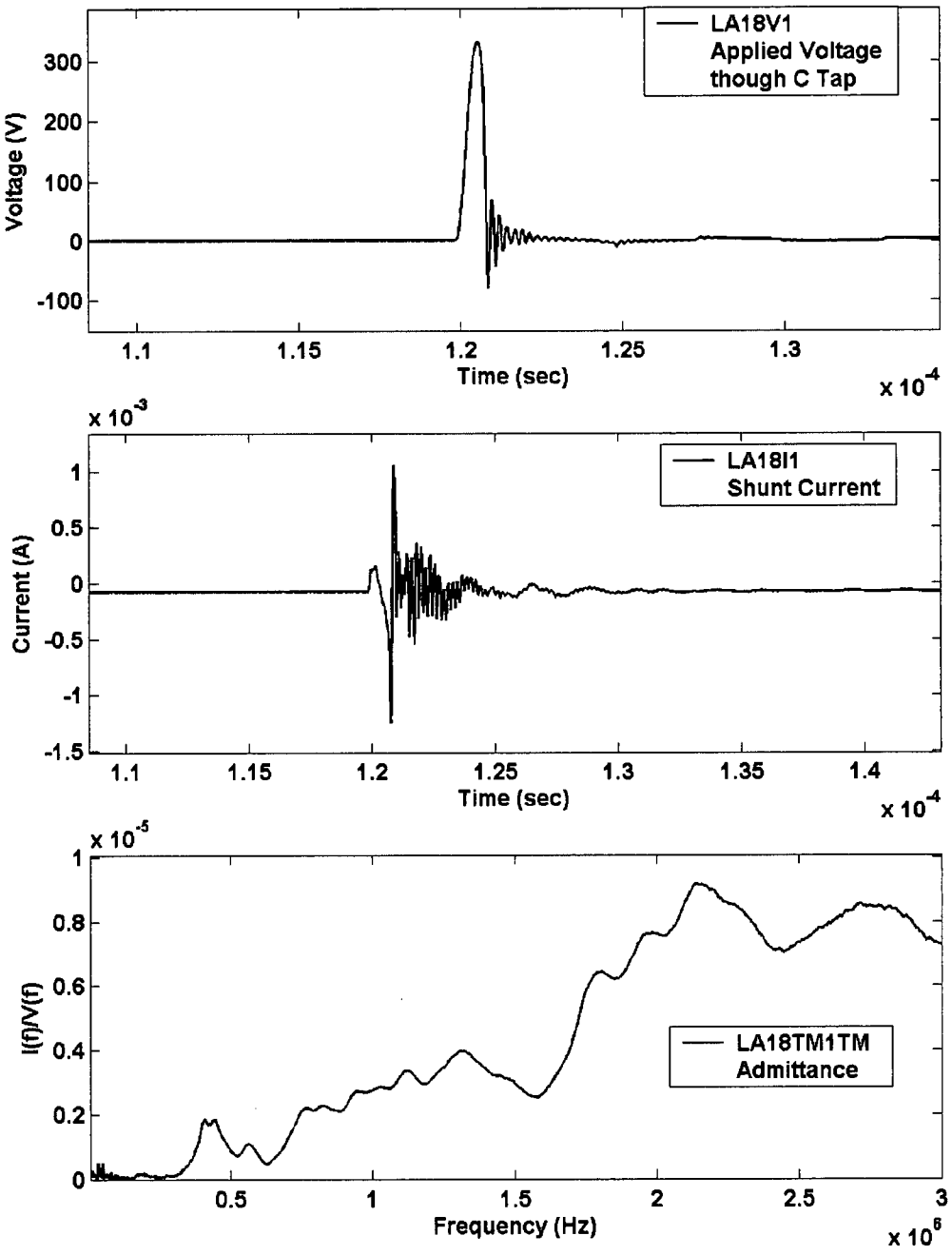


Figure 4.70 - 90 kV Test transformer with no bus on HV terminal (H1)
Input waveform – standard LVI pulse injected into bushing capacitance tap (C-tap), 250 shots avg., 50 Ms/s rate
Input measurement – C-tap
Output – X1 (through shunt)

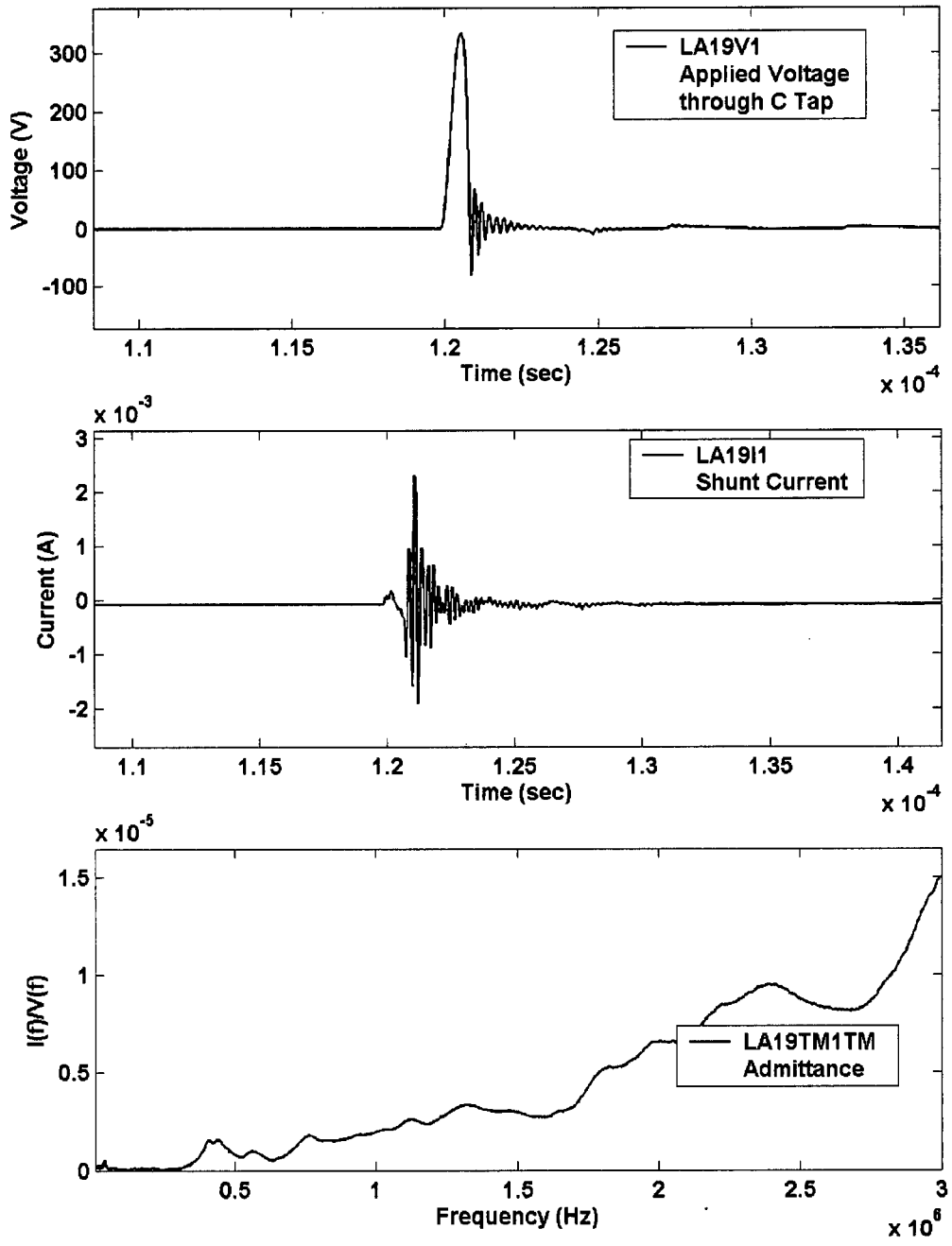


Figure 4.71 - 90 kV test transformer with 9.4 m bus on HV terminal (H1)
Input waveform – standard LVI pulse injected into bushing capacitance tap (C-tap), 250 shots avg., 50 Ms/s rate, injected into C-tap
Input measurement – C-tap
Output – X1 (through shunt)

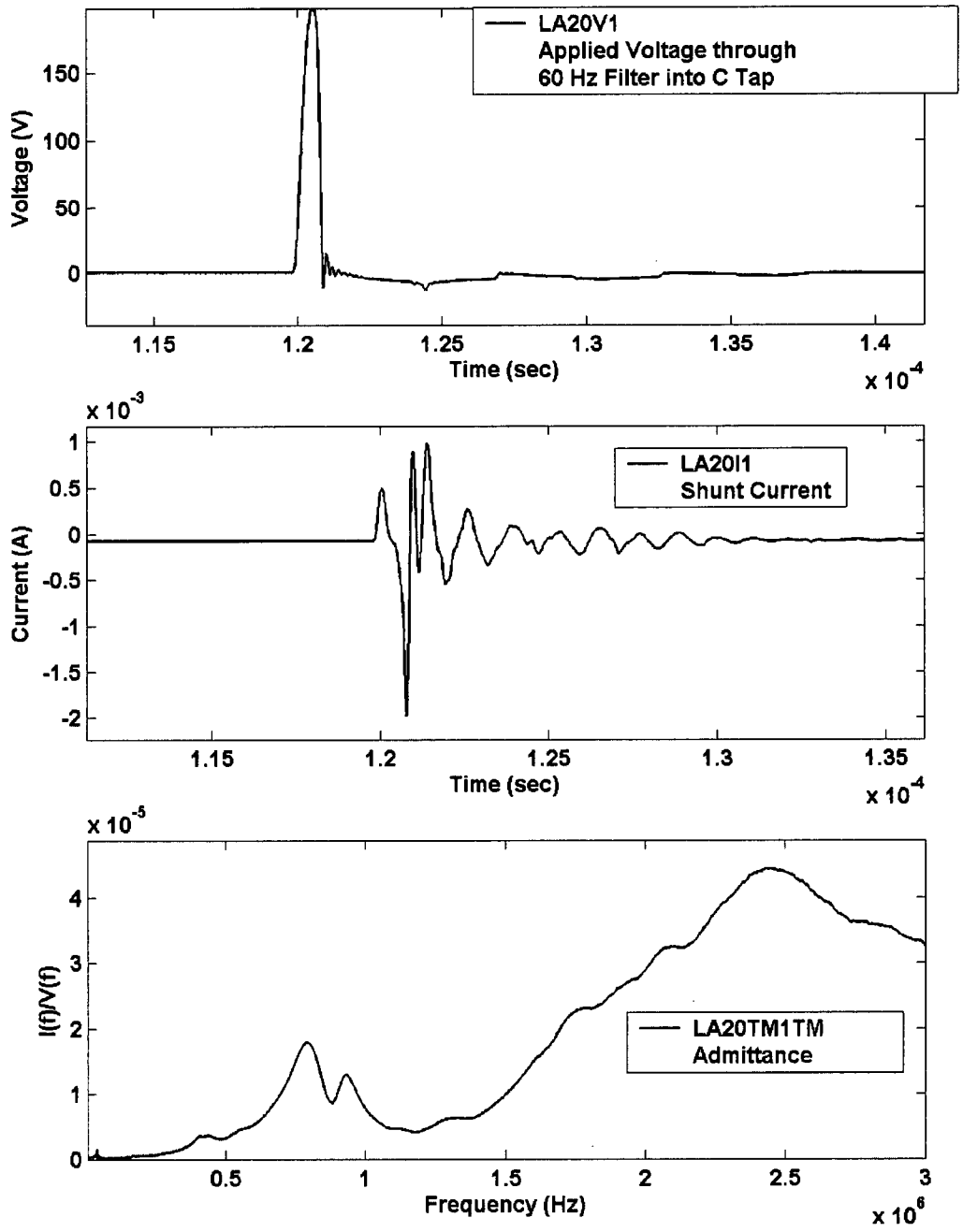


Figure 4.72 - 90 kV test transformer with 31' HV bus
Input waveform – standard LVI pulse, 250 shots avg.,
50 Ms/s rate, injected into bushing capacitance tap (C-tap) through
60 Hz filter
Input measurement – C-tap
Output – X1 (through shunt)

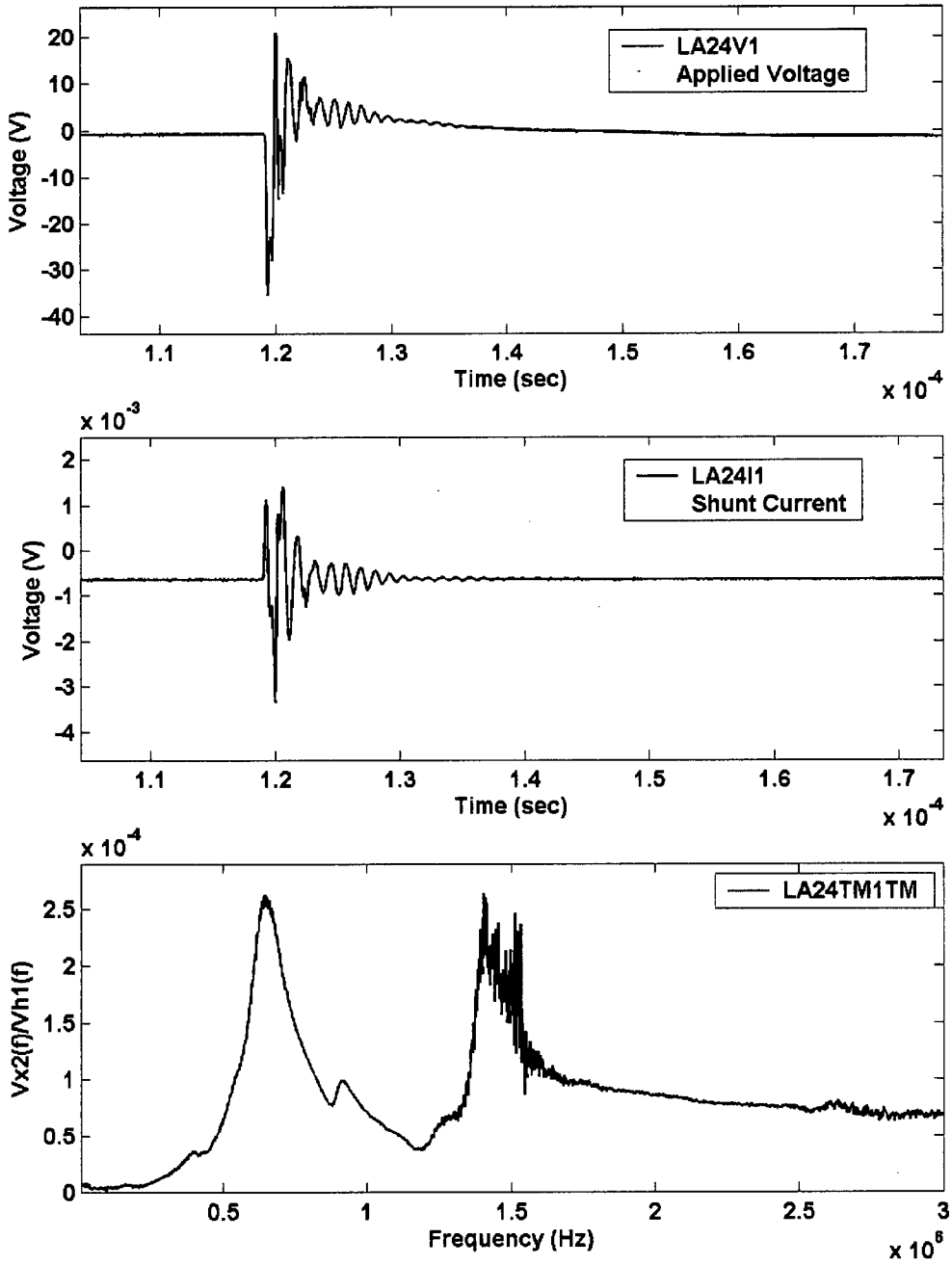


Figure 4.73 - 90 kV test transformer with 718 VAC on H1 bushing
Input waveform – standard LVI pulse, 250 shots avg.,
50 Ms/s rate, injected into bushing capacitance tap (C-tap) through 60 Hz filter
Input measurement – C-tap
Output – X1 (through shunt)

### 4.4.5 On-line Tests

Preliminary on-line FRA tests (transformer not isolated from the power system) were carried out on a single phase 63 MVA, 236-111 kV transformer and on a three-phase, 300 MVA, 330-138 kV transformer.

Two of the bushing tap coupling boxes described in Section 4.4.4 were used to carry out the tests. On the single-phase transformer, one coupling box was placed on the high voltage bushing and the other box was placed on one of the two low voltage bushings. On the three-phase transformer, the two coupling boxes were placed on two of the high voltage bushings. No coupling boxes were placed on the low voltage bushings on the three-phase transformer, as they had a tap design that required a different insert on the box.

The transformers were left connected to the power system but were first de-energized by opening a disconnect switch on the high voltage side of the transformer. The transformer was then re-energised by closing the disconnect switch. The transient signals generated were recorded with a conventional eight-bit oscilloscope. Figures 4.74 and 4.75 show the results of the measurements.

An analysis of the data shows that it is feasible to measure the signals at the bushing taps. The transients generated contained usable data up to a maximum frequency of about 0.8 MHz.

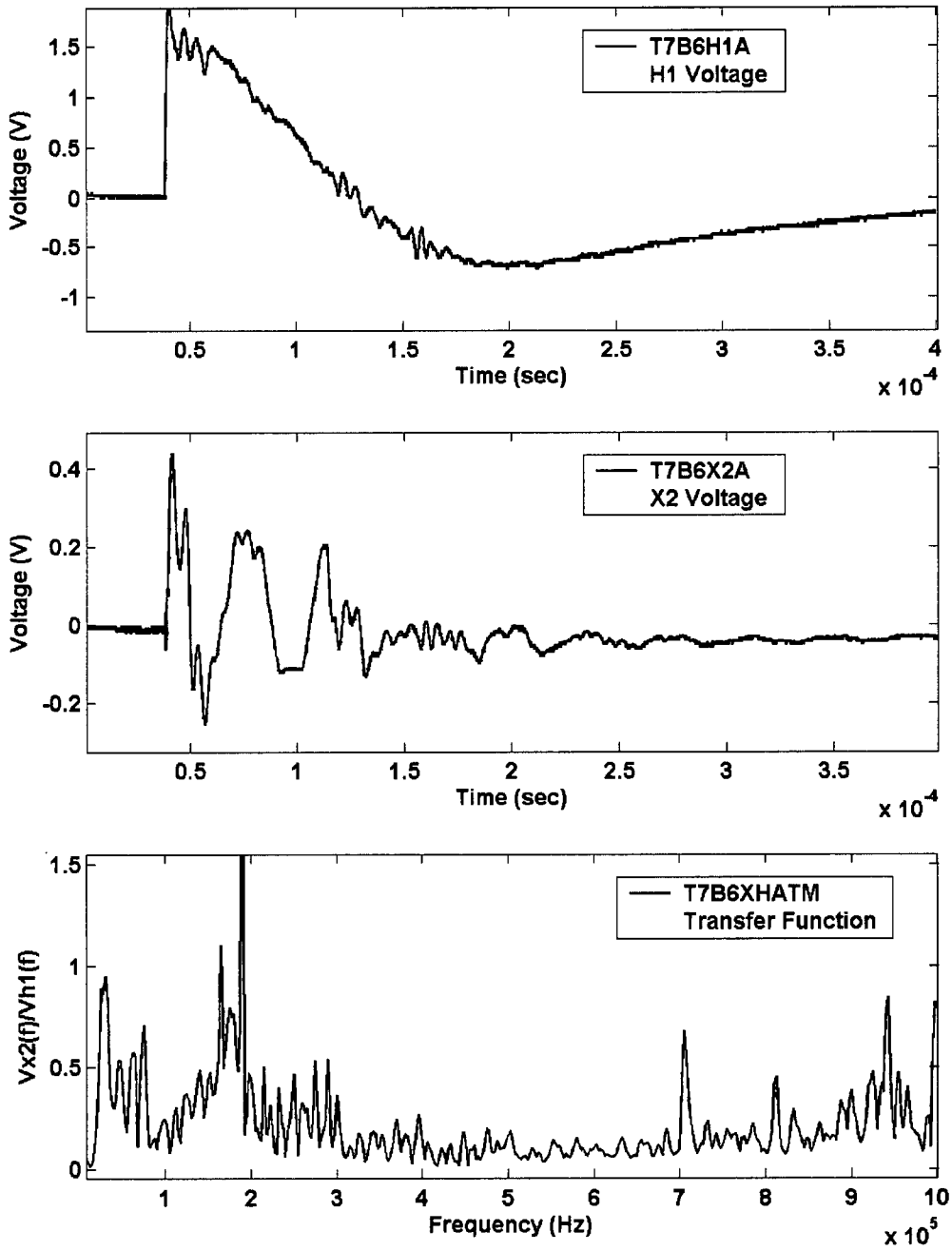


Figure 4.74 - 63 MVA transformer on-line transfer function

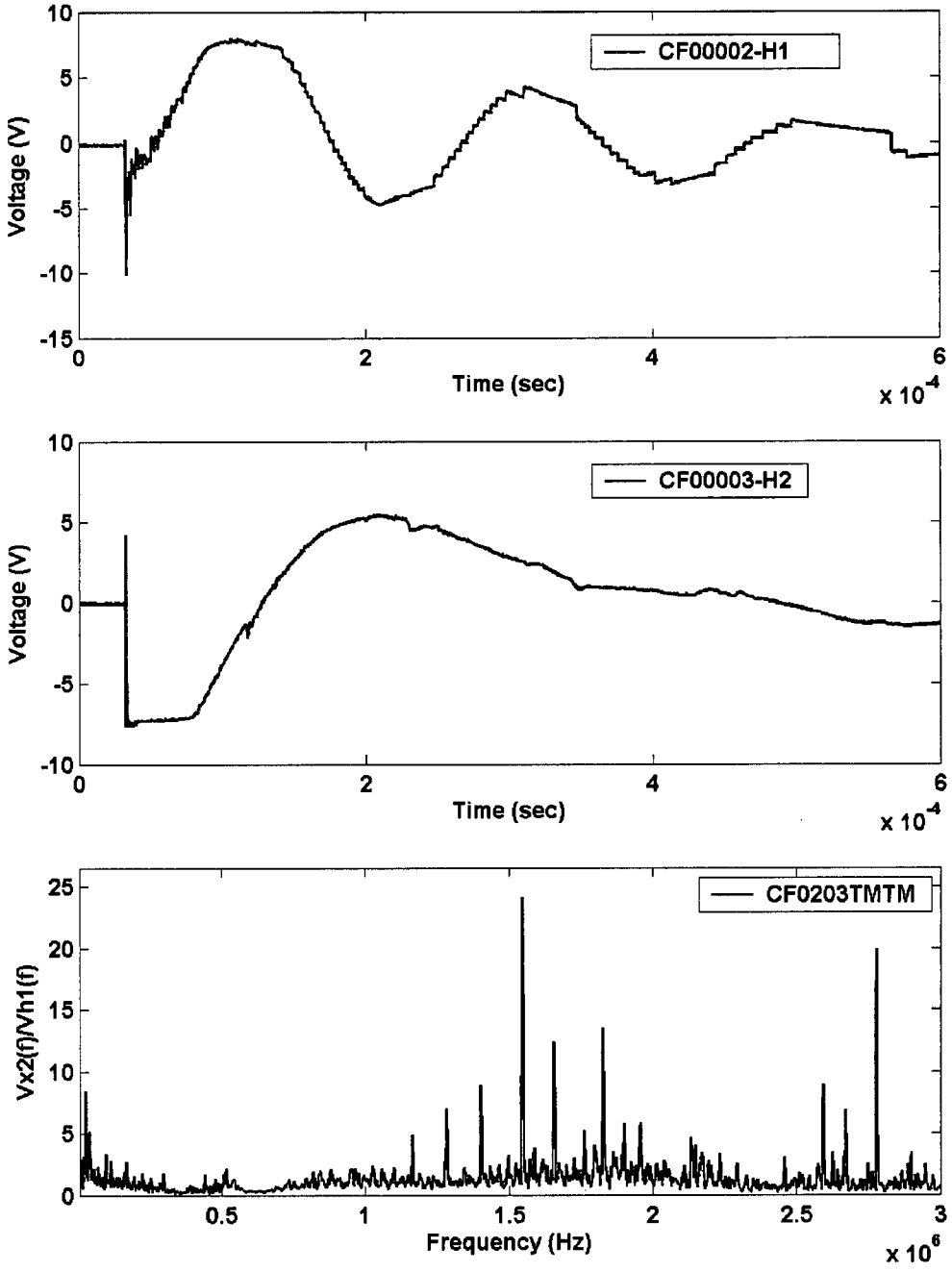


Figure 4.75 - 300 MVA transformer on-line transfer function

### 4.4.6 Discussion

The work to establish the feasibility of using the FRA test on-line shows that the transformer high voltage bushing capacitance taps can be used as a voltage divider to measure system transients for use as on-line FRA input signals. The on-line tests showed that applied voltage from disconnect switching can be measured using the bushing taps. The frequency content of the measured signals was not as high as is used for the off-line tests (0.8 MHz vs. 3 MHz). This means the on-line test will not be as sensitive to changes in the transformer as the off-line test. In general, a smaller winding movement usually shows in the higher frequency region. Both the computer simulation results in Appendix A and the measurement results in Chapter VI demonstrate this phenomenon. The bushing tap coupling box design was successfully used to carry out on-line tests on two transformers. A number of problems with this test method were apparent from the laboratory and field tests:

- The bushing tap termination output to input ratio (frequency response) is constant only to about 1 MHz.

- The signal available from the system transients is limited to less than 1 MHz.

- Injecting a signal in the bushing tap and measuring the input at the bushing capacitance tap does not produce measurements independent of the load external to the transformer

These problems limit the usefulness of this on-line test method.

## 4.5 Summary of Off-line and On-line Experimental Work

It is clear from the off-line tests (transformer de-energized and isolated) that both the impulse FRA (I) test method and the swept frequency FRA (S) method are capable of detecting winding deformation in laboratory experiments. Both methods are sensitive to changes in instrument location, lead and grounding arrangements, and measuring circuit impedances. Repeatability is dependent upon consistent arrangement of these parameters. Both methods are sensitive to axial winding deformation. Both methods are viable, but the measurement parameters are important to achieve the greatest sensitivity and repeatability. The transformer impedance at the higher frequencies is quite low (e.g., 1 Ω). The ground level instrument location and higher

series measurement impedance (50 Ω vs.10 Ω of the impulse shunt) cause the observed lower sensitivity of the FRA (S) method for some tests.

The on-line tests (transformer remains connected to the power system) showed that applied voltage from disconnect switching can be measured using the bushing taps. The frequency content of the measured signals was not as high as is used for the off-line tests (0.8 MHz vs. 3 MHz). This means that the on-line test will not be as sensitive to changes in the transformer as the off-line test. The limited energy content of power system transients at high frequencies limits the maximum frequency that can be measured with an on-line test using system transients. To improve the frequency range of the on-line test, other methods to obtain an input signal with higher bandwidth would need to be investigated.

The work to establish the feasibility of using the FRA test on-line shows that the transformer high voltage bushings capacitance taps can be used as a voltage divider to measure system transients for use as on-line FRA signals. The high voltage bushing capacitance tap has the potential to measure the input voltages below 2 MHz. At frequencies higher than 2 MHz, bushing capacitance tap measurement may still be workable but it will not be linear. The transformer secondary load has very little impact on the FRA measurement results in the 0.1 MHz to 3 MHz range.

# CHAPTER V DATA ANALYSIS

## 5.1 Introduction

The electromagnetic structure of a large power transformer is a very complex network that consists of distributed resistance, capacitance and inductance. When there is winding movement, the distributed parameters change and cause the FRA signature to change. When the winding movement is small, particularly for the loss of winding clamping pressure, it is more difficult to detect.

The equivalent circuit involved in an individual FRA measurement includes test leads and is affected by many factors: the size of the conductors, diameters of the coils, distance between the coils, distance between the windings, number of turns, type of core, winding configuration, type and thickness of insulation, geometry and size of supporting material. There is a direct relationship between the geometry of the core-winding configuration and the network of distributed resistive, capacitive and inductive elements of the equivalent circuit.

Since the admittance of the capacitive and inductive elements is frequency dependent, the contribution of each element to the transfer function varies with frequency, making the equivalent circuit unique at each frequency. Therefore, the signature uniquely describes the geometry of the core-winding configuration for a given unit and contains a great deal of diagnostic information. Since the transfer function is a complex variable, it is described by both the magnitude and the phase angle. In general, the FRA signature of a transformer is unique to that transformer design. Every change in the transformer or in the test set-up will have an impact on the shape of the signature. When signatures of different phases on the same transformer are examined, differences may be observed between phases. These differences can be due to minor design differences — for example, the differences associated with the layout of internal connections.

FRA data has been collected during years of research and field experimental work, yet it is still a challenge to evaluate a transformer's condition through its FRA measurement results. Some potential FRA data analysis methods were investigated.

## 5.2 Data Analysis

Very little research has been done on the analysis of the FRA data to assess the looseness of transformer windings. Using the FRA method to detect winding looseness is still new to most utilities, testing facilities and research laboratories. In most cases, a limited amount of data is available on a particular transformer for comparison. Many factors other than changes in the transformer can contribute to changes in the FRA results. If the measurements are not taken with a great deal of care, the data will not be valid.

The comparison of the FRA signatures on the transformer is normally done by visual comparison of the test results by personnel experienced in interpreting the data. An evaluation method is needed that can be effectively applied by inexperienced personnel. Three proposed evaluation techniques are described and evaluated in the following sections.

The techniques were compared using test data on seven identical 300 MVA, 3 phase transformers. FRA tests were done on each transformer using six configurations (two per phase). One of the transformers was in known good condition. The other six transformers were compared to the good transformer. The visual ranking is compared to the three proposed techniques.

### 5.2.1 Maximum Admittance Difference

The maximum difference in the admittance between the reference transformer and the tested transformer is measured.

$$Max\ [A_1(f) - A_2(f)]$$

The transformers are ranked according to the average of the difference for the six tested configurations.

### 5.2.2 Difference in Admittance Area

The area under the each admittance curve is calculated as follows:

$$\int [A(f)] * df$$

The transformers are then ranked according to the difference in the area between the two transformers being compared.

### 5.2.3 Difference in Absolute Value of Admittance Area

The admittance of the test transformers is lower than the reference transformer at some frequencies and higher at other frequencies. This leads to the admittance differences at different frequencies cancelling each other out. This can be corrected by taking the integral of the absolute value of the difference in the admittance of the two transformers, as follows:

$$\int \left| \{ [A_1(f)] - [A_2(f)] \} \right| * df$$

The transformers are ranked according to the difference in the area between the two transformers being compared.

## 5.3 Comparison of Evaluations

Table 5.1 compares the ranking according to the described evaluation techniques. The transformers are ranked from 1 to 6, with 1 showing the least movement and 6 the most. The values in brackets are the calculated values normalized to the value for the lowest ranked transformer.

Table 5.1 - Technique comparison

| Method | Ranking | | | | | |
|---|---|---|---|---|---|---|
| *Visual* | *1* | *2* | *3* | *4* | *5* | *6* |
| Max. Admit. Diff. | 1 (1) | 2 (3.7) | 4 (5.3) | 6 (23) | 3 (4.0) | 5 (6.0) |
| Diff. In Admit. Area | 1 (1) | 2 (1.7) | 5 (7.1) | 6 (7.9) | 3 (2.0) | 4 (3.9) |
| Diff. in Abs. Areas | 2 (1.8) | 1 (1) | 5 (23) | 6 (28) | 3 (5.3) | 4 (13) |

## 5.4 Discussion

The visual evaluation of FRA test data was similar to the three mathematical methods, but the rankings differed between the methods. Further investigation is required to determine the best evaluation method.

The new methods do provide assistance to decision makers on ranking transformer condition.

There are several other techniques that may prove useful in the comparison of FRA test results but which have not been evaluated in this work. These include:

1. Admittance pass bandwidth change
2. Admittance peak magnitude change
3. Admittance peak frequency peak shift
4. Admittance area difference vs. frequency
5. Admittance accumulated area curves vs. frequency
6. Analysis of transfer function phase data to obtain further information on transformer condition, such as insulation quality
7. Pattern recognition techniques
8. Expert systems to analyse the data

In the future, some of these techniques could be investigated for correlating changes in the transformer to changes in the signatures.

# CHAPTER VI KEY FACTORS AFFECTING FRA MEASUREMENTS

FRA results are not only related to transformer internal winding movement and condition, but are also affected by measurement systems such as leads arrangement, leads length, leads connection, shunt value and shunt connection as well as digital measuring technique etc. In order to identify all the key factors that contribute to FRA measurement results, the following experiments were performed. The results also show what the critical factors are over selected frequency ranges.

## 6.1 Voltage Source Effect

In order to obtain true measurement results from the FRA measuring system, it is important to identify that the voltage source signals have an adequate frequency range and output signal level. A 14.4 kV distribution class transformer was used in this investigation as a measurement object. Two signal generators were used for comparison, as follows:

A) RSG - recurrent surge generator
B) PEMI – high voltage pulse generator

Figure 6.1 shows the comparison of transformer FRA (admittance) results by using the RSG and PEMI generators in the frequency range of 0 to 3 MHz. Figure 6.2 shows the same results, but in the frequency range between 0 and 10 MHz. Figure 6.3 shows the results in the frequency range between 0 and 25 MHz. The shunt value for all the measurements was 10 Ω. From the published literature and utility practice, most research work on FRA work has been done to a maximum of a few MHz (3 MHz), mainly due to measurement difficulties. The study shows that the signals generated by the two generators were sufficient in this frequency range. Figure 6.1 demonstrates that identical results can be obtained in the 0 to 3 MHz range from these two signal generators.

Figures 6.4 and 6.5 and Figures 6.6 and 6.7 demonstrate the voltage signal frequency spectrum from the two generators. The plots illustrate that the signal energy from the RSG Generator is adequate only up to 5 MHz, while the signal energy from the PEMI generator can be adequate as high as 11 MHz when used for FRA measurements.

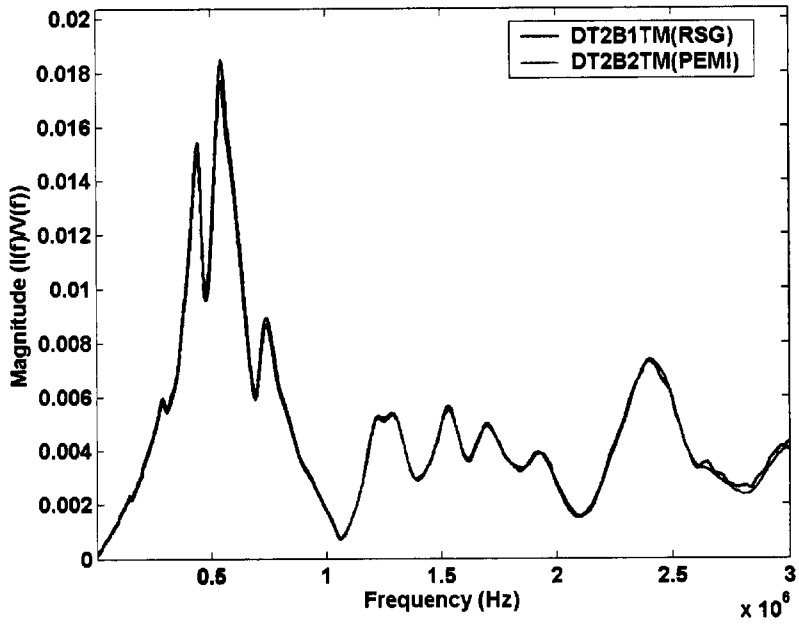


Figure 6.1 – Comparison of results with recurrent surge generator (RSG) and high voltage pulse generator (PEMI) to 3 MHz

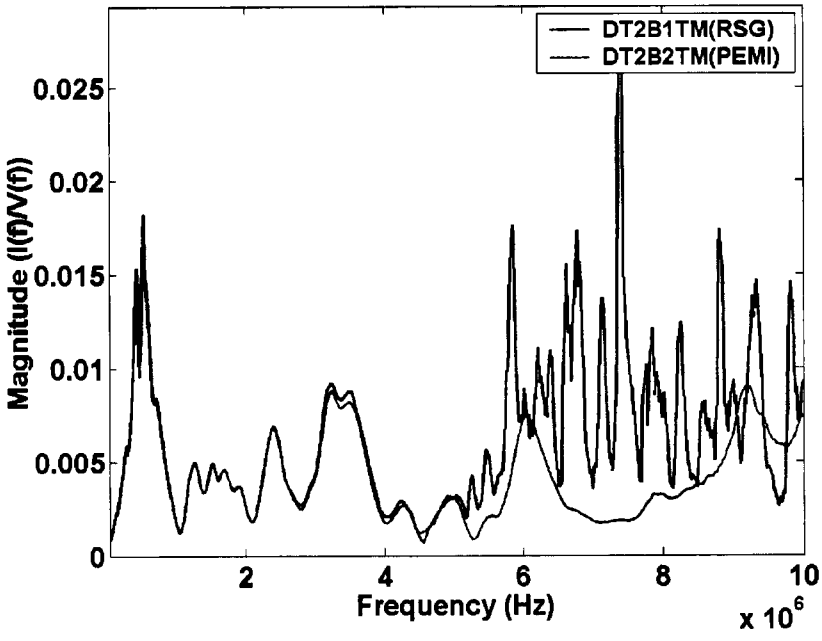


Figure 6.2 - Comparison of results with recurrent surge generator (RSG) and high voltage pulse generator (PEMI) to 10 MHz

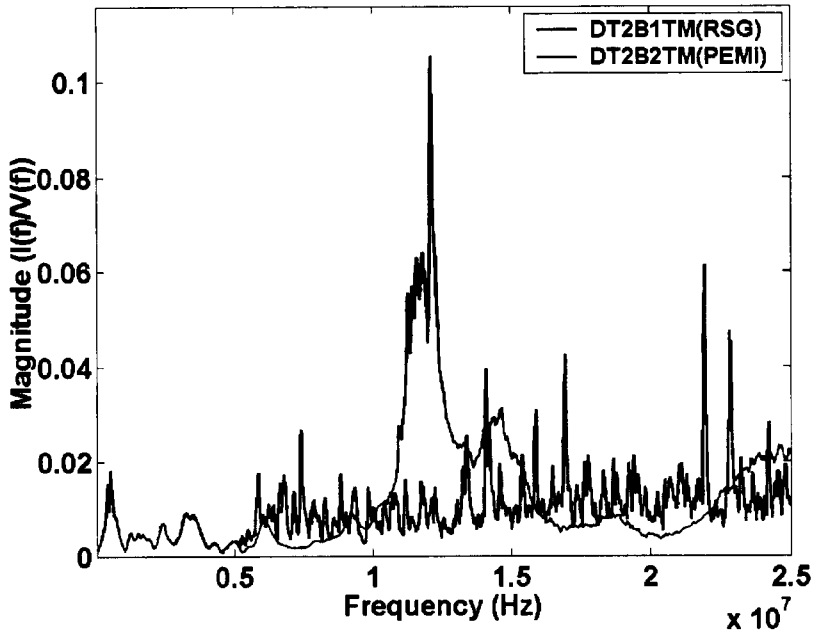


Figure 6.3 - Comparison of results with recurrent surge generator (RSG) and high voltage pulse generator (PEMI) to 25 MHz

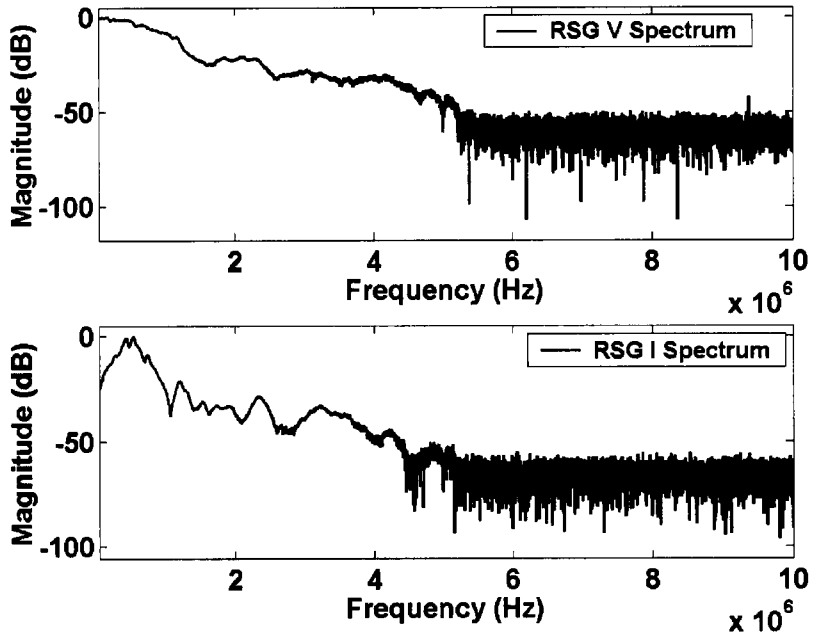


Figure 6.4 – RSG measurements spectrum to 10 MHz

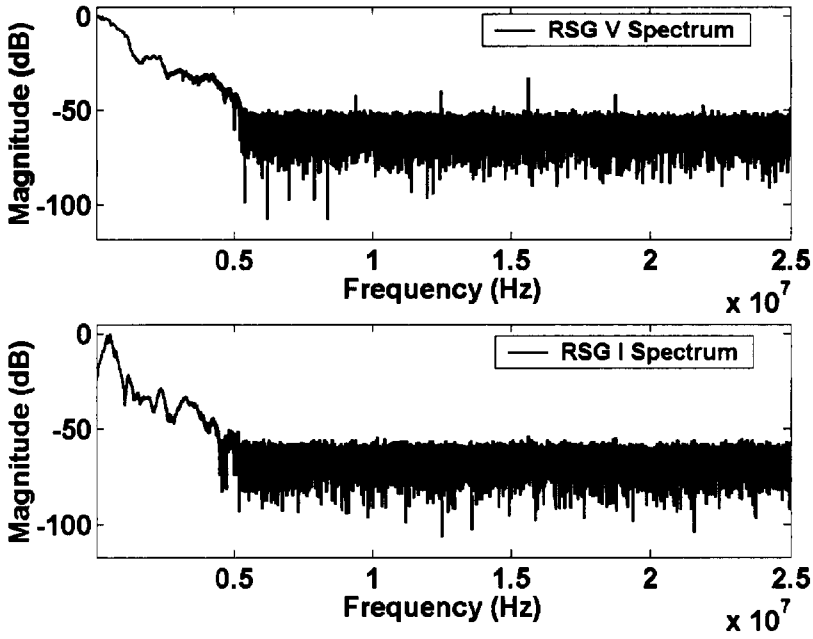


Figure 6.5 – RSG measurements spectrum to 25 MHz

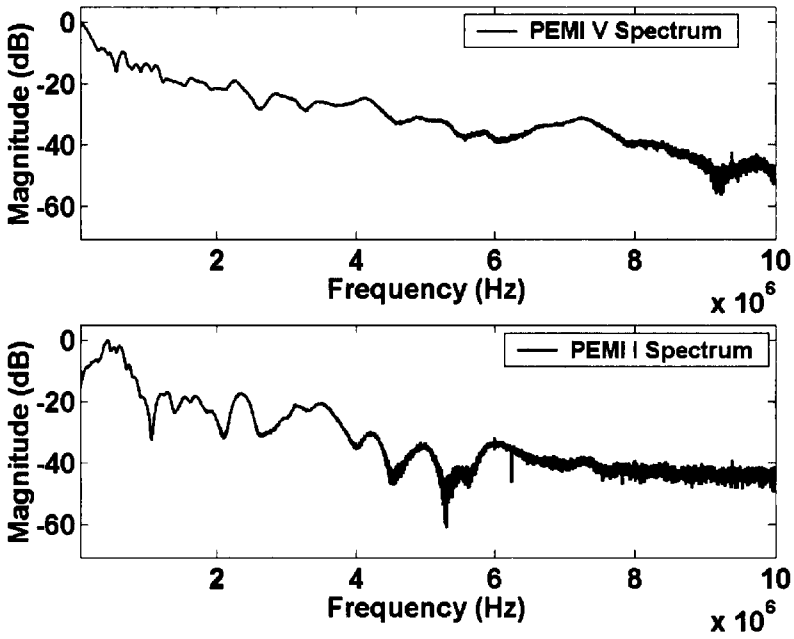


Figure 6.6 – PEMI measurements spectrum to 10 MHz

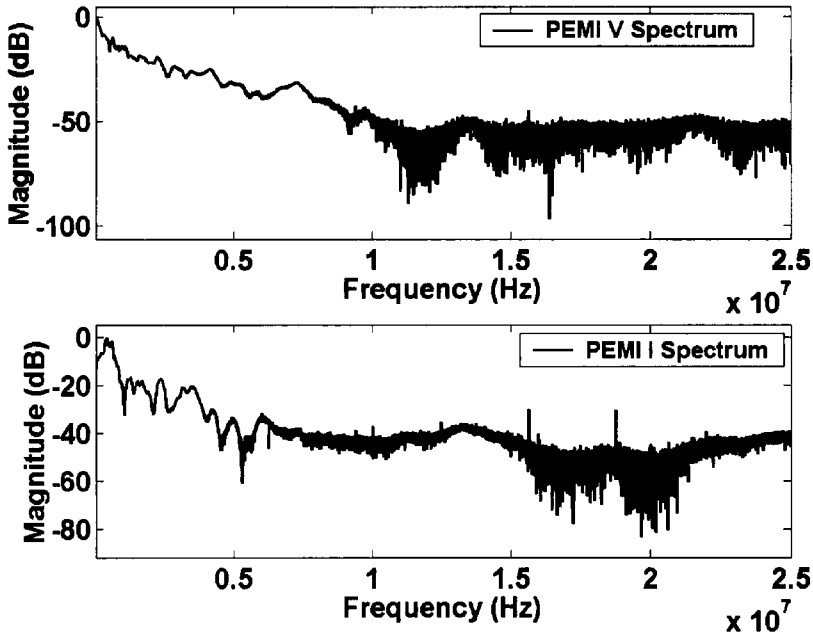


Figure 6.7 – PEMI measurements spectrum to 25 MHz

## 6.2 Effect of Sampling Rate

The sampling rate used in FRA measurement is another factor that could affect the FRA accuracy and results. To obtain good accuracy in the results, a high sampling rate should be used. However, at a higher sampling rate it takes longer to record the results, and the recording device has its own limitations. The minimum theoretical sampling rate required is double the recording signal frequency to avoid aliasing. In reality, the adequate sampling rate needs to be much higher than the theoretical one to obtain a good reproduction of frequency components. In general, a sampling rate of at least 5 times the Nyquist rate is required, depending on the type of signal being analyzed as well as noise level, etc.

Two sampling rates were applied to the experiments to evaluate the effects of the FRA results: 50 MHz and 500 MHz. In this study, two shunt values were used for comparison under different sampling rates: 1 Ω and 10 Ω.

Figures 6.8 and 6.9 show the FRA admittances recorded with a 50 MHz and 500 MHz sampling rate, respectively, with a 1 Ω shunt.

Figures 6.10 and 6.11 show the FRA admittance recorded with a 50 MHz and 500 MHz sampling rate, respectively, with a 10 Ω shunt.

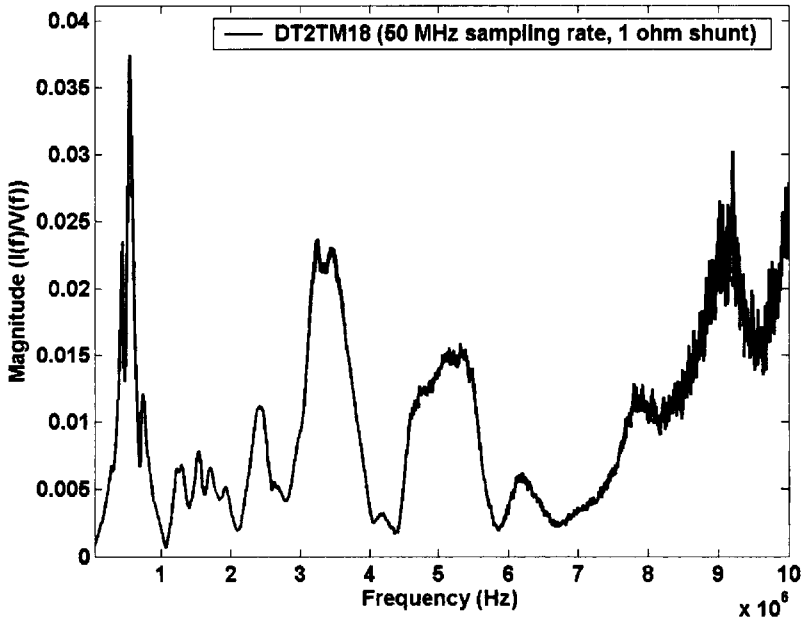


Figure 6.8 - Test with 50 MHz sampling rate - 1 Ω shunt.

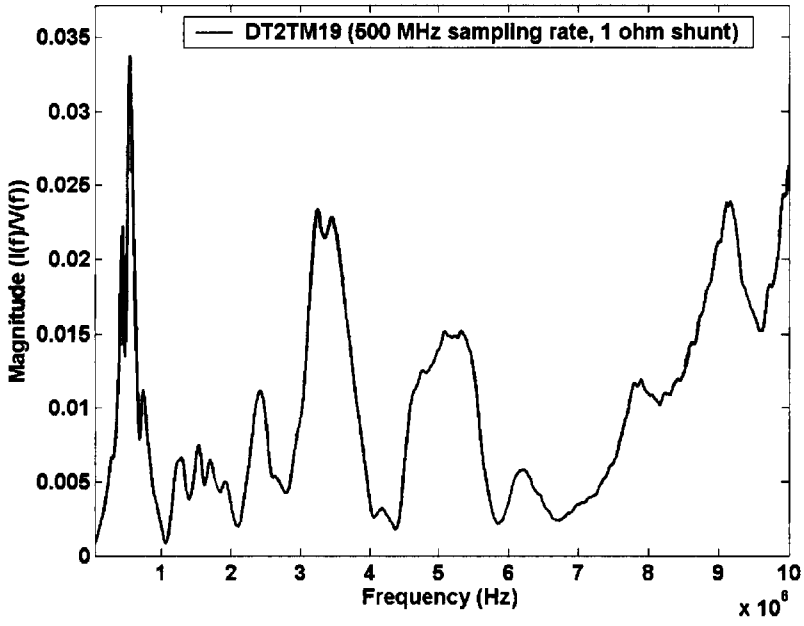


Figure 6.9 - Test with 500 MHz sampling rate - 1 Ω shunt

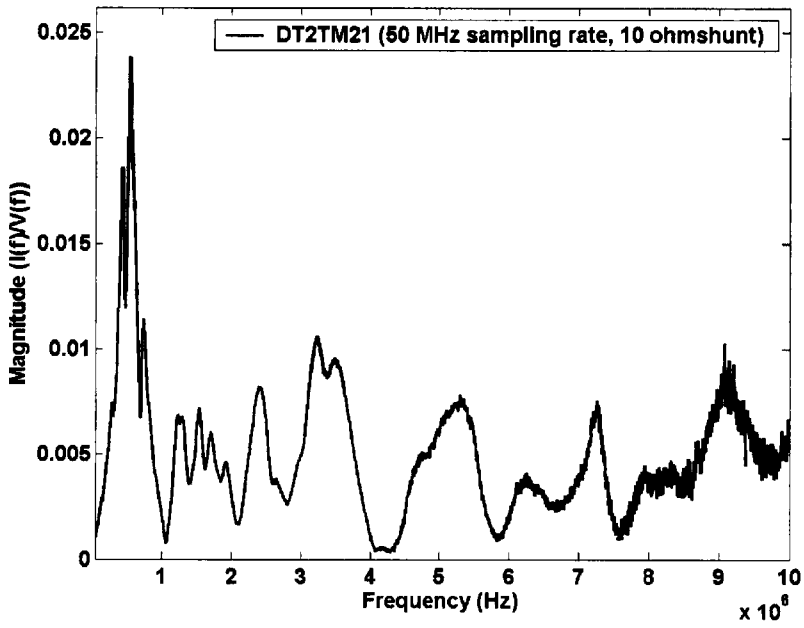


Figure 6.10 - Test with 50 MHz sampling rate - 10 Ω shunt

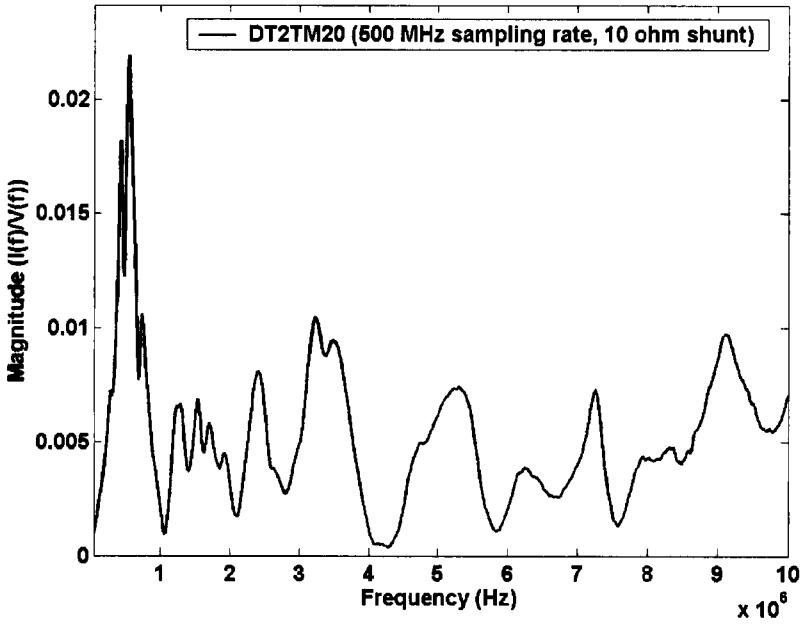


Figure 6.11 - Test with 500 MHz sampling rate - 10 Ω shunt

The FRA results demonstrate that the basic shapes of the admittance signatures obtained from the two sampling rates are the same. The noise level on the admittance obtained from a 50 MHz sampling rate increases above 4.5 MHz with both shunt resistances. The percentage of the noise at 9.2 MHz was up to 17% with the 1 Ω shunt, and up to 21% with the 10 Ω shunt. The admittance measured with the 500 MHz sampling rate up to 10 MHz still does not show any noise. Figure 6.12 demonstrates the noise levels from the two sampling rates.

The FRA results show that with a 500 MHz sampling rate, the admittance curve is noise--free up to about 14.9 MHz. This also demonstrates how increasing the sampling rate can improve the digitizer's vertical resolution. The relationship between sampling rate and vertical resolution is shown in the following calculations.

Vertical resolution improvement by increasing sampling rate:

$$\frac{500\,MHz}{50\,MHz} = 10 = 2^{3.3}$$

Noise start frequency: $4.5 MHz \times 3.3 = 14.9\,MHz$

$$50\,MHz\,Sampling\,Rate\,Noise\,Start\,Frequency - 4.5\,MHz$$

$$500\,MHz\,Sampling\,Rate\,Noise\,Start\,Frequency - 14.9\,MHz$$

The experiments demonstrate that the 50 MHz sampling rate is adequate for analysis of FRA results up to 4.5 MHz frequency, while the 500 MHz sampling rate is good up to 14.9 MHz frequency. This ratio is equivalent to an increase of 3.3 vertical bits. In practice, this method can reduce the signal noise level.

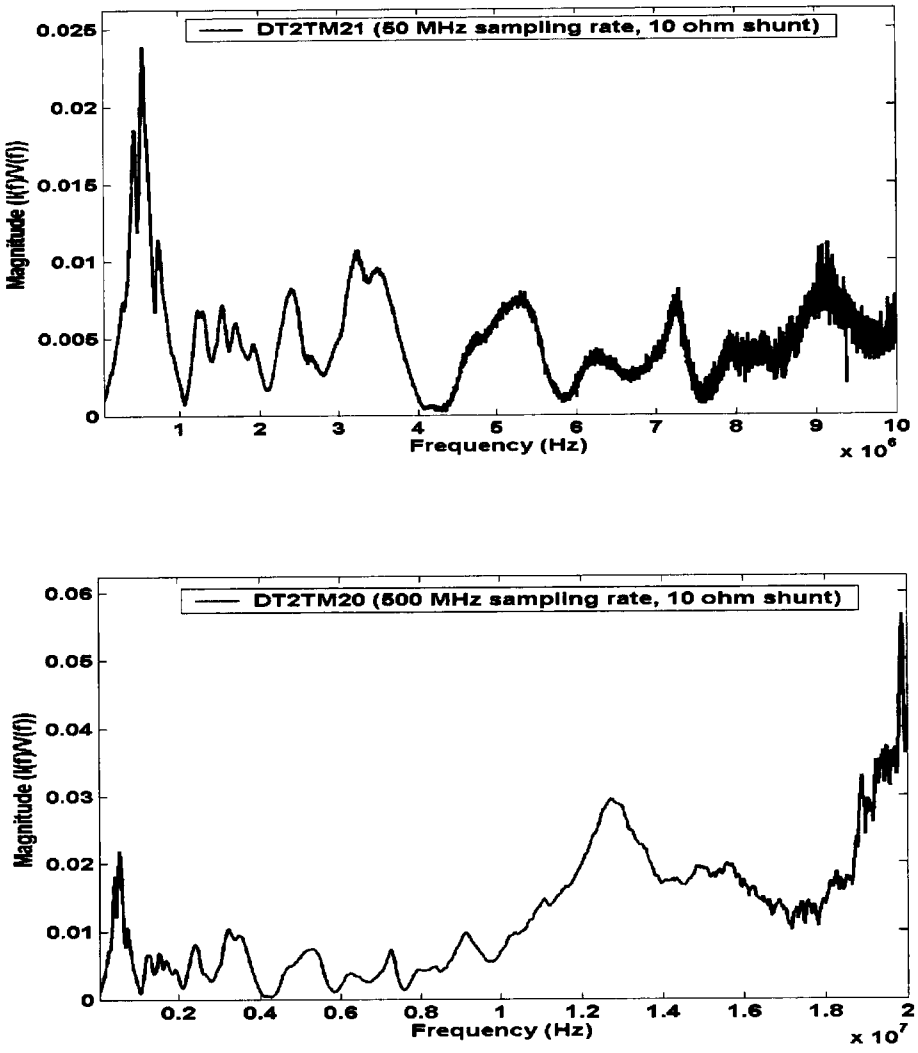


Figure 6.12 - Effect of sampling rate on noise

## 6.3 Shunt Value Effect

When measuring FRA, a resistive current shunt is used to measure the current from the transformer circuit. The FRA measurement covers a wide range of frequency. This is especially important for measuring small winding movements, such as winding looseness, that usually show in the high frequency range (>1 or 3 MHz from field experiment results). At lower frequencies (less than 1 MHz) the impedance of the current shunt (typically 10 Ω or 50 Ω) is not significant compared to the transformer impedance. However, at higher frequencies the shunt impedance becomes comparable to the transformer impedance. The FRA (I) method does not define the shunt resistance value, and in most cases the value is determined by picking a

convenient value or by the limitations of the test equipment (the equipment used for the FRA (S) method results in a 50 Ω shunt impedance). The shunt resistance used in this study was a 10 Ω non-inductive resistance. The equivalent shunt resistance value used in the FRA (S) method is 50 Ω, as this is the input impedance of the spectrum analyzers that were used. To evaluate the effect of shunt value on transformer FRA measurements, investigations were conducted on a distribution class transformer with a range of shunt resistance.

Three different shunt resistances were evaluated to demonstrate the effects of shunt value on the sensitivity of FRA results: 50 Ω, 10 Ω and 1Ω. The first two resistances represent the typical values used in FRA (S) and FRA (I) detection. The 1Ω resistance was chosen for analyzing the resistance sensitivity effect. The comparisons are show in Figure 6.13.

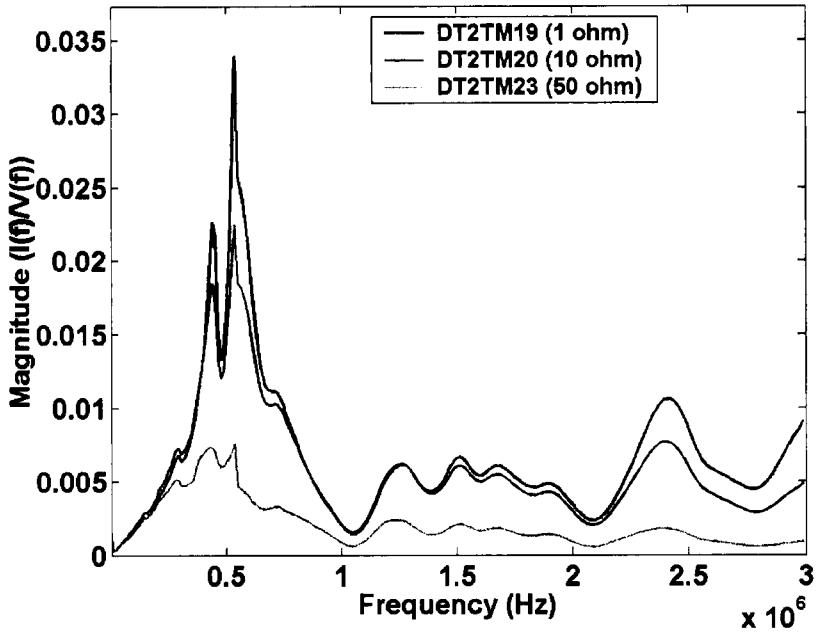


Figure 6.13 - Effect of shunt resistance to 3 MHz

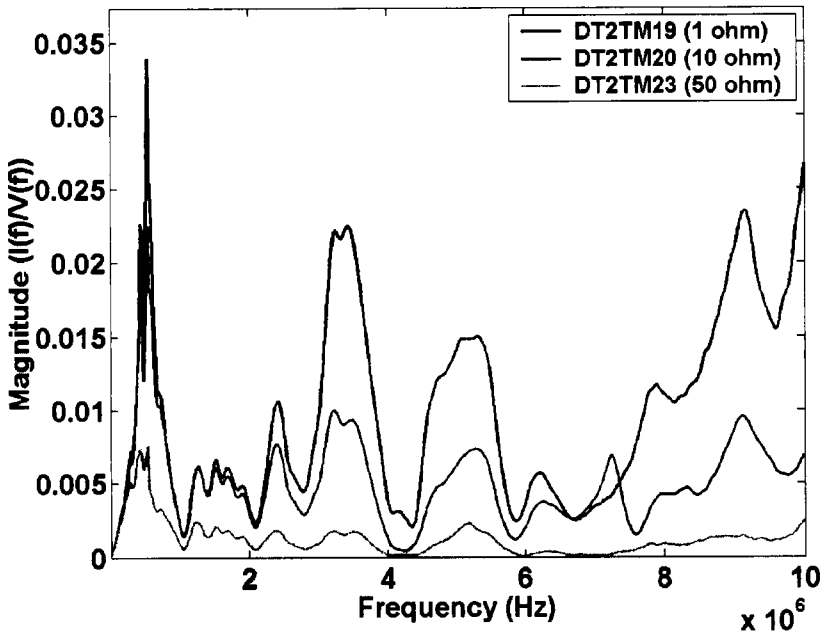


Figure 6.14 – Effect of shunt resistance to 10 MHz

The results from Figures 6.13 and 6.14 illustrate the effects of shunt resistances in the frequency range from 0 to 3 MHz and from 0 to 10 MHz, respectively. The results clearly show that the lower the shunt resistance value, the more sensitive the FRA measurement. Since the low resistance has a higher admittance value, especially in a higher frequency region, it would indicate a smaller winding movement.

The FRA admittance of this experiment also demonstrates that the shunt resistance dominates the transfer admittance in the higher frequency region, and could obscure detecting the change from a small winding movement. The higher the shunt value, the lower the FRA sensitivity. For example, for a 50 Ω shunt the FRA measurement will be insensitive when the frequency range is higher than 500 kHz. For a 10 Ω shunt, the sensitive frequency is up to 3 MHz. For a 1 Ω shunt, the sensitive frequency is higher than 10 MHz. The relative sensitivity of detection is also related to the size and type of transformer.

This investigation shows that transformer admittance still has several resonant peaks in the 2 MHz to 10 MHz range. This conflicts with some transformer models that show only the pure capacitive characteristic in the frequency range above 1 MHz.

In order to investigate the effects of shunt resistance, the test set-up had to be very carefully arranged, with all test leads and all external connecting leads made as short as possible. The significance of shunt resistance changes cannot be seen with lengthy leads in a high frequency range[5].

This shunt resistance evaluation also indirectly compared the detection sensitivity of the FRA (I) and FRA (S) methods. The FRA (I) method with a 10 Ω shunt value detected the change in the transformer, while the FRA (S) method with the equivalent 50 Ω shunt value did not detect any differences. In the FRA (S) method, the terminal resistance has to match the cable impedance, and is usually 50 Ω. The FRA (I) method can therefore detect smaller winding movements, such as winding looseness and small distortions that the FRA (S) method would not detect.

Since a transformer is a distributive network of real and reactive electrical components, it can be modeled as an RLC network and the network impedance/admittance is a function of frequency. The result is a transfer function representation of an RLC network in the frequency domain. In general, it is not difficult to lump elements together for a single frequency, but when system modeling requires a significant frequency interval, it becomes more of a challenge to produce a suitable lumped model. The FRA test then becomes very important. In a real FRA measurement, the transfer function of the measurement not only includes the transformer network function but also includes shunt resistance and leads impedance. The transfer function is shown in the following equation:

$$\frac{I_{out}}{V_{in}} = \frac{1}{Z_t(j\omega) + Z_{lead}(j\omega) + R_{shunt}} \qquad (6.1)$$

Equation 6.1 shows that the higher the shunt resistance and the longer the leads, the lower the sensitivity of the transformer response.

The estimated overall transformer admittance and impedance (with current shunt and leads) at different frequencies can be obtained from transformer FRA (I) measurements, as shown in Table 6.1.

[5] The effect of the leads will be discussed in Section 6.6

Table 6.1 – Shunt value effects

| Frequency (MHz) | 50 Ω shunt | | 10 Ω shunt | | 1 Ω shunt | |
|---|---|---|---|---|---|---|
| | Transfer Admittance (S) | Transfer Impedance (Ω) | Transfer Admittance (S) | Transfer Impedance (Ω) | Transfer Admittance (S) | Transfer Impedance (Ω) |
| 0.5 | 0.0075 | 133 | 0.0124 | 81 | 0.0126 | 79 |
| 1.0 | 0.001 | 1000 | 0.002 | 500 | 0.002 | 500 |
| 1.5 | 0.0025 | 400 | 0.006 | 167 | 0.0065 | 154 |
| 2.5 | 0.002 | 500 | 0.0075 | 133 | 0.011 | 91 |
| 3.0 | 0.001 | 1000 | 0.005 | 200 | 0.009 | 111 |
| 5.0 | 0.0025 | 400 | 0.0075 | 133 | 0.015 | 67 |
| 6.0 | 0.0001 | 10000 | 0.0015 | 667 | 0.0025 | 400 |
| 7.0 | 0.0001 | 10000 | 0.0025 | 400 | 0.0025 | 400 |
| 8.0 | 0.001 | 1000 | 0.004 | 250 | 0.012 | 83 |
| 9.0 | 0.0015 | 667 | 0.01 | 100 | 0.0235 | 43 |
| 10.0 | 0.0025 | 400 | 0.0065 | 154 | 0.0265 | 38 |

Table 6.2 - Nominal admittance based on 50 Ω shunt

| Frequency (MHz) | 50 Ω shunt | 50 Ω shunt | 10 Ω shunt | 10 Ω shunt | 1 Ω shunt | 1 Ω shunt |
|---|---|---|---|---|---|---|
| | Admittance (S) | Impedance (S) | Admittance (S) | Impedance (S) | Admittance (S) | Impedance (S) |
| 0.5 | 1 | 1 | 1.65 | 0.61 | 1.68 | 0.59 |
| 1.0 | 1 | 1 | 2.0 | 0.5 | 2 | 0.5 |
| 1.5 | 1 | 1 | 2.4 | 0.42 | 2.6 | 0.39 |
| 2.5 | 1 | 1 | 3.75 | 0.27 | 5.5 | 0.18 |
| 3.0 | 1 | 1 | 5.0 | 0.2 | 9 | 0.11 |
| 5.0 | 1 | 1 | 3.0 | 0.33 | 6 | 0.17 |
| 6.0 | 1 | 1 | 15 | 0.07 | 25 | 0.04 |
| 7.0 | 1 | 1 | 25 | 0.04 | 25 | 0.04 |
| 8.0 | 1 | 1 | 4.0 | 0.25 | 12 | 0.08 |
| 9.0 | 1 | 1 | 6.7 | 0.15 | 15.6 | 0.06 |
| 10.0 | 1 | 1 | 2.6 | 0.39 | 10.6 | 0.10 |

The shunt resistance not only adds to the impedance value of the circuit, which reduces the sensitivity of the measurement, but it also dampens the resonant so the effect could be very significant. The effect also depends on the Q value of the circuit. A high Q network will have a high sensitivity for detecting winding movement. When the current shunt resistance is low, the circuit Q value is relatively high. This is shown in the FRA results with three shunt resistances. For example, at 0.5 MHz and 1.7 MHz the resonant peaks of 10 Ω and 1 Ω shunt resistances were compatible, but they were not compatible with the 50 Ω shunt curve. The damping effect was significant above 0.5 MHz for the 50 Ω shunt. When the frequency was higher than 3 MHz, the damping effect was significant for the 10 Ω shunt. These results illustrate that the 50 Ω shunt is comparable to transformer impedance when the frequency is above 0.5 MHz, and the10 Ω shunt is comparable to transformer impedance in the 3 MHz range. With minor winding movement or looseness, the FRA change usually is shown at a higher frequency range (could be as high as 5 MHz or even higher).

The principal findings in this investigation are that the FRA test is more sensitive if a lower shunt resistance is used. For sensitive measurements, a 50 Ω shunt resistance is adequate for up to 0.5 MHz, a 10 Ω shunt is adequate to 3 MHz, and a1 Ω shunt is adequate 10 MHz.

Different sizes and types of transformers have different winding network impedances, so the shunt value could have different impacts. In general, for larger power transformers the major admittance resonant peak is usually at a lower frequency than for a distribution class transformer. The sensitive detection frequency could be different in large power transformers, but the trend in the effect of the shunt resistance will still be the same as the analysis in this study.

## 6.4 High Voltage Bushing Effect

### a) Effect of measurement from the top of the bushing vs. the bottom of the bushing

This experiment was done on a distribution class transformer. Originally the transformer used in this study only had a small porcelain bushing, 50 cm long. In order to perform the investigation on bushing effects, this porcelain bushing was replaced with a 27 kV oil-paper bushing, 90 cm long.

The bushing data is as follows:

| | |
|---|---|
| Manufacturer: | Lapp Co. |
| System Voltage: | 27.5 kV |
| BIL: | 150 kV |
| C1: | 294 pF |
| PF: | 0.70% |
| Length: | 90 cm |

The FRA measurements were performed with and without the bushing. The purpose of the investigation was to find out what role the high voltage bushing plays in the FRA measurement. In the discussion below, *top measurement* refers to FRA measurements with the input signal measured at the input terminal (top) of the bushing, while *bottom measurement* refers to FRA input signal measurements made directly at the high voltage winding lead inside the transformer.

Experiments were done on the same distribution class transformer as in the previous tests, under the following conditions:

Case 1: Pulse applied into the top of the high voltage bushing. The voltage measurement point was at the top of the high voltage bushing. The transfer current was obtained from the secondary winding though a 1 Ω shunt. The pulse source was the high voltage pulse generator (PEMI).

Case 2: Pulse applied into the top of the high voltage bushing. The voltage measurement point was at the bottom of the high voltage bushing. The transfer current was obtained from the secondary winding though a 1 Ω shunt. The pulse source was the high voltage pulse generator (PEMI).

The FRA measurements made with and without a bushing are shown in Figures 6.15 to 6.17. Figure 6.15 shows the overlay admittance plots of measurements at the top and the bottom of the bushing. Figures 6.16 and 6.17 show the input voltage spectrum and the output current spectrum of the top and bottom of the bushing, respectively.

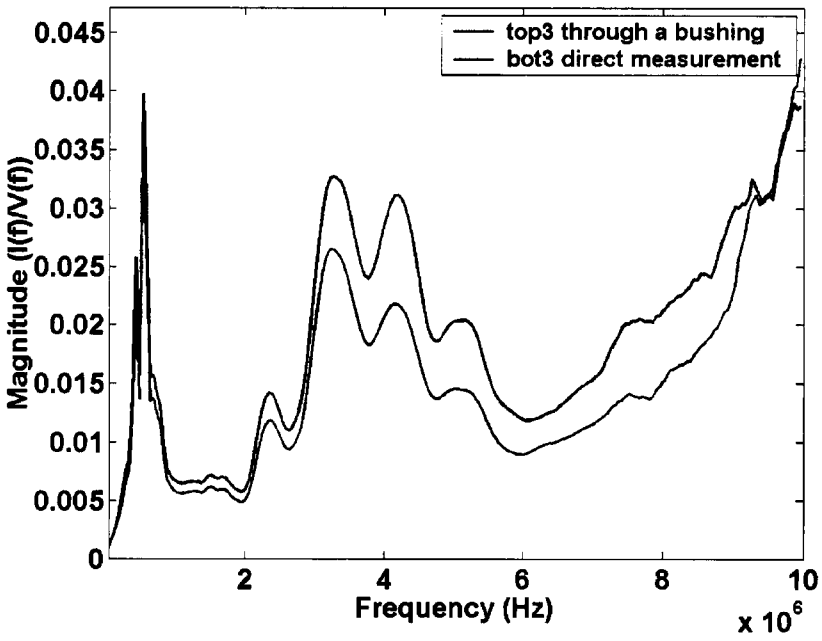


Figure 6.15 – FRA measurement the top and bottom of the bushing

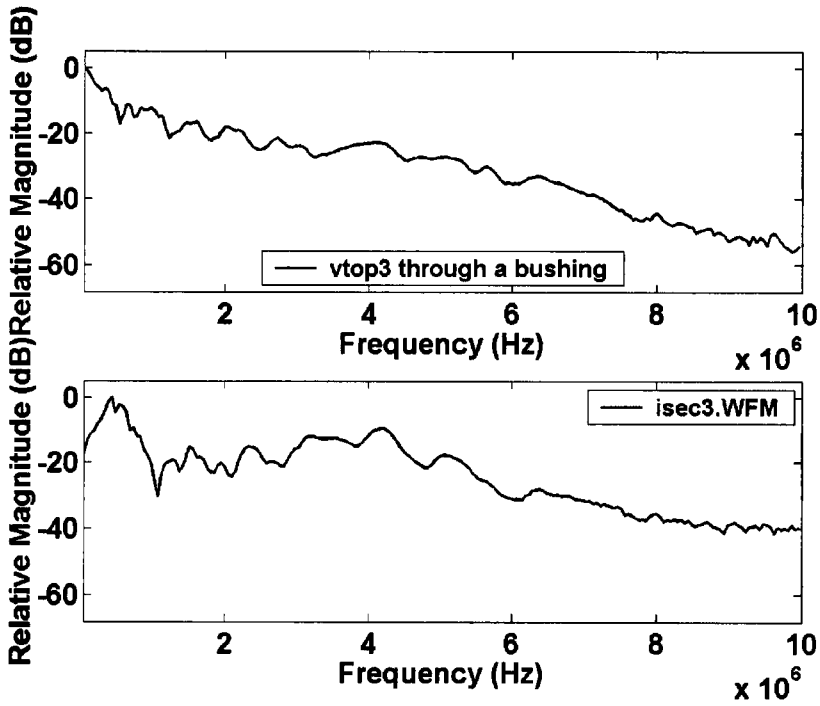


Figure 6.16 – Relative spectrum of signals measured signals
Top trace – signal at top of bushing
Bottom trace – measured current

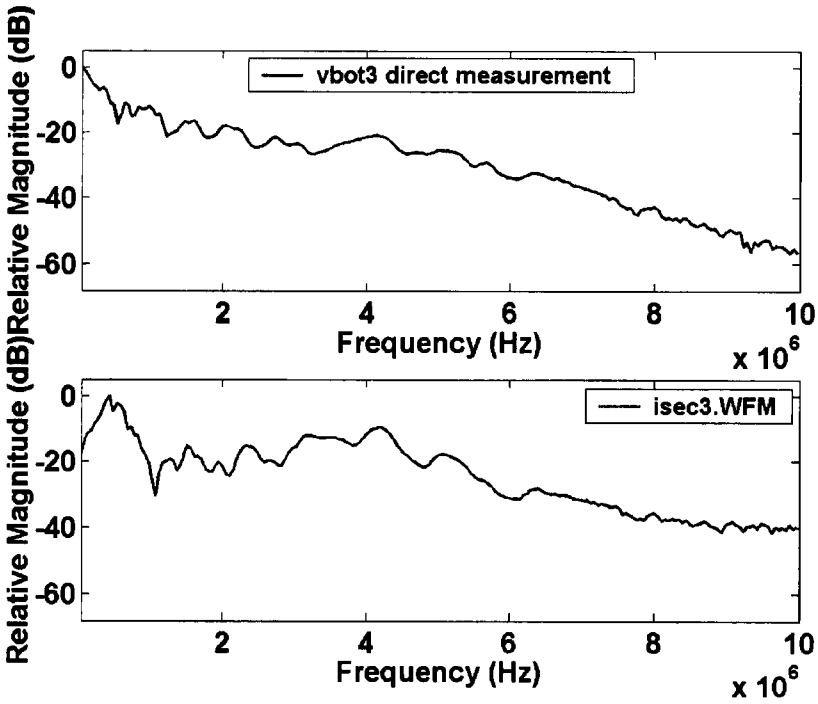


Figure 6.17 - Relative spectrum of measured signals
Top trace – signal at bottom of bushing
Bottom trace – measured current

The FRA results show that the transfer admittance measured directly from the terminal of the high voltage winding (bottom of the bushing) was lower than the measurement from the terminal on top of the bushing. The results imply that the equivalent impedance of the high voltage winding was capacitive dominant impedance from 1 MHz above. The bushing lead inductance cancelled the winding equivalent capacitance voltage so that the admittance measured at the top of the bushing was lower than at the bottom of the bushing.

$$I/V_{top} > I/V_{bottom};\ V_{top} < V_{bottom} \text{ in frequency range 1-9 MHz.}$$

This again shows that the measurement results are very sensitive to the test set-up, measurement location, and lead configuration. It is critical for the repeatability of the test that the test configuration is identical each time the test is done. Any changes in the test method that reduce the variability of the lead arrangements and condition will be very useful in improving the reliability and repeatability of the test.

b) Comparison of voltage directly applied to high voltage winding and though a bushing

Experiments were done on the same distribution class transformer as above. A comparison was done on the follow cases:

Case 3: Pulse applied directly to the high voltage winding. The voltage measurement point was at the high voltage terminal of the winding.

Case 4: Pulse applied through a high voltage bushing. The voltage measurement point was at the same point.

Case 3 and Case 4 were performed with a 1 Ω shunt value and at a 500 MHz sampling rate. The signal generator used in these cases was the PEMI.

The FRA overlay admittances of a transformer transfer function were obtained directly from the high voltage winding (Case 3) and through the high voltage bushing (Case 4). The experimental results from Cases 3 and 4 are shown in Figure 6.18.

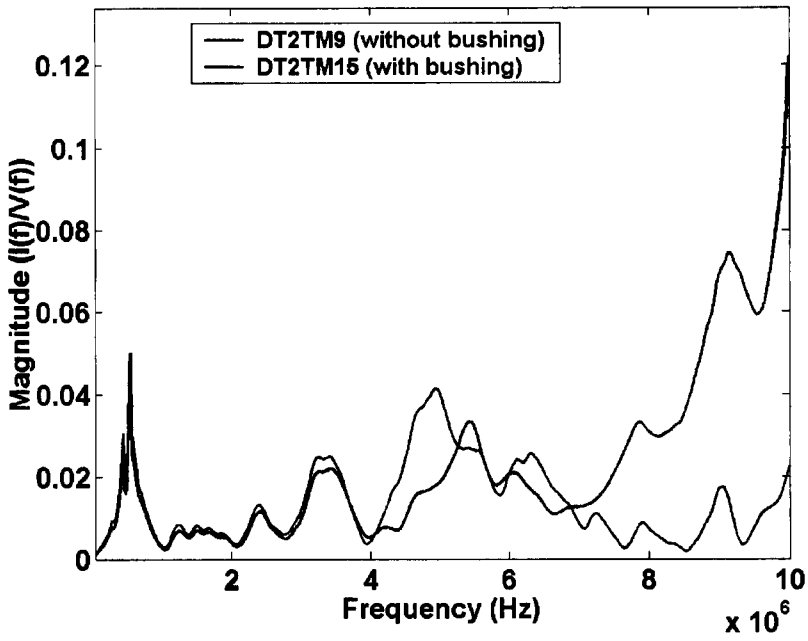


Figure 6.18 - Comparison FRA with and without HV bushing

The FRA admittances with and without the bushing are almost identical in the range below 3 MHz. The results from the direct input measurement at the winding are slightly lower than the admittance measured through the bushing. The admittance results measured at the top and the bottom of the bushing with the input voltage at the top of the bushing are very similar in the 0 to 3 MHz range. At the frequency range above 3 MHz, and in particular above 4 MHz, the FRA admittances are quite diversified between Case 3 and Case 4.

FRA admittances are very similar between direct measurement of windings and measurement through a bushing at 0 to 3 MHz, but the FRA admittance from the direct measurement was slightly lower than the FRA admittance from the bushing. This indicates that the equivalent FRA admittance is slightly capacitive at this frequency range.

The FRA admittances above 4 MHz are very diversified. The admittance from the direct measurement increased very quickly compared to the results through a bushing at the frequency range above 7 MHz.

In this investigation, all the measurements were made with a set of a very short leads. When measuring on site, especially on a large power transformer, a set of very short leads cannot be applied due to the physical size of the transformer and the high voltage bushing. A high voltage bushing, for example, can be as tall as 5 meters. The input fast pulse has to go through this length of lead to be applied to the bushing and then to the winding. The high frequency components from the source signal will be shunted to ground by the capacitance of the bushing, and the inductive impedance of the lead and bushing is significant compared to the impedance of the transformer at high frequencies. These factors mean that the fixed impedance of the leads and bushing will mask the changes in the transformer's impedance.

## 6.5 Effect of HV Winding Neutral Connection

During FRA measurement, how the transformer neutral is connected is also an important issue that could affect the results. Experiments were carried out to detect the influence of neutral connections in FRA measurement. The tests were performed on a distribution transformer under two conditions: with the high voltage winding neutral floating and with the neutral connected to the tank. Input voltage was applied and measured from the top of a bushing. The coupling current was measured from a 1 Ω shunt connected between the low voltage winding and tank. The FRA admittance was calculated based on the measured voltage and current.

The FRA results under these two neutral conditions (floating and connected to the tank) are shown in Figure 6.19 (up to 3 MHz) and Figure 6.20 (up to 10 MHz). The voltage and current frequency spectra for the two conditions are displayed in Figure 6.21 (neutral floating) and 6.22 (neutral connected to tank). The spectrum plots show that the input signal did not contain adequate frequency components above 7 MHz.

These experiments illustrate that the neutral ground connections do have some impact on the FRA results, but below 1.5 MHz the impact is not significant. When the frequency is below 1.5 MHz, the FRA results are actually quite similar between the neutral floating and the neutral connected to the tank. The FRA admittances show more differences above 2 MHz. Therefore, to detect minor winding movements the FRA comparison must be done using the same neutral connections.

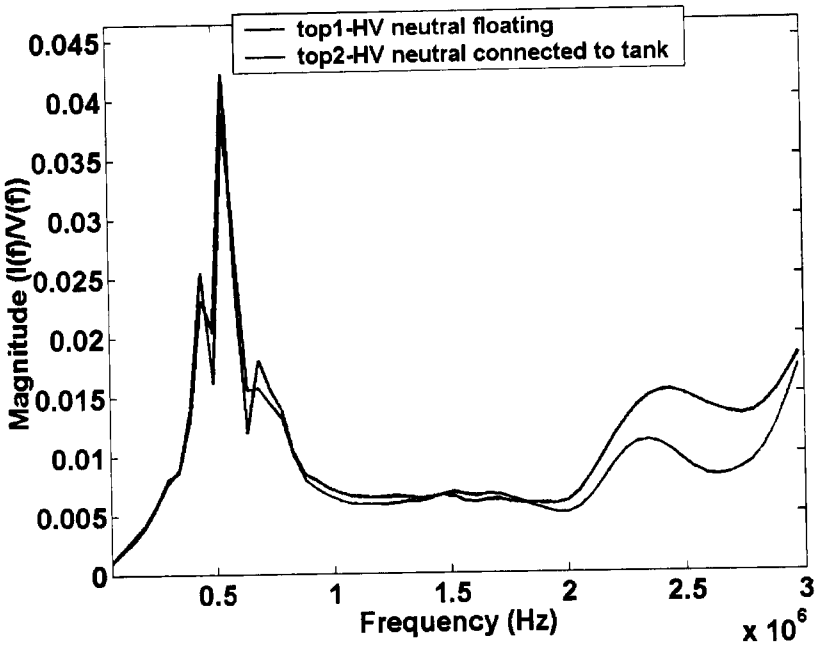


Figure 6.19 – Effect of neutral floating vs. grounded to 3 MHz

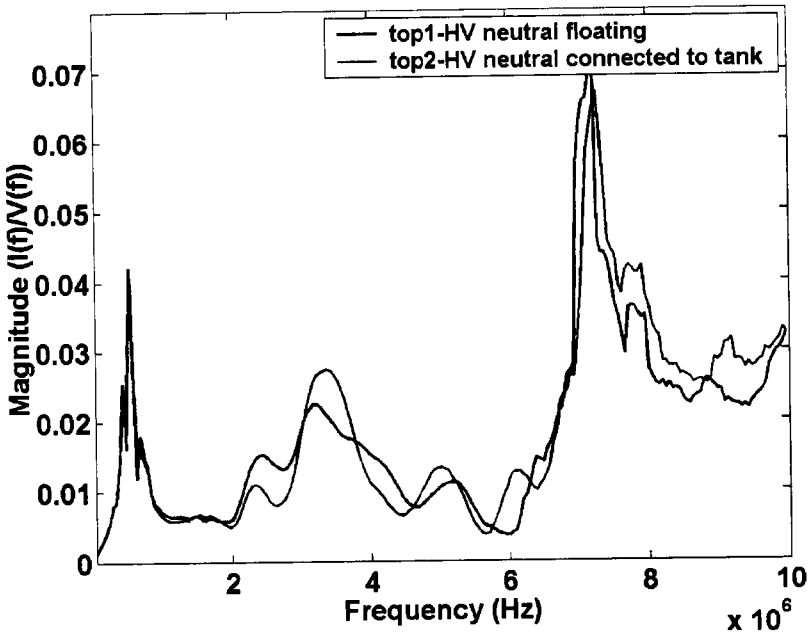


Figure 6.20 – Effect of neutral floating vs. grounded to 10 MHz

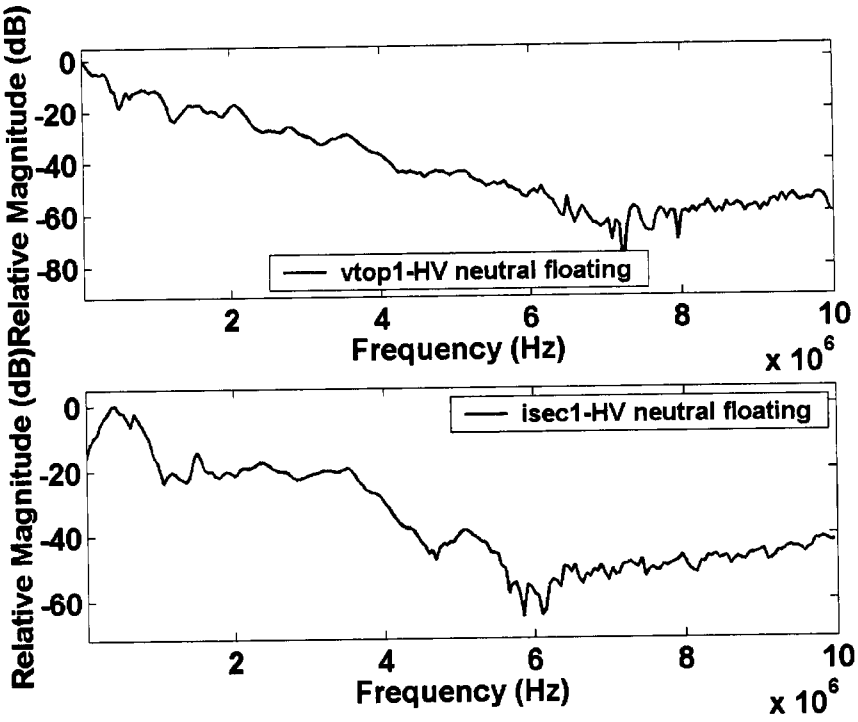


Figure 6.21 – Relative spectrum of measured signals with floating neutral
Top trace – signal at top of bushing
Bottom trace – measured current

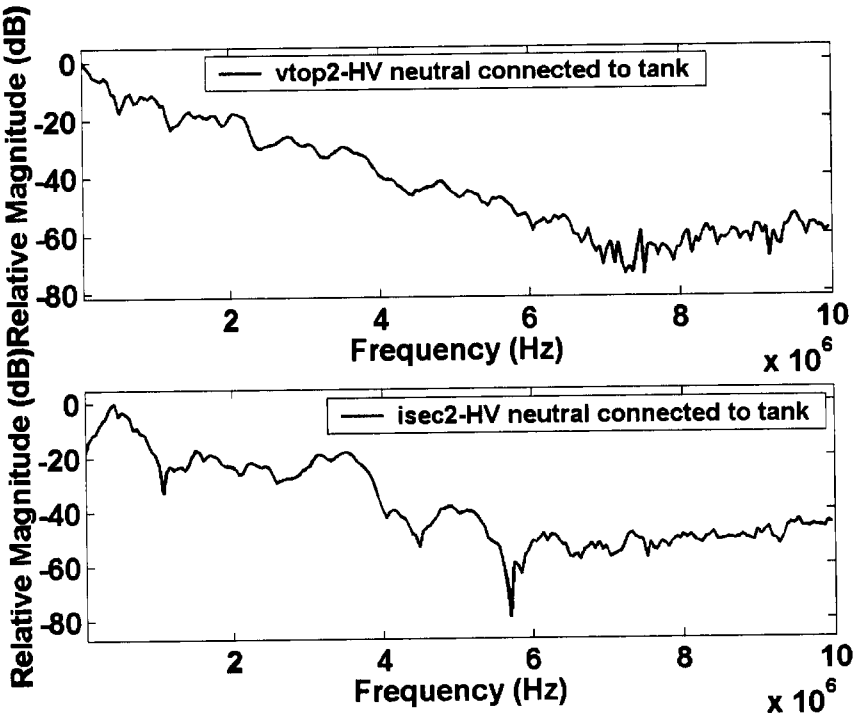


Figure 6.22 – Relative spectrum of measured signals with grounded neutral
Top trace – signal at top of bushing
Bottom trace – measured current

## 6.6 Effects of Measurement Leads

The transformer network impedance, the shunt resistance and the lead impedance all contribute to the FRA measurement. In Section 6.3, shunt effects were presented and analyzed. In this section the effects from the measuring leads will be presented and analyzed.

The analysis of high voltage and grounding leads effects was performed with three sets of test leads. One was the "standard" set of leads with lengths suitable for most on-site FRA measurements on top of the transformer. The second set of leads were long leads used to measure very large power transformers, or for FRA measurements with the equipment on the ground. The third set of leads were kept as short as physically possible with the FRA measurements done on a distribution size transformer. Investigations were performed mainly on two particular leads in the lead sets. One was the grounding lead that connects the shunt, the probe and the voltage pulse generator to the transformer tank. The other was the lead/cable that connects the signal source to the transformer and the measurement signal from the transformer to the measuring device. The circuit lead arrangement and labelling were as shown in Figure 4.2.

Standard Lead Set

The standard leads set consists of the following:

L1-#10 twin lead, 2.5 m
L2-#10 twin lead, 0 m
L3-#10 5.5 m
L4-#2 single 2.5 m
L6-#10 twin 3.21 m
C1- 10x probe, 3.0 m 10 MΩ
C2- RG58, 6 m
C3- RG58, 2.11 m

Long Lead Set

The long leads set, required for larger transformers or for measurements on the ground, consists of the following leads in addition to the standard lead set:

C2- RG58, 15 m
L1-#10 twin lead, 7.0 m

Short Lead Set

The short leads set consists of the following:

L1-#10 twin lead, 10 cm

L2-#10 twin lead, 0 m

L3-#10 0.5 m

L4-#2 single 10 cm

L6-#10 twin 0.5 m

C1- 10x probe, 3.0 m 10 MΩ

C2- single, 0.6 m

C3- single wire, 1 m

For the short lead set, the input signal lead from the signal generator to the high voltage bushing was shortened to 0.6 meter, the lead from the shunt to the transformer secondary was shortened to 0.1 meter and all leads to ground were kept as short as possible.

FRA measurements were carried out on the transformer with the three sets of leads (long, standard and short), then with the long and standard lead sets with the transformer out of the circuit (equivalent to shorting the transformer). The individual lead changes were as follows:

1) Lead from the input signal generator to H1 (HV winding input) changed from a 0.6 m #12 wire to a 6.0 m coaxial cable.
2) Lead from the current shunt to X1 (LV winding) changed from a 2.5 m twin #10 wire to a 6.0 m twin #10 wire.
3) Extension leads from the voltage measurement probe to H1 (L2) and the probe grounding lead (L3) changed from L2 = 0 m and L3 = 0 m to L2 = 2.5 m and L3 = 5.5 m (twin #10 wire).
4) Lead from shunt ground to transformer tank: a) 0.1 m #12 wire, b) 2.5 m #2 wire.

All of these tests were done with a 100 MHz sampling rate, averaging 250 pulses and using a 1 Ω shunt. The measurement results are shown in Figures 6.23 to 6.36.

The impact of the lead set used is compared in Figures 6.23 and 6.24 (3 MHz range) and Figures 6.25 and 6.26 (10 MHz range). The following comparisons are made:

1) standard test leads with transformer
2) standard leads without transformer
3) long leads without transformer

The figures show both the admittance and the impedance curves.

The results indicate that the admittance of the standard leads is similar to the admittance of the transformer with the standard leads above 2.3 MHz. With the long leads, the admittance becomes similar to the admittance of the transformer with the standard leads above 0.5 MHz. This means that above these frequencies (0.5 MHz for long leads and 2.3 MHz for standard leads), the lead admittance becomes the component being measured. The sensitivity to changes in the transformer would be dramatically reduced. The leads also have an impact below this frequency, but the influence rapidly decreases. With this typical circuit, it is clear that the FRA measurement sensitivity range of the long leads arrangement is approximately 0.5 MHz and below, and the range of the standard arrangement is below 2.3 MHz.

The FRA measurements on the transformer with the short lead set and the standard lead set are shown in Figures 6.27 and 6.28. It is interesting to note that between 0 and 0.4 MHz the two admittances are the same, between 0.4 MHz and 2 MHz the admittances have some minor differences, but above 2 MHz the differences are dramatic. The lead length does have a great impact on the FRA results. This analysis shows that the short lead arrangement has a much higher admittance compared with the standard long leads arrangement above 2 MHz. The short leads arrangement will give much higher sensitivity to changes in the transformer compared with the standard lead arrangement in the high frequency range.

Figures 6.29 and 6.30 demonstrate the effects of the lead from the signal generator to the high voltage winding. Above 4 MHz, the change in the lead has an impact. Even with the longer lead the admittance can have resonance at some frequencies, so that the admittance with the

longer lead is higher than the admittance with the short lead. However, the general trend is that the admittance at higher frequencies is higher with the short lead. The admittance differences below 4 MHz are very minor one in this case. Figures 6.31 and 6.32 show the effects of the lead from the low voltage winding to the shunt input. The experimental results demonstrate that the shorter the lead from the shunt to X1, the higher the sensitivity in the high frequency range. The admittance differences are minor below 1.2 MHz.

Figures 6.33 and 6.34 present the effects of the voltage probe extension leads. On large bushings it is often necessary to extend the voltage probe by adding these leads, as longer voltage probes are not available. The results have some differences above the 6 MHz range. In general, the impact from the probe ground and extension lead to the high voltage winding terminal is not severe. In particular, below 3 MHz the lead change has no impact on the results.

Figures 6.35 and 6.36 show the effects from the lead from the current shunt to the tank ground point. The effect of the lead change starts at 2 MHz, and after 3 MHz the admittance changes are significant. The experimental results show the significance of the contribution of this lead in the high frequency region. The analysis of these results shows that the admittance increases at some frequencies, as the leads are made longer. This confirms that the optimum measurement requires the lead length to be as short as possible and the lead length must remain constant in the test configuration for repeated tests. The higher the frequency range used, the more critical this becomes.

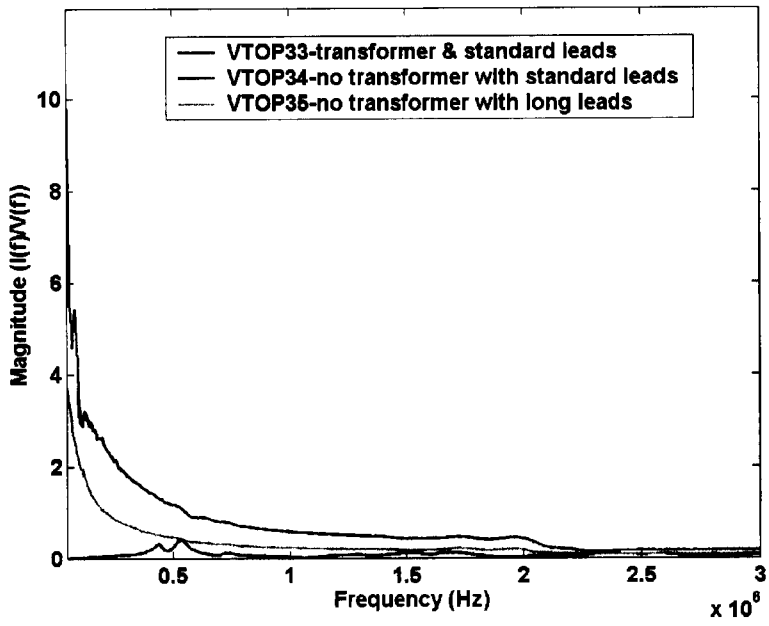


Figure 6.23 – Comparison of lead sets admittance to 3 MHz
Trace 1 – test with transformer using standard lead set
Trace 2 – test with standard lead set only, no transformer
Trace 3 – test with long lead set only, no transformer

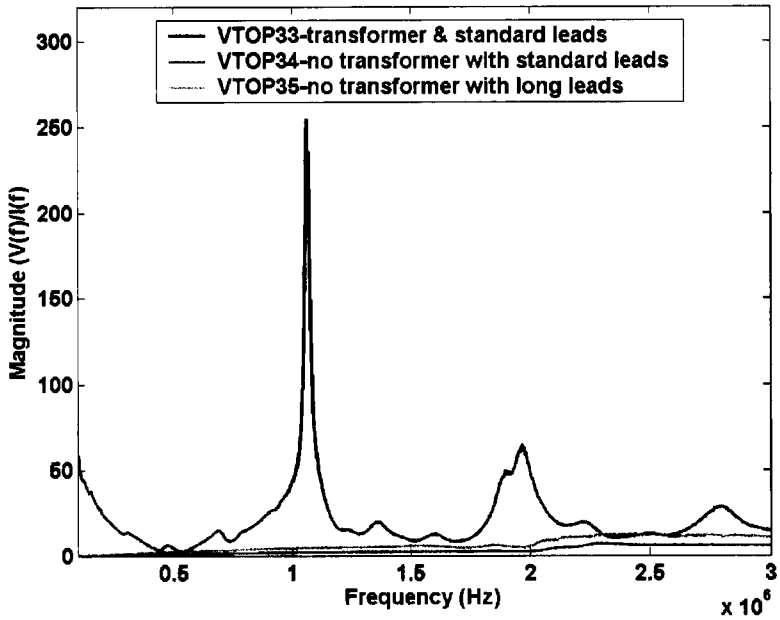


Figure 6.24 – Comparison of Lead Sets Impedance to 3 MHz
Trace 1 – Test with Transformer using standard lead set
Trace 2 – Test with standard lead set only, no transformer
Trace 3 – Test with long lead set only, no transformer

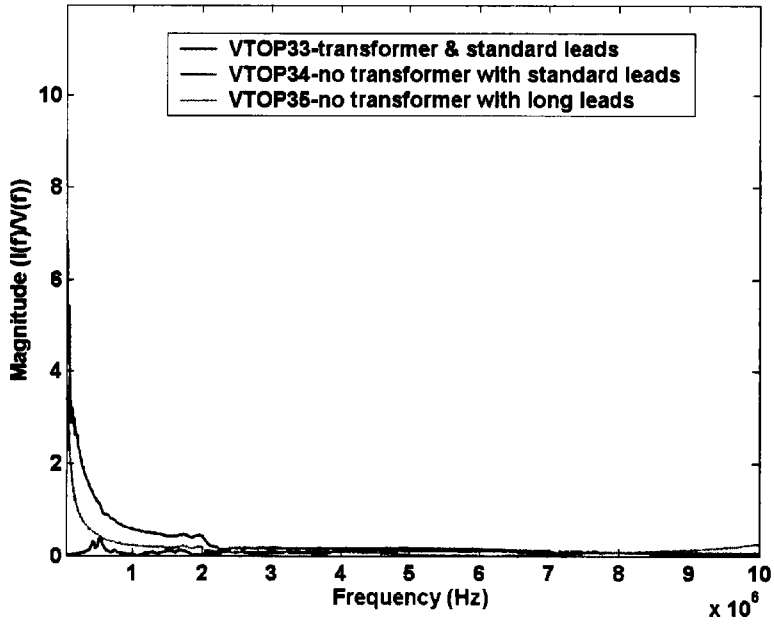


Figure 6.25 – Comparison of lead sets admittance to 10 MHz
Trace 1 – test with transformer using standard lead set
Trace 2 – test with standard lead set only, no transformer
Trace 3 – test with long lead set only, no transformer

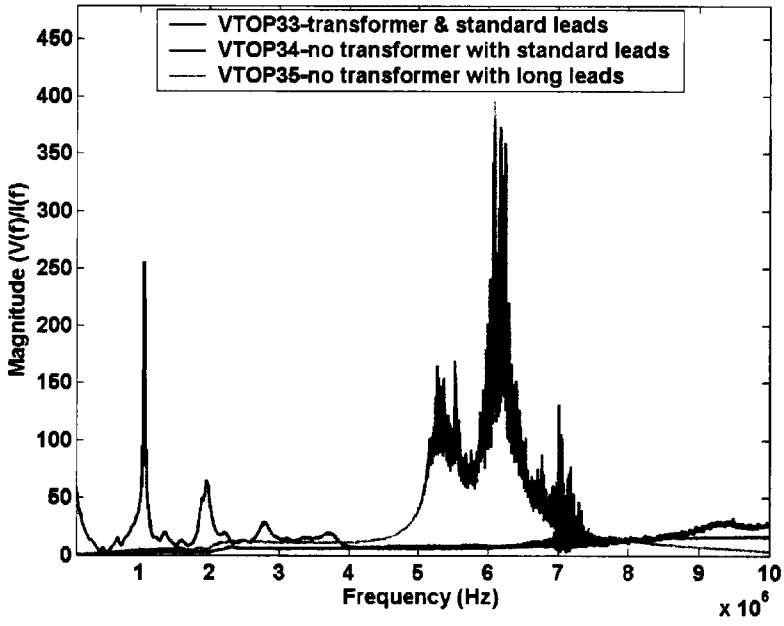


Figure 6.26 – Comparison of lead sets impedance to 10 MHz
Trace 1 – test with transformer using standard lead set
Trace 2 – test with standard lead set only, no transformer
Trace 3 – test with long lead set only, no transformer

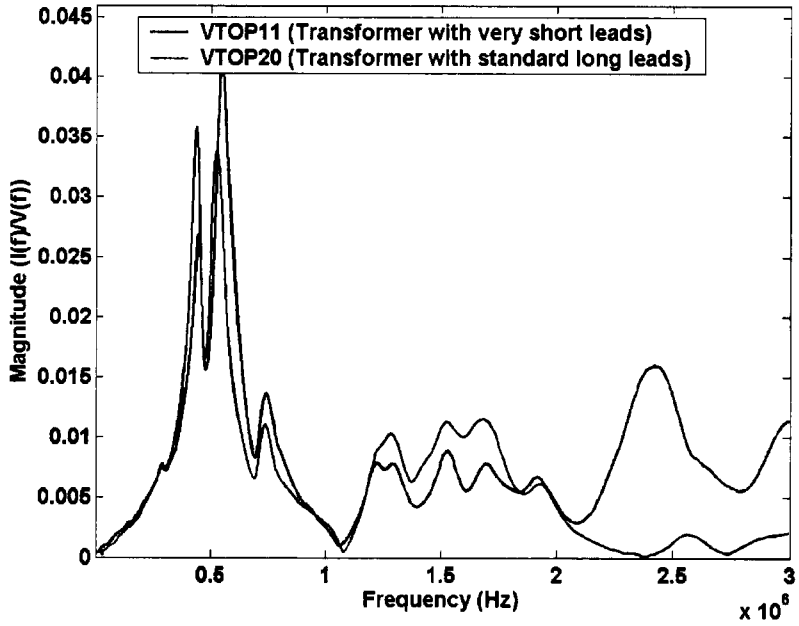


Figure 6.27 - Comparison of tests with short and long lead sets to 3 MHz

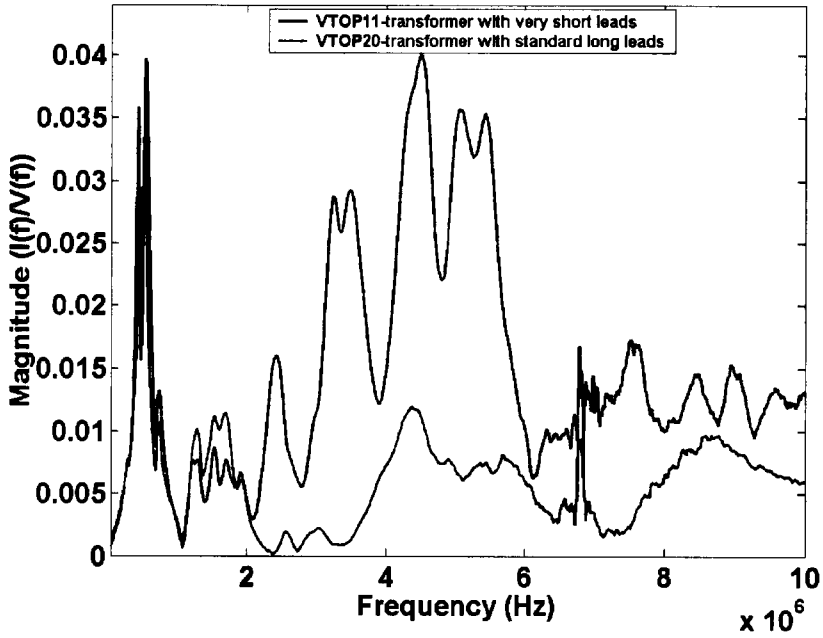


Figure 6.28 - Comparison of tests with short and long lead sets to 10 MHz

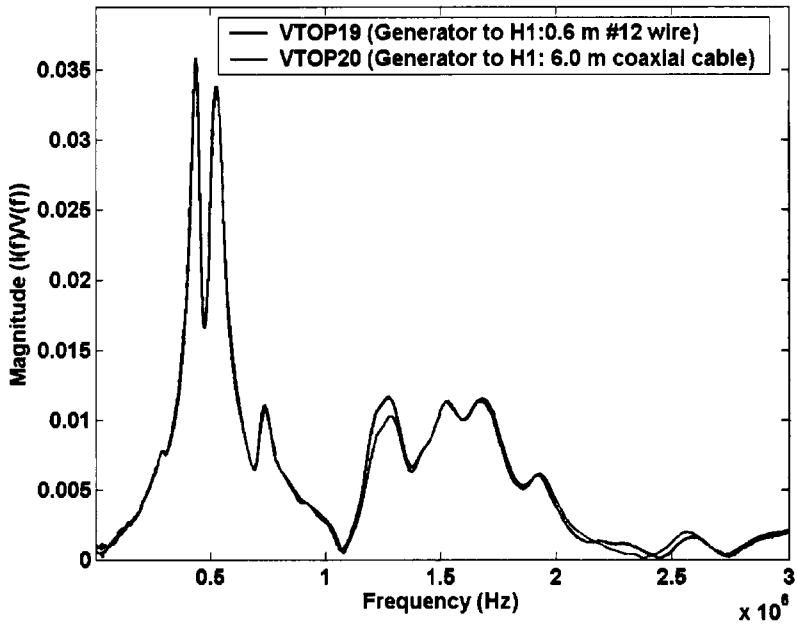


Figure 6.29 – Effect of lead from signal generator to input to 3 MHz
Trace 1 – 0.6 m #12 wire
Trace 2 – 6 m coaxial cable

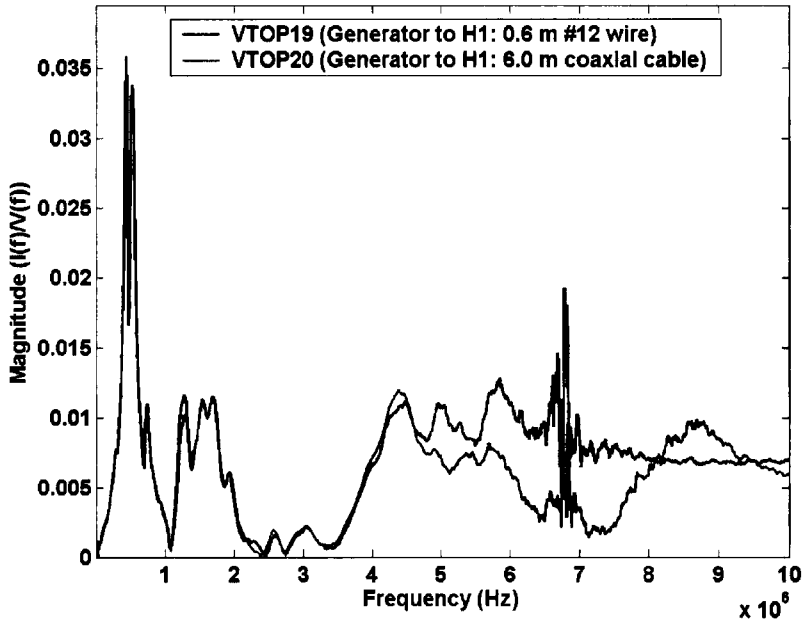


Figure 6.30 – Effect of lead from signal generator to input to 10 MHz
Trace 1 – 0.6 m #12 wire
Trace 2 – 6 m coaxial cable

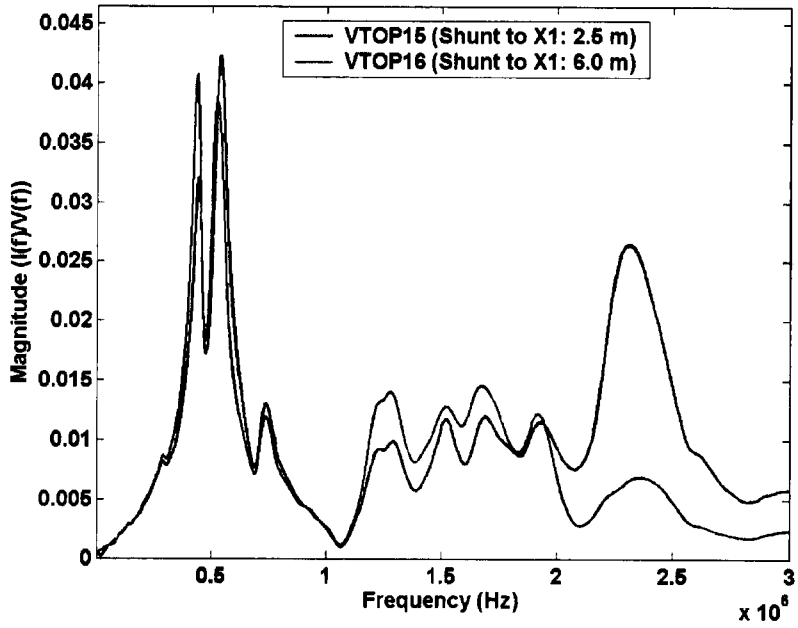


Figure 6.31 – Effect of lead from LV winding to shunt to 3 MHz
Trace 1 – 2.5 m twin #12 wire
Trace 2 – 6 m twin #12 wire

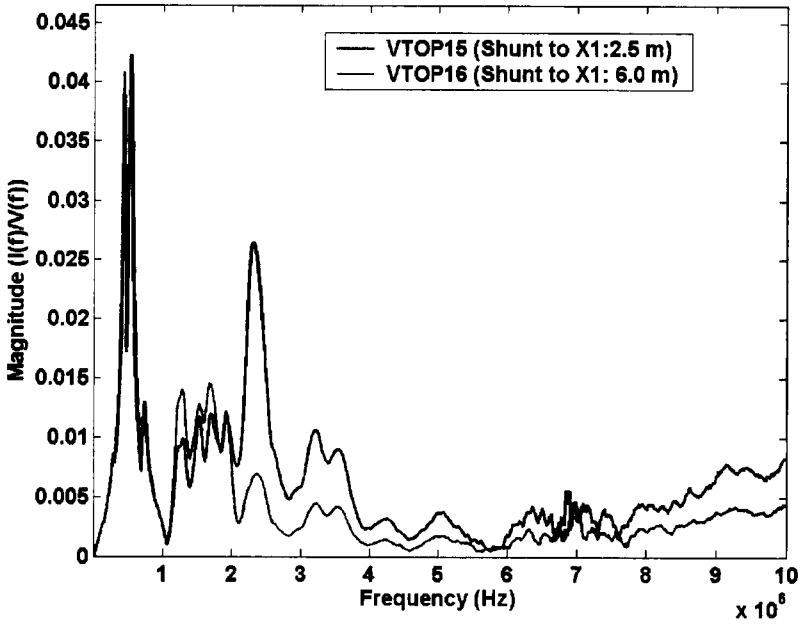


Figure 6.32 – Effect of lead from LV winding to shunt to 10 MHz
Trace 1 – 2.5 m twin #10 wire
Trace 2 – 6 m twin #10 wire

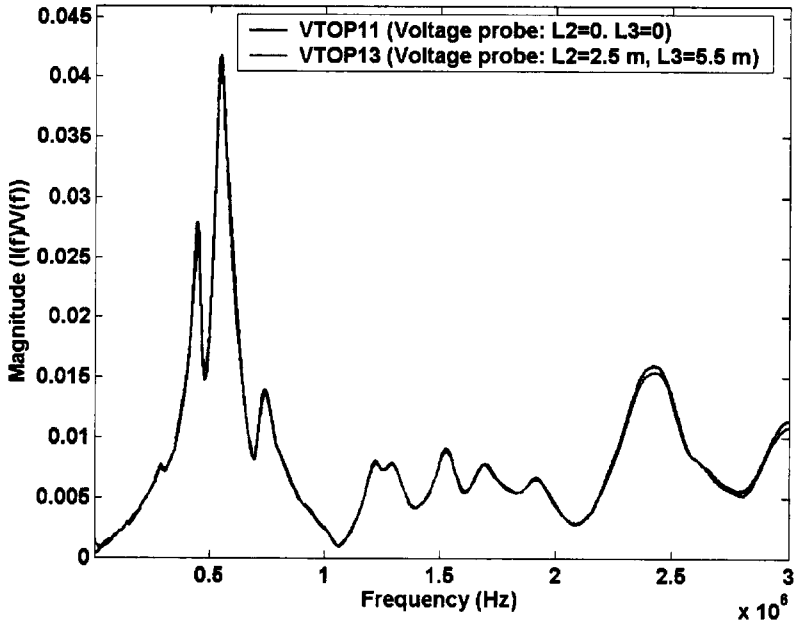


Figure 6.33 – Effect of extension to voltage probe input and ground lead to 3 MHz
Trace 1 – 2.5 m twin #10 wire
Trace 2 – 6 m twin #10 wire

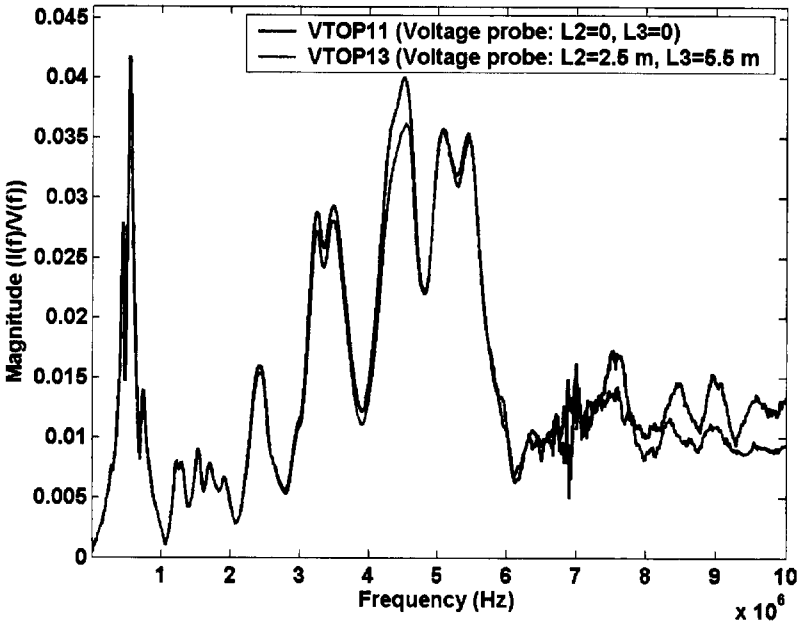


Figure 6.34 – Effect of extension to voltage probe input and ground lead to 10 MHz
Trace 1 – 2.5 m twin #10 wire
Trace 2 – 6 m twin #10 wire

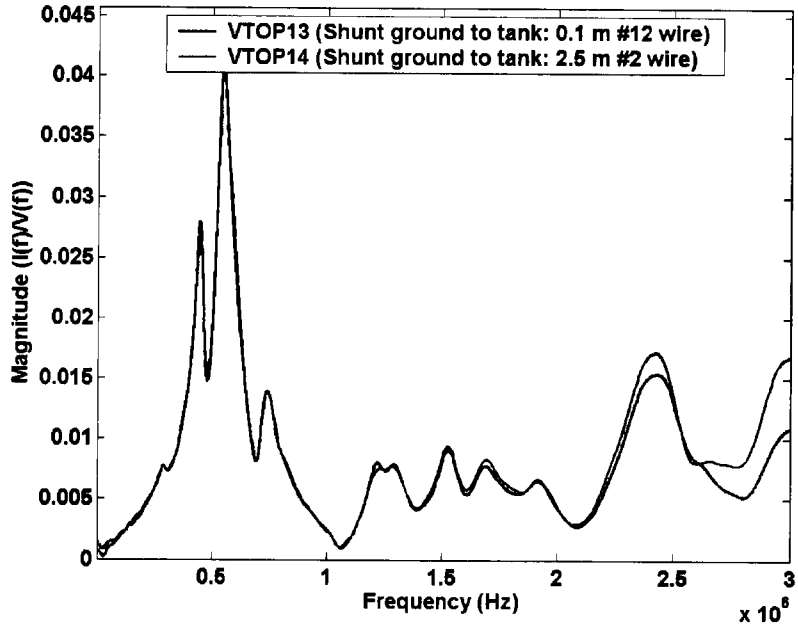


Figure 6.35 – Effect of lead from current shunt to tank ground to 3 MHz
Trace 1 – 0.1 m #2 wire
Trace 2 – 2.5 m #2 wire

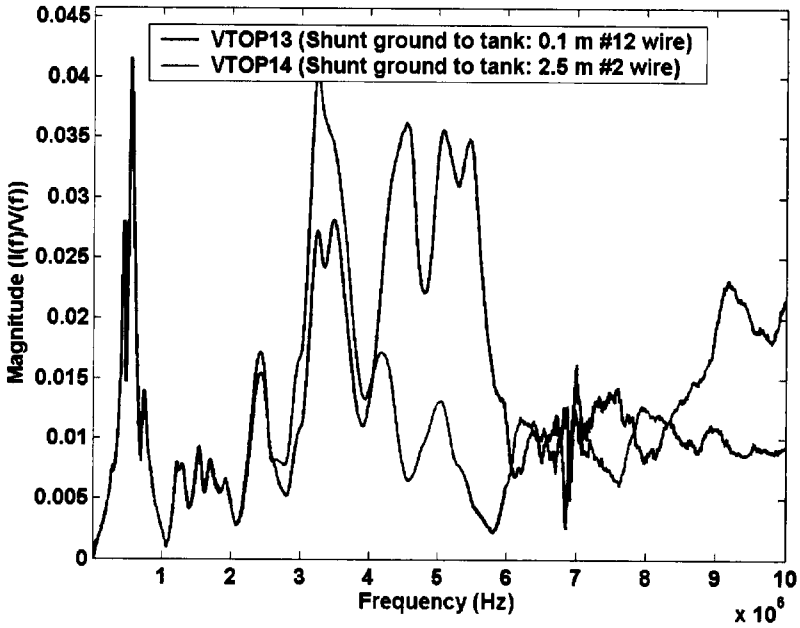


Figure 6.36 – Effect of lead from current shunt to tank ground to 10 MHz
Trace 1 – 0.1 m #2 wire
Trace 2 – 2.5 m #2 wire

## 6.7 Effects of Winding Movement

The distribution transformer winding was used to study the effect of winding movement. The winding has dimensions of 38 cm wide x 56 cm deep by 31 cm high, with 882 turns on the primary winding (high voltage) and 21 turns on the secondary winding (low voltage). The winding was first moved in the axial direction by prying up the upper four turns of one layer of the winding near the high voltage lead. A section of three turns of the winding was pried up a maximum of about 1.5 cm over a length of 5 cm, so that approximately 0.01% of the winding was moved. The radial movement was done by placing a wedge between layers of the winding to a depth of 9.5 cm. This produced a maximum radial movement of about 1 cm over a width of about 6 cm. The distortion was done at about the top of the middle layer of the winding. FRA measurements were recorded before and after the winding was distorted. All of these FRA tests were done with a 100 MHz sampling rate, averaging 250 pulses and using a 1 Ω shunt. All lead lengths were kept as short as possible to minimize their effect. The measurement results are shown in Figures 6.37 to 6.41.

Figures 6.37 and 6.38 show the experimental results for the minor axial winding distortion. In the 0 to 3 MHz frequency range, the distortion is completely undetectable. Above 4 MHz, the distortion is very apparent. Figures 6.39 and 6.40 show the frequency spectrum of the measured signals, indicating that there was good signal strength right up to 10 MHz.

Figures 6.41 and 6.42 show the experimental results for the minor radial winding distortion. In the 0 to 3 MHz frequency range, the distortion is undetectable. Above 3 MHz, small changes become visible, and major changes occur above 7.5 MHz. The differences are not as great as for the axial movement, but the movement is still detectable. Figures 6.43 and 6.44 show the frequency spectrum of the measured signals, indicating that there was good signal strength up to 10 MHz, except around 7 MHz.

From this investigation and past experience, it is apparent that minor winding movement or winding looseness generally shows in the high frequency region of the FRA admittance. This investigation shows the desirability for an alternative measurement method that would optimize the test sensitivity by testing the transformer at higher frequencies without the measurement being swamped by the external test equipment impedances.

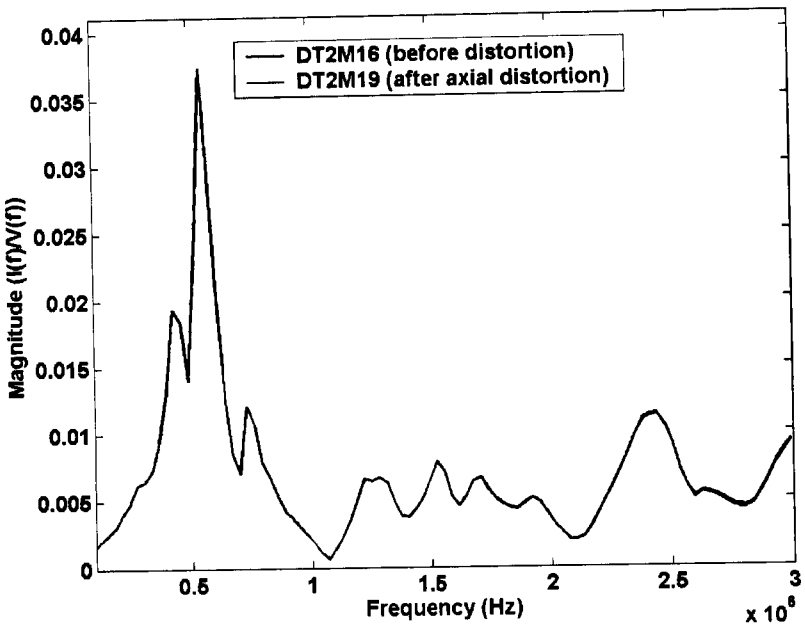


Figure 6.37 – Effect of minor axial movement to 3 MHz
Trace 1 – before axial distortion
Trace 2 – after axial distortion

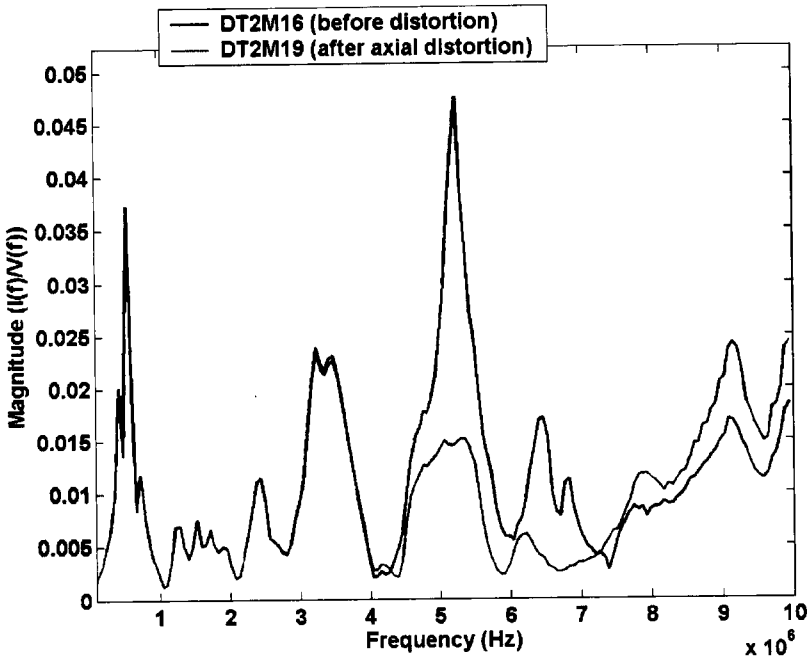


Figure 6.38 – Effect of minor axial movement to 10 MHz
Trace 1 – before axial distortion
Trace 2 – after axial distortion

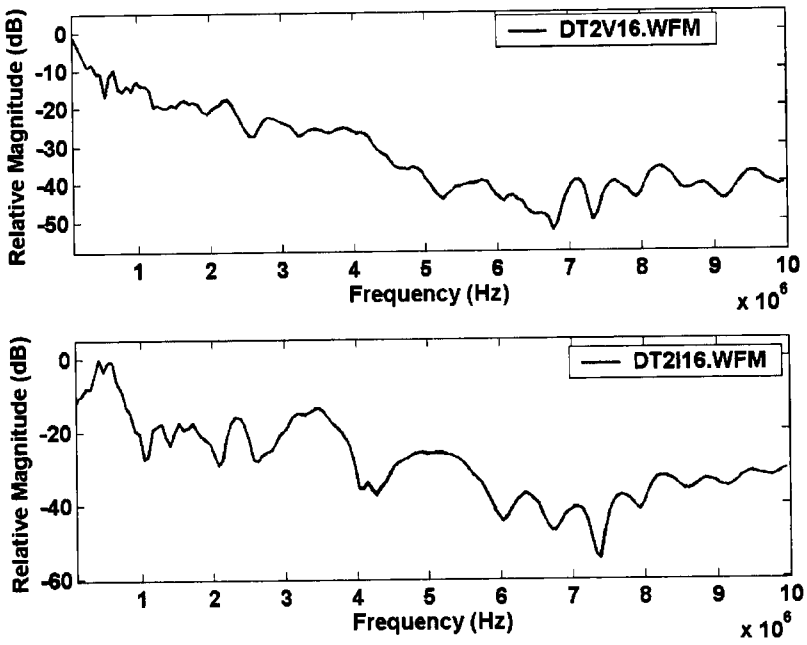


Figure 6.39 – Signal spectrum for test before axial winding distortion
Top Trace – Input signal spectrum
Bottom Trace – Current shunt signal spectrum

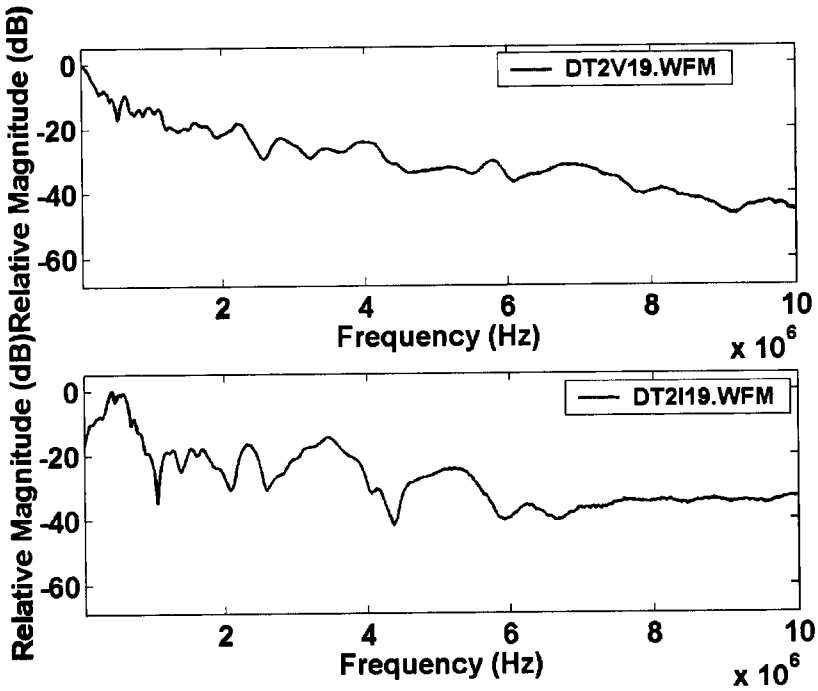


Figure 6.40 - Signal spectrum for test after axial winding distortion
Top Trace – Input signal spectrum
Bottom Trace – Current shunt signal spectrum

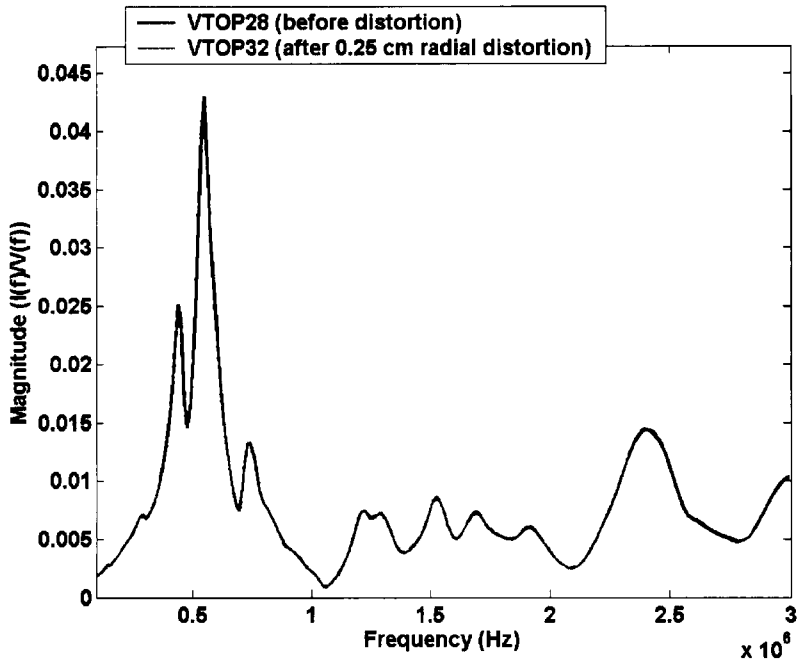


Figure 6.41 – Effect of minor radial movement to 3 MHz
Trace 1 – before radial distortion
Trace 2 – after radial distortion

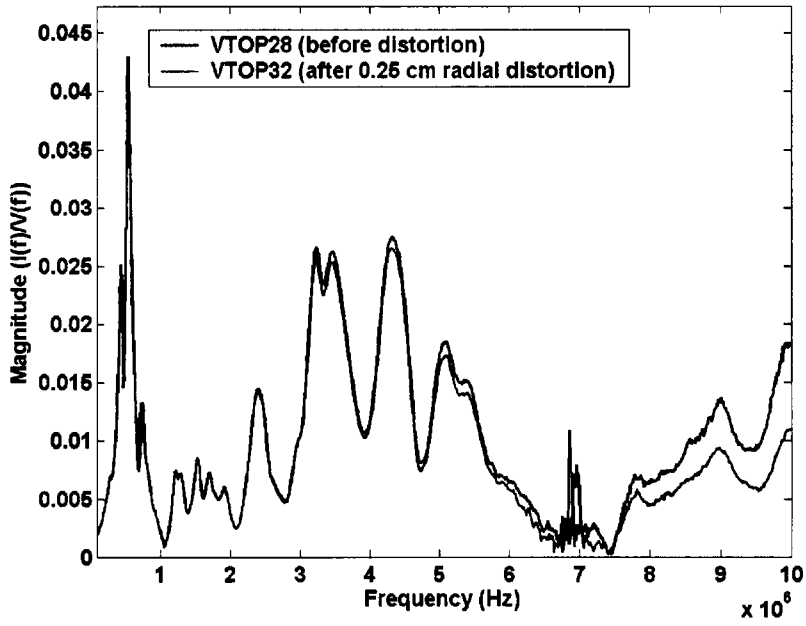


Figure 6.42 – Effect of minor radial movement to 10 MHz
Trace 1 – before radial distortion
Trace 2 – after radial distortion

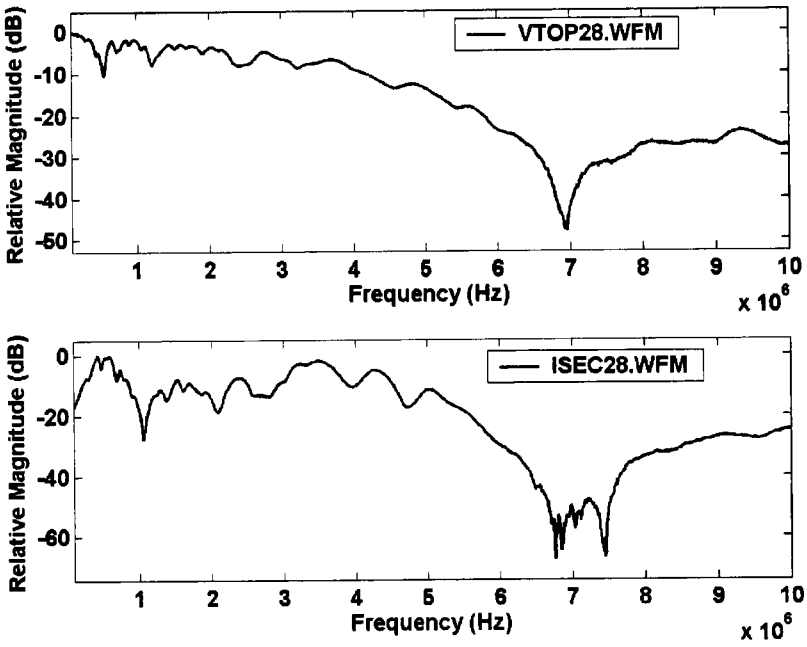


Figure 6.43 – Signal spectrum for test before radial winding distortion
Top Trace – Input signal spectrum
Bottom Trace – Current shunt signal spectrum

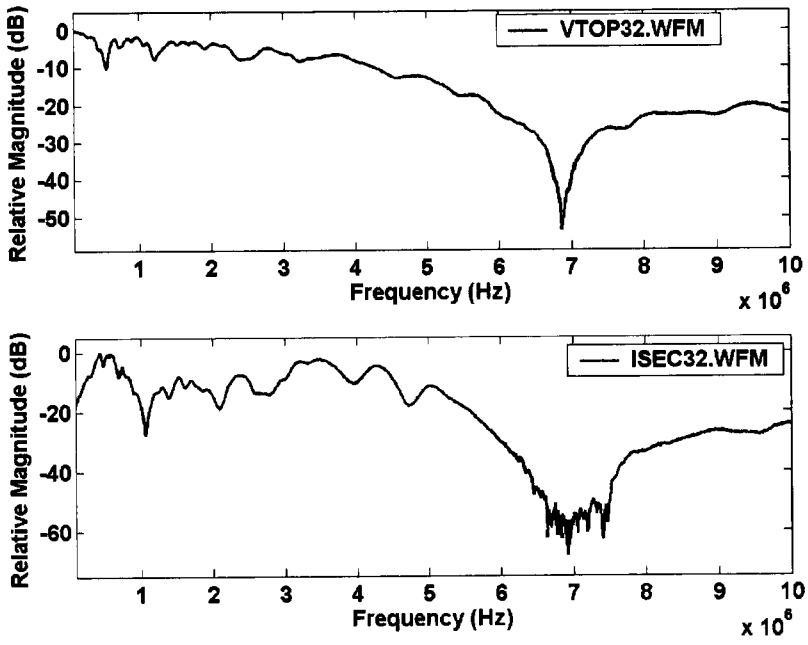


Figure 6.44 – Signal spectrum for test after radial winding distortion
Top Trace – Input signal spectrum
Bottom Trace – Current shunt signal spectrum

## 6.8 Summary of the Investigation

Experiments were performed to study the factors that influence the FRA results. The parameters analyzed were:

- effect of input signal sources
- effect of sampling rate
- effect of shunt
- effect of high voltage bushing
- effect of transformer neutral connection
- effect of measurement leads
- effect of winding movement

### 6.8.1 Effect of input signal source

Two different input signal voltage pulse generators were compared. The admittance results in the range of 0 to 3 MHz showed that the results are independent of the input wave-shape as long as they have sufficient signal energy in the frequency range to be measured. This confirms that the network being tested (transformer with set-up) can be treated as a linear time invariant network and that the FRA test measurement is not dependent on the wave-shape of the input signal (assuming sufficient energy content). Both the voltage spectrum results and the FRA results demonstrated that the RSG generator does not have sufficient signal energy at frequencies above 4.5 MHz, while the PEMI generator has sufficient signal energy up to 11 MHz.

### 6.8.2 Effect of sampling rate

The experiments demonstrated that, for an eight-bit digitizer, a 50 MHz sampling rate is adequate to analyze FRA results up to the 4.5 MHz frequency range, and 500 MHz is adequate for 14.9 MHz.

### 6.8.3 Effect of shunt

The principal findings in this investigation are that the FRA detection sensitivity significantly decreases as the shunt resistance is increased. As the shunt resistance is increased, the maximum frequency range that is sensitive to winding changes decreases. In the cases studied it was found that sensitive measurement could be made to only 0.5 MHz with a 50 Ω shunt resistance. With a 10 Ω shunt and a 1 Ω shunt, the range increases to 3 MHz and 10 MHz, respectively. These limits are dependent to some extent on the individual transformer, as the limits are determined by the magnitude of the winding network impedance compared to the shunt impedance.

### 6.8.4 Effect of high voltage bushing

FRA signatures are not strongly affected by the high voltage bushing and leads impedances, up to about 3 MHz. Above 3 MHz, these impedances start to have an impact. Above 4 MHz the effect is very significant. At the higher frequencies, measurement of the input signal should be done inside the transformer, at the input lead to the transformer, for the measurements to be useful.

On site measurements, especially on a large power transformer, cannot bypass the bushing. This means that the fixed impedance of the bushing can mask changes in the transformer.

### 6.8.5 Effect of transformer neutral connection

The experiments illustrated that having the neutral grounded or having floating connections does have some impact on the FRA results, but below 1.5 MHz the impact was not significant. Above 2 MHz, the FRA admittances show more differences. It is concluded that to detect minor winding movements the FRA comparison has to be done using the same neutral connections each time.

### 6.8.6 Effect of measurement leads

The analysis of the effects of the high voltage and grounding leads was performed with three sets of test leads (standard, long and short). The results indicate that the admittance with the standard leads is similar to the admittance of the transformer with the standard leads above 2.3 MHz. With the long leads, the admittance is similar to the admittance of the transformer with the standard leads above 0.5 MHz. This means that above these frequencies (0.5 MHz for long leads and 2.3 MHz for standard leads), only the lead admittance is being measured. Hence, the sensitivity to changes in the transformer would be dramatically reduced. The leads also have an impact below this frequency, but the influence rapidly decreases. This shows that with a typical circuit the FRA measurement sensitivity range of the long leads arrangement is approximately 0.5 MHz and below, and the range of the standard arrangement is below 2.3 MHz. The standard leads are of a length that would be adequate for most transformers rated below 500 kV. The long leads are of a length that would be required for larger 500 kV transformers and for 750 kV transformers.

The experimental results demonstrate that the shorter the lead from the shunt to X1 terminal, the higher the sensitivity in the high frequency range. The admittance differences are minor below 1.2 MHz. The experimental results also show the significance of the contribution of this lead in the high frequency region. The analysis of these results shows that the admittance increases at some frequencies, as the leads are made longer. This confirms that the optimum measurement requires the lead length to be as short as possible, and the test configuration must remain constant for repeated tests. The higher the frequency range used, the more critical this becomes.

### 6.8.7 Effect of winding movement

For tests in a high voltage laboratory, a distribution transformer winding was used to study the effect of winding movement at frequencies above 3 MHz. The windings were made accessible, then the winding was moved in the axial direction by prying up the upper four turns of one layer of the winding near the high voltage lead. This means that approximately 0.01% of the winding was moved. Radial movement was done by placing a wedge between layers of the winding to a depth of 9.5 cm. This produced a maximum radial movement of about 1 cm over a width of about 6 cm. The distortion was done at about the top of the middle layer of the winding. In the

0 to 3 MHz frequency range, the distortion was completely undetectable. Above 3 MHz small changes were noted. and major changes occurred above 7.5 MHz.

From this investigation and past experience, it is apparent that minor winding movement or winding looseness generally shows in the high frequency region of the FRA admittance. This investigation shows the desirability for an alternative measurement method that would optimize the test sensitivity by testing the transformer at higher frequencies without the measurement being swamped by the external test equipment impedances.

# CHAPTER VII DISCUSSION AND A NEW APPROACH

## 7.1 Introduction

All the existing FRA methods found in the literature have focused on the FRA frequency results at the range of a few tens of kHz to about 1 MHz. The 3 MHz range has been the upper frequency limit of FRA measurements. Measurements made at higher frequencies have not been considered to contain useful information. In discussions with other researchers it has been suggested that at higher frequencies the transformer becomes a pure capacitor and changes in the winding do not affect the FRA signature.

Researchers in reference [122] reported measuring unexpected high frequency overvoltages in the winding due to internal winding resonances in the 1 MHz to 10 MHz frequency range. This supports the contention that there is useful information at the higher frequencies. From a theoretical viewpoint, if we consider the transformer from the lumped element point of view the resonant frequency of a section of winding = $1/2\pi\sqrt{LC}$ (circuit resonant inductance and capacitance). The inductance (L) in the winding does not change significantly with movement; however, the capacitance C changes as the winding moves. Small changes in capacitance $\Delta C$ will have more impact at the high resonant frequencies due to the fact that $f_2/f_1 = 1/\sqrt{(1+\Delta C/C)}$ ($f_2$ and $f_1$ are the resonant frequencies with and without movement respectively). In the higher frequency resonance circuit C is smaller than in the lower frequency resonance, so that the $\Delta C$ will take a bigger percentage of the capacitance change resulting in greater detection sensitivity.

From a transmission line point of view, the transformer winding can be considered as a transmission line with discontinuities such as interlayer connections. Winding movement can be considered as a discontinuity or as a change in impedance of a section of the transmission line. The effect of a change in impedance of a section of transmission line depends on the length of line that has changed. The shorter the wavelength of the frequency used to probe the transmission line, the smaller the winding change that can be resolved. The frequency and wavelength have the following relationship:

wavelength = 300E6/frequency.

For example, at 60 Hz the quarter wavelength is 1250 kilometres, at 1 MHz the quarter wavelength is 75 meters, and at 10 MHz the quarter wavelength is 7.5 meters. It can be seen from these wavelengths that higher frequencies are required to see the smaller changes, and smaller changes will only have an impact at higher frequencies.

These considerations point to the need to study the factors that could be causing the effect of winding changes not to be detected at higher frequencies using existing test methods. The key factors affecting FRA measurement, reported in Chapter VI, showed that the external measurement leads and shunt impedance have a big impact on the FRA results at higher frequencies. The measurement leads and high shunt impedance mask the high frequency information. For example, in order to do an FRA test on a large-sized power transformer, a set of long leads has to be used. Unfortunately, these leads will mask the changes in the winding. This research work has found that the transformer is not a pure capacitor at frequencies above 3 MHz, and that measurements at higher frequencies have greater sensitivity to winding changes once external effects are eliminated.

## 7.2 Limitation of Existing Off-line and On-line FRA Methods

Winding looseness and minor movements are not easy to detect below the 1 MHz frequency range, as seen in the investigations of key factors affecting FRA measurement from Chapter VI. Minor winding movement was easiest to detect above 6 MHz. In the 1 MHz to 3 MHz range, minor winding movement can be detected but the measuring leads arrangement and set-up are very critical. These critical factors were analyzed in Chapters IV and VI, and in Appendix A. At frequencies above 3 MHz, the measurements are even more difficult since many factors contribute significantly to the FRA results, including connecting leads to and from the transformer and bushings, shunt and common ground leads, and the ground connection location on the transformer.

In this study, FRA measurements in the frequency range above 3 MHz were investigated and a wide range of factors were analyzed and discussed. Experiments and analyses were carried out on on-line FRA measurements. It was found that the bushing tap termination output to input signal ratio is constant to approximately 1 MHz, the signal available from the system switching transients is limited to less than 1 MHz, and injecting a signal in the bushing tap and measuring the input at the bushing capacitance tap does not produce measurements independent of the

load external to the transformer. These problems mean that this on-line method is not useful for detecting minor winding movement and winding looseness that is in the range 3 MHz and above.

All the off-line and on-line FRA techniques tested and analyzed in the previous chapters have limitations for detecting minor winding movement to give the earliest possible indication of damage to the transformer winding. High frequency measurements are required (above 3 MHz), which are difficult or impossible to do with the existing methods.

An extensive literature search was carried out, but no method was found to perform such high frequency FRA on-line tests. Based on the research, an alternative method needs to be developed to meet the requirements for an improved test. The new method should be able to detect minor winding movement in a higher frequency range, both off-line and on-line. This chapter investigates a new approach that would enhance measurement sensitivity and perform measurements on-line.

As changes in the power industry towards deregulation lead to changes in maintenance procedures from time-based maintenance to condition-based maintenance, better diagnostic and monitoring tools are needed to assess the condition of transformers on-line, so that if there is a problem the transformer can be repaired or replaced before it fails. The new approach presented in this chapter, called the High-frequency Internal Frequency Response Analysis (HIFRA) method, addresses this requirement.

## 7.3 Results from Transformer Simulations

In order to thoroughly analyse the existing FRA methods and the new concept, transformer model simulations were carried out[6]. The basic parameters for a medium-sized transformer were taken from reference [138]. A number of modifications were made on this model to tailor it to simulating FRA winding movement detection. Components were added to the basic transformer model, including a high voltage bushing, ground lead, parallel ground resistance and resistance in parallel with the series winding capacitance. The majority of the simulations were carried out on a 67-section transformer model. The aim of this simulation was to

[6] Detailed results are in Appendix A.

determine the principal factors affecting FRA measurement and to provide clues as to how to relate changes in the transformer signature to the type and location of winding movement.

The simulation results show that the FRA method for the detection of winding movement is more sensitive at a high frequency range (6 MHz to 10 MHz). Most of the simulation cases show that the most significant frequency shifts and magnitude changes occur in this high frequency region. Figure 7.1 demonstrates the frequency shift and magnitude change patterns from the simulations of winding movement. The movements were simulated at three winding positions, and the results are the average of these three simulations. The results show that the changes from winding movement increase as the resonant frequency increases. The general trend in sensitivity to winding movement detection is that it increases with frequency.

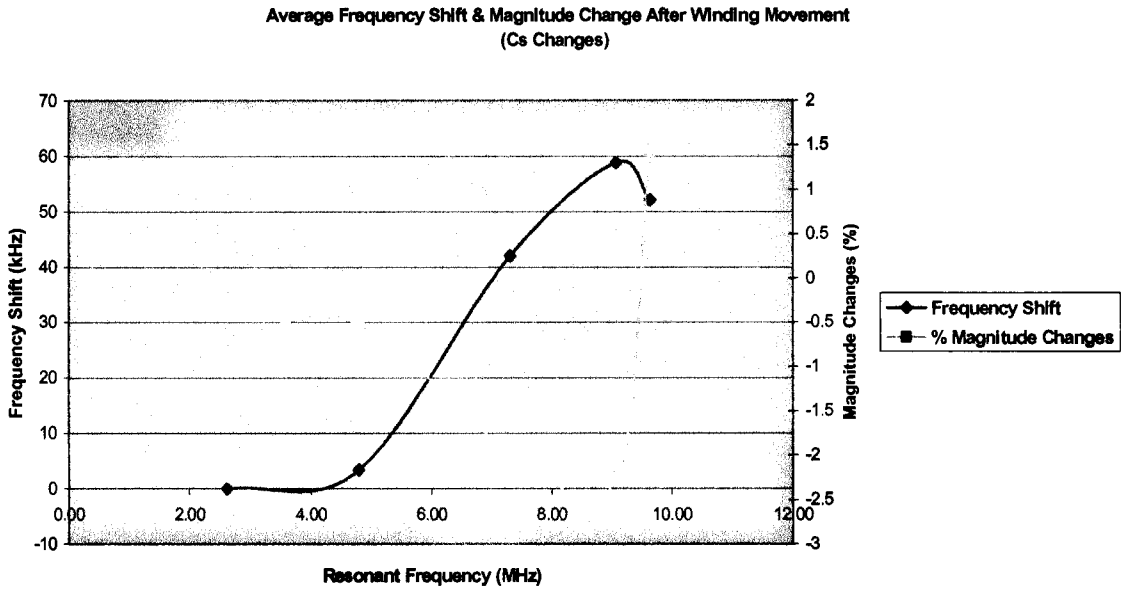


Figure 7.1 – Average frequency shift & magnitude change after winding movement

The case of the transformer model with a high voltage bushing and ground lead was studied. The magnitude of admittance with ground lead and bushing decayed much faster in the high frequency region (7 MHz to 10 MHz) than the magnitude of admittance without a bushing and ground lead. This simulation shows that the admittance magnitude can be higher in the high frequency region if the effect of the ground lead and bushing can be eliminated.

Both axial movement (Cs changes, Figure A.16) and radial movement (Cg changes, Figure A.27) in a winding were simulated. The simulation results show that they can be detected at this high frequency region (5 MHz to 10 MHz) and that the detection is more sensitive in this range. Locally shorted windings can be detected, but not necessarily in the very high frequency range.

Winding movements in different locations are simulated in Appendix A (Figures A.17, A.18, A.28 and A.29). The results clearly show that movement causes changes in frequency and magnitude of the admittance peaks. The correlation of movement location with FRA results needs to be investigated further. There was no obvious simple pattern to the results. Further work using pattern recognition techniques may be useful.

Winding clamping pressure changes were simulated and were found to have a significant impact on the FRA results. The simulation results (Appendix A, simulation 17, Figure A.33) also explain the phenomenon that after re-clamping, the admittance magnitude reduces. After re-clamping, the thickness of the dielectric between winding layers is reduced and results in a slight reduction of dielectric resistance. The simulation results show that the resistance parallel with the main winding series capacitance also had a significant impact (Appendix A simulation 16, Figure A.32). The parallel ground resistance ($R_s$) with series capacitance shows a reduction on the resonant magnitude as well.

Simulation of signal injection into the bushing capacitance tap was carried out. The simulation measured the input signal at the top and bottom of the bushing. The bushing bottom measurement was found to have a slightly higher sensitivity compared with the measurement at the top of the bushing. The high voltage terminal load did not affect measurement at the bottom of the bushing, but the load did affect the measurement at the top of the bushing. Tables 7.1 and 7.2 show the simulation results of the injection method for a load of 300 Ωin parallel with 2 nF. The data with no load are used as the baseline data. The change in the resonant peak frequency and magnitude is compared with the baseline (no load) data. The results in the table clearly show that the measurements at the top of the bushing are affected by the high voltage load, while the measurement at the bottom of the bushing (inside transformer measurement) are not affected by the high voltage external loads.

Table 7.1 – Measurement at top of bushing with and without load - 300 Ω parallel with 2 nF

| Baseline* resonant frequency (no load) | Baseline* resonant magnitude (no load) | Frequency change comparing with baseline (Δf ) | Magnitude change comparing with baseline | Note |
|---|---|---|---|---|
| 2.62 MHz | 5.64e-3 | 0 kHz | -62.20% | 1st resonance |
| 4.80 MHz | 7.30e-3 | 0 kHz | 283.70% | 2nd resonance |
| 7.30 MHz | 4.27e-3 | 0 kHz | 1019.76% | 3rd resonance |
| 9.07 MHz | 3.17e-3 | 0 kHz | 1857.94% | 4th resonance |
| 9.64 MHz | 2.02e-3 | 0 kHz | 2199.19% | 5th resonance |

* Baseline – no load test data, effect of load is compared to this reference data.

Table 7.2 – Measurement at bottom of bushing with and without load - 300 Ω parallel with 2 nF

| Baseline* resonant frequency (no load) | Baseline* resonant magnitude (no load) | Frequency change comparing with baseline Δf | Magnitude change comparing with baseline | Note |
|---|---|---|---|---|
| 2.62 MHz | 5.71e-3 | 0 kHz | -0.15% | 1st resonance |
| 4.80 MHz | 7.31e-3 | 0 kHz | -0.14% | 2nd resonance |
| 7.31 MHz | 4.30e-3 | 0 kHz | -0.27% | 3rd resonance |
| 9.08 MHz | 3.22e-3 | 0 kHz | -0.19% | 4th resonance |
| 9.64 MHz | 1.93e-3 | 0 kHz | 0.13% | 5th resonance |

* Baseline – no load test data, effect of load is compared to this reference data.

The transformer model simulation lead and the tests in the laboratory and in the field led the research towards measurement at higher frequencies. The simulations showed the potential strength of this measurement method.

## 7.4 New Concept

### 7.4.1 Problems with Conventional FRA Methods

Measuring the input signal outside the transformer has a frequency limitation (about 3 MHz for the pulse test method) due to the impedance of the external leads and the sensitivity of lead placement at higher frequencies. The lead length limits the frequency response of the signal measurement. Due to the physical size of the transformer bushings, it is not possible to shorten the leads to improve the frequency response. At higher frequencies even minor changes in the location of the leads will cause changes in the transfer function. These problems make the test unusable at the higher frequencies.

### 7.4.2 High-frequency Internal Frequency Response Analysis (HIFRA) Test Method

The new concept that was developed is to measure the signals inside the transformer by using appropriate non-contact sensors on the transformer winding leads. The transfer function would then be calculated from the measured signals. The new method, called High-frequency Internal Frequency Response Analysis (HIFRA), was tested in the laboratory.

The measured signal for the HIFRA test can be either a voltage or a current. To measure voltage, either a capacitive voltage sensor or an electric field sensor is used. If an electric field sensor (optical or electrical) is used, the sensor position is fixed in place such that the output is always directly proportional to voltage. To measure current, a high frequency current transformer (optical or electrical) or a Rogowski coil is used.

The output of the capacitive voltage sensor, electrical current transformer or Rogowski coil is connected to a coaxial cable that is brought through the transformer tank wall to the outside and connected to the recording instrument (e.g., an oscilloscope). If an electric field sensor is used, the output signal could be optical or electrical. If optical, optical fibres are brought through the transformer tank wall to the instrumentation that converts the optical signal to an electrical signal.

The input signal can be obtained from a number of different sources, as long as the signal contains measurable energy in the frequency range of interest. The signal can be a swept frequency source or a pulse as in the conventional measurement.

Three signal sources were originally considered for the HIFRA method. One is transients generated by power system switching operations. However, the on-line experiments showed that the signal does not have the desired frequency range (see Chapter IV). The other signal source that was investigated is the signal from a transmission line conductor, since the transmission line acts as an antenna and could pick up radiated signals. These signals were also evaluated for the application of measuring the transfer function of a transformer. A preliminary test was performed on a test transmission line. The results showed that the transmission line as an antenna did not pick up sufficient signal for the purpose of the FRA measurement. The third method proposed is the signal injection method. The principle of this method is to inject the input signal through a high voltage bushing capacitance tap. A detailed analysis and discussion of this method will be presented later in this chapter.

Figure 7.2 shows the new concept. Figures 7.3 and 7.4 show the transfer function measured up to 10 MHz inside the transformer on the winding leads, with and without minor winding movement. It can be seen that there is no difference in the transfer function below about 4 MHz. Figures 7.5 and 7.6 show the transfer function measured using the conventional impulse method (FRA (I)). This signal is "noisy" above 5 MHz due to a lack of energy content in the input signal at the higher frequencies.

There are a number of advantages to measuring the signals inside a transformer:

1. It eliminates the frequency limitation imposed by the length of the leads required for external measurement, and makes measurements at higher frequencies (10 MHz) possible. By measuring at higher frequencies, much smaller winding movements can be detected which will allow for earlier warning of changes in the transformer.

2. By permanently mounting the measuring sensors inside the transformer, the risk of the test set-up being changed from one measurement to the next is eliminated. With the conventional test method, a change in set-up can cause changes in the transfer function that appear to be changes in the transformer.

3. The permanently mounted sensors make it easier to do the test, thereby reducing the cost of testing and making it possible to test more often and monitor the transformer more closely.

4. If the required input signals can be injected into the high voltage bushing capacitance tap, the test can be done without taking the transformer out of service.

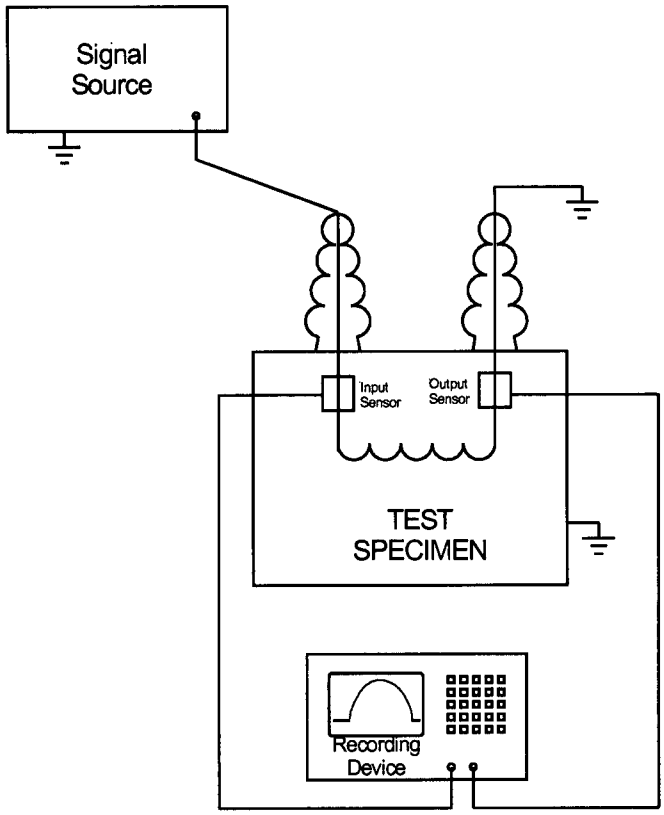


Figure 7.2 - Proposed new measurement circuit

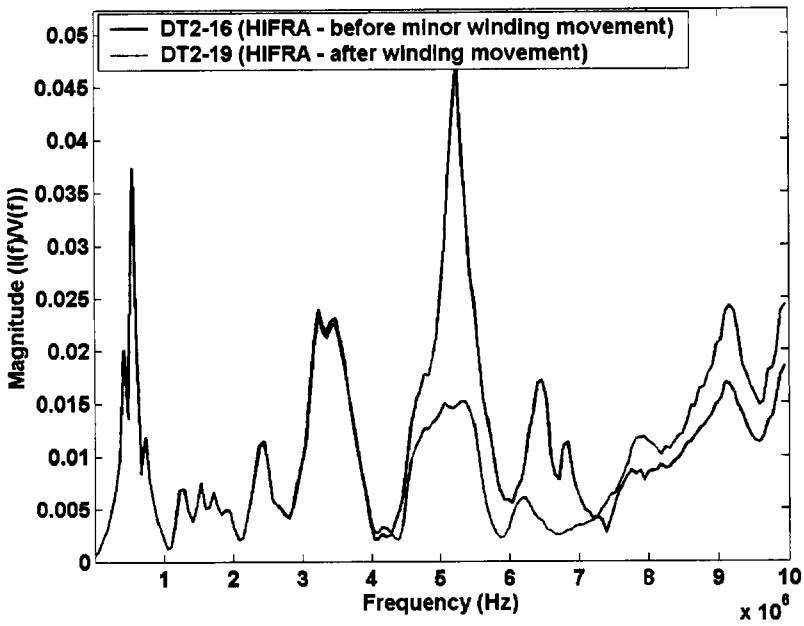


Figure 7.3 - New method showing the effect of using higher frequencies (linear plot)

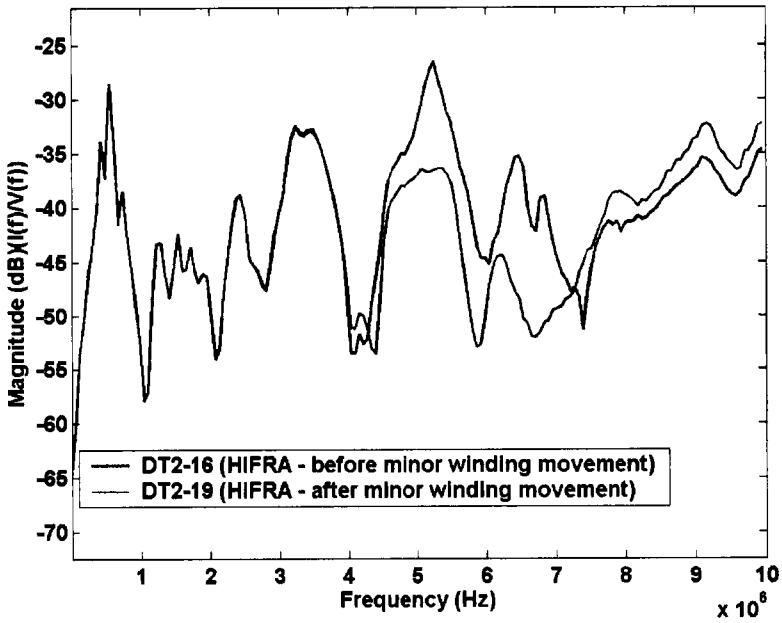


Figure 7.4 - New method showing the effect of using higher frequencies (dB plot)

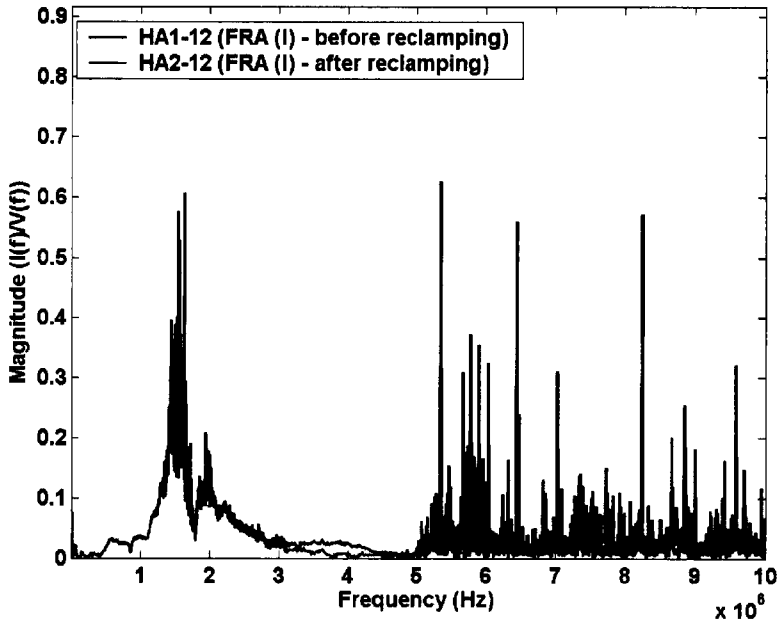


Figure 7.5 - Conventional FRA method showing noise at higher frequencies (linear plot) (caused by inadequate signal strength)

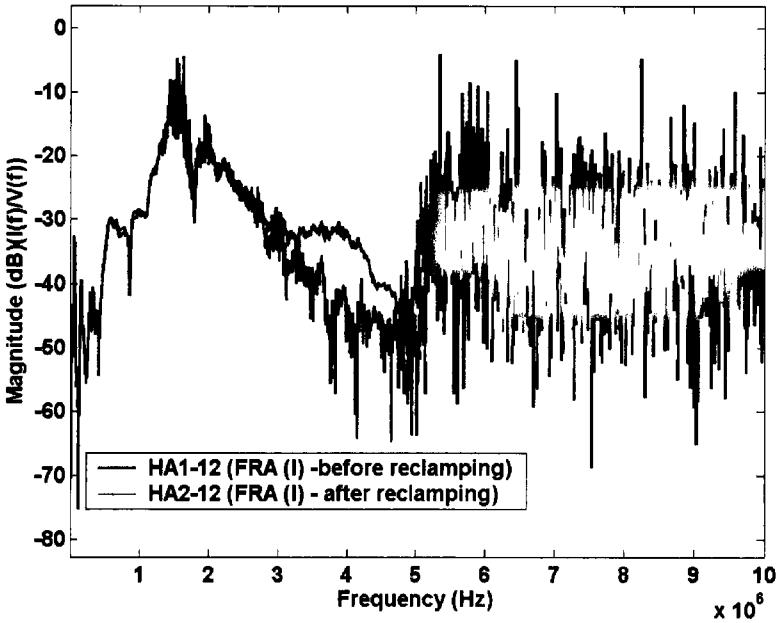


Figure 7.6 - Conventional FRA method showing noise at higher frequencies (dB plot) (caused by inadequate signal strength)

### 7.4.3 Laboratory experiments on the HIFRA method

Three potential input signal sources for the HIFRA method on-line test were investigated: system switching transients, pickup of random transmission line signals and signal injection through the bushing tap. These are preliminary tests of the on-line application of the HIFRA method. The experiment results are reviewed in the following sections.

#### 7.4.3.1 System switching transient measurement

Disconnect switches and circuit breakers generate transient voltage in a power system when they operate. These transients could be used for the HIFRA method as an input signal source. Experiments were performed on measuring the switching transients, which were generated by closing a disconnect switch to energize the high voltage winding of the transformer under test. The measurements were recorded at a capacitance tap on a nearby transformer's high voltage bushing. The bushing was equipped with a bushing coupling box, as described in Section 4.4.4.

Figures 7.7 and 7.8 show the frequency spectrum from two examples of switching transients measured from two different transformers in two different substations. They were measured on the low voltage winding bushings. In the first case (Figure 7.7), the sufficient frequency span reached approximately from 1.5 MHz to 2.5 MHz. In the second case (Figure 7.8), the sufficient frequency span only extended to about 0.8 MHz. These recorded data show that switching transients can potentially be used for on-line FRA measurement, but the frequency content is not sufficient to perform sensitive FRA measurements, which require higher frequencies.

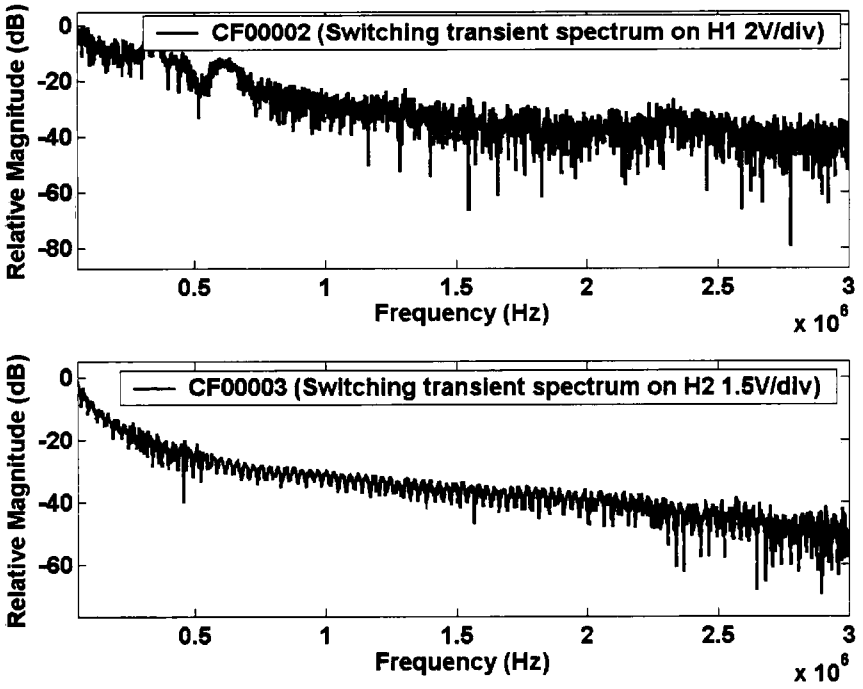


Figure 7.7 – System switching transient spectrum - Example 1

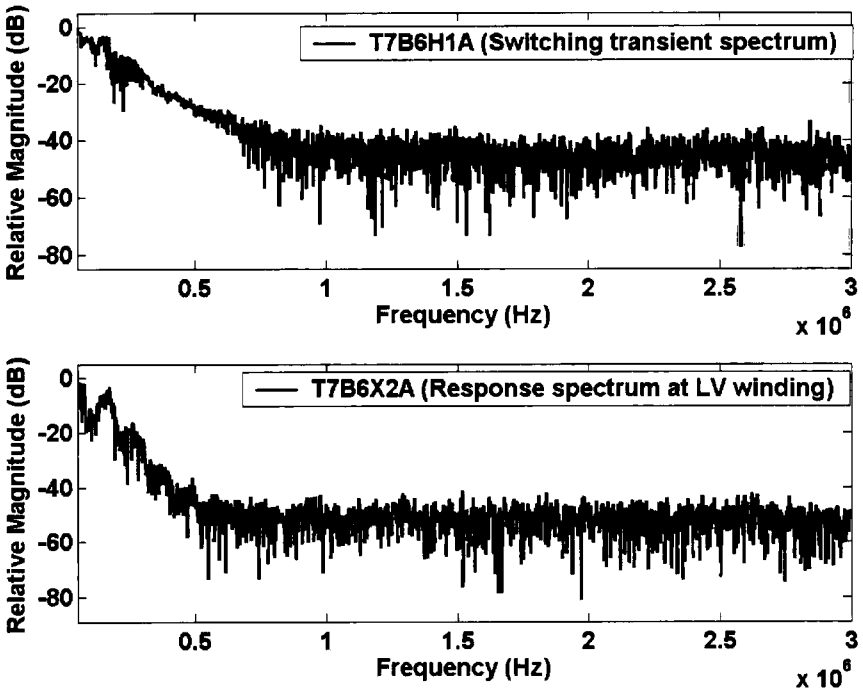


Figure 7.8 – System switching transient spectrum - Example 2

7.4.3.2 Transmission line signal pickup measurements

There may be sufficient high frequency noise on a transmission line to use this noise as the input signal to carry out the HIFRA test, with the transformer energized in the power system. The high frequency noise on the transmission line would be transferred into the transformer winding through the transformer bushings. In order to find out whether there are high frequency signals on a transmission line that could be used by the HIFRA test method, measurements were made on a short (0.5 km long) de-energized transmission line. A connection was made to the transmission line with a 12 m lead and input to a Tektronix scope. Measurements were made at different sample rates (10 MHz/s and 50 MHz/s), and single and multiple (50) sweep averages were used. The frequency spectrum of the measurements is shown in Figures 7.9 to 7.11. Figure 7.9 shows the results of single and multiple sweeps with a 10 MHz sampling rate and plotted up to 3 MHz. Figures 7.10 and 7.11 show the results of single and multiple sweeps with a 50 MHz sampling rate plotted to 3 MHz and to 10 MHz, respectively.

The measurement results show that the transmission line had a reasonable signal level below 2 MHz. Above 2 MHz the signal level was not sufficient for the HIFRA measurement.

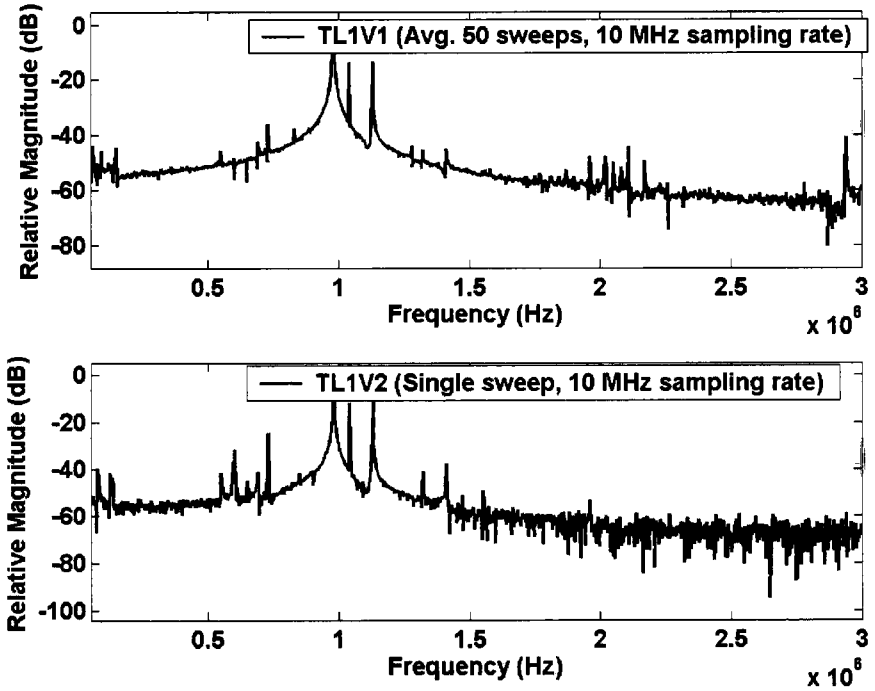


Figure 7.9 – Transmission line pickup signal spectrum with 10 MHz sampling rate

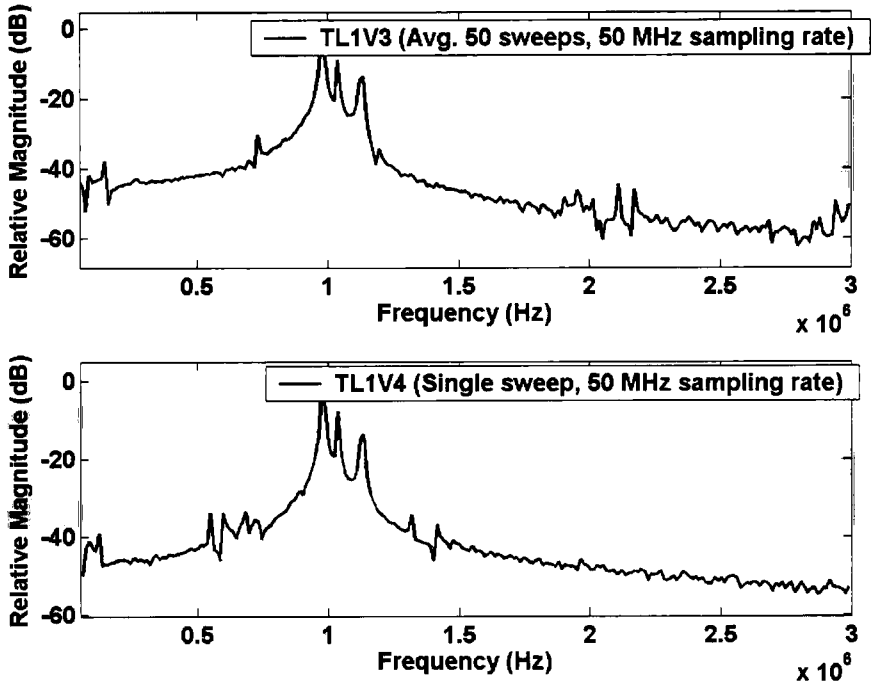


Figure 7.10 – Transmission line pickup signal spectrum to 3 MHz - 50 MHz sampling rate

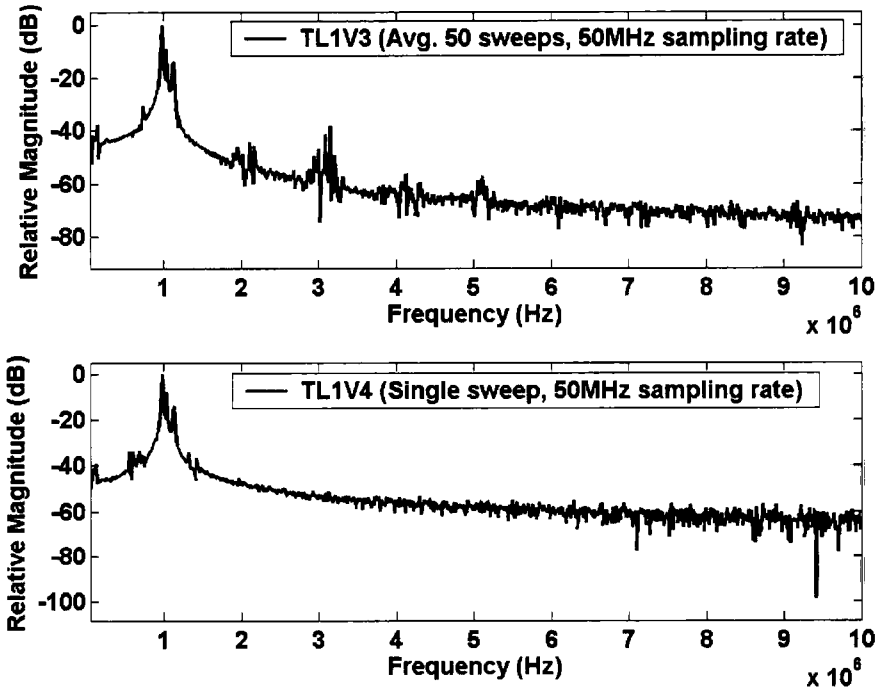


Figure 7.11 - Transmission line pickup signal spectrum to 10 MHz - 50 MHz sampling rate

7.4.3.3 Signal Injection Method

Injecting a signal into a transformer bushing capacitance tap as the input signal for the HIFRA test has great advantages in moving the HIFRA test method to an on-line measurement. Preliminary experiments were performed in the laboratory using a distribution transformer. A Monsanto pulse generator was used to generate a repeatable 20 ns duration pulse with a 5 ns rise time. This pulse was injected into the bushing capacitance tap. Figure 7.12 shows the test circuit. The HIFRA method was then used for the FRA test measurement. A coupled current at the low voltage winding was measured with a 1 Ω shunt. The input signal spectrum is shown in Figures 7.13 and 7.14. The measurement results show that the signal injected through a bushing tap can have a broad frequency range. From the conceptual point of view, there is no problem in injecting a signal up to the 10 MHz frequency range into the high voltage winding terminal inside the transformer.

Figures 7.15 and 7.16 show the transfer functions obtained with different high voltage external leads. The purpose was to study the effect of the external connections at the high voltage bushing terminal. If the external load affects the transfer function measured by the HIFRA method with signal injection, this technique will not be useable on-line since the external impedance changes with system condition changes. The results show that the transfer functions are basically the same right up to 10 MHz. There are some slight differences at the high end of the frequency range (7 MHz to 10 MHz). The comparison of the transfer function with the baseline case without a lead connected to the HV bushing terminal shows that the transfer function with the long (15 meter) and short (4.3 meter) coaxial cables has a slightly larger deviation in the high frequency region than with the short lead (1 meter conductor). In the frequency range to 1 MHz, the transfer function also has some minor differences with different external leads. Overall, the agreement of the transfer functions with different lengths of leads on top of the high voltage bushing is very good.

In addition to the above investigation, transformer tests were carried out using the injection method with loads applied to the secondary winding of the transformer. The loads used in the tests were 1 Ω (12% load) and 10 Ω (120% load) low inductive resistors. The purpose of the experiment was to check the influence of the secondary load on the transfer function. The measurement results using the HIFRA concept (measured at the bottom of the bushing) are

shown in Figures 7.17 and 7.18. A measurement at the top of the high voltage bushing was performed at the same time. The results of this measurement are shown in Figures 7.19 and 7.20.

The measurements at the top and bottom of the high voltage bushing with the signal injection method both show significant admittance differences with different loads in the frequency region of 0.8 MHz to 5.5 MHz. Both measurement locations show almost no effect from the load in the higher frequency region (5.5 MHz to 10 MHz). These results indicate that the effect of the secondary winding load can be avoided by using the high frequency part of the transfer function.

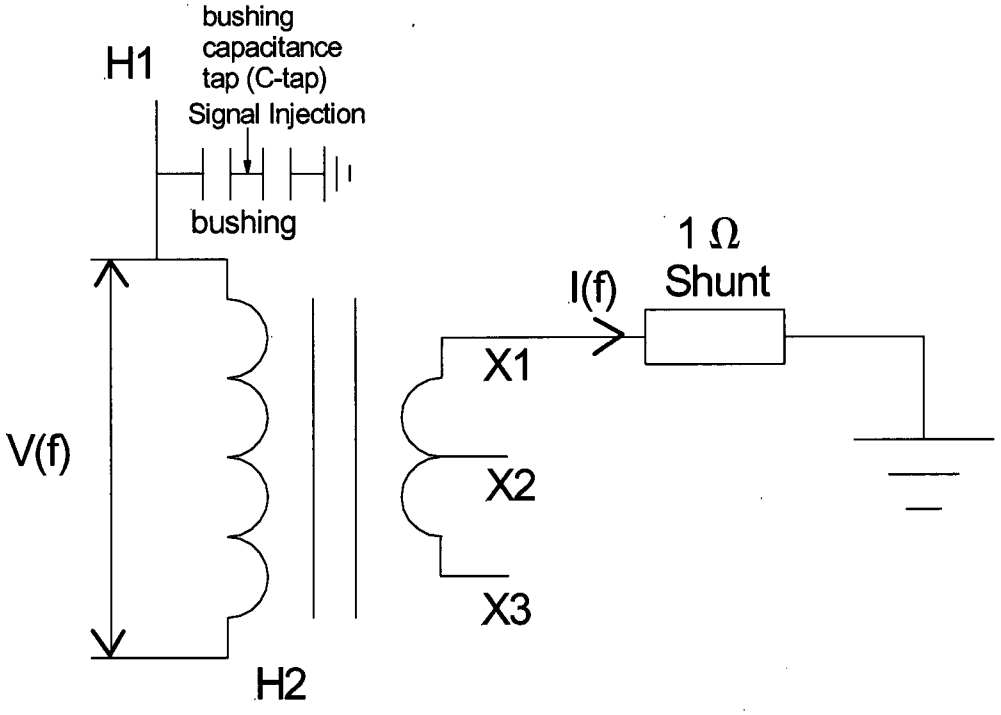


Figure 7.12 – Signal injection method test circuit

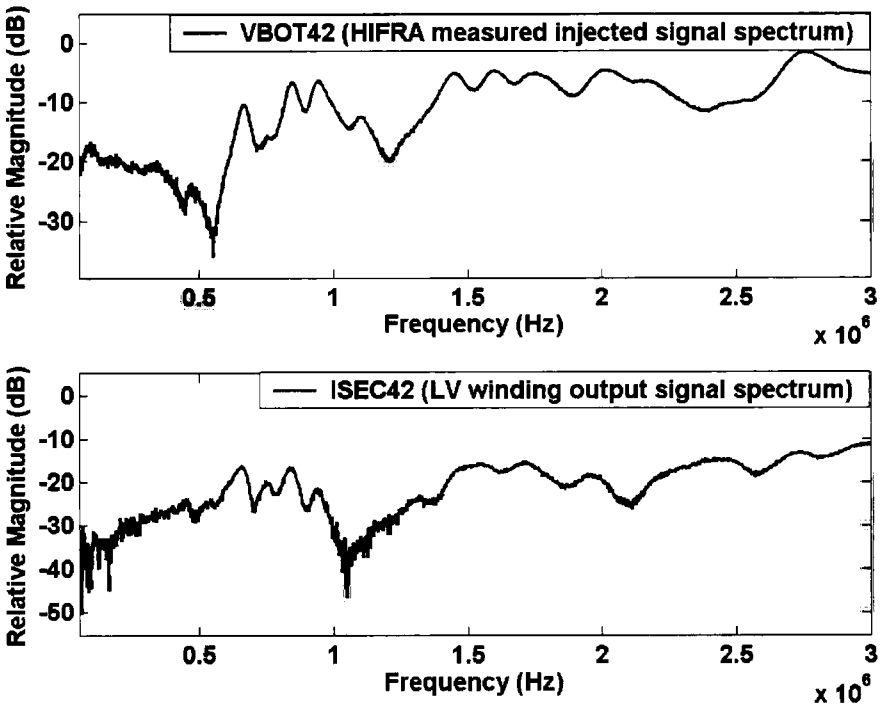


Figure 7.13 – HIFRA measured signals spectrum to 3 MHz range

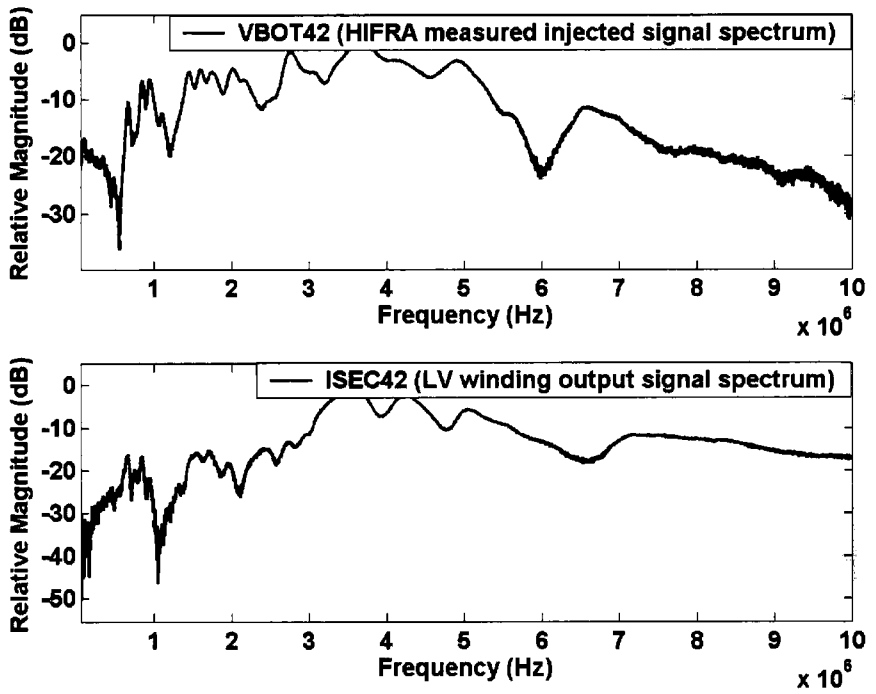


Figure 7.14 – HIFRA measured signals spectrum to 10 MHz range

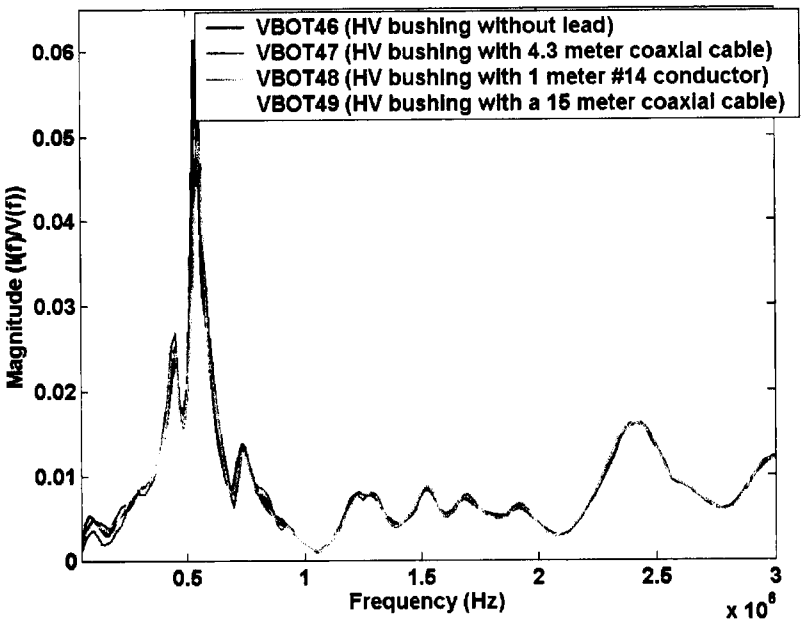


Figure 7.15 – Transfer function from bottom of bushing by HIFRA with signal injection method using different leads connected on top of HV bushing (3 MHz range)

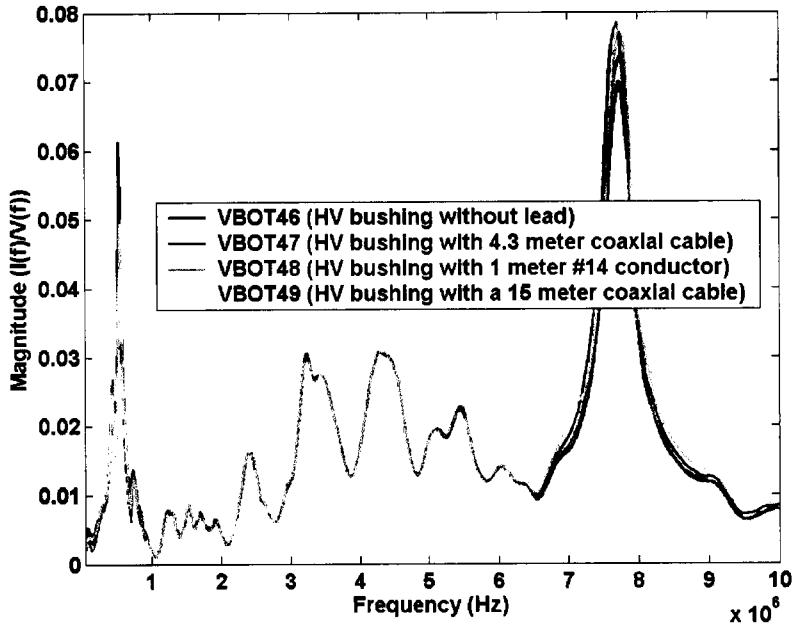


Figure 7.16 – Transfer function from bottom of bushing (HIFRA) with signal injection method using different leads connected on top of HV bushing (10 MHz range)

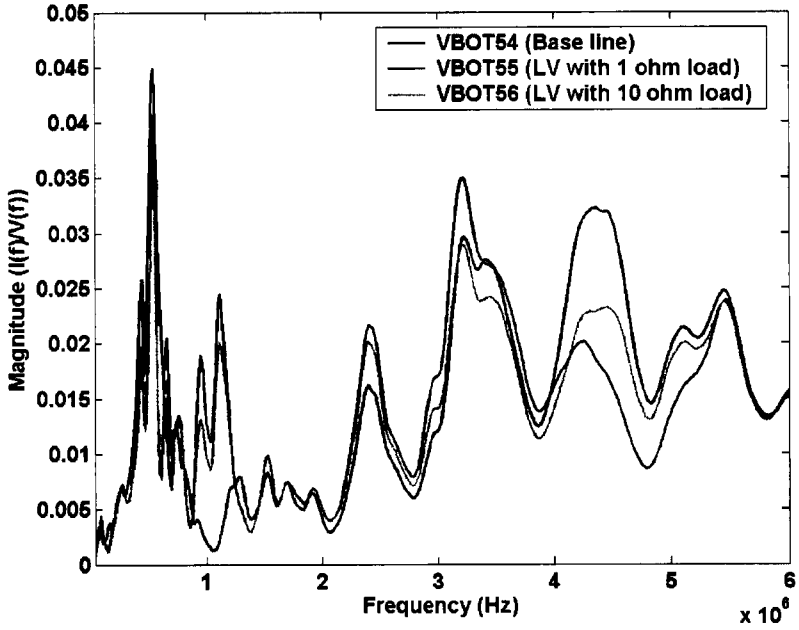


Figure 7.17 - Transfer function from bottom of bushing (HIFRA) and injection method with different LV winding loads (6 MHz range)

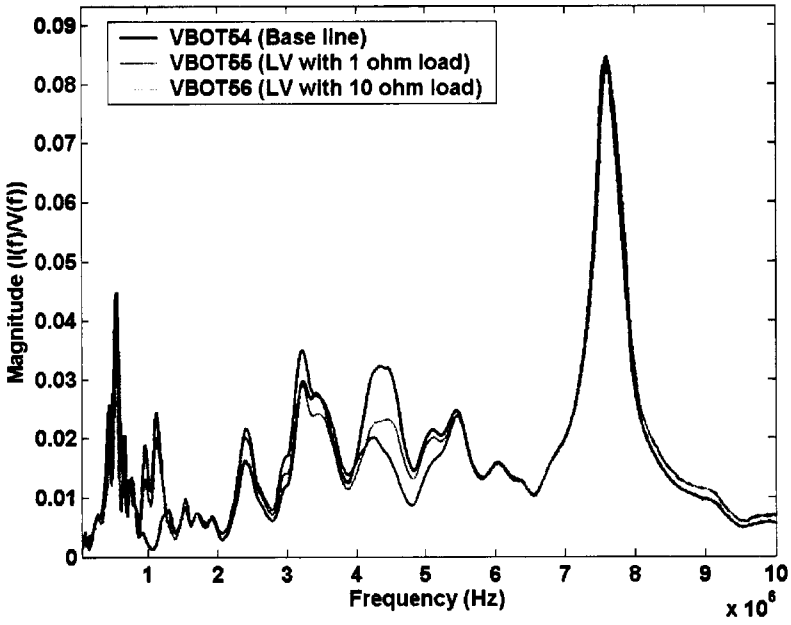


Figure 7.18 - Transfer function from bottom of bushing (HIFRA) and injection method with different LV winding loads (10 MHz range)

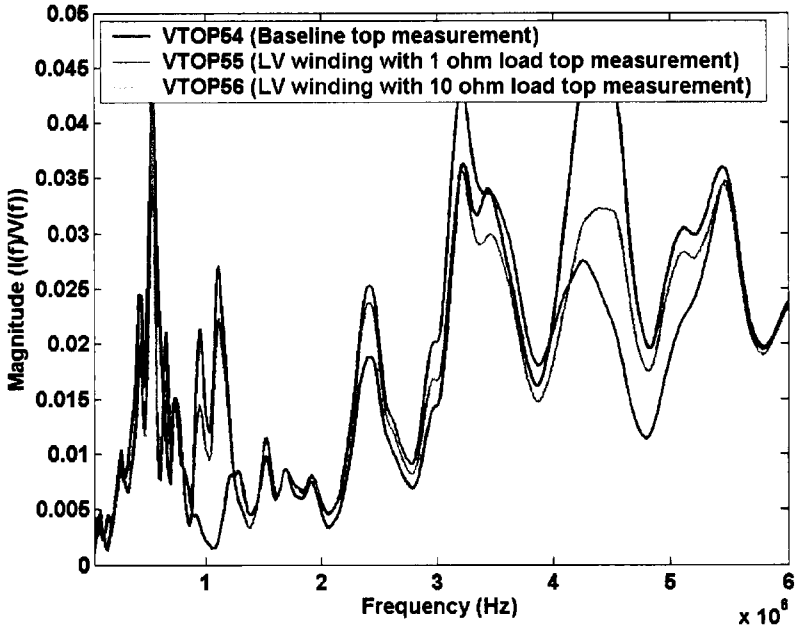


Figure 7.19 - Transfer function obtained from top of bushing and injection method with different LV winding loads (6 MHz range)

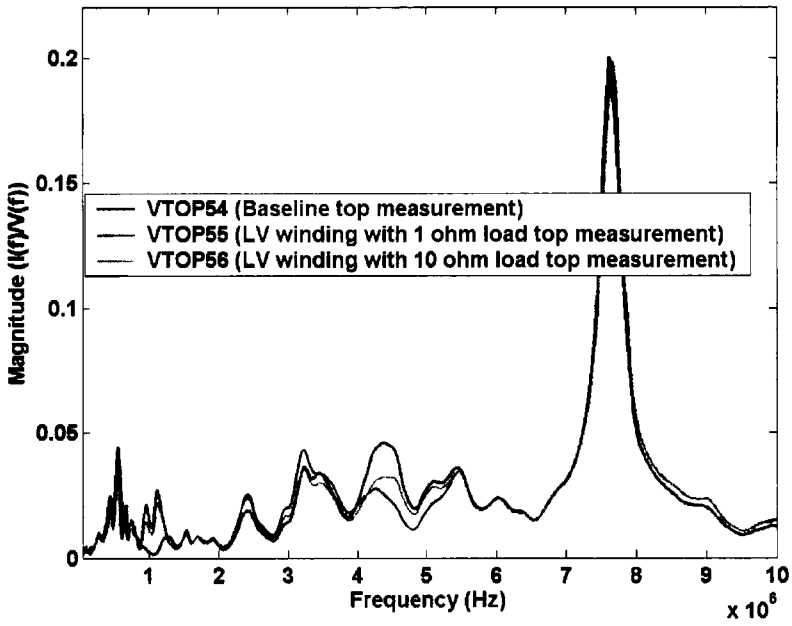


Figure 7.20 - Transfer function obtained from top of bushing and injection method with different LV winding loads (10 MHz range)

### 7.4.4 Feasibility of Using an Electric Field Sensor with the HIFRA Test Method

A simple electric field sensor was constructed using a parallel plate capacitor made from a 1.5 mm thick, 1 cm wide x 1.5 cm long, double-sided printed circuit board. This sensor was connected to a short coaxial cable and the output was measured with an oscilloscope. The sensor was mounted next to the transformer primary high voltage lead (H1), between the high voltage bushing and the start of the high voltage winding. The sensor was electrically isolated from the high voltage lead. FRA tests were done with this electric field sensor with both output terminals electrically floating and with one terminal grounded. Comparison tests were performed by the HIFRA method, using this internal sensor and direct measurement of the signal at the same location on the high voltage lead. The measurements were done using a 500 MHz sampling rate and with a 100 MHz filter hi-pass filter. The comparison results with one electrode of the sensor grounded are shown in Figures 7.21 and 7.22 (3 MHz and 10 MHz range, respectively). A 1 Ω shunt was used in this measurement.

A second experiment was conducted on the sensor with both electrodes floating. This test simulated a true electric field sensor measurement. Figures 7.23 and 7.24 show the measurement results of this test. The output signal was 25 times lower in this arrangement compared to the test with one grounded electrode. The simple electrical field sensor used for these tests had a weaker signal than the conventional measurement, but the transfer function results have the same characteristics.

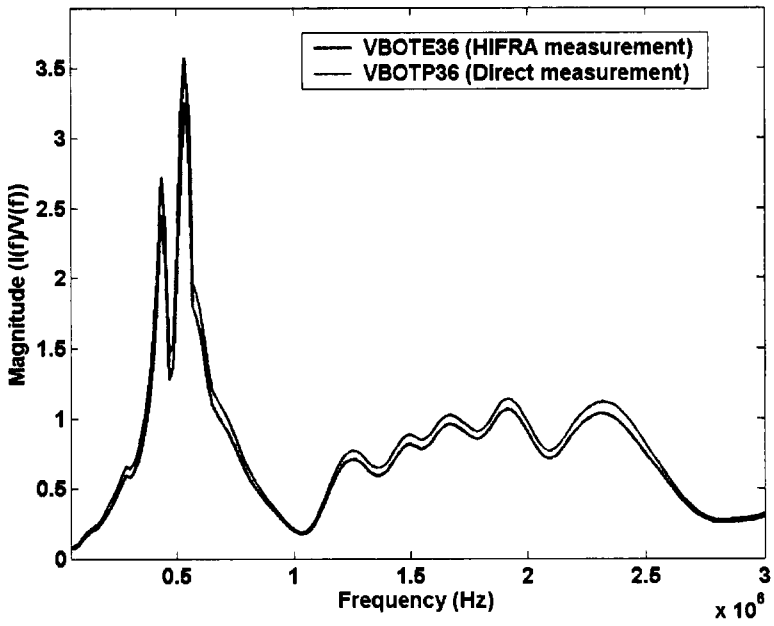


Figure 7.21 - Transfer function measured directly and measured by HIFRA sensor with one electrode grounded (3 MHz range)

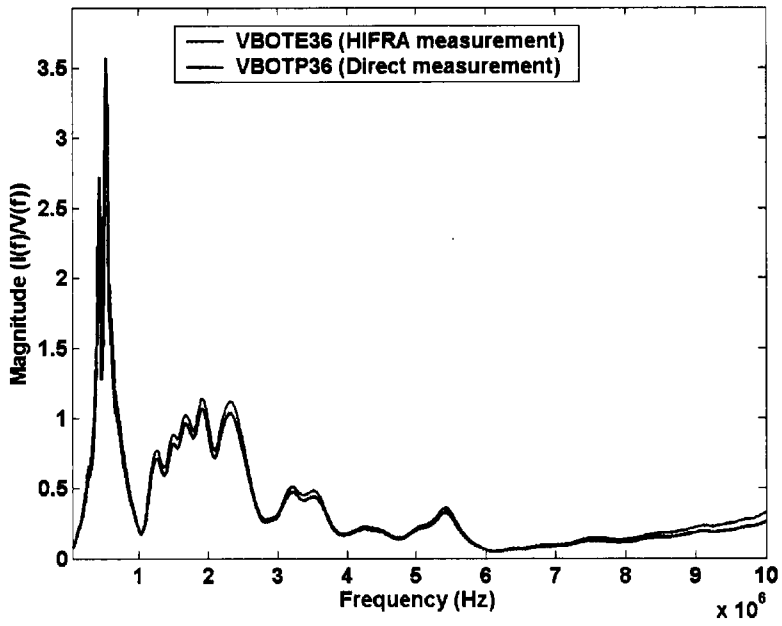


Figure 7.22 - Transfer function measured directly and measured by HIFRA sensor with one electrode grounded (10 MHz Range)

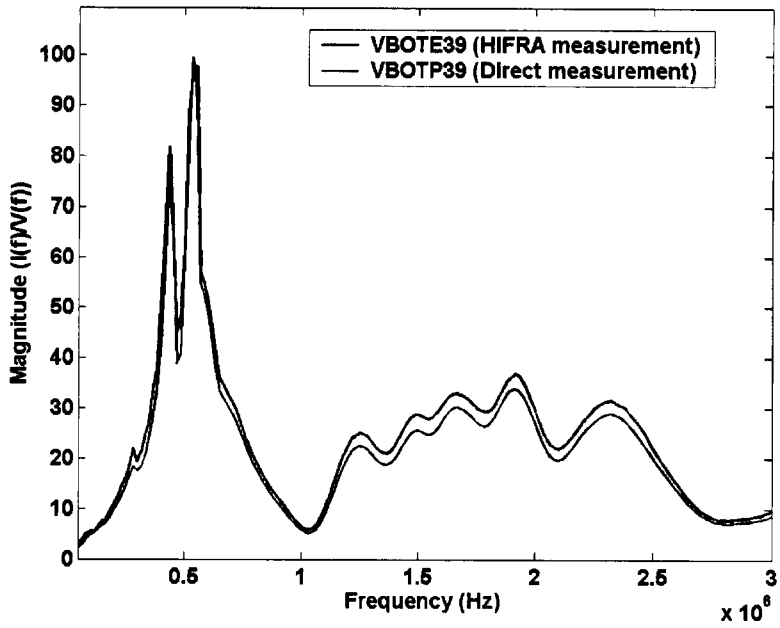


Figure 7.23 - Transfer function measured directly and measured by HIFRA sensor with both electrodes floating (3 MHz range)

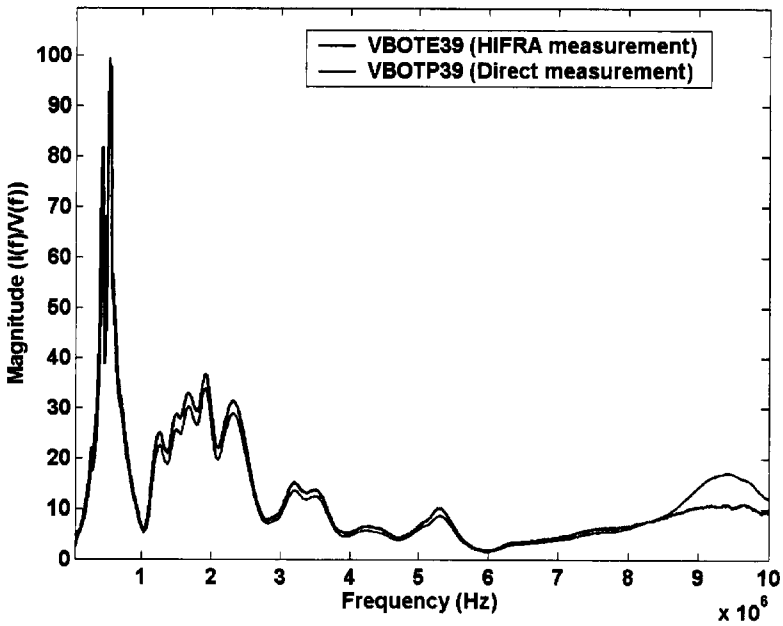


Figure 7.24 - Transfer function measured directly and measured by HIFRA sensor with both electrodes floating (10 MHz range)

## 7.5 Summary of HIFRA Method

The new HIFRA method looks very promising as a method to improve the sensitivity of the FRA test so that winding problems can be detected at an earlier stage, and for application as an on-line FRA test. The results show the HIFRA works well to at least the 10 MHz frequency range. Three potential signal sources for an on-line HIFRA measurement were investigated and compared: power system switching transients, transmission line random signal pickup and signal injection at the bushing capacitance tap. The results show that the injected signal from the bushing tap had a very broad frequency range. The injected signal technique combined with the HIFRA method is a very promising approach for the detection of transformer winding movement on-line. Further research needs to be carried out on this combined technique, and issues such as the proper location and method for mounting the internal sensors need to be worked out. Rugged low cost sensors and associated measuring systems need to be developed for field application.

It is important to accumulate field data with the HIFRA method in order to correlate the measurement results with changes in transformer internal condition. At the current stage of development (above 3 MHz), there is little experience in evaluating the results in order to make a decision on opening the transformer. A patent on this method has been applied for with the United States Patent Office [148].

## 7.6 Contribution to the State of-the-art

The following summarizes the contribution made by this work:

- A systematic comparison of the impulse FRA test method (FRA (I)) and the swept frequency FRA (FRA (S)) methods show that both are capable of detecting winding deformation below 3 MHz.
- It is feasible to do the FRA test on-line, but if system switching transients are used as the input signal source the on-line test is not as sensitive to changes in the transformer as the off-line test.

- The following key factors were determined to have a significant impact on the FRA test:
  - A 50 MHz sampling rate is adequate for performing FRA tests up to approximately 4.5 MHz.
  - A 500 MHz sampling rate is adequate for performing FRA tests up to approximately 15 MHz.
  - As the shunt resistance increases, the maximum frequency range that is sensitive to changes in the transformer winding decreases. A 50 Ω shunt is sensitive up to 0.5 MHz and a 1 Ω shunt is sensitive up to 10 MHz.
  - The high voltage bushing impedance has a significant impact on the FRA results above 3 MHz.
  - The test leads should be as short as possible and the test configuration (leads and instruments) must remain unchanged for repeated tests. The higher the frequency, the more critical this becomes.
  - Minor winding movement and looseness show changes in the transformer signature above 3 MHz.
  - The new concept of FRA measurements inside the transformer - HIFRA works well up to at least 10 MHz and is more sensitive to winding movement than conventional measurements.
- The HIFRA test method could significantly reduce the cost of repetitive tests on a transformer and could make it feasible to effectively monitor a transformer for winding movement on a continuous basis.
- Injecting a test signal into a bushing capacitance tap can be used over a very broad frequency range with the HIFRA test method to improve the detection of transformer winding movement on-line.
- The simulation study carried out confirmed the experimental data.
- The simulation study provided an understanding of why the resonant peaks of the transfer function reduce in magnitude after the transformers are re-clamped.
- The simulation study showed that the bushing tap signal injection technique is feasible for performing on-line tests.

# CHAPTER VIII CONCLUSIONS AND FUTURE RESEARCH

## 8.1 Conclusion

Prevention of power transformer failure is extremely important to utilities as they try to reduce maintenance costs while delivering reliable service. Winding looseness and winding movement are potential causes of transformer failure. The frequency response analysis (FRA) method has started to be used in detecting winding movement, but there are still many unanswered questions. The influencing factors that need to be better understood and an improved analysis of the results have been addressed in this study. Some of the issues that were considered are:

- How do the external measurement leads and high voltage bushing affect the test results?
- How does the measuring shunt impedance affect the test results?
- What frequency range should be used?
- What is the relationship between frequency range and the amount of winding movement?
- What criteria should be used for winding movement ranking?
- Is it feasible to do the FRA test on-line to eliminate the need to have an outage?

It was concluded from the research work that both the impulse FRA test method (FRA (I)) and the swept frequency FRA (FRA (S)) method are capable of detecting winding deformation at below 3 MHz. Both methods are viable, but the correct choice of measurement parameters is very important to achieve the highest sensitivity and repeatability. The experimental work established the feasibility of using the FRA test on-line. The investigation shows that the on-line test will not be as sensitive to changes in the transformer as the off-line test, if system switching transients are used as the input signal source.

FRA data analysis methods were investigated. The visual evaluation of FRA results was compared with three mathematical methods. These methods give different rankings of transformer condition, but they do provide assistance in decision making. Further investigations are required to establish analysis techniques that do not require the interpretation of experts.
The laboratory investigations found a number of key factors that influence FRA measurements:

- Effect of input signal sources – Two commonly available signal sources were investigated. The recurrent surge generator (RSG) was found to be usable for FRA testing up to a maximum of 4.5 MHz. A fast high voltage pulse generator, such as the PEMI, has signal energy up to 11 MHz.

- Effect of sampling rate – A 50 MHz sampling rate is adequate for performing FRA tests up to approximately 4.5 MHz. A 500 MHz sampling rate is adequate for tests up to approximately 15 MHz.

- Effect of shunt – As the shunt resistance increases, the maximum frequency range that is sensitive to changes in the transformer winding decreases. A 50 Ω shunt is sensitive up to 0.5 MHz and a 1 Ω shunt is sensitive up to 10 MHz.

- High voltage bushing effect – The bushing impedance has a significant impact on the FRA results above 3 MHz.

- Effect of transformer neutral connection – The neutral connection can affect the FRA results. It is important that the connection is kept constant for repeated tests.

- Effects of the measurement leads – Three different sets of leads were investigated (long, standard and short). The experiments confirm that to optimize the measurement sensitivity and repeatability, the lead length should be as short as possible and the test configuration must remain constant for repeated tests. The higher the frequency, the more critical this becomes.

- Effect of winding movement – Smaller winding movement shows at above 3 MHz, and winding looseness usually appears in a higher frequency region of FRA results.

The investigations show the need for an alternative measurement method to obtain more sensitive FRA measurements that will help detect winding movement at an earlier stage than is possible with the present test methods. A new concept called the High-frequency Internal Frequency Response Analysis (HIFRA) test method was developed. It improves the sensitivity of the FRA test and it looks very promising for application to on-line FRA testing which could significantly reducing the cost of repetitive tests on a transformer. It could make it feasible to

effectively monitor a transformer for winding movement on a continuous basis. The results show that the HIFRA method works well in the high frequency range, up to at least 10 MHz. Measurements at this higher frequency range are more sensitive to winding movement if done using the new test method.

Three potential signal sources for use with HIFRA on-line measurement were investigated and compared: system switching transients, transmission line random signal pickup and signal injection into the bushing tap. The results showed that injecting a signal into the bushing tap can be used over a very broad frequency range. The injected signal technique combined with the HIFRA method is a very promising approach for improving the detection of transformer winding movement on-line. Further research needs to be carried out on this combined technique, and issues such as the on-line application of the injection signal source and details of mounting the internal sensors need to be worked out. Sophisticated sensors and measuring devices need to be developed for field application. The transmission line signal pick up method had limited success but it still warrants further investigation.

A simulation study was carried out, based on a reduced detail transformer equivalent circuit model (Appendix A). The simulation attempted to use a reasonably detailed transformer model to demonstrate how changes inside a transformer affect the FRA measurement. The transformer bushing, current shunt and ground lead effects were also simulated.

Models with a different number of sections were found to have different resonant frequencies, but the general characteristics of the admittance from these models are similar. Even the transformer model with 74 sections is still not detailed enough to simulate the actual measured response in the megahertz frequency range. A more complex transformer model is required, or other innovative types of models need to be developed, to accurately model the transformer physical changes in the megahertz frequency range. The model used was adequate for this research, since the work focused on the FRA measurement parameters. Developing a more detailed transformer model was beyond scope of this work program.

Three current shunt resistances were simulated on the 67-section model. The results show that the sensitivity of the measurement is significantly improved by using a lower shunt value, particularly when looking at very high frequencies (above 3 MHz).

The transformer bushing was also modeled in this investigation using an LCR T circuit for the bushing model. The high voltage bushing has a significant impact on the FRA results and cannot be ignored. The model also shows that the bushing reduces the test sensitivity.

Two ground leads were simulated in this investigation. The ground lead contributed a shift in the resonant frequencies. The model with bushing and ground lead further reduced the sensitivity to the detection of winding movement.

Minor winding movements were simulated at three different winding locations (top, middle and bottom). The results showed both magnitude and frequency changes as the winding movement was introduced to the model. The higher frequencies showed greater changes than at the lower frequencies for all three winding movement simulations. A short occurring on a portion of the winding was also simulated in this study. The results show that the predominant change caused by the short was a shift in the resonant frequencies.

Changes in the ground capacitance were simulated at three winding locations (top, middle and bottom). The top and middle winding ground capacitance changes contributed more to the resonant frequency shift and the bottom winding ground capacitance changes caused more magnitude changes. Ground capacitance losses and winding series capacitance losses were also simulated. This simulation shows that introducing parallel resistance to the model significantly reduces the magnitude of the resonant admittance. The known phenomenon of reduced resonant magnitude after re-clamping can be explained by the reduction in the distances between turns/discs. This also reduces the parallel equivalent resistances and opens up a potential application for future development of the FRA test as a means to evaluate transformer dielectric condition, such as moisture level.

The bushing tap injection method was also investigated in the simulations. The results showed that this method had great promise for further development, especially if the injection method is combined with the application of signal measurement inside the transformer at the bottom of the bushing. The simulation results showed that the high voltage terminal load did not affect the injection method when it is combined with internal measurement. The simulations show that the injection method is a very feasible way to apply the test to on-line monitoring of winding movement.

## 8.2 Future Work

This study showed that the HIFRA method has the potential to be applied to transformer on-line FRA measurement. Further work needs to be done on this new method to realize its full potential. The on-line measurement equipment needs development and suitable signal sources need to be identified that can be injected into the transformer, along with methods to couple these signals into the transformer. Work needs to be done to determine the type of sensors to use for HIFRA measurements (optical vs. electrical, high frequency shunt vs. Rogowski coil, etc.). It is important to accumulate field data with the HIFRA method in order to correlate the measurement results with changes in transformer internal condition. At the current stage of development, there is little experience in evaluating the results in order to make a decision on opening the transformer.

Further research should be carried out on the potential of using random noise on the transmission line as the signal source. If there is a noise signal over an adequate frequency range, it could be used as the input signal and the signal injection source could be eliminated. Further signal analysis methods, such as pattern recognition, needs to be studied for analysis of the on-line data.

A more detailed transformer model could be investigated for the high frequency modeling of the transformer winding. The model should include the simulation of parts such as the inter-winding leads, the internal high voltage leads and the ground leads, since they contribute to the transformer transfer admittance as well the transformer windings. Improved high frequency modeling of the transformer winding could lead to improvements in the understanding of the relationship between the type and location of winding movement and the effect it has on the FRA test results. This work could also aid in establishing test result evaluation methods that will be able to rank the condition of a transformer without requiring the interpretation of an engineer experienced in FRA testing.

Further work should be carried out to develop techniques that can be used to simplify the interpretation of test results. Analysis of the results, such as admittance pass bandwidth change, admittance peak magnitude change, admittance peak frequency peak shift, admittance area difference vs. frequency, admittance accumulated area curves vs. frequency and pattern recognition methods should be investigated. Expert software systems that are based on input

from experienced experts in the interpretation of FRA test data should be examined as a means to allow non-experienced personnel to interpret FRA test results. Further analysis of the transfer function phase data should also be studied, as it may contain information on transformer conditions such as insulation quality.

## REFERENCES


[1] CIGRE Working Group 05, "An International Survey on Failures in Large Power Transformers in Service", Electra, No.88, May 1983.

[2] Kogan, V.I., et al., "Failure Analysis of EHV Transformers", IEEE Transactions on Power Delivery, Vol. 3, No. 2, pp. 672-683, April 1988.

[3] Sparling, B., "Transformer Monitoring and Diagnostics", IEEE Power Engineering Society 1999 Winter Power Meeting, Vol. 2, pp. 978-980, New York, USA, 31 January - 4 February 1999.

[4] Grechko, O.N., and Kalacheva, I., "Current Trends in the Development of In-Service Monitoring and Diagnostic Systems for 110-750 kV Power Transformers", Applied Energy: Russian Journal of Fuel, Power, and Heat Systems, Vol. 34, No. 5, pp. 84-97, 1996.

[5] McElroy, A.J., "On the Significance of Recent EHV Transformer Failures Involving Winding Resonance", IEEE Transactions on Power Apparatus and Systems, Vol. PAS-94, No. 4, pp. 1301-1316, July/August 1975.

[6] Lee, K.H., and Schneider, J.M., "Rockport Transient Voltage Monitoring System: Analysis and Simulation of Record Waveforms", IEEE Transactions on Power Delivery, Vol.4, No. 3, pp. 1794-1805, July 1989.

[7] Minhas, M., Reynders, J. P. and de Klerk, P.J., "Failure in Power System Transformers and Appropriate Monitoring Techniques", 11th International Symposium on High Voltage Engineering, paper 1.94.S23, London, England, 23-27 August 1999.

[8] Sahu, R., "Optimization of the Transmission and Subtransmission Transformer Spares on the AEP System", 42nd American Power Conference, pp. 701-705, Chicago, USA, 21-23 April 1980.

[9] CIGRE Working Group 09 of Study Committee 12, "Lifetime Evaluation of Transformers", Electra, No. 150, pp. 39-51, October 1993.

[10] Pettersson, L., "Estimation of the Remaining Service Life of Power Transformers and their Insulation", Electra, No. 133, pp. 65-71, December 1990.

[11] Darveniza, M., et al., "Investigations into Effective Methods for Assessing the Condition of Insulation in Aged Power Transformers", IEEE Transactions on Power Delivery, Vol. 13, No. 4, pp. 1214-1223, October 1998.

[12] Lapworth, J. A., Jarman, P. N., and Funnell, I. R., "Condition Assessment Techniques for Large Power Transformers", Second International Conference on the Reliability of Transmission and Distribution Equipment, Coventry, England, Conf. Publ. No. 406 pp. 85-90, March 29-31 1995.

[13] Kazmierski, M., Sobocki, R., and Olech, W., "Selected Elements of Life Management of Large Power Transformers – A Polish Experience", CIGRE, paper 12-203, Paris, France, 1998.

[14] Pettersson, L., Fantana, N. L., and Sundermann, U., "Life Assessment: Ranking of Power Transformers Using Condition Based Evaluation. A New Approach", CIGRE, paper 12-204, Paris, France, 1998.

[15] Jarman, P. N., Lapworth, J. A., and Wolson, A., "Life Assessment of 275 and 400 kV Transmission Transformers", CIGRE, paper 12-210, Paris, France, 1998.

[16] Breen, G., "Essential Requirements to Maintain Transformers in Service", CIGRE, paper 12-103, Paris, France, 30 August-5 September 1992.

[17] Agou, S., et al., "Increasing the Reliability of Online Insulation Condition Assessment of MV-HV Equipment", Electricity Today, Vol. 12, No. 6, pp., 22-27 August 2000.

[18] Aschwanden, T.H., et al., "Development and Application of New Condition Assessment Methods for Power Transformers", CIGRE, paper 12-207, Paris, France, 1998.

[19] Basak, A., "Condition Monitoring of Power Transformers", Engineering Science and Education Journal, Vol. 8, No. 1, pp. 41-46, February 1999.

[20] Belanger, M., "Transformer Diagnosis: Part 1: A Statistical Justification for Preventative Maintenance", Electricity Today, Vol. 11, No. 6, pp. 5-8, June 1999.

[21] Belanger, M., "Transformer Diagnosis: Part 2: A Look at the Reference Data for Interpreting Test Results", Electricity Today, Vol. 11, No. 7, pp. 19-26, August 1999.

[22] Belanger, M., "Transformer Diagnosis: Part 3: Detection Techniques and Frequency of Transformer Testing", Electricity Today, Vol. 11, No. 8, pp. 19-26, September 1999.

[23] Bengtsson, C., "Status and Trends In Transformer Monitoring", IEEE Transactions on Power Delivery, Vol. 11, No. 3, pp. 1379-1384, July 1996.

[24] Blackburn, T.R., et al., "On-Line Partial Discharge Measurement on Instrument Transformers", International Symposium on Electrical Insulating Materials, Toyohashi, Japan, 27-30 September 1998.

[25] Bolduc, L., et al., "Detection of Transformer Winding Displacement by the Frequency Response of Stray Losses (FRSL)", CIGRE, paper 12/33-02, Paris, France, 2000.

[26] Bolduc, L. and Aubin, J., "Determination of Transformer Winding Displacement by FRSL Diagnostic Method", Final Report on CEA Project, RP 77-47, March 1981.

[27] Aubin, J., Bolduc, L. and Trinh, N.G., "Dielectric and Short-Circuit Tests of Used Transformers", CEA Fall Meeting Electrical Apparatus Section, Winnipeg, October 1983.

[28] Boss, P., et al., "Economical Aspects and Practical Experiences of Power Transformers On-line Monitoring", CIGRE, paper 12-202, Paris, France, 2000.

[29] Cardoso, A. J. M. and Oliveira, L. M. R., "Condition Monitoring and Diagnostics of Power Transformers", International Journal of COMADEM, pp. 5-11, Sunderland, England, 1999.

[30] Carreau, D., et al., "Condition Monitoring Diagnostics Expert Systems: A Project Roadmap", Electricity Today, Vol. 12, No. 4, pp.8-14, May 2000.

[31] Crowley, T. H., "Automated Diagnosis of Large Power Transformers Using Adaptive Model-Based Monitoring", A Thesis of Master and Bachelor Science at Massachusetts Institute of Technology, June 1990.

[32] DiGiorgio, J.B., et al., "Cut Failures by Analyzing Transformer Oil", Electrical World, Vol. 192, No. 7, pp. 52-54, 1 October 1979.

[33] Dominelli, N., "Furanic and Non-Furanic Analysis as a Transformer Diagnostic", EPRI Substation Equipment Diagnostics Conference IV, New Orleans, USA, 5-7 February 1996.

[34] Duke, G., "Predictive Maintenance a Case Study in Infrared Thermography", Electrical Maintenance, pp. 11-12, October 1998.

[35] Farquharson, R., and Caird, K., "An Overview of Substation Equipment Monitoring and Diagnostics: Part 1", Electricity Today, Vol. 12, No.5, pp.23-26, June/July 2000.

[36] Feser, K., et al., "General Trends in Condition Monitoring of Electrical Insulation", Stockholm Power Tech International Symposium on Electric Power Engineering, Vol. 1, Stockholm, Sweden, 18-22 June 1995.

[37] Eleftherion, P.M., "Partial Discharge XXI: Acoustic Emission-Based PD Source Location in Transformers", IEEE Insulation Magazine, Vol. 11, No. 6, pp. 22-26, November/December 1995.

[38] Feser, K., et al., "The Transfer Function Method for Detection of Winding Displacements on Power Transformers after Transport, Short Circuit or 30 Years Service", CIGRE, paper 12/33-04, 2000.

[39] Gockenbach, E., and Borsi, H., "Diagnostic Methods for Transformers On-Site", International Symposium on Electrical Insulating Materials, pp. 2-36, Toyohashi, Japan, 27-30 September, 1998.

[40] Guuinic, P., "Progress Report of Study Committee 12 (Transformers)", Electra, No. 178, paper 12.19, pp. 17-21, June 1998.

[41] Hanique, E., Reijnders, H.F., and Vaessen, P.T.M., "Frequency Response Analysis as a Diagnostic Tool", Journal of Elektotechniek, Vol. 68, No. 6, pp. 549-558, June 1990.

[42] Harley, J.W., "CIGRE Working Group 12.18 TF02 Survey on Diagnostics & Monitoring Techniques Transformer Subsystems", CIGRE SC 12, Sydney Colloquium, Sydney, 6-10 October 1997.

[43] Harley, J.W., and Sokolov, V.V., "Diagnostic Techniques for Power Transformers", CIGRE, paper P1-06, Paris, France, 2000.

[44] Huang, X., and Yan, Z., "Study on Trend Analysis Method for On-Line Insulation Diagnosing of Capacitive-Type Equipment", International Symposium on Electrical Insulating Materials, paper P2-40, Toyohashi, Japan, 27-30 September 1998.

[45] Hyde, T.R., "On-line Condition Monitoring Technology and Applications", ERA Technology, Report No. 95-0546R, July 1995.

[46] Jaksts, A., et al., "A Major Breakthrough in Transformer Technology", CIGRE, paper 12-101, Paris, France, 2000.

[47] Judd, M.D., et al., "Transformer Monitoring using the UHF Technique", 11th International Symposium on High Voltage Engineering, paper 5.362.P5, London, England, 22-27 August 1999.

[48] Kachler, A.J., "Diagnostic and Monitoring Technology for Large Power Transformers", CIGRE SC 12, Sydney Colloquium, Sydney, Australia, 6-10 October 1997.

[49] Kannan, S.R., Tech, M. and Rao, N., "Generator loading limits for impulse testing low-inductance windings", Proceedings of the IEE, Vol. 122, No. 5, pp. 535-538, May 1975.

[50] Kirtley, J.L., et al., "Monitoring the Health of Power Transformers", IEEE Computer Applications in Power, Vol. 9, No. 1, pp. 18-23, January 1996.

[51] Lachman, M.F., Walter W., and von Guggenberg P.A., "On-Line Diagnostics of High-Voltage Bushings and Current Transformers Using the Sum Current Method", IEEE Transactions on Power Delivery, Vol. 15, No. 1, pp. 155-162, January 2000.

[52] Leemans, P., et al., "Control, Diagnostic and Monitoring of Power Transformers", CIGRE, paper 12-213, Paris, France, 1998.

[53] Leibfried, T., "Online Monitors Keep Transformers in Service", IEEE Computer Applications in Power, Vol. 11, No. 3, pp. 36-42, July 1998.

[54] Leibfried, T., et al., "On-line Monitoring of Power Transformers - Trends, New Developments and First Experiences", CIGRE, paper 12-211, Paris, France, 1998.

[55] Leibfried, T., and Feser, K., "Monitoring of Power Transformers using the Transfer Function Method", IEEE Transactions on Power Delivery, Paper PE-053-PWRD-1-08-1998, 1998.

[56] Leibfried, T., "Online Monitoring of Power Transformers – System Technology and Data Evaluation", 11th International Symposium on High Voltage Engineering, paper 5.184.P5, London, England, 22-27 August 1999.

[57] Macor, P., et al., "The Short-Circuit Resistance of Transformers: The Feedback in France Based on Tests, Service and Calculation Approaches", CIGRE, paper 12-102, Paris, France, 2000.

[58] Malewski, R., Douville, J., and Belanger, G., "Insulation Diagnostic System for HV Power Transformers in Service", CIGRE, paper 12-01, 1986.

[59] Malewski, R., and Kazmierski, M., "Diagnostic Techniques for Power Transformers", CIGRE, paper P1-07, Paris, France, 2000.

[60] Malewski, R., et al., "Instruments for HV Insulation Testing in Substations", CIGRE, paper 12/33-06, Paris, France, 2000.

[61] Mizokami, M., Yabumoto, M., and Okazaki, Y., "Vibration Analysis of a 3-Phase Model Transformer Core", Electrical Engineering in Japan, Vol. 119, No. 1, 1997.

[62] Mollmann, A., and Pahlavanpour, B., "New Guidelines for Interpretation of Dissolved Gas Analysis in Oil-filled Transformers", Electra, No. 186, paper 15.01.01, pp. 30-51, October 1999.

[63] Noonan, T., "Power Transformer On-site Condition Assessment Testing", CIGRE, paper 12/33-05, Paris, France, 2000.

[64] Pemen, A.J.M., et al., "On-Line Partial Discharge Monitoring of HV Components", 11th International Symposium on High Voltage Engineering, paper 5.136.S16, London, England, 22-27 August 1999.

[65] Poyser, T.D., et al., "On-Line Monitoring of Power Transformers", IEEE Transactions on Power Apparatus and Systems, Vol. PAS-104, No. 1, January 1985.

[66] Provanzana, J.H., et al., "Transformer Condition Monitoring-Realizing an Integrated Adaptive Analysis System", CIGRE, paper 12-105, 30 August-5 September 1992.

[67] Ruijin, L. et al., "On-Line Detection of Gases Dissolved in Transformer Oil and the Faults Diagnosis", International Symposium on Electrical Insulating Materials", paper P2-44, Toyohashi, Japan, 27-30 September 1998.

[68] Rushford, B.G., "Business Case Development for On-Line Equipment", Electrical Maintenance, pp. 5-10, October 1998.

[69] Saha, T.K., et al., "Electrical and Chemical Diagnostics of Transformers Insulation-Part A: Aged Transformers Samples", IEEE Transactions on Power Delivery, Vol. 12, No. 4, pp. 1547-1554, October 1997.

[70] Saha, T.K., et al., "Electrical and Chemical Diagnostics of Transformers Insulation-Part B: Accelerated Aged Insulation Samples", IEEE Transactions on Power Delivery, Vol. 12, No. 4, pp. 1555-1561, October 1997.

[71] Schwabe, R.J., et al., "On-Line Diagnostics of Oil Paper Insulated Instrument Transformers", CIGRE, paper 12-105, Paris, France, 2000.

[72] Tenbohlen, S., et al., "Enhanced Diagnosis of Power Transformers using On- and Off-Line Methods: Results, Examples and Future Trends", CIGRE, paper 12-204, Paris, France, 2000.

[73] Tian, Y., et al., "PD Pattern Identification using Acoustic Emission Measurement and Neural Networks", 11th International Symposium on High Voltage Engineering, paper 5.41.S8, London, England, 22-27 August 1999.

[74] Tomsovic, K., Tapper, M., and Ingvasrsson, T., "Performance Evaluation of a Transformer Condition Monitoring Expert System", CIGRE, paper 110-24, Berlin, Federal Republic of Germany, 1993.

[75] Vandermaar, A.J., and Wang, M., "Transformer Condition Monitoring By Frequency Response Analysis" 10th International Symposium High Voltage Engineering, Vol. 4, pp. 119-122, Montreal, Canada, 25-29 August 1997.

[76] Wang, C., et al., "Analysis and Suppression of Continuous Periodic Interference for On-Line PD Monitoring of Power Transformers", 11th International Symposium on High Voltage Engineering, paper 5.212.P5, London, England, 22-27 August 1999.

[77] Wang, M., Vandermaar, A.J., and Srivastava, K.D., "Condition Monitoring of Transformers in Service by the Low Voltage Impulse Test Method", 11th International Symposium on High Voltage Engineering, paper 1.45.S3, London, England, 22-27 August 1999.

[78] Wang, M., Vandermaar, A.J, and Srivastava, K.D., "Transformer Condition Monitoring by the Low Voltage Impulse Test Method", CIGRE Third South African Regional Conference, Session 1, Item No. 3, Johannesburg South Africa, 19-21 May 1998.

[79] Wang, Z., Liu, Y., and Griffin, P.J., "Neural Net and Expert System Diagnose Transformer Faults", IEEE Computer Applications in Power, Vol. 13, No. 1, pp. 50-55, January 2000.

[80] Al-Khayat, N., and Haydock, L., "Swept Frequency Response Test for Condition Monitoring of Power Transformer", Proceedings of the Electrical/Electronics Insulation Conference, Rosemount, USA, 18-21 September 1995.

[81] Drobishevskey, A., Levitzkaya, E., and Filatova, M., "Application of LV Impulses for Diagnostics of Transformers During Tests and In Service", 8th International Symposium on High Voltage Engineering, paper 65.07, pp. 189-192, Yokohama, Japan, August 23-27, 1993.

[82] Kachler, A.J., et al., "High Voltage Impulse Tests on Power Transformers Using A Digital Measuring System", Fifth International Symposium on High Voltage Engineering, Vol. 3 paper 72.05, Braunschweig, Stadthalle, 24-28 August 1987.

[83] White, E.L., "Monitoring Transformers in Service for Winding Displacement Using the Low Voltage Impulse Method", ERA Technology, Report No. 81-62R, June 1981.

[84] Tantin, P., Goosen, P.V., and Christensen, P., "CIGRE SC 12 Power Transformers Special Report 1998", CIGRE, paper 12-00, Paris, France, 1998.

[85] "Guide for the Sampling of Gases and Oil from Oil-Filled Electrical Equipment and for the Analysis of Free and Dissolved Gases", IEC Publication 567, 1992.

[86] "IEEE Guide for the Interpretation of Gases Generated in Oil-Immersed Transformers", IEEE Std. C57.104-1991, 1991.

[87] Roger, R. R., "IEEE And IEC Codes To Interpret Incipient Faults In Transformers, Using Gas In Oil Analysis", IEEE Transaction Electrical Insulation, Vol. EI-13 No. 5, pp. 349-354, October 1978.

[88] "Interpretation of the Analysis of Gases in Transformers and Other Oil-Filled Electrical Equipment in Service", IEC Publication 599, 1978.

[89] Duval, M., "Dissolved Gas Analysis: It Can Save Your Transformer", IEEE Electrical Insulation Magazine, Vol. 5, No. 6., pp. 22-27, November/December 1989.

[90] Burton, P.J., et al., "Recent Developments by CEGB to Improve the Prediction and Monitoring of Transformer Performance", CIGRE, paper No. 12-09, Paris, France, 1984.

[91] Fallou, B., "Detection of and Research for the Characteristics of an Incipient Fault from Analysis of Dissolved Gases in the Oil of an Insulation", Electra, No. 42, pp.31-52, October 1975.

[92] CIGRE 15-01, "Detection of and Research for the Characteristics of an Incipient Fault form Analysis of Dissolved Gases in the Oil of an Insulation", Electra, No. 42, October 1975, pp 31-52.

[93] De Pablo, A., and Mollmann, A., "New Guidelines for Furans Analysis as well as Dissolved Gas Analysis in Oil-Filled Transformers", CIGRE, paper 15/21/33-19, Paris, France, 1996.

[94] Kopaczynski, D., "AC Dielectric-Loss, Power-Factor and Capacitance Measurements as Applied to Insulation Systems of High-Voltage Power Apparatus in the Field (a review) - Part 1: Dielectric Theory and Part 2: Practical Applications (Doble testing)", Doble Client Conference Proceedings, April 1993.

[95] "IEEE Standard Test Code for Liquid Immersed Distribution, Power, and Regulating Transformers and IEEE Guide for Short-circuit Testing of Distribution and Power Transformer", IEEE Std. C57.12.90-1999, 1999.

[96] Zargari, A., and Blackburn, T. R., "Application of Optical Fiber Sensor for Partial Discharge Detection in High-voltage Power Equipment", 1996 IEEE Annual Report – Conference on Electrical Insulation and Dielectric Phenomena, pp.541-544, Millbrae, USA, 20-23 October, 1996.

[97] Dorr, R, et al., "On-Line Transformer Monitoring: Detection of Partial Discharges from HF Measurements Using FFT and Time Domain Filters", 12th International Symposium on High Voltage Engineering, Vol. 5, pp.1230-1233, Bangalore, India, 20-24 August 2001.

[98] Brooks, R. S., and Urbana, G.S., "Using the Recovery Voltage Method to Evaluate Aging In Oil-Paper Insulation", IEEE International Conference on Conduction and Breakdown in Solid Dielectrics, pp. 93-97, Vaster as, Sweden, 22-25 June 1998.

[99] Csepés, G., et al., "Recovery Voltage Method for Oil/Paper Insulation Diagnosis", 1998 Annual Report Conference on Electrical Insulation and Dielectric Phenomena, Vol. 1, pp. 345-355, Atlanta, Georgia, 25-28 October 1998.

[100] Schlag, A. G., "The Recovery Voltage Method for Transformer Diagnosis", Tettex Instruments, 1995

[101] Bognar, A., et al, "Diagnostic Tests of High Voltage Oil-Paper Insulating Systems (In Particular Transformer Insulation) Using DC Dielectrometrics", CIGRE, paper 15/33-08, Paris, France, 1990.

[102] Nemeth, E., "Measuring Voltage Response: a Non-destructive Diagnostic Test Method of HV Insulation", IEE Proceedings, Science, Measurement and Technology, Vol. 146, No.5, pp. 249-252, September 1999.

[103] Sanz-Bobi, M.A., et al., "Experiences Learned from the on-line Internal Monitoring of the Behaviour of a Transformer", IEEE International Electric Machines and Drives Conference, Milwaukee, USA, 1997.

[104] Mechefske, C.K., "Correlating Power Transformer Tank Vibration Characteristics to Winding Looseness", Insight, Vol. 37, No. 8, pp. 599-604, 1985.

[105] Bengtsson, T., et al., "Acoustic Diagnosis of Tap Changers", CIGRE, paper 12-101, 1996.

[106] Golubev, A., et al., "On-Line Vibro-Acoustic Alternative to the Frequency Response Analysis and On-line Partial Discharge Measurements on Large Power Transformers", Tech Con'99 Annual Conference of TJ/H2b, New Orleans, USA, 18-19 February 1999.

[107] Denis, R.J., An, S.K., Vandermaar, J., and Wang, M., "Comparison of Two FRA Methods to Detect Transformer Winding Movement", EPRI Substation Equipment Diagnostics Conference VIII, New Orleans, USA, 20-23 February 2000.

[108] Dick, E.P. and Erven, C.C., "Transformer Diagnostic Testing by Frequency Response Analysis", IEEE Transactions on Power Apparatus and Systems, Vol. PAS-97, No. 6, Nov/Dec. 1978.

[109] Lech, W., and Tyminski, L., "Detecting Transformer Winding Damage – The Low Voltage Impulse Method", Electrical Review, No. 18, 1966.

[110] McDowell, G., "Condition Monitoring of Power Transformers to Assess Residual Life and Fault Damage", ERA Report 88-0566R, June 1989.

[111] Wang, M. and Vandermaar, A. J., "Low-Voltage Impulse (LVI) & Vibration Tests on DC Terminal Rectifier Transformers", Powertech Labs Inc. Report - Project No. 7795-27, May 1996.

[112] Birlasekaran, S. and Fetherston, F., "Off/On-Line FRA Condition Monitoring Technique for Power Transformer", IEEE Power Engineering Review, pp. 54-56, August 1999.

[113] Caldecott, R., et al., "HVDC Converter Station Tests in the 0.1 to 5 MHz Frequency Range", IEEE Transactions on Power Delivery, Vol. 3, No. 3, pp. 971-977, July 1988.

[114] Caldecott, R., et al., "Measurement of the Frequency Dependent Impedance of Major HVDC Converter Station Equipment", IEEE Transactions on Power Delivery, Vol. 5, No. 1, pp. 474-480, January 1990.

[115] Liu, Y., et al., "Power Transformer Resonance - Measurements and Predictions", IEEE Transactions on Power Delivery, Vol. 7, No. 1, pp. 245-253, July 1992.

[116] Vandermaar, A.J., "On-Line Transformer Winding and Dielectric Monitoring-Laboratory and Field Test Results", EPRI, Final Report TR-113650, September 1999

[117] Vaessen, P. T. M., "Transformer Model for High Frequencies", IEEE Transactions on Power Delivery, Vol. 3, No. 4, pp. 1761-1768, October 1988.

[118] Chimklai, S. and Marti, J.R., "Simplified Three-Phase Transformer Model for Electromagnetic Transient Studies", IEEE Transactions on Power Delivery, Vol. 10, No. 3, pp. 1316-1325, July 1995.

[119] Morched, A., Marti, L. and Ottevangers, J., "A High Frequency Transformer Model for the EMTP", IEEE Transactions on Power Delivery, Vol. 8, No. 3, pp. 1615-1626, July 1993.

[120] Shibuya, Y., Fujita, S. and Hosokawa, N., "Analysis of very fast transient overvoltage in transformer winding", IEEE Proceedings.-Generation, Transmission, Distribution., Vol. 144, No. 5, pp. 461-468, September 1997.

[121] Brandwajn, V., Dommel, H. and Dommel, I., "Matrix Representation of Three-phase N-winding Transformers for Steadu-state and Transient Studies", IEEE Transaction on Power Apparatus and Systems, Vol. PAS-101, No. 6, pp. 1369-1378, June 1982.

[122] Gharehpetian, G.B., Mohseni, H. and Möller, K., "Hybrid Modelling of Inhomogeneous Transformer Windings for Very Fast Transient Overvoltage Studies", IEEE Transactions on Power Delivery, Vol. 13, No. 1, pp. 157-163, January 1998.

[123] Singh, B. P. et al., "Experimental and Analytical Studies of Resonant Frequencies of a Generator Transformer Using Transfer Function Method", Fourth Workshop & Conference on EHV Technology, CSIC Auditorium, Indian Institute of Science, Bangalore, India, pp. 95-157, 15-16 July 1998.

[124] Prabhakar, N., Kamaraju, J. N. and Singh, B. P., "Sensitivity Analysis of the Power Transformer Windings by Transfer Function Method", 10th International Symposium on High Voltage Engineering, Montreal, Quebec, pp. 517-520, 25-29 August 1997.

[125] Wenzel, D., Borsi, H. and Gockenbach, "Analytical Computation of the Transfer Functions of Transformers", Proceedings of 1998 International Symposium on Electrical Insulating Materials, P2-48, pp. 787-790, Toyohashi, Japan, 27-30 September 1998.

[126] Bak-Jensen, J., et al., "Parametric Identification in Potential Transformer Modelling", IEEE Transactions on Power Delivery, Vol. 7 No. 1, pp. 70-76, January 1992.

[127] Jacques, R. N., Liu, K. and Miller, D. W., "Identification of High Accurate Low Order State Space Models in the Frequency Domain", Signal Processing, 52, pp. 195-207, 1996.

[128] Sidman, M. D., DeAngelis, F. E. and Verghese, G. C., "Parametric System Identification on Logarithmic Frequency Response Data", IEEE Transaction on Automatic Control, Vol. 36, No. 9, pp. 1065-1070, September 1991.

[129] Liu, K., Jacques, R. N. and Miller, D. W., "Frequency Domain Structural System Identification by Observability Range Space Extraction", Journal of Dynamic Systems, Measurement, and Control Transaction of the ASME, Vol. 118, pp. 211-220. June 1996.

[130] Mckelvey, T., Akcay, H. and Ljung, L., "Subspace-based Multivariable System Identification from Frequency Response Data", IEEE Transaction on Automatic Control, Vol. 41, No. 7, pp. 960-979, July 1996.

[131] Pintelon, R., et al., "Parametric Identification of Transfer Functions in the Frequency Domain – A Survey", IEEE Transactions on Automatic Control, Vol. 39, No. 11, pp. 2245-2260, November 1994.

[132] Islam, S. M., Coates, K. M. and Ledwich, G., "Identification of High Frequency Transformer Equivalent Circuit Using Matlab from Frequency Domain Data", IEEE Industry Applications Society, Annual Meeting, New Orleans, Louisiana, pp. 357-364, 5-9 October, 1997.

[133] Akcay, H., Islam, S. M. and Ninness, B., "Subspace Based Identification of Power Transformer Models from Frequency Response Data", Proceedings of the American Control Conference, Philadelphia, Pennsylvania, pp. 3398-3402, June 1998.

[134] Islam, S. M., Coates, K. M. and Ledwich, G., "Identification of High Frequency Transformer Equivalent Circuit Using Matlab from Frequency Domain Data", IEEE Industry Applications Society, Annual Meeting, New Orleans, Louisiana, pp. 357-364, 5-9 October 1997.

[135] Liu, Y., et al., "Modeling of Converter Transformers Using Frequency Domain Terminal Impedance Measurements", IEEE Transactions on Power Delivery, Vol. 8, No. 1, pp. 66-72, January 1993.

[136] Liu, Y., et al., "Transient Response Prediction of Power System Equipment using a Frequency Domain Impedance Function Model", International Journal of Power and Energy Systems, Vol. 15, No. 1, pp. 14-21, 1995.

[137] Rao, M. R. and Bopardikar, A. S., "Wavelet Transforms, Introduction to Theory and Applications", Addison Wesley Longman (Publishers) Inc., Reading, Massachusetts, 1998.

[138] Purkait, P. and Chakravorti, S, "Pattern Classification of Impulse Faults in Transformers by Wavelet Analysis", IEEE Transactions on Dielectrics and Electrical Insulation, Vol. 9, No. 4, pp. 555 – 561, August 2002.

[139] Satish, L., "Short-Time Fourier and Wavelet Transforms for Fault Detection in Power Transformers During Impulse Tests", IEE Proceedings: Science, Measurement and Technology, Vol. 145, No. 2, pp. 77-84, March 1998.

[140] Pandey. S.K. and Satish, L., "Multiresolution Signal Decomposition: A New Tool for Fault Detection in Power Transformers During Impulse Tests", IEEE Transactions on Power Delivery, Vol. 13, No. 4, pp. 1194-1200, October 1998.

[141] Waters, M., "The Short-Circuit Strength of Power Transformers", Macdonald & Co. (Publishers) Ltd., London, 1996.

[142] Moser, H. P., et al., "Transformerboard", EHV-Weidmann Ltd., St. Johnsbury, Vermont

[143] Malewski, R. and Poulin, B., "Impulse Testing of Power Transformers Using the Transfer Function Method", IEEE Transactions on Power Delivery, Vol. 3, No. 2, April 1988.

[144] de Klerk, P.J. and Reynders, J.P, "Winding Slackness Monitoring as a Diagnostic for Insulation Aging in Oil-paper Insulated Power Transformers", 11th International Symposium on High Voltage Engineering, London, England, paper 1.185.P3, 23-27 August 1999.

[145] Hori, Y. and Fujisawa, F., "Electromechanical Coupling Vibration of Power Transformer under Short Circuit Conditions", Nippon Kikai Gakkai Ronbunshu, C Hen/Transaction of the Japan Society, Part C, Vol. 59, No. 563, July 1993.

[146] RF Patent No. 2117955, "Transformer diagnostics method".

[147] Malewski, R., Douville, J. and Lavallee, L., "Measurement of Switching Transients in 735-kV Substations and Assessment of their Severity for Transformer Insulation", IEEE Transactions on Power Delivery, Vol. 3, No. 4, pp. 1380 – 1390, October 1988.

[148] Provisional United States Patent No. 6,466,034 "Transformer Winding Movement Detection By High Frequency Internal Response Analysis"; Granted on October 15, 2002.

[149] AlFuhaid, A. S., "Frequency Characteristics of Single-Phase Two-Winding Transformers Using Distributed-Parameter Modeling", IEEE Transactions on Power Delivery, Vol. 16, No. 4, pp. 637-642, October 2001.

[150] Adielson, T., et al., "Resonant Overvoltages In EHV Transformers – Modeling and Application", IEEE Transactions on Power Apparatus and Systems, Vol. PAS-100, No. 7, pp. 3563-3572, July 1981.

[151] Akbari, A, et al., "A Continuous Parameter High Frequency Model Based on Travelling Waves for Transformer Diagnostic Purposes", Conference Record of the 2002 IEEE International Symposium on Electrical Insulation, Boston, MA USA, pp. 154-157, April 7-10, 2002.

[152] Degeneff, R.C., "A Method for Constructing Terminal Models for Single-Phase n-Winding Transformers", IEEE PES Summer Meeting, Los Angeles, CA, A 78 539-9, July 16-21, 1978

[153] Degeneff, R. C., et al. "A Method for Constructing Reduced Order Transformer Models for System Studies from Detailed Lumped Parameter Models", IEEE Transactions on Power Delivery, Vol. 7, No. 2, pp. 649-655, April 1992.

[154] de Leon, F. and Semlyen, A., "Reduced Order Model for Transformer Transients", IEEE Transactions on Power Delivery, Vol. 7, No. 1, pp. 361-369, January 1992.

[155] Keyhani, A., Tsai, H., and Abur, A., "Maximum Likelihood Estimation of High Frequency Machine and Transformer Winging Parameters", IEEE Transactions on Power Delivery, Vol. 5, No. 1, pp. 212-219, January 1990.

[156] Keyhani, A., Miri, S. M., and Hao, S., "Parameter Estimation for Power Transformer Models from Time-Domain Data", IEEE Transactions on Power Delivery, Vol.PWRD-1, No. 3, pp. 140-146, July 1986.

[157] Keyhani, A., et al, "Identification of High Frequency Transformer Model Parameters", Electric Power System Research, 42, pp. 127-133, 1997.

[158] Soysal, A., "A Method for Wide Frequency Range Modeling of Power Transformers and Rotating Machines", IEEE Transactions on Power Delivery, Vol. 8, No. 4, pp. 1802-1808, October 1993.

[159] Woivre, V, et al. "Transient Overvoltage Study and Model for Shell-Type Power Transformers", IEEE Transactions on Power Delivery, Vol. 8, No. 1, pp. 212-222, January 1993.

# APPENDIX A TRANSFORMER MODELING

## A.1 Introduction

There has been a great deal of research work done on transformer modeling [117 – 136,138, 149-159]. Due to different purposes for the models, different types of transformer models have been constructed and used. In general, there are two main categories of transformer models. One is the terminal or black box model, which provides the terminal characteristics of a transformer and is not necessarily related to a transformer internal condition and physical configuration. This type of model mainly describes the terminal performance and characteristics, and can be constructed by various methods (e.g., mathematical equations or network analysis (poles and zeros)).

The other type of transformer model is the physical model. The physical model can either model all parts of the transformer in great detail or can be constructed according to gross physical components such as the winding layers. These types of models use network equivalent parameters (resistances, inductances and capacitances) to construct the model and focus on the frequency range of interest. Transformer models can be classified as power frequency range, medium frequency range (kHz) or high frequency range (MHz).

This thesis is studying what influence the transformer internal changes have on the FRA transadmittance signature changes. In the case of the FRA test, it is desirable to see small changes in the transformer so that any movement can be detected as early as possible. This means that the focus of the model has to be on the high frequency range. To model this situation, a terminal model is not suitable as it is mainly used for system performance studies rather than being focused on transformer internal condition changes. A detailed model is preferred, but detailed design information for a transformer is very difficult to obtain, as it needs detailed proprietary manufacturing design data that manufacturers do not want to divulge. A reduced model is more suitable for the work in this thesis.

A reduced transformer model on time domain calculation was therefore carried out. The modeling work did not focus on a particular transformer, but instead used a general model testing different parameters related to FRA measurement to see how these factors influence the

FRA results. The transformer model simulation is intended to explain the observations from the experimental work and to test how the proposed new method works in principle.

## A.2 Simulation Model and Cases Studied

The purpose of the transformer modeling for this study is to analyse the principal changes in FRA transadmittance, which are caused by transformer internal factors and by the measurement circuit itself. A high frequency time domain reduced model is used for the simulation since the megahertz range is of most interest for this study. In the megahertz frequency range transformer excitation inductance can be ignored. The Electro-Magnetic Transients Program (EMTP) was used for the simulations.

The FRA measurements were done on many different power transformers that varied in voltage and kVA rating, number of phases and in internal design. Future measurements will also be done on a large variety of power transformers. Due to the lack of detailed transformer internal design data, and since a detailed transformer model for this frequency range would need to be very complicated, an alternative approach was taken. The model used is not based on a fit to any of the tested transformers, but is based on experimental and published data. The purpose of this model is to interpret the FRA admittance caused by internal changes. The basic components of the model transformer are from a paper [138] with some modifications. Parallel ground capacitances were added to each section of the winding to simulate the dielectric loss of the insulation, since this factor has potential influence on FRA results. High voltage bushings and ground leads were also introduced in some of the case simulations. Only one winding was simulated in this model to simplify the analysis. The model separates the winding into identical sections that simulate individual winding discs. The number of sections is a compromise between closeness to the real transformer and limitations of capability of the program to perform the calculations. An R, L, C equivalent network circuit simulates the transformer winding. Each section of the circuit consists of a ground capacitance ($C_g$), series capacitance ($C_s$), series inductance (L) and resistance (R). The number of sections used in this model is 12, 67, and 74, which simulates the number of transformer discs. The series inductance represents the winding lead inductance, the parallel ground capacitance represents the capacitance between the discs and ground, the series capacitance represents the turn-to-turn or disc-to-disc capacitance and the series resistance represents the winding resistance.

Figure A.1 shows the basic model. Parallel resistance ($R_g$) was added in some simulations to represent the dielectric losses between the winding and tank. Resistance ($R_p$) in parallel with the series capacitance was also added in some simulations to represent the dielectric losses between winding turns/discs.

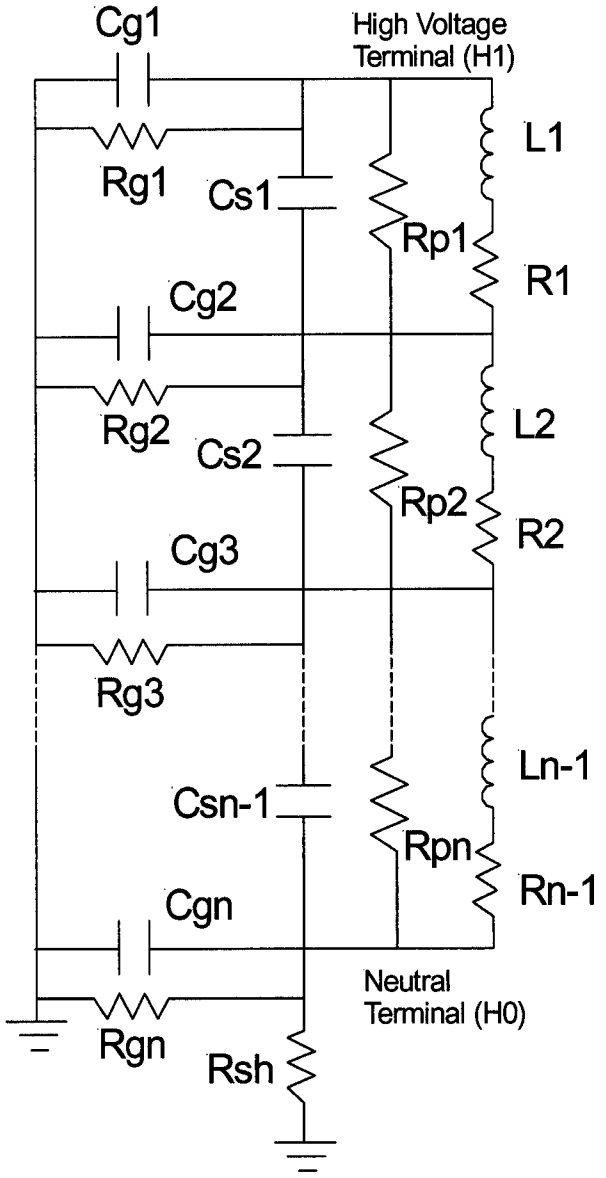


Figure A.1 – Base line model used for simulations

The following simulations were carried out in this study:

1) Minor winding movement, simulated by changing the series capacitance
2) Minor winding movement, simulated by changing the ground capacitance
3) Winding movements occurring in different winding locations, simulated by changing the series capacitance in different winding locations
4) Winding series resistance changes, simulated by changing winding resistance
5) Shorts in winding turns, simulated by shorting several sections
6) High voltage bushing effects
8) Ground lead effects
9) Shunt resistance effects
10) Parallel ground capacitance effects
11) Series resistance effects
12) Effects of parallel resistance with series capacitance
13) Effects of different number of modeling sections
14) Simulation injection method comparing the differences of top and bottom bushing measurement
15) Comparison of top and bottom bushing measurement on injection method with and without a resistive load at bushing terminal
16) Comparison of top and bottom bushing measurement on injection method with and without a capacitive load at bushing terminal

The baseline model parameters used were based on those used in Reference [138]. They were as follows:

Basic 67 Section Model Data:

| | |
|---|---|
| Cs - Series capacitance per disc: | 5.1 pF |
| Cg - Ground capacitance per disc: | 0.12 pF |
| R - Resistance per disc: | 0.43 Ω |
| L – Total inductance per disc: | 0.025 mH |
| Rg – Parallel resistance on Cg per disc: | 67 MΩ |
| S – Total number of sections: | 67 |

Basic 12 Section Model Data:

| | |
|---|---|
| Cs - Series capacitance per disc: | 0.91 pF |
| Cg - Ground capacitance per disc: | 0.67 pF |
| R - Resistance per disc: | 2.4 Ω |
| L – Total inductance per disc: | 0.14 mH |
| Rg – Parallel resistance on Cg per disc: | 12 MΩ |
| S – Total number of sections: | 12 |

Basic 74 Section Model Data:

| | |
|---|---|
| Cs - Series capacitance per disc: | 5.6 pF |
| Cg - Ground capacitance per disc: | 0.11 pF |
| R - Resistance per disc: | 0.39 Ω |
| L – Total inductance per disc: | 0.023 mH |
| Rg – Parallel resistance on Cg per disc: | 74 MΩ |
| S – Total number of sections: | 74 |

Local winding movement was simulated in the 67-section model by changing the series capacitance in three adjacent sections as follows:

| | |
|---|---|
| Section A: | from 5.1 pF to 2.1 pF |
| Section B: | from 5.1 pF to 1.1 pF |
| Section C: | from 5.1 pF to 2.1 pF |

Partial parallel capacitance changes in three sections of Cg (out of 67 sections) were simulated by the following changes:

| | |
|---|---|
| Section A: | from 0.12 pF to 0.052 pF |
| Section B: | from 0.12 pF to 0.022 pF |
| Section C: | from 0.12 pF to 0.052 pF |

Ground resistance changes in the 12-section model by adding 10 MΩ to each section

| | |
|---|---|
| EMTP time interval: | 20 ns |
| Total calculating point: | 10,000 |
| Time length: | 200 microseconds |
| Current shunt resistance: | 10 Ω, 1 Ω |
| Ground lead: | 100 μH, 10 μH |
| Bushing: | "T" circuit with R = 0.4 Ω, L = 5 μH pF |

Details of the simulation cases are listed in Table A.1.

Table A.1 – Simulation cases

| Simulation No | Purpose of the simulation | Conditions |
|---|---|---|
| Simulation 1 | Baseline model | 67 section winding, 1 Ω shunt |
| Simulation 2 | Shunt resistance effects | 67 section winding, 1 Ω, 10 Ω & 50 Ω shunt |
| Simulation 3 | Top 1/3 winding moved (axial), measured by 1 Ω shunt | Simulated by reducing Cs from 5.1 pF to 2.1 pF in three sections (section 19 – 21), 1 Ω shunt, 67 sections |
| Simulation 4 | Top 1/3 winding moved (axial), measured by 50 Ω shunt | Simulated by reducing Cs from 5.1 pF to 2.1 pF in three sections (section 19 – 21), 50 Ω shunt, 67 sections |
| Simulation 5 | Bushing effect | A "T" circuit added simulating the HV bushing (two 0.2 μH and two 0.2 Ω in series, 400 pF in series with 2000 pF to grd), 67 sections |
| Simulation 6 | Ground lead effect | Ground lead between shunt ground terminal to ground, 67 sections |
| Simulation 7 | Comparison of models with/without bushing and ground lead | With & without both bushing and ground lead, 1 Ω shunt, 67 sections |
| Simulation 8 | Investigate sensitivity of detecting winding movement (axial) with bushing only | With bushing & moved winding 1/3 down from top, 1 Ω shunt, 67 sections |
| Simulation 9 | Investigate sensitivity of detecting winding movement (axial) with bushing and ground lead | With bushing & ground lead, moved winding 1/3 down from top, 1 Ω shunt, 67 sections |
| Simulation 10 | Investigate movement (axial) at different locations with no bushing or ground lead | Top, middle & bottom winding movement, 1 Ω shunt, 67 sections |
| Simulation 11 | Investigate movement (axial) in different locations of the winding with ground lead only | Top, middle & bottom winding movement, 1 Ω shunt, 67 sections |

| Simulation No | Purpose of the simulation | Conditions |
|---|---|---|
| Simulation 12 | Investigate a winding short | Section on top of top winding shorted, 1 Ω shunt, 67 sections |
| Simulation 13 | Investigate radial winding movement by reducing winding to tank capacitance (Cg) | Cg changed from 5.1 pF to 1.1 & 2.1 pF in upper section of winding sections, 1 Ω shunt, 67 sections |
| Simulation 14 | Investigate radial movement in different locations of the winding | Top, middle, and bottom winding movement, 1 Ω shunt, 67 sections |
| Simulation 15 | Study effect of different number of sections to simulate winding | Winding formed by 12, 67 and 74 sections, the total parameters are the same, 1 Ω shunt |
| Simulation 16 | Effect of dielectric loss from winding to tank | Adding an additional 10 MΩ parallel resistance to ground, 67 section model, 1Ω shunt |
| Simulation 17 | Effects of dielectric loss between winding discs | Adding additional 1 MΩ parallel resistance to Cs, 67 section model, 1Ω shunt |
| Simulation 18 | Simulate effect of winding movement using the injection method | Comparison of measurement at top and bottom of bushing using injection method with and without winding movement |
| Simulation 19 | Simulate injection test method with a bushing and various external loads on the bushing | Bushing "T" circuit two 0.2 μH and two 0.2 Ω in series, 400 pF in series with 2000 pF to grd, 67 sections |

## A.3 Simulation Results

The analysis provides both magnitude and phase angle data. Only the magnitude data is presented here as only the magnitude is commonly used. Experience has shown that the phase angle data does not provide useful additional information.

**Simulation 1**

The results of the baseline model calculation are shown in Figure A.2. The baseline case was done with a 67-layer transformer model based on the modified IEEE paper model. This model has no high voltage bushing, no ground lead and a 1 Ω current shunt connected between the neutral of the winding and ground. The 1 Ω shunt value was chosen based on the experiment results that 1 Ω has the highest sensitivity. Figure A.2 demonstrates the admittance results from the simulation. The admittance is calculated from shunt current and high voltage to ground voltage. The admittance results show that there are five major resonant frequencies in the 500 kHz to 10 MHz frequency range. The majority of the following simulations were based on this model.

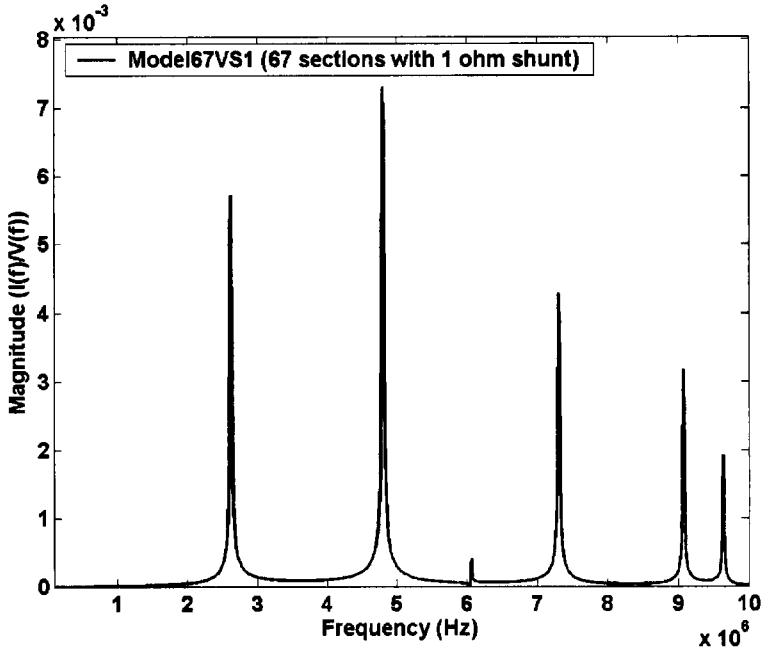


Figure A.2 – Baseline model simulated admittance

**Simulation 2**

The basic model was used to simulate the effect of using different shunt resistances. Three shunt resistances were used in the simulation (1Ω, 10 Ω and 50 Ω). A 50 Ω shunt is normally used in FRA (S) measurements, and 10 Ω is commonly used in FRA (I) measurements. A 1 Ω shunt is the proposed value for the high frequency FRA measurement. Figure A.3 shows the comparison results of the three shunt resistances. The quality factor (Q) of the admittance resonant peak values decreases as the shunt resistance increases. This would correspond to a reduction in sensitivity to changes in the transformer. This simulation agrees with actual measurements on transformers, where it has been found that using a higher shunt resistance reduces the FRA measurement sensitivity to changes. There is no frequency shift between different shunt resistances. Table A.2 demonstrates the effects of using different shunt resistances. The admittance magnitude has a reduction ranging from 2% to 13% by using the 10 Ω shunt. The reduction in magnitude is 9% to 45% when using the 50 Ω shunt. This simulation results again show that the shunt resistance is significant compared with transformer impedance in the megahertz frequency range. In order to increase the sensitivity of the FRA measurement, a lower shunt resistance value is more appropriate. From simulation and experiments, a 1 Ω shunt is a compromise choice.

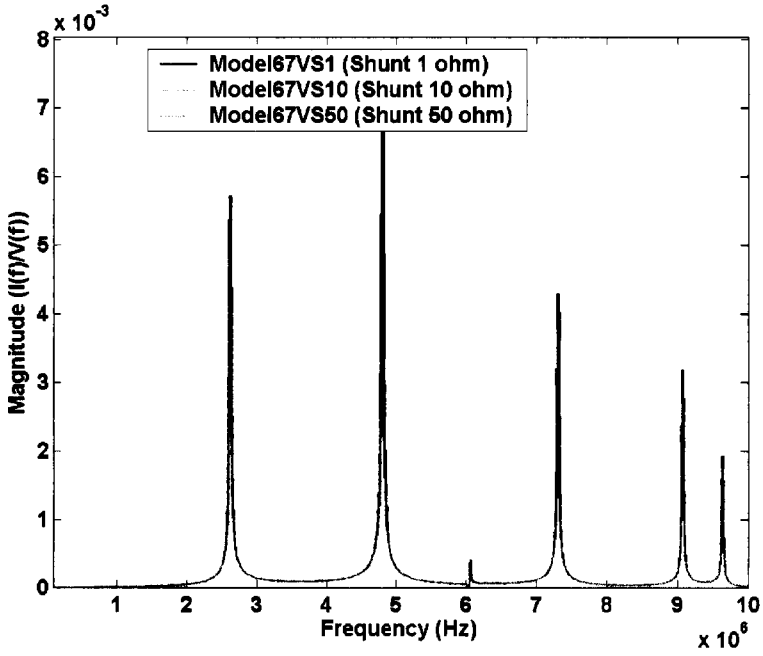


Figure A.3 – Simulation results of shunt resistance

Table A.2 – Shunt resistance simulations

| Baseline resonant frequency | Baseline resonant magnitude | Magnitude change comparing with baseline (10 Ω shunt) | Magnitude change comparing with baseline (50 Ω shunt) | Note |
|---|---|---|---|---|
| 2.62 MHz | 5.72e-3 | -1.97% | -9.87% | 1st resonance |
| 4.80 MHz | 7.31e-3 | -13.04% | -45.27% | 2nd resonance |
| 7.31 MHz | 4.28e-3 | -2.29% | -11.36% | 3rd resonance |
| 9.08 MHz | 3.17e-3 | -3.07% | -14.72% | 4th resonance |
| 9.64 MHz | 1.93e-3 | -1.79% | -9.02% | 5th resonance |

**Simulation 3**

This simulation modeled localized winding movement at a location one-third of the way down from the top of the winding. The changes simulate winding axial movement, which mainly causes a change in the capacitance between winding discs. Figure A.4 and Table A.3 show the results of reducing the series capacitance in sections 19 to 21 of the winding (out of 67 sections). The first section was reduced from 5.1 pF to 2.1 pF, the second to 1.1 pF, and the third to 2.1 pF. This change is to simulate mild bulging of about 2% of the winding in an outward direction. The series capacitance of the winding would be reduced due to an increase in the distance from the winding section to the neighbouring winding sections. The simulation results demonstrate more frequency shift on the higher frequency range. In this case, the 9.64 MHz resonant shows the most frequency shift. The percentage changes of resonant magnitude vary among the five major resonant frequencies. The 9.64 MHz resonant frequency shows the largest change in magnitude (4%) and the 9.08 MHz resonant frequency had the largest frequency shift (56 kHz). This simulation shows that the transformer winding axial measurement can cause both frequency shifts and magnitude changes. In this case, the higher frequency shows more frequency changes than the lower frequency resonance. After the axial movement at the top of the winding, the resonant frequencies shifted to higher frequencies and the magnitude slightly reduced below 9 MHz and increased above 9 MHz.

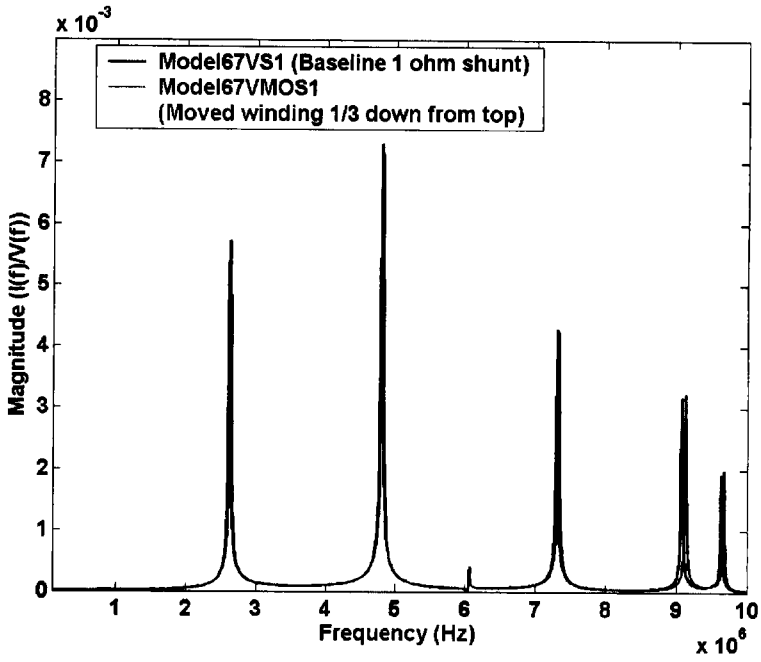


Figure A.4 – Winding movement in the upper sections of the winding

Table A.3 – Winding movement simulations with 1 Ω shunt

| Baseline resonant frequency | Baseline resonant magnitude | Frequency change comparing with baseline | Magnitude change comparing with baseline | Note |
|---|---|---|---|---|
| 2.62 MHz | 5.72e-3 | 0 | -1.55% | 1st resonance |
| 4.80 MHz | 7.31e-3 | 0 | -0.71% | 2nd resonance |
| 6.07E+06 | 4.14E-04 | 0 | 0.00% | Minor resonance |
| 7.31 MHz | 4.28e-3 | 15.2 kHz | -1.00% | 3rd resonance |
| 9.08 MHz | 3.17e-3 | 55.6 kHz | 2.02% | 4th resonance |
| 9.64 MHz | 1.93e-3 | 35.4 kHz | 3.76% | 5th resonance |

**Simulation 4**

This case simulates the 50 Ω shunt model and compares the results before and after an axial winding movement, one-third of the way down from the top of the winding, modeled by reducing the series capacitance in sections 19 to 21 of the winding (out of 67 sections). The winding movement used in this simulation is same as Simulation 3. Figure A.5 and Table A.4 show the simulation results before and after winding movement. The admittance value is lower than the 1 Ω shunt model. This result agrees with the actual FRA measurements in Chapter IV. The admittance magnitude of the transformer is much lower than the shunt resistance. This means that the shunt admittance will dominate the measurement, and therefore effectively the shunt is being tested instead of the transformer. After the winding moved, the resonant frequency shifted more in the higher frequency region than the lower frequency region. The frequency shifts before and after winding movements are the same as for the 1 Ω shunt results. The magnitude changes are less than for the 1 Ω shunt model. The percentage changes are only slightly different than the 1 Ω shunt model, but the absolute magnitude reduction is significant (30% at 2.8 MHz).

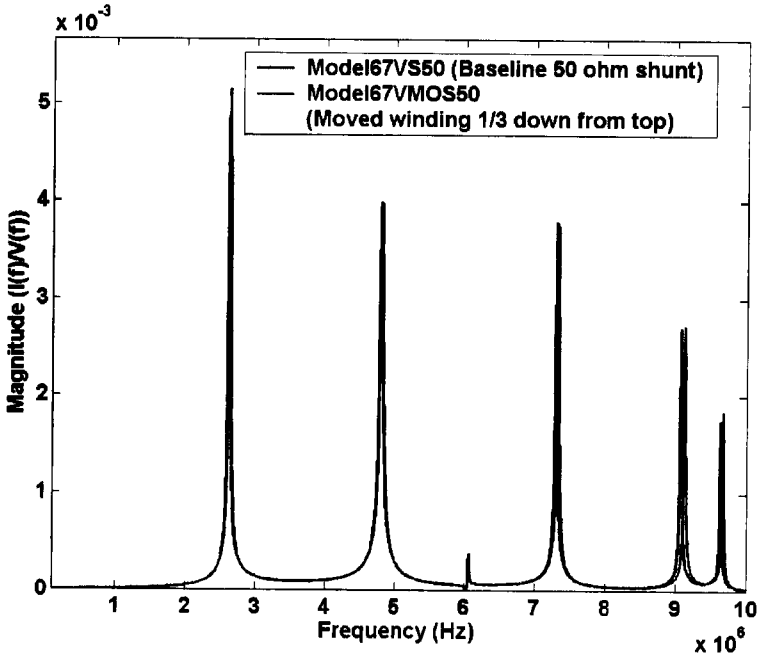


Figure A.5 - Winding movement in the upper section of the winding with 50 Ω shunt

Table A.4 – Winding movement simulations with 50 Ω shunt

| Baseline resonant frequency | Baseline resonant magnitude | Frequency change comparing with baseline | Magnitude change comparing with baseline | Note |
|---|---|---|---|---|
| 2.62 MHz | 5.15e-3 | 0 | -1.43% | 1st resonance |
| 4.80 MHz | 4.00e-3 | 0 | -0.05% | 2nd resonance |
| 6.07 MHz | 3.83e-4 | 0 | 0.09% | Minor resonance |
| 7.31 MHz | 3.80e-3 | 15.2 kHz | -1.23% | 3rd resonance |
| 9.08 MHz | 2.70e-03 | 55.6 kHz | -0.73% | 4th resonance |
| 9.64 MHz | 1.75e-03 | 35.4 kHz | 5.34% | 5th resonance |

**Simulation 5**

This case investigates the effect of the high voltage bushing on the FRA measurement. The model of the transformer bushing was simulated by the LRC "T" circuit shown in Figure A.6. The results are shown in Figure A.7 and Table A.5. After adding the bushing, the transformer admittance developed a new large resonant peak at 5.31 MHz. The magnitude at the first two resonant frequency peaks increased after adding the bushing model. The magnitude of the other three major peaks reduced. The simulation shows that by including a bushing model the admittance characteristics change significantly.

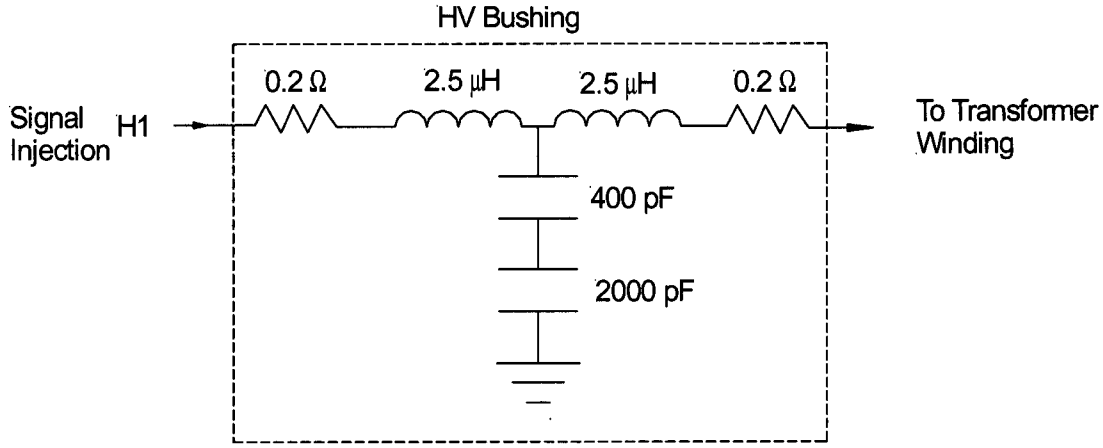


Figure A.6 – Bushing simulation

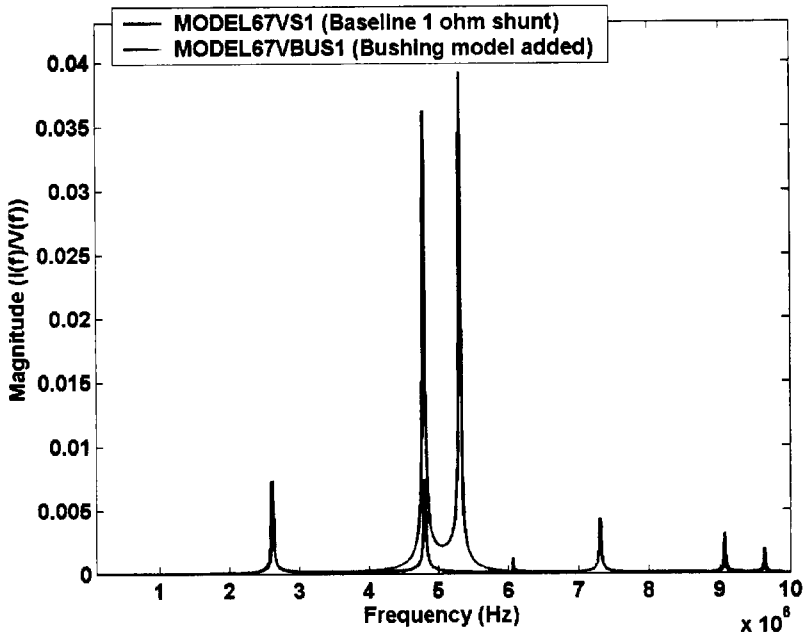


Figure A.7 – Effect of the bushing

Table A.5 – Simulating high voltage bushing

| Baseline resonant frequency | Baseline resonant magnitude | Frequency change comparing with baseline Δf | Magnitude change comparing with baseline | Note |
|---|---|---|---|---|
| 2.62 MHz | 6.19e-3 | -12.2 kHz | 37.02% | 1st resonance |
| 4.80 MHz | 7.85e-3 | -12.2 kHz | 389.44% | 2nd resonance |
| - | - | 5.32 MHz | New peak | New resonance |
| 6.07 MHz | 4.79e-4 | - | No peak | 3rd resonance |
| 7.31 MHz | 4.52e-3 | -6.1 kHz | -3.18% | 4th resonance |
| 9.08 MHz | 4.09e-3 | 0 kHz | -61.50% | 5th resonance |
| 9.42 MHz | 8.43e-5 | -9.42 MHz | -100% | 6th resonance |
| 9.64 MHz | 2.34e-3 | 0 kHz | -63.71% | 7th resonance |

**Simulation 6**

This case simulates the effect of the ground lead, which connects the shunt to ground. Figures A.8 and A.9 and Tables A.6 and A.7 show the comparison of the base model with the model with a short lead (10 μH) and a long lead (100 μH), respectively. Adding the short lead causes some frequency shift to lower frequencies (up to 45.5 kHz) and magnitude changes (up to 4.2%). Adding the long ground lead caused significant resonant frequency shifts to lower frequencies (up to 434 kHz) and magnitude changes (up to 11.8%). The ground lead causes changes spread over all frequency regions.

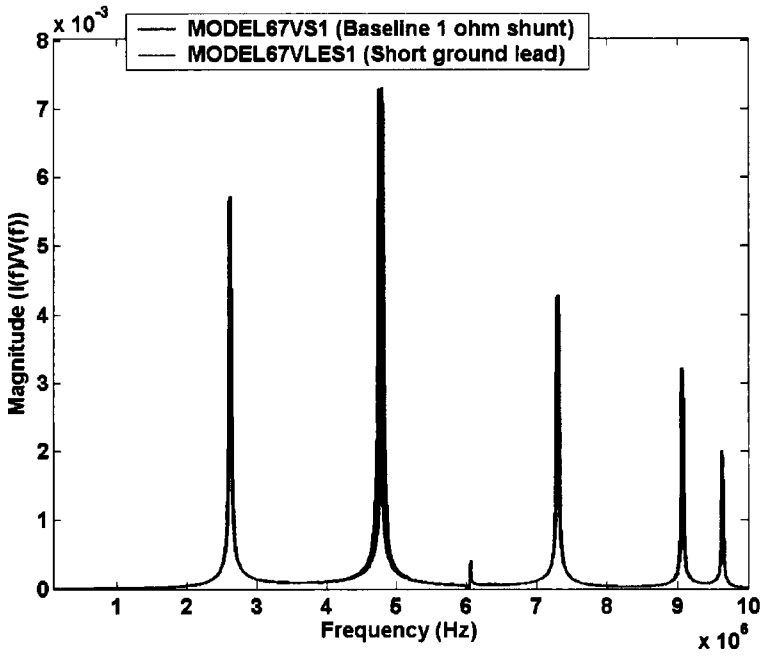


Figure A.8 – Effect of 10 μH ground lead

Table A.6 – Simulating 10 μH grounding lead

| Baseline resonant frequency | Baseline resonant magnitude | Frequency change comparing with baseline Δf | Magnitude change comparing with baseline | Note |
|---|---|---|---|---|
| 2.62 MHz | 5.72e-3 | -5.05 kHz | -0.93% | 1st resonance |
| 4.80 MHz | 7.31e-3 | -45.5 kHz | -0.19% | 2nd resonance |
| 7.31 MHz | 4.28e-3 | -10.1 kHz | -0.84% | 3rd resonance |
| 9.08 MHz | 3.17e-3 | -15.2 kHz | 1.46% | 4th resonance |
| 9.64 MHz | 1.93e-3 | -5.05 kHz | 4.19% | 5th resonance |

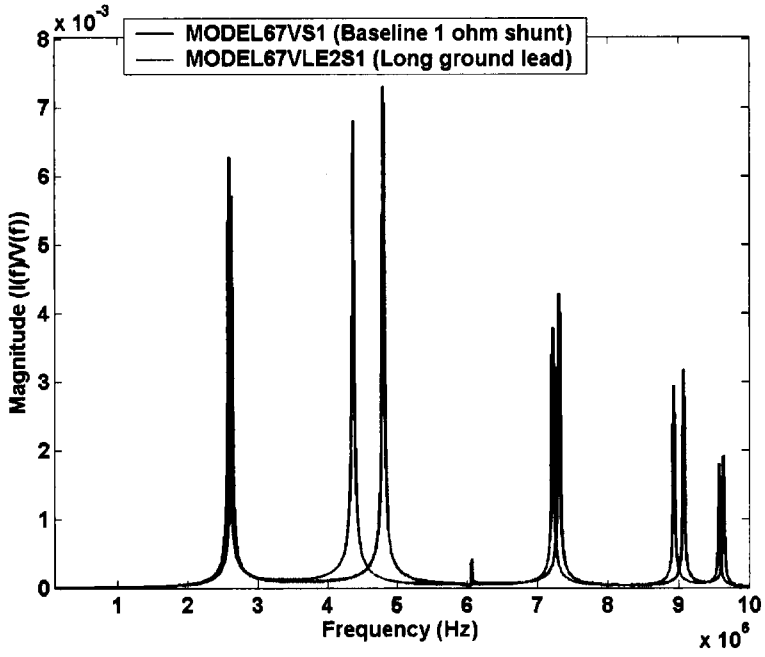


Figure A.9 – Effect of 100 μH ground lead

Table A.7 – Simulating 100 μH grounding lead

| Baseline resonant frequency | Baseline resonant magnitude | Frequency change comparing with baseline Δf | Magnitude change comparing with baseline | Note |
|---|---|---|---|---|
| 2.62 MHz | 5.72e-3 | -3.03 kHz | 9.84% | 1st resonance |
| 4.80 MHz | 7.31e-3 | -434 kHz | -6.67% | 2nd resonance |
| 7.31 MHz | 4.28e-3 | -90.9 kHz | -11.77% | 3rd resonance |
| 9.08 MHz | 3.17e-3 | -136 kHz | -7.04% | 4th resonance |
| 9.64 MHz | 1.93e-3 | -60.6 kHz | -6.11% | 5th resonance |

**Simulation 7**

This simulation compares the model with and without a bushing and a ground lead. The bushing used is the same model as in Simulation 5, an LCR "T" circuit. The ground lead used here is the short lead model. In a real measurement, a bushing and a lead are both in the measurement circuit. Figure A.10 shows the comparison of the transformer baseline model and a model with both a short ground lead and bushing model. Table 6.8 shows the differences with and without the bushing and ground lead. A new resonant frequency occurred at 4.88 MHz after the bushing and ground lead were added. All the resonant frequency shifted slightly to a lower frequency. The resonant frequency magnitude changed from –7.6% to 78.7%.

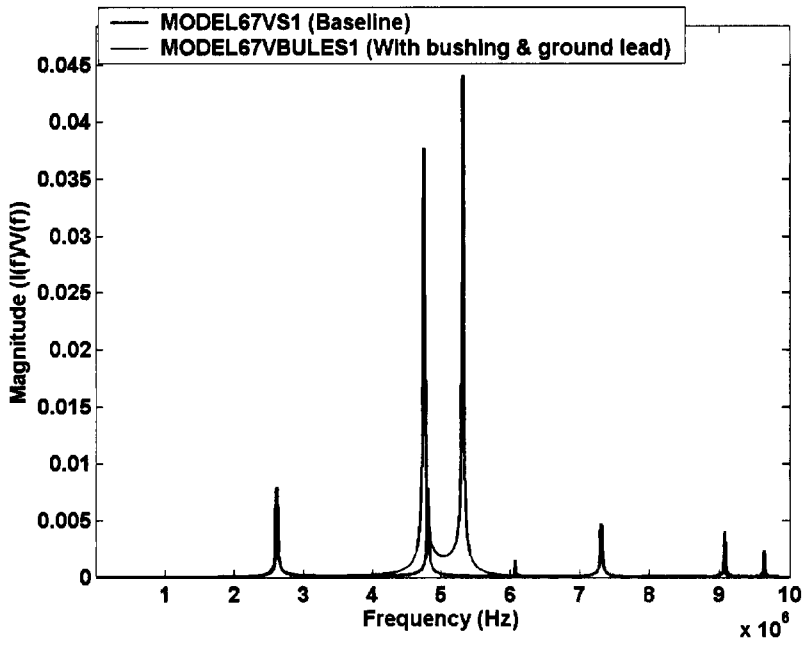


Figure A.10 – Results from the models with and without bushing and ground lead

Table A.8 – Transformer model with and without bushing and grounding lead

| Baseline resonant frequency | Baseline resonant magnitude | Frequency change comparing with baseline Δf | Magnitude change comparing with baseline | Note |
|---|---|---|---|---|
| 2.62 MHz | 6.19e-3 | -12.2 kHz | 28.10% | 1st resonance |
| 4.80 MHz | 7.85e-3 | -54.9 kHz | 379.97 | 2nd resonance |
| 5.32 MHz | - | 5.32 MHz | New | New |
| 6.07 MHz | 4.79e-4 | -6.1 kHz | 224.11% | 3rd resonance |
| 7.31 MHz | 4.52e-3 | -12.2 kHz | 4.64% | 4th resonance |
| 9.08 MHz | 4.09e-3 | -12.2 kHz | -64.83% | 5th resonance |
| 9.64 MHz | 2.34e-3 | -6.1 kHz | -62.38% | 6th resonance |

**Simulation 8**

This case simulates the influence of axial winding movement with the high voltage bushing only added. Figure A.11 and Table A.9 show the comparison of the model with and without winding movement with the high voltage bushing added. The winding movement is the same as in Simulation 3, in which the series capacitance at sections 19 to 21 of the winding was reduced. The results show that the largest changes both at frequency shift and percentage magnitude happened at the highest frequency range (8 MHz to 10 MHz).

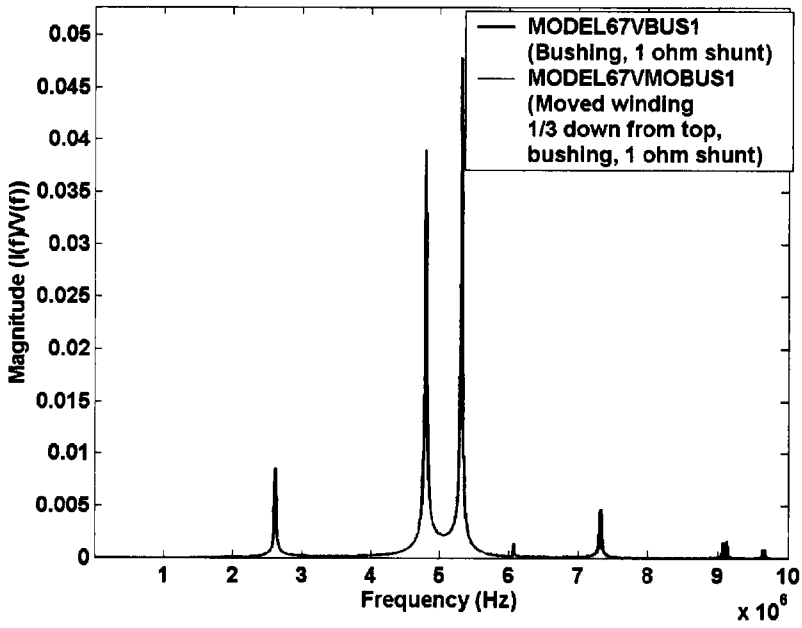


Figure A.11 – Winding movement with bushing

Table A.9 – Simulating winding movement with high voltage bushing

| Baseline resonant frequency | Baseline resonant magnitude | Frequency change comparing with baseline Δf | Magnitude change comparing with baseline | Note |
|---|---|---|---|---|
| 2.61 MHz | 8.48e-3 | 0 kHz | -4.92% | 1st resonance |
| 4.79 MHz | 3.84e-2 | 6.1 kHz | 1.43% | 2nd resonance |
| 5.32 MHz | 4.78e-2 | 0 kHz | -0.03% | 3rd resonance |
| 6.07 MHz | 1.42e-3 | 0 kHz | -0.02% | 4th resonance |
| 7.31 MHz | 4.37e-3 | 18.3 kHz | 7.30% | 5th resonance |
| 9.08 MHz | 1.57e-3 | 54.9 kHz | 5.83% | 6th resonance |
| 9.64 MHz | 8.51e-4 | 30.5 kHz | 2.61% | 7th resonance |

**Simulation 9**

This case simulates the effects of the transformer with both a bushing and a ground lead. The bushing model used is the same as in Simulation 5, an LCR "T" circuit. The ground lead used here is the short lead model. The winding movement simulated is the same as the axial winding movement described in Simulation 3. In a real measurement, a bushing and a lead are both in the measurement circuit. Figure A.12 shows the comparison of the transformer model with both a short ground lead and bushing model before and after the axial winding movement. The winding movement is the same as in Simulation 3. The simulation shows that the winding movement is hard to detect after adding the ground lead and the bushing to the transformer model.

Table A.10 shows the differences before and after winding movement. This simulation shows that the higher frequency demonstrates more magnitude change and frequency shift. The results show that the FRA at higher frequencies (8 MHz to 10 MHz) is more sensitive than the FRA at lower frequencies (below 6 MHz) in this case. However the absolute magnitude greatly reduced after the bushing and ground lead were added into the circuit.

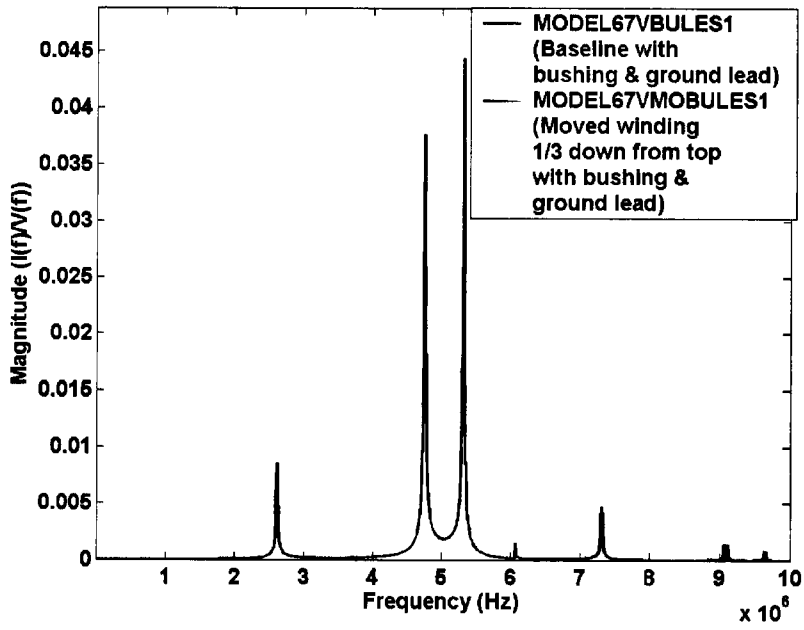


Figure A.12 – Winding movement with bushing and ground lead

Table A.10 – Simulating winding movement with bushing and grounding lead

| Baseline resonant frequency | Baseline resonant magnitude | Frequency change comparing with baseline Δf | Magnitude change comparing with baseline | Note |
|---|---|---|---|---|
| 2.61 MHz | 7.92e-3 | 0.0 kHz | 8.02% | 1st resonance |
| 4.74 MHz | 3.77e-2 | 0.0 kHz | -0.03% | 2nd resonance |
| 5.32 MHz | 4.40e-2 | 0.0 kHz | 0.80% | 3rd resonance |
| 6.07 MHz | 1.55e-3 | 0.0 kHz | -0.04% | 4th resonance |
| 7.30 MHz | 4.73e-3 | 12.2 kHz | -8.01% | 5th resonance |
| 9.06 MHz | 1.44e-3 | 54.9 kHz | 1.46% | 6th resonance |
| 9.63 MHz | 8.82e-4 | 30.5 kHz | -1.13% | 7th resonance |

**Simulation 10**

This case simulates the influences of axial winding movement at different locations with the winding and no bushing and no ground lead. The axial winding movement is simulated as described in Simulation 3. Three winding movement locations were simulated: top, middle and bottom of the winding. Figure A.13 to Figure A.15 shows the simulation results for movement at the three locations. Figure A.13 shows the overall results from 2 MHz to 10 MHz. Figure A.14 and Figure A.15 show the admittance differences at the first resonant peak (2.62 MHz) and the last two resonant peaks (9.08 & 9.64 MHz), respectively. The resonance peak at 9.08 MHz showed the greatest frequency shift and magnitude changes. The changes in the major resonances are shown in Table A.11.

In general, there are more significant changes, on average, at the higher frequencies. The frequency changes increase as the resonant frequency increases. This phenomenon is demonstrated in Figure A.16. The figure shows the average frequency shift and percentage magnitude changes at top, middle and bottom locations. The graph clearly shows that the trend of average frequency shift increases as the resonant frequency increases. The individual frequency shifts and magnitude changes at each location are shown in Figures A.17 and A.18, respectively.

The simulation results indicate that the high frequency region is more sensitive to the axial winding movement in general. The average percentage magnitude changes are also higher as the resonant frequency increases, but the average increases are not as significant as the frequency shift.

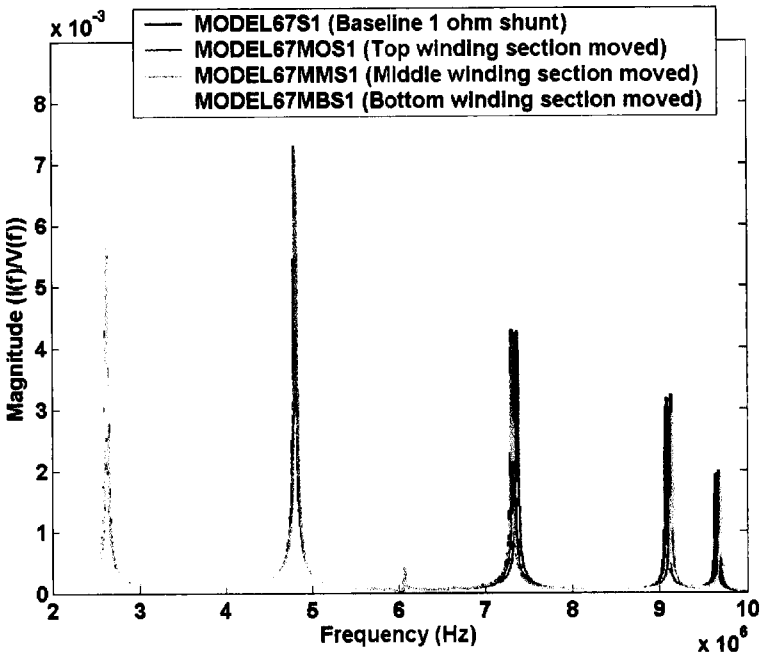


Figure A.13 - Effect of winding movement

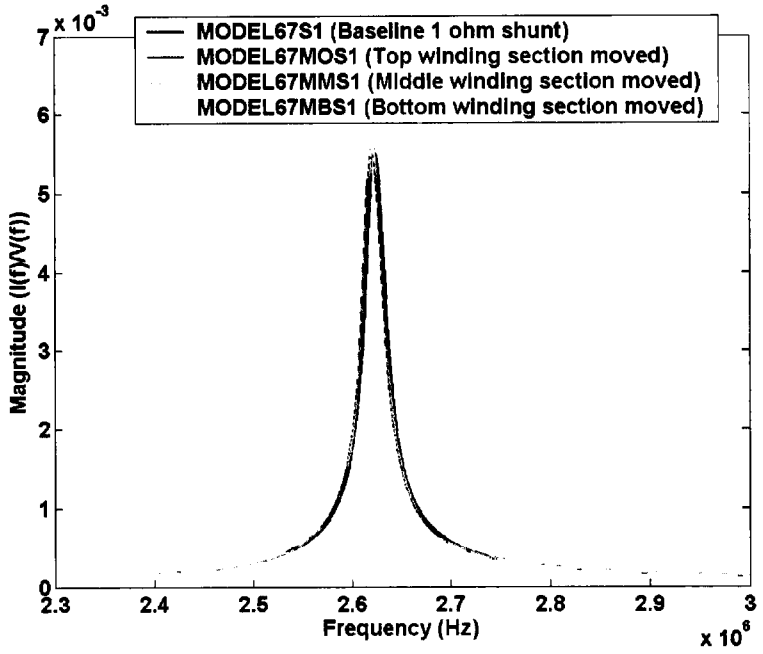


Figure A.14 – First resonant peak

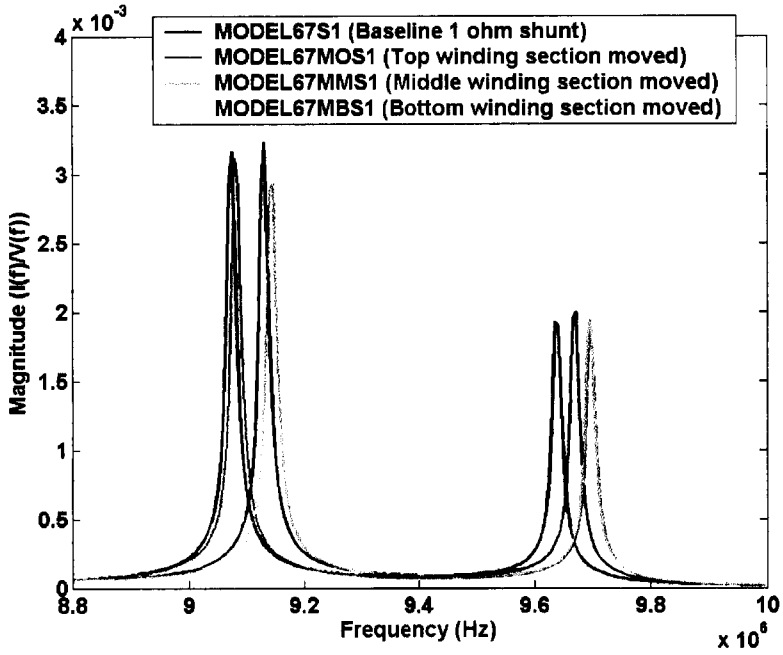


Figure A.15 – Fourth and fifth resonant peaks

Table A.11 – Winding movement simulations at different locations

| Location | Resonant peak | Frequency change comparing with baseline Δf | Magnitude change comparing with baseline | Note |
|---|---|---|---|---|
| Baseline | 2.62 MHz | - | - | 1st resonance |
| Top | 2.62 MHz | 0 kHz | -1.55% | 1st resonance |
| Middle | 2.62 MHz | 0 kHz | -0.32% | 1st resonance |
| Bottom | 2.62 MHz | 0 kHz | -0.04% | 1st resonance |
| Average after move | 2.62 MHz | 0 kHz | -0.64% | 1st resonance |
| Baseline | 4.80 MHz | - | - | 2nd resonance |
| Top | 4.80 MHz | 0 kHz | -0.71% | 2nd resonance |
| Middle | 4.80 MHz | 0 kHz | -0.54% | 2nd resonance |
| Bottom | 4.81 MHz | 10.1 kHz | -0.30% | 2nd resonance |
| Average after move | 4.80 MHz | 3.4 kHz | -0.52% | 2nd resonance |
| Baseline | 7.31 MHz | - | - | 3rd resonance |
| Top | 7.32 MHz | 15.2 kHz | -1.0% | 3rd resonance |
| Middle | 7.37 MHz | 60.6 kHz | -0.31% | 3rd resonance |
| Bottom | 7.31 MHz | 50.5 kHz | -4.58% | 3rd resonance |
| Average after move | 7.33 MHz | 42.1 kHz | -1.96% | 3rd resonance |
| Baseline | 9.08 MHz | - | - | 4th resonance |
| Top | 9.13 MHz | 55.6 kHz | 2.02% | 4th resonance |
| Middle | 9.08 MHz | 50.5 kHz | -1.54% | 4th resonance |
| Bottom | 9.15 MHz | 70.7 kHz | -7.25% | 4th resonance |
| Average after move | 9.12 MHz | 58.9 kHz | -2.26% | 4th resonance |
| Baseline | 9.64 MHz | - | - | 5th resonance |
| Top | 9.67 MHz | 35.4 kHz | 3.76% | 5th resonance |
| Middle | 9.70 MHz | 60.6 kHz | -0.66% | 5th resonance |
| Bottom | 9.70 MHz | 60.6 kHz | 1.23% | 5th resonance |
| Average after move | 9.69 MHz | 52.2 kHz | 1.44% | 5th resonance |

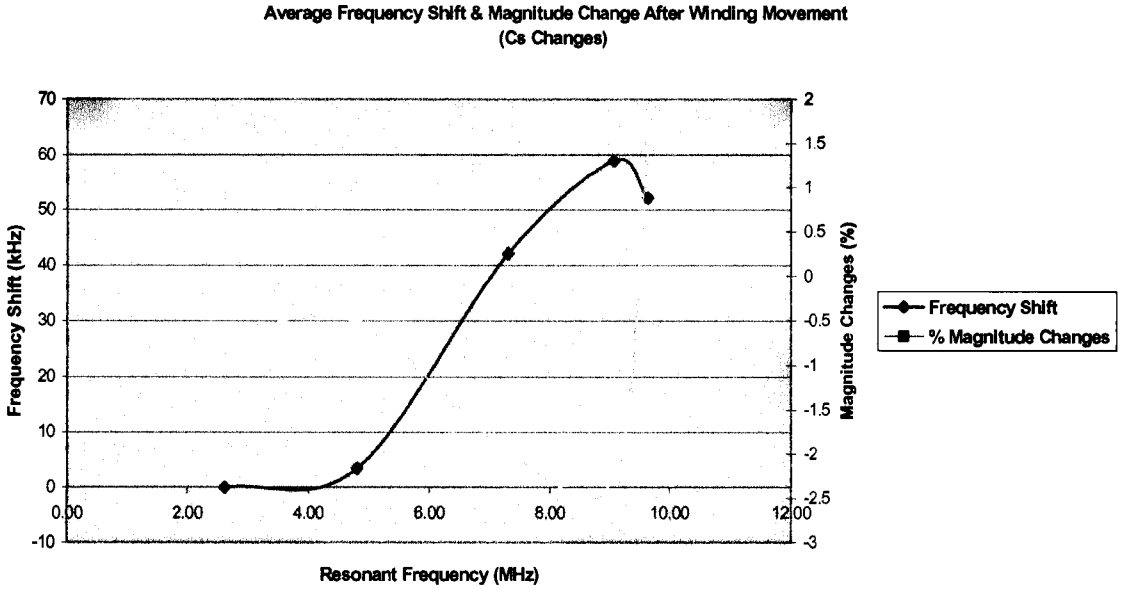


Figure A.16 – Average frequency shift & magnitude change after winding movement (Cs Changes)

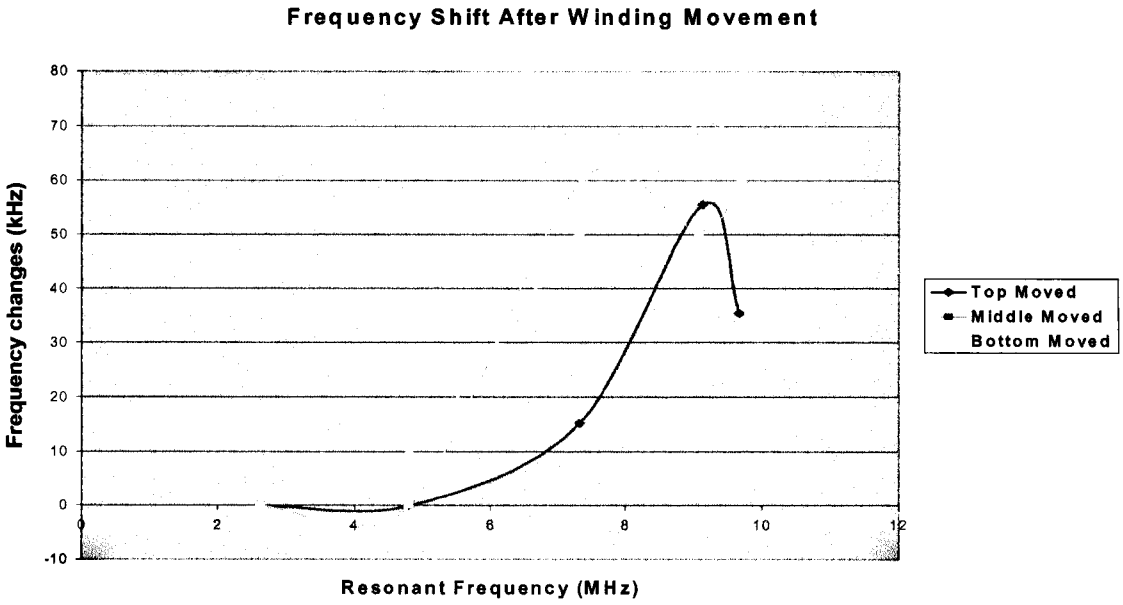


Figure A.17 – Frequency shift at each location after winding movement (Cs Changes)

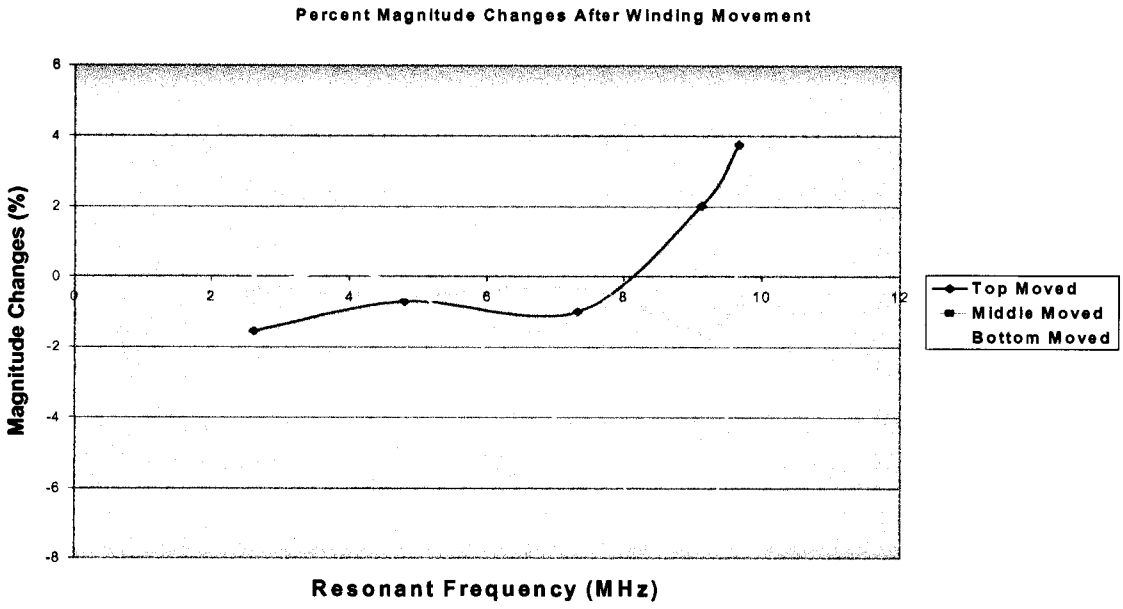


Figure A.18 – Percentage magnitude changes after winding movement at each location (Cs Changes)

**Simulation 11**

This case simulates the axial winding movement with a model including a 10 μH ground lead (short lead). Figure A.19 show the simulation results. A comparison was made of the base model and the model with the ground lead. Both models have no bushing added. The simulation shows that the higher resonant frequencies had larger frequency shifts after the winding moved. The 4$^{th}$ resonant frequency had the largest shift. Table A.12 summarizes the changes.

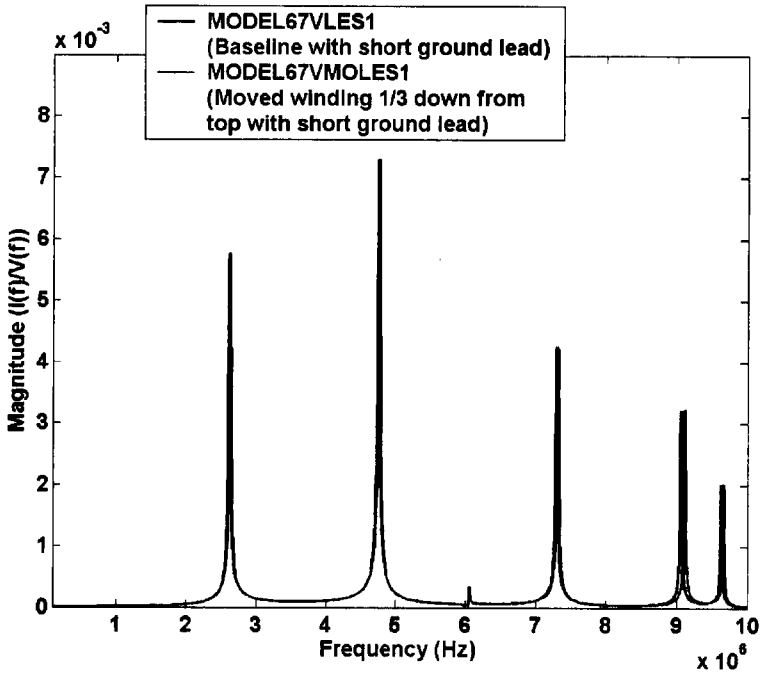


Figure A.19 – Winding movement with ground lead only

Table A.12 – Simulating winding movement with ground lead only

| Baseline resonant frequency | Baseline resonant magnitude | Frequency change comparing with baseline Δf | Magnitude change comparing with baseline | Note |
|---|---|---|---|---|
| 2.62 MHz | 5.63e-3 | 5 kHz | 1.76% | 1st resonance |
| 4.75 MHz | 7.29E-03 | 0 kHz | -0.08% | 2nd resonance |
| 7.30 MHz | 4.25E-03 | 15.2 kHz | -0.79% | 3rd resonance |
| 9.06 MHz | 3.22E-03 | 55.6 kHz | 0.76% | 4th resonance |
| 9.63 MHz | 2.01E-03 | 30.3 kHz | 0.66% | 5th resonance |

**Simulation 12**

This case simulates a short in the winding. The location of the short was at winding section 19-21 of the 67-section model. Figure A.20 shows the simulation results of shorting the three sections (19-21) of the winding. The four resonant frequencies all slightly shifted to higher frequencies and the change in magnitude of the resonance peaks ranged from –4.78% to +11.29%. The magnitude of the first, second and fifth major resonances increased after the winding section was shorted, while the magnitudes of the third and fourth major resonances were reduced. Table A.13 shows the simulation frequency shifts and magnitude changes before and after the partial winding short. Figure A.21 shows the plot of frequency shifts and magnitude changes. The local winding short caused both frequency shifts and magnitude changes. All the major resonances shifted to higher frequencies. The magnitude changes were in both directions.

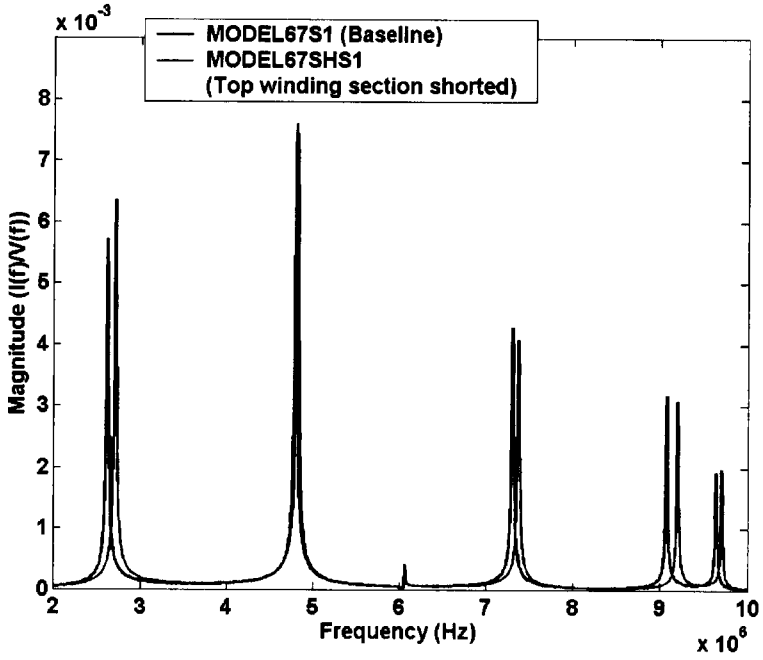


Figure A.20 – Before and after partial winding shorted

Table A.13 – Winding shorted simulations

| Baseline resonant frequency | Baseline resonant magnitude | Frequency change comparing with baseline | Magnitude change comparing with baseline | Note |
|---|---|---|---|---|
| 2.62 MHz | 5.72e-3 | 90.9 kHz | 11.29% | 1st resonance |
| 4.80 MHz | 7.31e-3 | 10.1 kHz | 4.31% | 2nd resonance |
| 7.31 MHz | 4.28e-3 | 70.7 kHz | -4.78% | 3rd resonance |
| 9.08 MHz | 3.17e-3 | 126.3 kHz | -2.57% | 4th resonance |
| 9.64 MHz | 1.93e-3 | 65.7 kHz | 2.85% | 5th resonance |

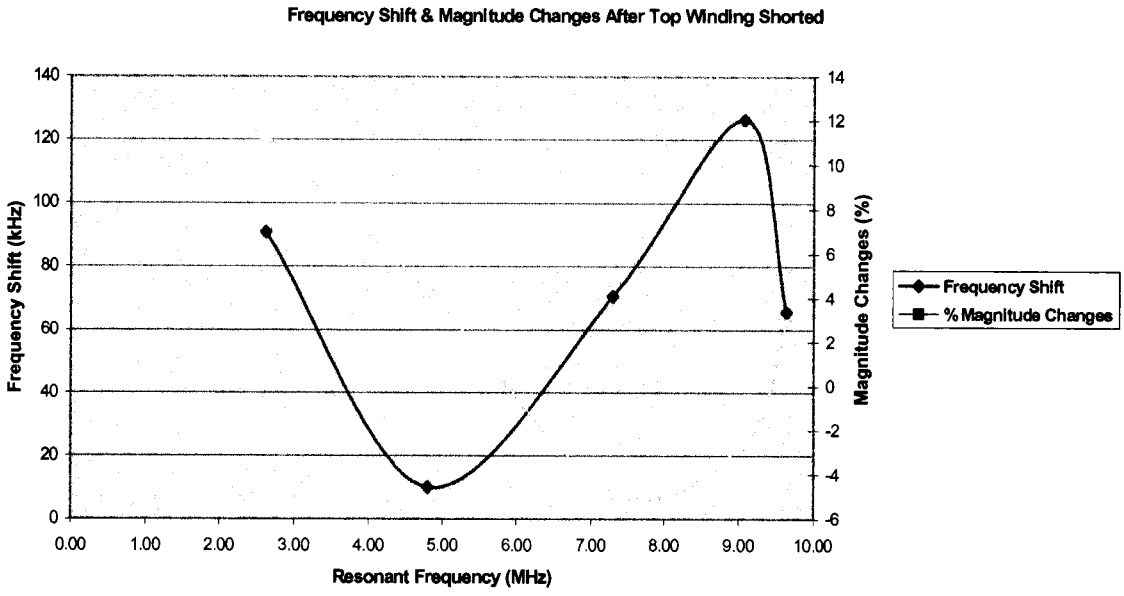


Figure A.21 – Frequency shift & magnitude changes after top winding partially shorted

**Simulation 13**

This case simulates radial winding movement. This type of movement is assumed to introduce changes in the ground capacitance of a winding. In order to simulate this type of winding movement the parallel ground capacitance were changed as follows:

Layer 19 from 0.12 pF to 0.052 pF
Layer 20 from 0.12 pF to 0.022 pF
Layer 21 from 0.12 pF to 0.052 pF

Figure A.22 and Table A.14 show the simulation results of radial movement (parallel ground capacitance change) at section 19-21 of the winding. The simulation results show both frequency shifts and magnitude reduction. The peak changes occurred in the higher frequency region (7 MHz to 10 MHz). All the resonant frequencies slightly shifted to higher values and all the resonant frequency magnitudes reduced.

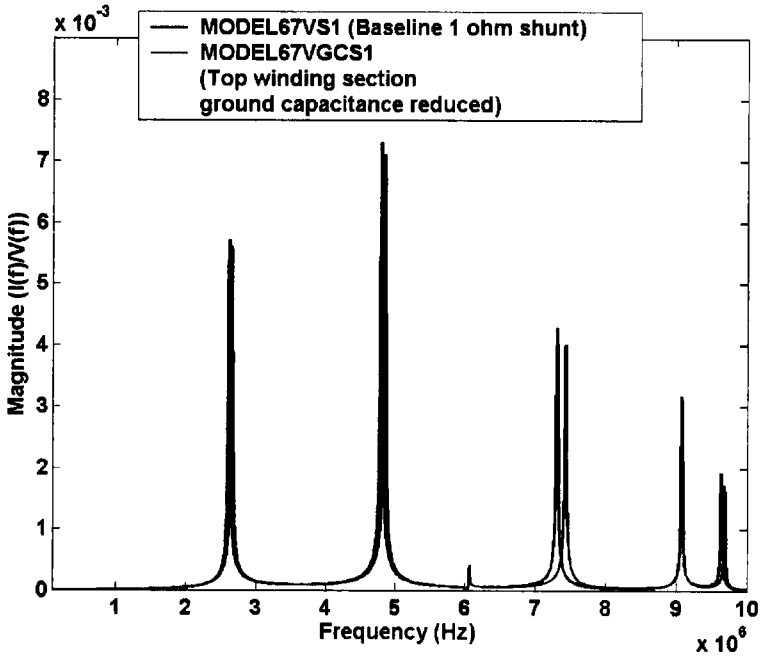


Figure A.22 – Effect of radial winding movement

Table A.14 – Top winding section radial movement

| Baseline resonant frequency | Baseline resonant magnitude | Frequency change comparing with baseline Δf | Magnitude change comparing with baseline | Notes |
|---|---|---|---|---|
| 2.62 MHz | 5.72e-3 | 25.3 kHz | -2.08% | 1st resonance |
| 4.80 MHz | 7.31e-3 | 40.4 kHz | -2.71% | 2nd resonance |
| 7.31 MHz | 4.28e-3 | 121 kHz | -6.51% | 3rd resonance |
| 9.08 MHz | 3.17e-3 | 5.05 | -1.69% | 4th resonance |
| 9.64 MHz | 1.93e-3 | 45.5 kHz | -10.51% | 5th resonance |

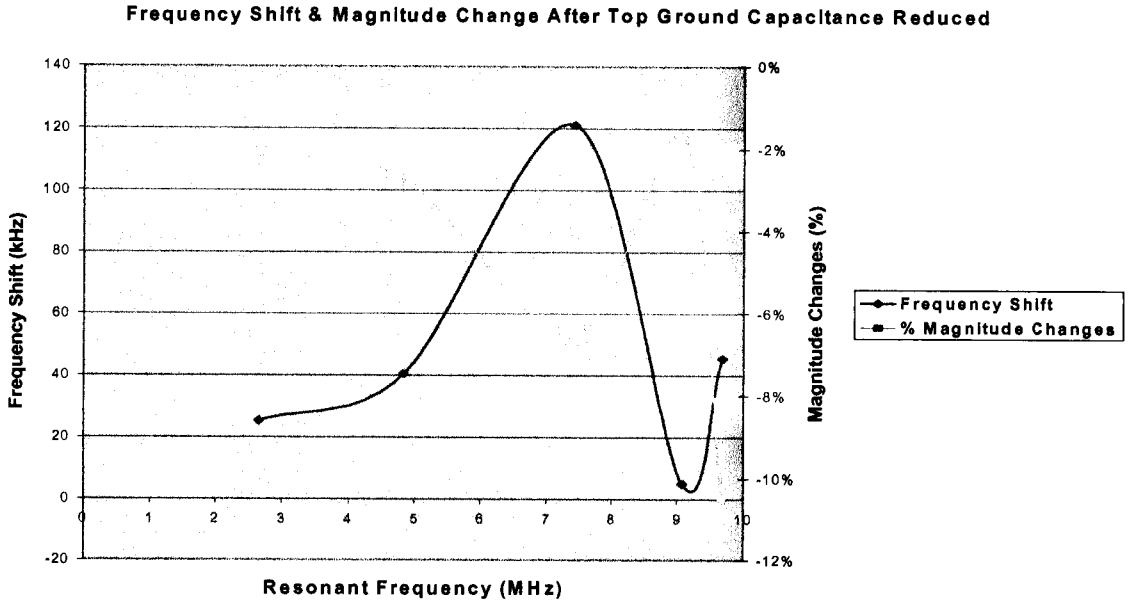


Figure A.23 – Frequency shift & magnitude changes after top ground capacitance reduced

**Simulation 14**

This simulation is a continuation of the investigation of Simulation 13, which simulates radial movement by changing the parallel ground capacitance (Cg). In this case, changes in three locations were simulated (top, middle and bottom).

Figures A.24 to A.26 show the overlaid results of the baseline case and the cases with the parallel ground capacitance (Cg) changed in three different locations. Table A.15 shows the changes caused by simulated radial movement at different locations of the transformer winding. Figure A.27 demonstrates the pattern of average frequency shift and magnitude changes from three simulations (top, middle and bottom). Figures A.28 and A.29 show the frequency shift and the magnitude changes each location (top, middle & bottom). In general, the magnitude and frequency changes increase as the resonant frequency is increased. The pattern of the changes caused by the radial movement change as the movement location is changed. There is no simple pattern to the changes, but it may be possible to use pattern recognition to provide an indication of the failure location.

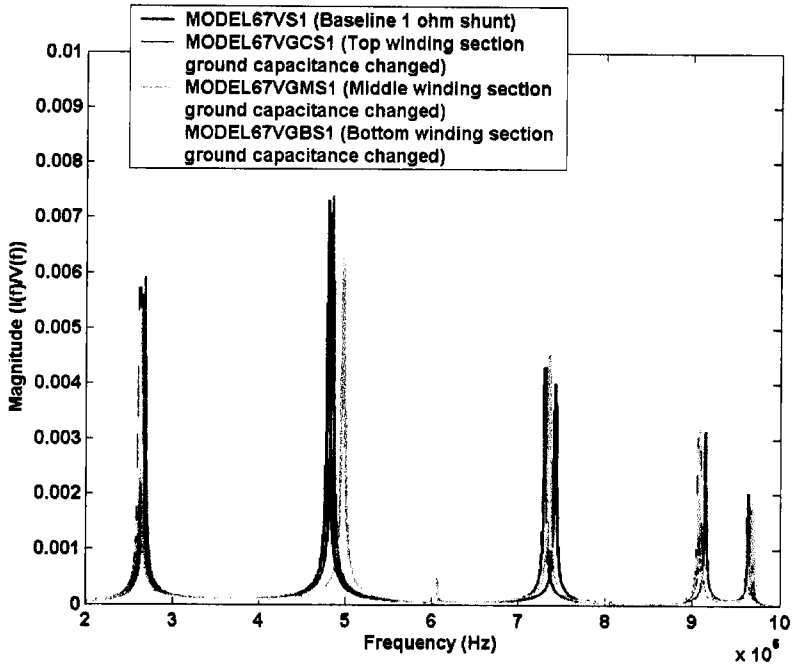


Figure A.24 – Radial winding movement at different locations (2 MHz to 10 MHz)

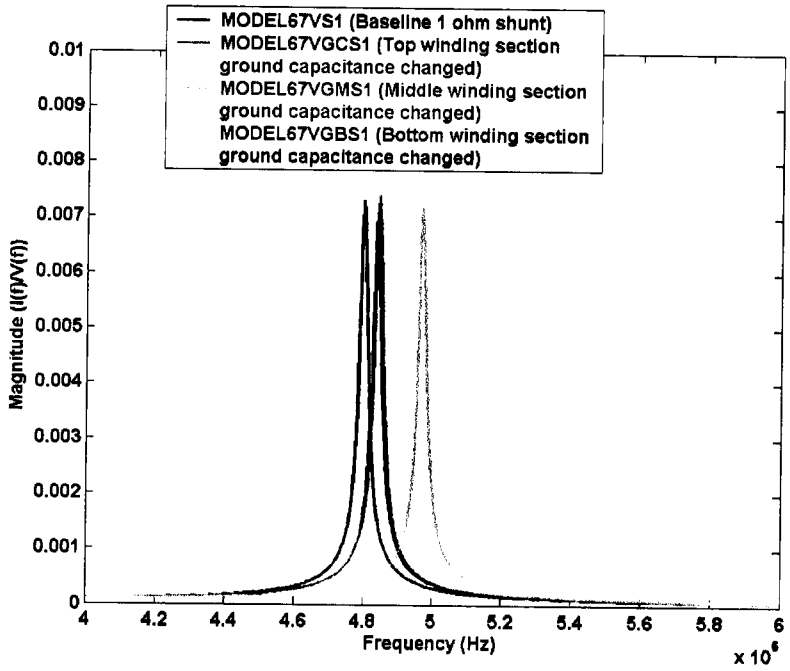


Figure A.25 – Radial winding movement at different locations (2 MHz to 4 MHz)

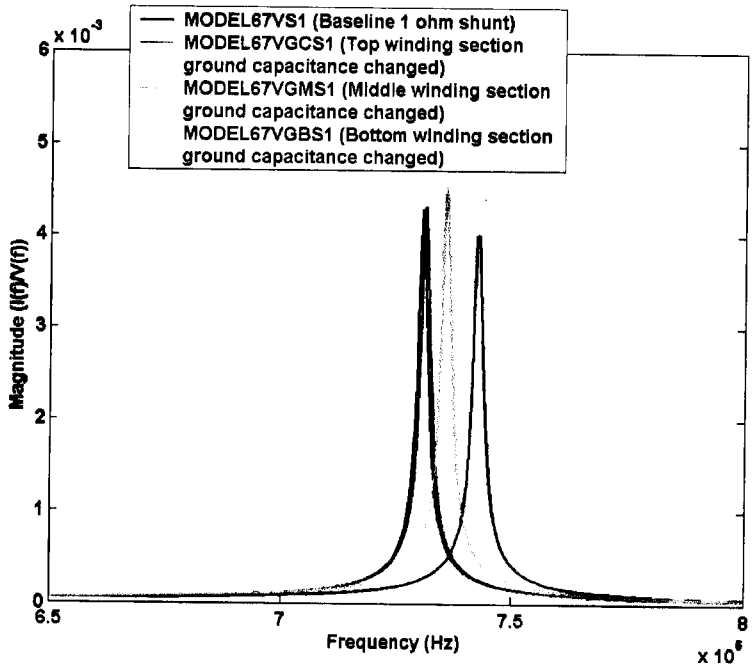


Figure A.26 – Radial winding movement at different locations (6 MHz to 8 MHz)

Table A.15 – Effect of changes in capacitance to ground

| Location | Resonant peak | Frequency change comparing with baseline Δf | Magnitude change comparing with baseline | Note |
|---|---|---|---|---|
| Baseline | 2.62 MHz | - | - | 1st resonance |
| Top | 2.65 MHz | 25.3 kHz | -2.08% | 1st resonance |
| Middle | 2.68 MHz | 55.6 kHz | 3.56% | 1st resonance |
| Bottom | 2.63 MHz | 5.05 kHz | 5.67% | 1st resonance |
| Average after move | 2.65 MHz | 28.6 kHz | -1.40% | 1st resonance |
| Baseline | 4.80 MHz | - | - | 2nd resonance |
| Top | 4.84 MHz | 40.4 kHz | -2.71% | 2nd resonance |
| Middle | 4.84 MHz | 45.5 kHz | 1.30% | 2nd resonance |
| Bottom | 4.97 MHz | 172 kHz | -1.57% | 2nd resonance |
| Average after move | 4.88 MHz | 85.9 kHz | -0.99% | 2nd resonance |
| Baseline | 7.31 MHz | - | - | 3rd resonance |
| Top | 7.43 MHz | 121 kHz | -6.51% | 3rd resonance |
| Middle | 7.31 MHz | 5.05 kHz | 0.72% | 3rd resonance |
| Bottom | 7.36 MHz | 50.5 kHz | 6.07% | 3rd resonance |
| Average after move | 7.37 MHz | 58.9 kHz | 0.9% | 3rd resonance |
| Baseline | 9.08 MHz | - | - | 4th resonance |
| Top | 9.08 MHz | 5.05 kHz | -1.69% | 4th resonance |
| Middle | 9.15 MHz | 70.7 kHz | -0.86% | 4th resonance |
| Bottom | 9.08 MHz | 0.00 kHz | 0.97% | 4th resonance |
| Average after move | 9.10 MHz | 25.3 kHz | -0.53% | 4th resonance |
| Baseline | 9.64 MHz | - | - | 5th resonance |
| Top | 9.68 MHz | 45.5 kHz | -10.51% | 5th resonance |
| Middle | 9.64 MHz | 5.05 kHz | 5.18% | 5th resonance |
| Bottom | 9.69 MHz | 50.05 kHz | -3.05% | 5th resonance |
| Average after move | 9.67 MHz | 33.7 kHz | -2.79% | 5th resonance |

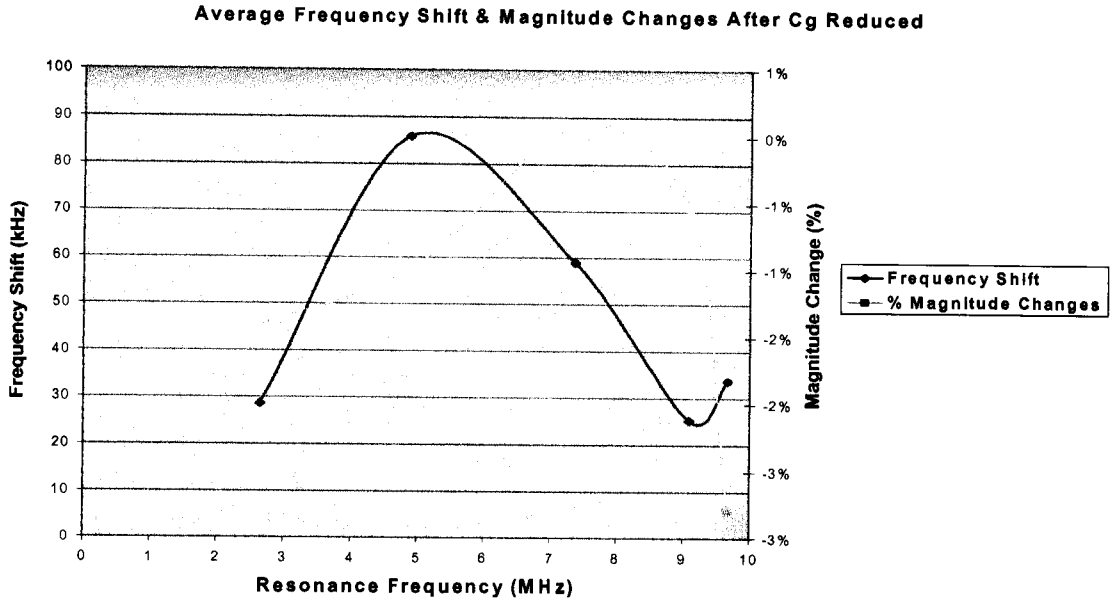


Figure A.27 – Average frequency shift & magnitude changes after Cg reduced at top, middle & bottom of the winding

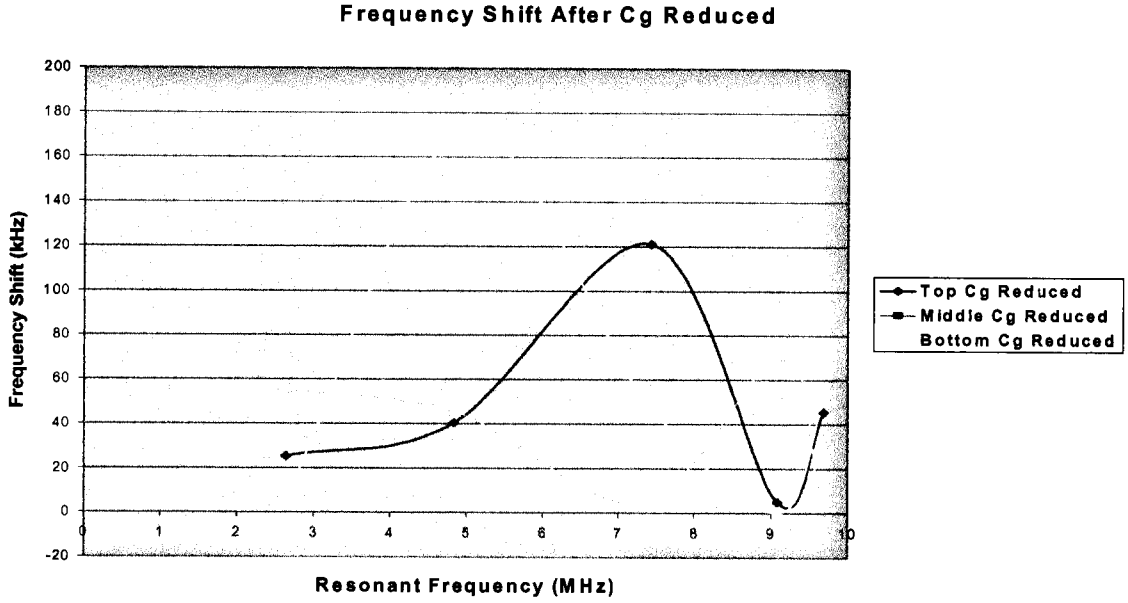


Figure A.28 – Frequency shift after Cg reduced at each locations

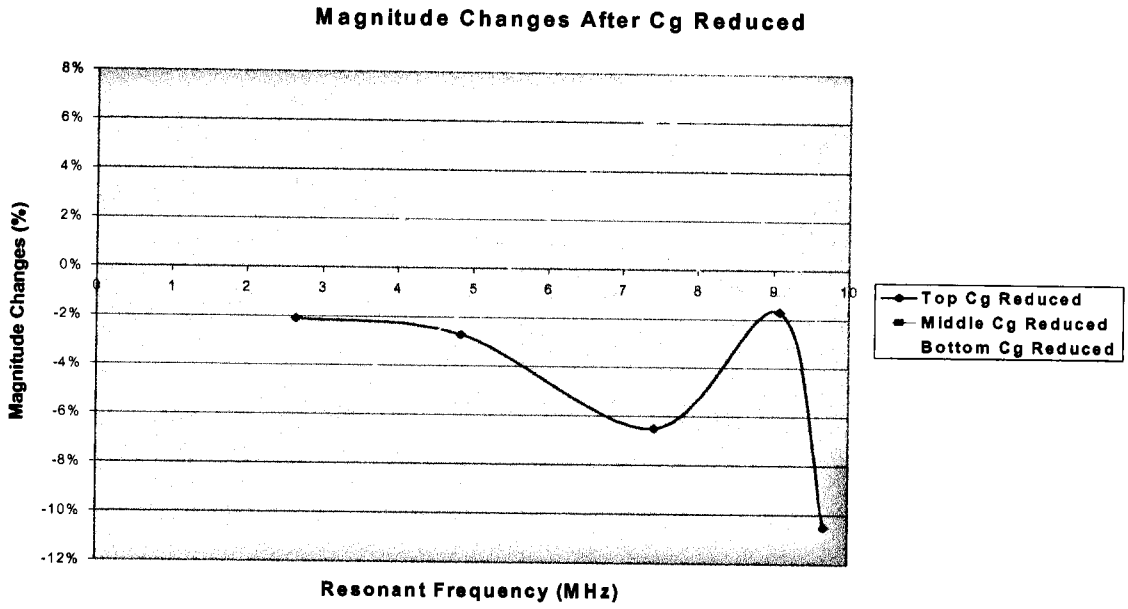


Figure A.29 - Percentage magnitude changes after Cg reduced at each locations

**Simulation 15**

This simulation investigates the significance of the impact of changing the number of sections. The basic total magnitude of the transformer's LRC circuit is the same, but the transformer is simulated with a different number of sections. The simulations were done with 12 sections, 67 sections and 74 sections. Figures A.30 and A.31 and Table A.16 show the simulation results (to 10 MHz and 20 MHz, respectively). The general trend is that the model with more sections has more resonant peaks. The 12-section model has stronger low frequency components. The 74-section model frequency shifts vary in both directions relative to the 67-layer model. It is observed that there is no resonance above 12 MHz in any of the three models.

From the simulation results, it can be concluded that the number of sections has a significant impact on the transformer admittance results. The admittances are smoother and have more high frequency resonances as the number of sections is increased.

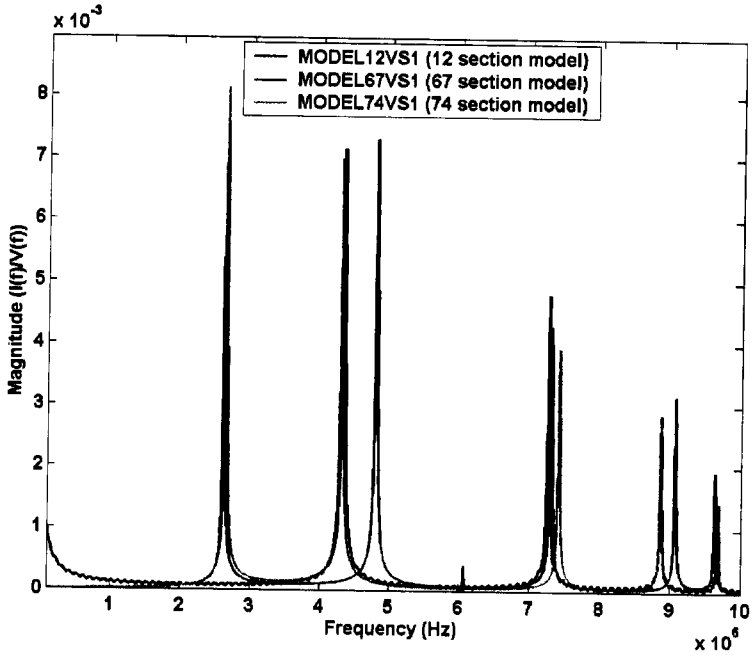


Figure A.30 – Transformer model simulated by 12, 67 & 74 sections (10 MHz range)

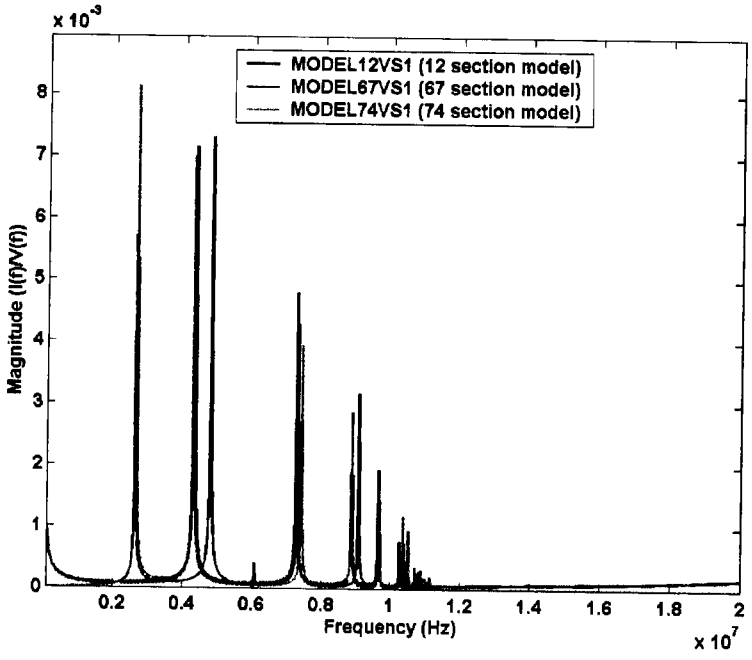


F

Figure A.31 - Transformer model simulated by 12, 67 & 74 sections (20 MHz range)

Table A.16 – Simulation of different number of winding sections

| Models sections | Resonant peak | Frequency change comparing with baseline Δf | Magnitude change comparing with baseline | Note |
|---|---|---|---|---|
| 67 - baseline | 2.62 MHz | - | - | 1st resonance |
| 12 | - | - | - | 1st resonance |
| 74 | 2.65 MHz | 25.3 kHz | 42.14% | 1st resonance |
| 67 - baseline | 4.80 MHz | - | - | 2nd resonance |
| 12 | 4.33 MHz | -470 kHz | -2.24% | 2nd resonance |
| 74 | 4.30 MHz | -500 kHz | -4.45% | 2nd resonance |
| 67 - baseline | 7.31 MHz | - | - | 3rd resonance |
| 12 | 7.27 MHz | -35.4 kHz | 11.62% | 3rd resonance |
| 74 | 7.42 MHz | 111 kHz | -8.21% | 3rd resonance |
| 67 - baseline | 9.08 MHz | - | - | 4th resonance |
| 12 | 8.87 MHz | -202 kHz | -9.93% | 4th resonance |
| 74 | 9.68 MHz | -207 kHz | -15.38% | 4th resonance |
| 67 - baseline | 9.64 MHz | - | - | 5th resonance |
| 12 | 9.68 MHz | 40.4 kHz | -25.34% | 5th resonance |
| 74 | 9.69 MHz | 50.5 kHz | -28.37% | 5th resonance |

**Simulation 16**

This case simulates the effects of the ground resistance in parallel with the ground capacitance ($C_g$). Figure A.32 and Table A.17 show the effects of the resistance. After adding the 67 MΩ parallel resistance, the magnitude of the admittance resonance reduced 32% at 9.6 MHz and 39% at 2.6 MHz. The percentage reduction of magnitude was similar over all frequencies. The parallel ground resistance, which simulates the dielectric losses, shows a very significant impact on the FRA results. This finding indicates that it may be possible to give information on the dielectric condition of overall transformer insulation condition, such as moisture level in transformer oil and paper. However, dielectric condition issues are beyond the research scope of this thesis. Future investigations could be done on this subject.

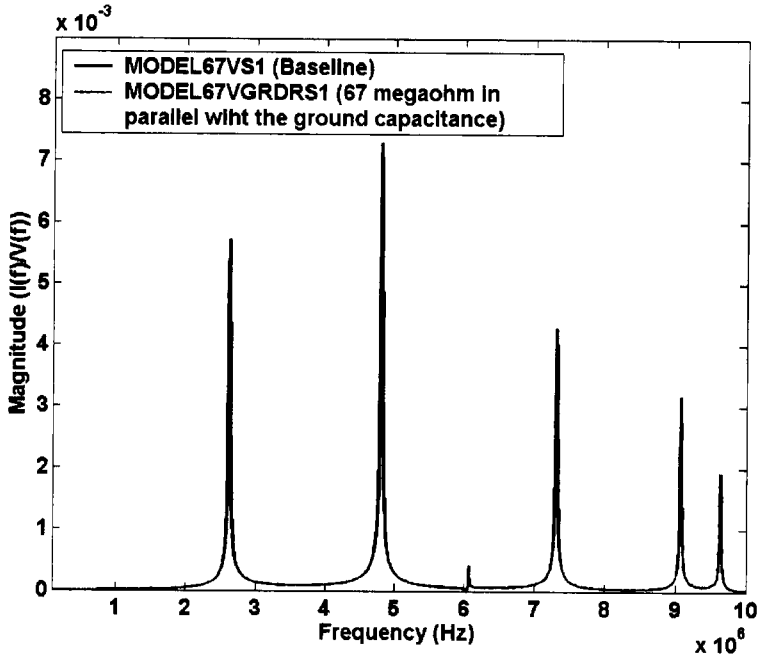


Figure A.32 – Simulated winding to ground dielectric loss

Table A.17 – Parallel resistance (67 MΩ) added to ground capacitance ($C_g$)

| Baseline resonant frequency | Baseline resonant magnitude | Frequency change comparing with baseline Δf | Magnitude change comparing with baseline | Note |
|---|---|---|---|---|
| 2.62 MHz | 5.72e-3 | 0 | -38.84% | 1st resonance |
| 4.80 MHz | 7.31e-3 | 0 | -41.00% | 2nd resonance |
| 7.31 MHz | 4.28e-3 | 0 | -40.07% | 3rd resonance |
| 9.08 MHz | 3.17e-3 | 0 | -34.29% | 4th resonance |
| 9.64MHz | 1.93e-3 | 0 | -32.04% | 5th resonance |

**Simulation 17**

This case simulates the winding clamping pressure changes that cause a reduction in the resistance (Rs) in parallel with the winding disc-to-disc capacitances (Cs). This phenomenon can be explained as follows; after re-clamping, the "thickness" of the dielectric between winding layers is reduced and results in a slight reduction of dielectric resistance. This case models this

dielectric resistance change between winding discs. A 1 MΩ resistance was added in parallel with each series capacitance. This simulation was done using the 67-section model. Figure A.33 and Table A.18 show the influence of the parallel resistance. Adding the parallel resistance reduced the admittance magnitude significantly. Compared with the parallel ground resistance case in simulation 16, the magnitude reduction increases as the resonant frequency increases. There is no frequency shift in this simulation result. A number of FRA field test results show that the admittance magnitude was reduced after re-clamping with no resonant frequency shift. This simulation result helps to explain the admittance magnitude reduction after re-clamping. The insulation distance is reduced after re-clamping and this reduction in physical distance may result in the reduction of dielectric resistance. The simulation results indicate the dielectric resistance changes have a significant impact on the FRA results. Before this simulation there was no viable explanation that could explain the phenomenon of reduction of the admittance resonant magnitude after re-clamping.

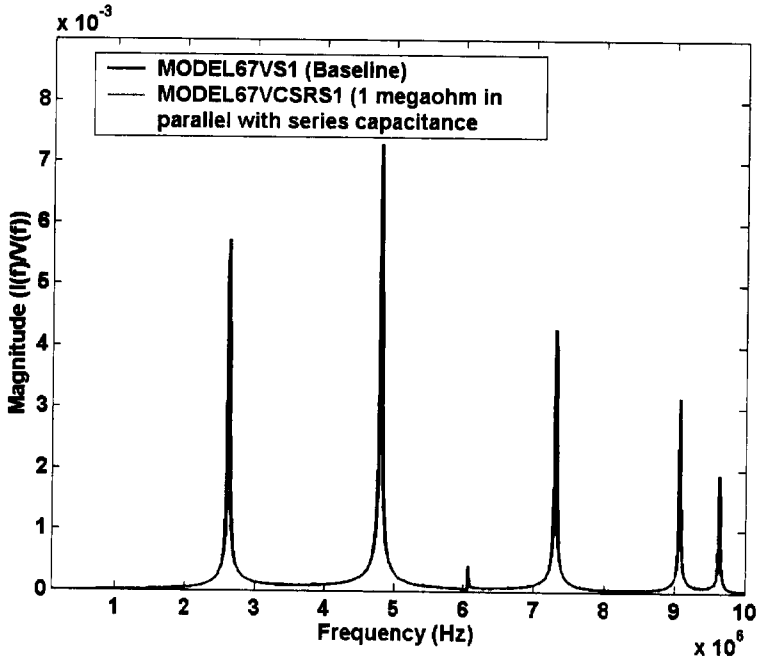


Figure A.33 – Before and after adding a parallel resistance ($R_s$)with series ($C_s$) capacitance

Table A.18 – Parallel resistance (1 MΩ) added to series capacitance

| Baseline resonant frequency | Baseline resonant magnitude | Frequency change comparing with baseline Δf | Magnitude change comparing with baseline | Note |
|---|---|---|---|---|
| 2.62 MHz | 5.72e-3 | 0 | -49.7% | 1st resonance |
| 4.80 MHz | 7.31e-3 | 0 | -33.6% | 2nd resonance |
| 7.31 MHz | 4.28e-3 | 0 | -36.3% | 3rd resonance |
| 9.08 MHz | 3.17e-3 | 0 | -52.7% | 4th resonance |
| 9.64MHz | 1.93e-3 | 0 | -54.71% | 5th resonance |

**Simulation 18**

The purpose of this case is to simulate the proposed bushing tap injection method. The injection method has the potential advantage of measuring winding movement on-line and eliminating the measurement leads effects. The simulation aims to investigate the feasibility of this method and important issues related to the bushing tap injection method. The transformer was modeled with 67 sections. The high voltage bushing was modeled with a LCR "T" circuit. Figure A.34 shows the circuit of the injection method and its parameters.

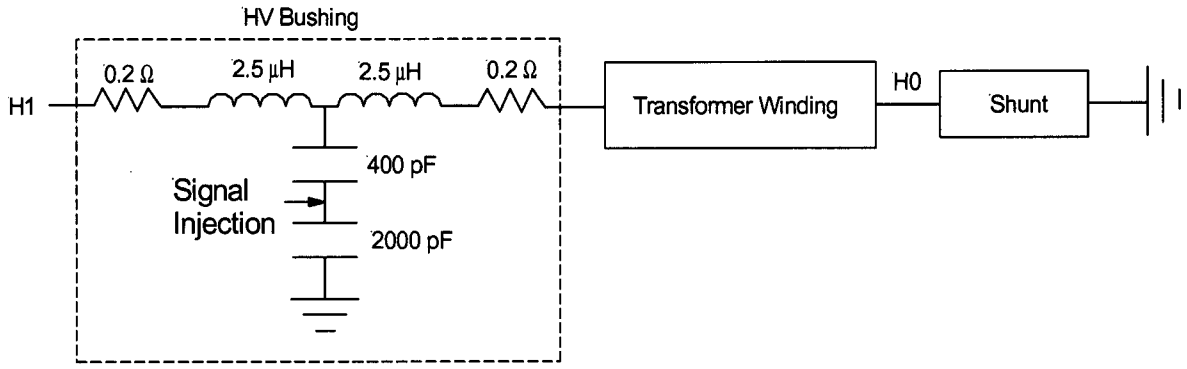


Figure A.34 – Injection method simulation model

The transformer admittances were calculated both from the top and bottom bushing voltages. The admittance calculated from the bottom bushing voltage simulates an FRA measurement done on the inside of a transformer. This simulation has no load at the high voltage bushing terminal. The simulation results are shown in Figure A.35. The data in Table A.19 shows slight differences between the measured admittances at the top and the bottom of the bushing.

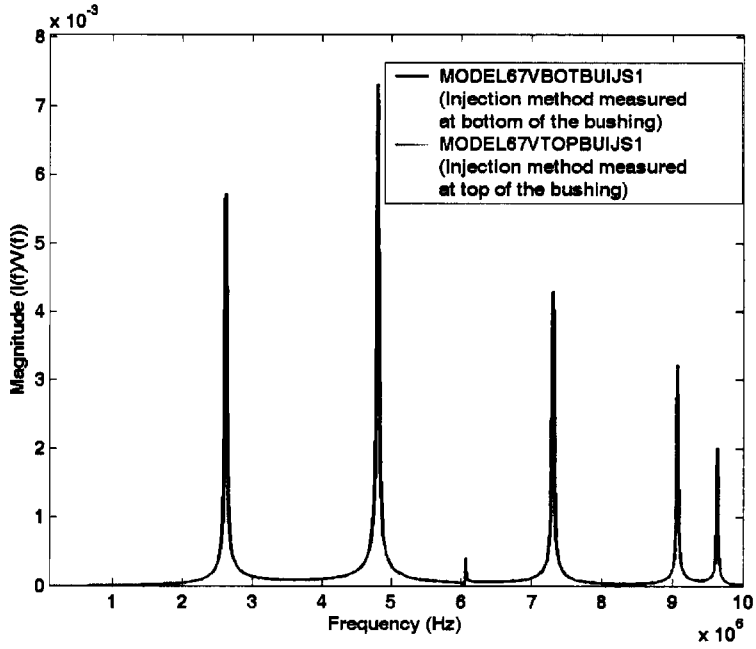


Figure A.35 – Simulation on injection method made both bottom and top of the bushing

Table A.19 – Measuring at the top vs. the bottom of the bushing

| Baseline resonant frequency (top) | Baseline resonant magnitude (top) | Frequency change comparing with baseline Δf | Magnitude change comparing with baseline | Note |
|---|---|---|---|---|
| 2.62 MHz | 5.64e-3 | 5.1 kHz | 1.24% | 1st resonance |
| 4.80 MHz | 7.30e-3 | 0 kHz | 0.20% | 2nd resonance |
| 6.07 MHz | 4.14e-4 | 0 kHz | 0.21% | 3rd resonance |
| 7.30 MHz | 4.27e-3 | 5.1 kHz | 0.63% | 4th resonance |
| 9.07 MHz | 3.17e-3 | 5.1 kHz | 1.67% | 5th resonance |
| 9.64 MHz | 2.02e-3 | 0 kHz | -4.39% | 6th resonance |

Figures A.36 and A.37 show the results with and without winding movement measured at the top and the bottom the bushing by using the bushing tap injection method. After the winding movement, the admittances measured at the top and the bottom of the winding show similar frequency shifts and magnitude changes compared to the normal test method (Simulation 3). The results showed the bottom measurement had slightly higher sensitivity than the top measurement. The average magnitude change was 0.51% for the bottom vs. 0.12% for the top.

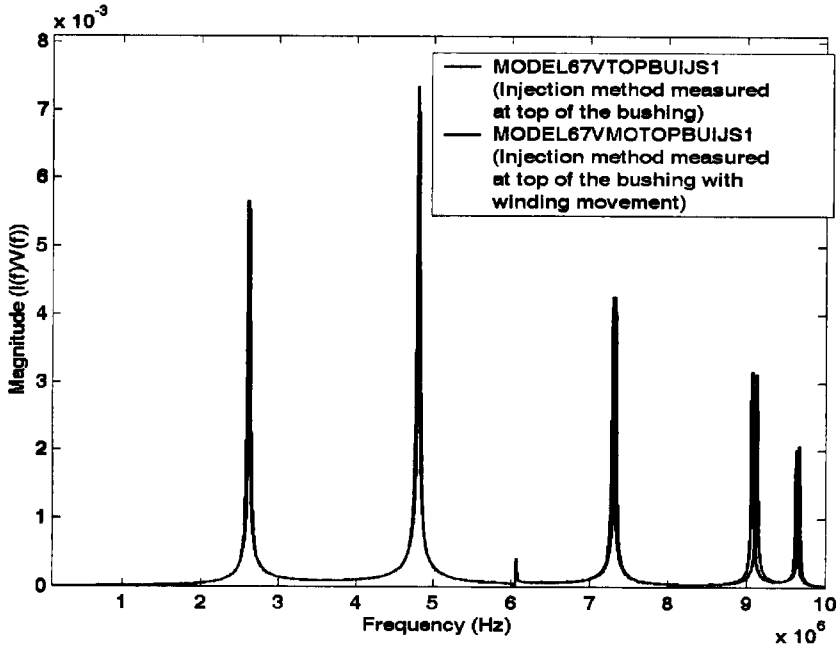


Figure A.36 – Comparison made by injection method measured at top of the bushing by injection method with and without winding movement

Table A.20 – Admittance measured at top of bushing with and without winding movement

| Baseline resonant frequency (top) | Baseline resonant magnitude (top) | Frequency change comparing with baseline Δf | Magnitude change comparing with baseline | Note |
|---|---|---|---|---|
| 2.62 MHz | 5.64e-3 | 5.1 kHz | -2.05% | 1st resonance |
| 4.80 MHz | 7.30e-3 | 0 kHz | 0.84% | 2nd resonance |
| 6.07 MHz | 4.14e-4 | 0 kHz | -0.10% | 3rd resonance |
| 7.30 MHz | 4.27e-3 | 15.2 kHz | 0.04% | 4th resonance |
| 9.07 MHz | 3.17e-3 | 55.6 kHz | -1.22% | 5th resonance |
| 9.64 MHz | 2.02e-3 | 30.3 kHz | 3.20% | 6th resonance |

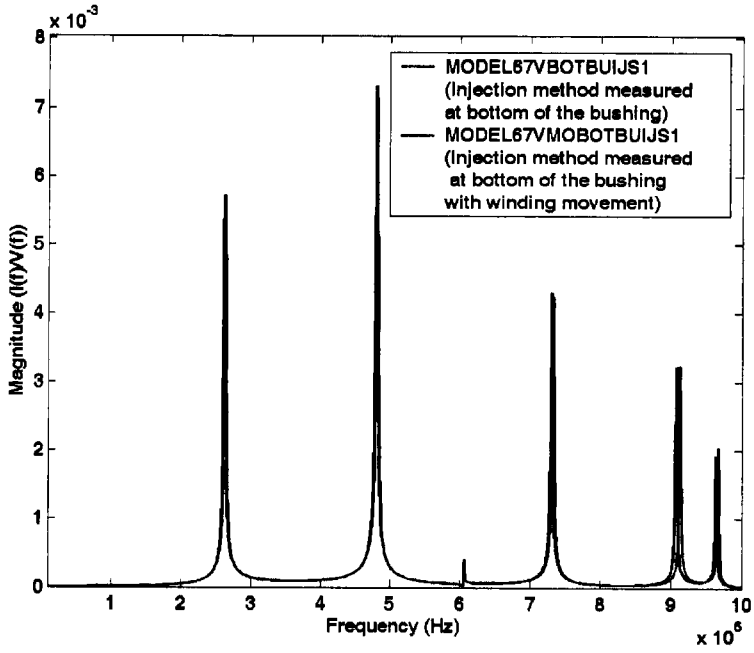


Figure A.37 – Comparison of admittances measured at bottom of the bushing by using injection method with and without winding movement

Table A.21 – Admittance measured at bottom of bushing with and without winding movement

| Baseline resonant frequency (bottom) | Baseline resonant magnitude (bottom) | Frequency change comparing with baseline Δf | Magnitude change comparing with baseline | Note |
|---|---|---|---|---|
| 2.62 MHz | 5.71e-3 | 0 kHz | -1.36% | 1st resonance |
| 4.80 MHz | 7.31e-3 | 0 kHz | -0.68% | 2nd resonance |
| 6.07 MHz | 4.15e-4 | 0 kHz | -0.06% | 3rd resonance |
| 7.31 MHz | 4.30e-3 | 15.2 kHz | -1.53% | 4th resonance |
| 9.08 MHz | 3.22e-3 | 55.6 kHz | 0.46% | 5th resonance |
| 9.64 MHz | 1.93e-3 | 35.4 kHz | 6.23% | 6th resonance |

**Simulation 19**

The aim of this case is to investigate the influences of a load at the bushing terminal with the capacitance tap injection method. The simulation has the purpose of finding out the best location for on-line measurement, and whether the results are affected by bushing load conditions. Two loads were used in this simulation. They were 300 Ω and 300 Ω in parallel with 2 nF. The admittances were measured at the top and bottom of the bushing under these load conditions.

Figure A.38, Table A.22, Figure A.39 and Table A.23 show the simulation results with and without a 300 Ω resistive load at the bushing terminal measured at the top and bottom of the bushing, respectively.

Figure A.40, Table A.24, Figure A.41, and Table A.25 show the simulation results with and without a load - 300 Ω parallel with 2 nF at the bushing high voltage terminal. The measurements were done at the top and the bottom of the bushing, respectively.

The simulations showed that the admittance measured from the bottom of the bushing has almost no impact from the different types of load, compared to the very significant impact from different terminal loads to the admittance measured from the top of the bushing using the injection method. The simulation results demonstrated that the FRA measurement has to be done at the bottom of the bushing if the bushing tap injection method is used.

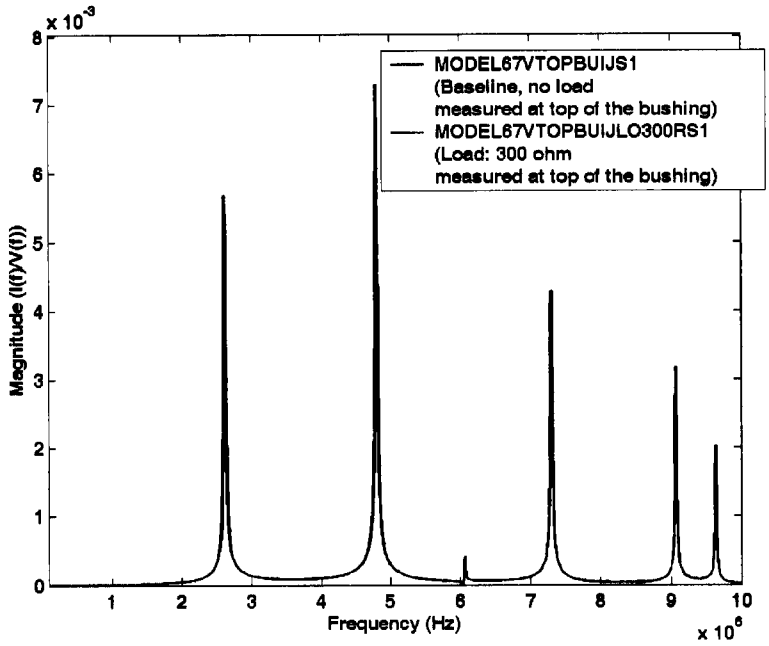


Figure A.38 – Simulation results measured at top of the bushing with and without 300 Ω load

Table A.22 – Comparison measured at top of the bushing with and without 300 Ω load

| Baseline resonant frequency (no load) | Baseline resonant magnitude (no load) | Frequency change comparing with baseline Δf | Magnitude change comparing with baseline | Note |
|---|---|---|---|---|
| 2.62 MHz | 5.64e-3 | 0 kHz | 0.50% | 1st resonance |
| 4.80 MHz | 7.30e-3 | 0 kHz | 0.15% | 2nd resonance |
| 6.07 MHz | 4.14e-4 | 0 kHz | 0.19% | 3rd resonance |
| 7.30 MHz | 4.27e-3 | 0 kHz | 0.16% | 4th resonance |
| 9.07 MHz | 3.17e-3 | 0 kHz | 0.36% | 5th resonance |
| 9.64 MHz | 2.02e-3 | 0 kHz | 0.19% | 6th resonance |
| Average | | | 0.26% | |

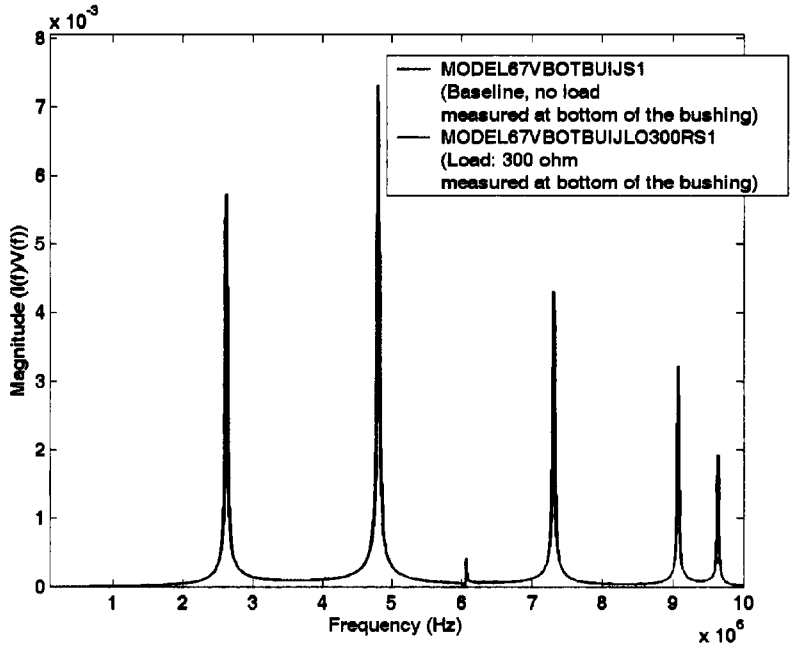


Figure A.39 – Simulation results measured at bottom of the bushing with and without 300 Ω load

Table A.23 – Admittance measured at bottom of bushing with and without 300 Ω load

| Baseline resonant frequency (no load) | Baseline resonant magnitude (no load) | Frequency change comparing with baseline Δf | Magnitude change comparing with baseline | Note |
|---|---|---|---|---|
| 2.62 MHz | 5.71e-3 | 0 kHz | 0.15% | 1st resonance |
| 4.80 MHz | 7.31e-3 | 0 kHz | 0.05% | 2nd resonance |
| 6.07 MHz | 4.15e-4 | 0 kHz | 0.12% | 3rd resonance |
| 7.31 MHz | 4.30e-3 | 0 kHz | -0.14% | 4th resonance |
| 9.08 MHz | 3.22e-3 | 0 kHz | 0.15% | 5th resonance |
| 9.64 MHz | 1.93e-3 | 0 kHz | -0.03% | 6th resonance |
| Average | | | 0.05% | |

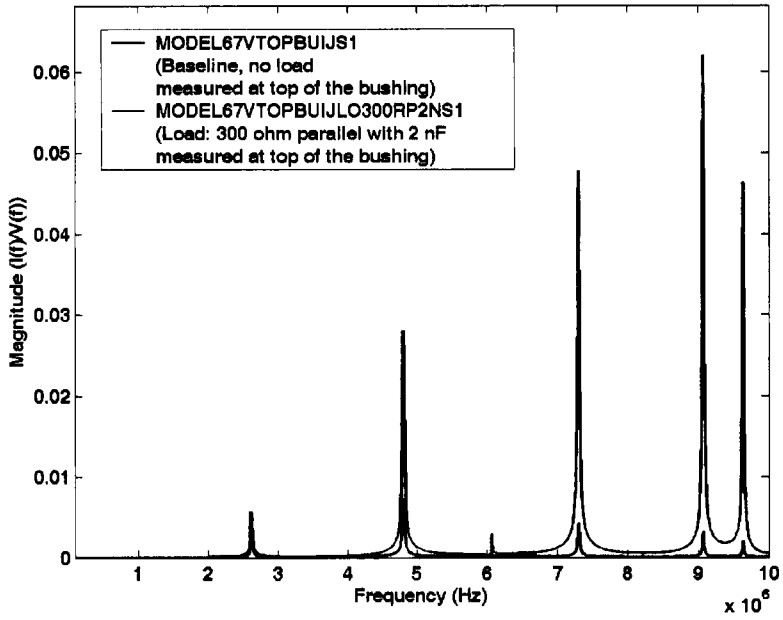


Figure A.40 - Simulation results measured at top of the bushing with and without load – 300 Ω parallel with 2 nF

Table A.24 – Measurement at top of bushing with and without load - 300 Ω parallel with 2 nF

| Baseline resonant frequency (no load) | Baseline resonant magnitude (no load) | Frequency change comparing with baseline Δf | Magnitude change comparing with baseline | Note |
|---|---|---|---|---|
| 2.62 MHz | 5.64e-3 | 0 kHz | -62.20% | 1st resonance |
| 4.80 MHz | 7.30e-3 | 0 kHz | 283.70% | 2nd resonance |
| 6.07 MHz | 4.14e-4 | 0 kHz | 601.79% | 3rd resonance |
| 7.30 MHz | 4.27e-3 | 0 kHz | 1019.76% | 4th resonance |
| 9.07 MHz | 3.17e-3 | 0 kHz | 1857.94% | 5th resonance |
| 9.64 MHz | 2.02e-3 | 0 kHz | 2199.19% | 6th resonance |
| Average | | | 983.36% | |

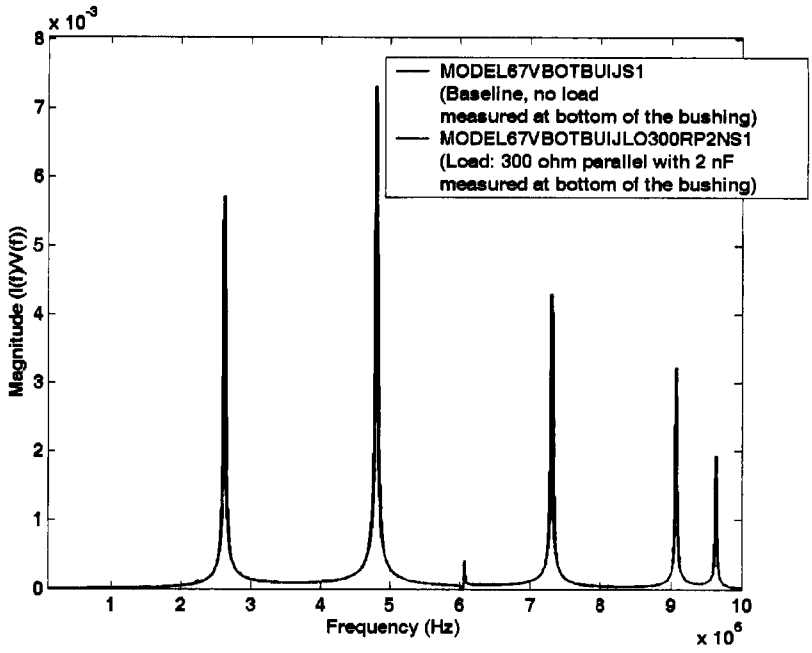


Figure A.41 – Simulation results measured at bottom of the bushing with and without load – 300 Ω parallel with 2 nF

Table A.25 – Measurement at bottom of bushing with and without load - 300 Ω parallel with 2 nF

| Baseline resonant frequency (no load) | Baseline resonant magnitude (no load) | Frequency change comparing with baseline Δf | Magnitude change comparing with baseline | Note |
|---|---|---|---|---|
| 2.62 MHz | 5.71e-3 | 0 kHz | -0.15% | 1st resonance |
| 4.80 MHz | 7.31e-3 | 0 kHz | -0.14% | 2nd resonance |
| 6.07 MHz | 4.15e-4 | 0 kHz | -0.34% | 3rd resonance |
| 7.31 MHz | 4.30e-3 | 0 kHz | -0.27% | 4th resonance |
| 9.08 MHz | 3.22e-3 | 0 kHz | -0.19% | 5th resonance |
| 9.64 MHz | 1.93e-3 | 0 kHz | 0.13% | 6th resonance |
| Average | | | -0.16% | |

## A.4 Discussion and Conclusions of Simulation Results

The simulations are based on a reduced detail transformer equivalent circuit model. The model did not simulate any transformer cases measured in the field FRA. The field and laboratory FRA measurements were performed on different types of transformers and there was no internal design information for these transformers. The simulation attempted to use a reasonably detailed transformer model to demonstrate how the changes inside a transformer affect the FRA measurement. The transformer bushing, current shunt and ground lead effects were also simulated.

The basic model used had 67 sections. In addition, two more models were investigated for comparison, a 12-section model and a 74-section model. The comparisons were made between the three models. The models with a different number of sections have different resonant frequencies, but the general characteristics of the admittance from these models are similar. Even the transformer model having 74 sections is still not detailed enough to simulate the actual measured response in the megahertz frequency range. At the megahertz frequency range, a more complex transformer model is required. The task of this research is targeted to the FRA measurement parameters, and for this purpose this model was adequate. Developing a more detailed transformer model was beyond scope of this work program.

Three current shunt resistances were simulated on the 67-section model. The results show that the resistance value has a significant impact on the admittance magnitude. The 1 Ω shunt has the highest resonant magnitude signal at the resonant peaks in the signatures and the 50 Ω shunt has the lowest values. The results show the sensitivity of the measurement is much better with the lower shunt value, particularly when looking at the very high frequencies (above 3 MHz).

A bushing model was simulated in this investigation, using a pi circuit. The high voltage bushing has a significant impact on the FRA results and cannot be ignored. This result shows that a comparison of the FRA measurement to a baseline case has to be done either with or without the high voltage bushing. The practice of some utilities to obtain a baseline without the bushings in the factory or in the field is not valid, unless the subsequent measurements are also done without the bushings. The model also shows that the bushing reduces the test sensitivity.

Two ground leads were simulated in this investigation. The ground lead contributed a shift in the resonant frequencies. The model with bushing model 1 and a ground lead further reduced the sensitivity to the detection of winding movement.

Minor winding movements were simulated at three different winding locations (top, middle and bottom). The results showed both magnitude and frequency changes as the winding movement was introduced to the model. The higher frequencies showed greater changes than at the lower frequencies for all three winding movement simulations.

A short on a portion of the winding was also simulated in this study. The results show that the predominant change caused by the short was a shift in the resonant frequencies. There were some magnitude changes in both directions. Some frequencies had an increase in magnitude while other frequencies had a decrease in magnitude.

Changes in the ground capacitance were simulated on three winding locations (top, middle and bottom). The top and middle winding ground capacitance changes contributed more on the resonant frequency shift and the bottom winding ground capacitance changes caused more magnitude changes.

Ground capacitance losses and winding series capacitance losses were simulated in the 12-section model. Both cases show that the resonant magnitudes reduce with resistance in parallel with this capacitance. These results are very interesting, since before this simulation it was not understood why the magnitude of the admittance was reduced after re-clamping the transformer. It was not realized that the dielectric losses were significant enough to reduce the resonant magnitude sufficiently to affect the transformer signature. This simulation shows that introducing parallel resistance to the model significantly reduces the magnitude of the resonant admittance. Therefore, the phenomenon of reduced resonant magnitude after re-clamping can be explained as due to the reduction in the distances between turns/discs. This also reduces the parallel equivalent resistances. This phenomenon also opens up the potential application for future development of the FRA test as a means to evaluate transformer dielectric condition such as moisture level.

The bushing tap injection method was investigated in the simulations. The simulation results showed that this method is very promising for future development, especially by using the

injection method combined with the application of the measurement inside the transformer at the bottom of the bushing. The simulation results showed that the high voltage terminal load did not affect the injection method with internal measurement (bushing bottom measurement). The simulation showed that the injection method is a very feasible way to apply the test to monitoring of on-line winding movement.